Háskólinn á Akureyri
University of Akureyri

Per- and polyfluoroalkyl substances (PFASs) meet Arctic and sub-Arctic marine diatoms and associated symbionts

Ashani Arulananthan

DOCTORAL THESIS

University of Akureyri
School of Health, Business and Natural Sciences

October 2026

Per- and polyfluoroalkyl substances (PFASs) meet Arctic and sub-Arctic marine diatoms and associated symbionts

Ashani Arulananthan

Doctoral thesis

Natural Resource Sciences

Doctoral committee

Oddur Þór Vilhelmsson: Main supervisor

Bettina Scholz: Co-supervisor

Auður Sigurbjörnsdóttir: Co-supervisor

Óttar Rolfsson: Co-supervisor & Secondment host

Hans-Peter Grossart: Co-supervisor & Secondment host

Ulf Karsten: Advisor & Secondment host

Háskólinn á Akureyri
Sólborg, Norðurslóð 2
600 Akureyri

Printing: Prentmet Oddi
Akureyri, October, 2026

ISBN: 978-9935-505-35-4
ORCID: https://orcid.org/0000-0003-0514-9878

Áhrif fjölflúorsetinna alkýlefna á kísilþörunga og sambýlisörverur þeirra á Norðurslóðum

Ashani Arulananthan

Doktorsritgerð

í auðlindafræðum

Doktorsnefnd:

Oddur Þór Vilhelmsson: aðalleiðbeinandi

Bettina Scholz: leiðbeinandi

Auður Sigurbjörnsdóttir: leiðbeinandi

Óttar Rolfsson: leiðbeinandi og umsjónarmaður rannsóknardvalar

Hans-Peter Grossart: leiðbeinandi og umsjónarmaður rannsóknardvalar

Ulf Karsten: ráðgjafi og umsjónarmaður rannsóknardvalar

Háskólinn á Akureyri
University of Akureyri

Háskólinn á Akureyri
Sólborg, Norðurslóð 2
600 Akureyri

Prentun: Prentmet Oddi
Akureyri, Október, 2026

ISBN: 978-9935-505-35-4
ORCID: https://orcid.org/0000-0003-0514-9878

Dedicated to my loving parents, who gave me roots; my caring brothers, who gave me belonging; my husband, who gave me wings; my loving friends, who walked beside me; my dear teachers and mentors, who lit the way; and to nature, which inspired it all.

Acknowledgments

The work presented in this thesis was carried out in North Iceland, far from where my journey first began. Reflecting on the path from the tropical warmth of Sri Lanka to the stark and beautiful landscapes of Iceland, I realize that this journey has been one of challenge, resilience, growth, and transformation.

The road was not always easy. Long hours in the laboratory, often working alone, were filled with trial and error, failed experiments, and the continuous process of learning and adapting. The first year was particularly demanding as I struggled to establish cultures, refine protocols, and find my place in a new research field. Through perseverance, however, I found confidence, clarity, and the determination that ultimately shaped this thesis.

My deepest gratitude goes to my doctoral committee, Prof. Oddur Þór Vilhelmsson, Dr. Bettina Scholz, Associate Prof. Auður Sigurbjörnsdóttir, Prof. Óttar Rolfsson, Prof. Hans-Peter Grossart, and Prof. Ulf Karsten, for their guidance, encouragement, and unwavering support throughout this PhD journey. Their expertise, timely advice, and constructive feedback were instrumental in the successful completion of this research. I will always be grateful for their trust, encouragement, and belief in my potential, especially during moments when I doubted myself.

I sincerely thank Sjávarlíftæknisetrið BioPol ehf., Halldór G. Ólafsson, and the Icelandic Research Fund (RANNIS ID: 239548-051) for providing this PhD opportunity. I am also grateful for the Erasmus Mobility Grants, which enabled valuable international research experiences and professional development.

My sincere thanks go to my collaborators, Prof. Helmut Hillebrand, Prof. Klaus Herburger, Prof. Rodrigo Almeda, Prof. Ralf Ebinghaus, Prof. Hanna Joerss, Prof. Bernardo Duarte, and Prof. Zophonías O. Jónsson, for their expertise, guidance, and opportunities to broaden my scientific horizons.

I warmly thank Dr. Guðrún Rósa Þórsteinsdóttir, Director of the Centre for Doctoral Studies, for her continuous guidance, encouragement, and genuine interest in my academic progress and well-being. I am equally grateful to Hildur Friðriksdóttir, International Coordinator, for her support in pursuing international research opportunities, and to Pia Susanna Sigurlína Viinikka for her kindness and support throughout my time at the university.

Special thanks go to the lab manager, Andrés Tryggvi Jakobsson and Dr. Sean Scully for their invaluable technical assistance and support in the laboratory. I also thank my colleagues, Dr. Natalia Ramirez Carrera, Lada Zelinski, Eva María Ingvadóttir, and Alexandra Georganti-Ntaliape, whose companionship made this journey less solitary.

I have never forgotten those who guided and shaped my academic and research journey. I am thankful to Prof. Sepalika Jeyamanne, Prof. Sivashanthini Kuganathan, Prof. Venura Herath, Prof. Terney Pradeep Kumara, Dr. Anura Upasanta Kumara, Dr.Akila Harishchandra, Prof. Jes Vollertsen, Associate Prof. Alvise Vianello, and Associate Prof. Claudia Lorenz, whose mentorship and support laid the foundation for my research career.

My heartfelt thanks go to my dear friends, Dr. Lara Wilhelmine Hoffmann, Dr. Thineshkaran Abirami, Ainkaran Vithiyarani, Gabriela Galecka, Urmila Selvakumar, and Misriya Rinas for their friendship and unconditional love during difficult times. Their care and positivity reminded me that I was never alone.

Finally, my deepest gratitude goes to my family, my father, Markandu Arulananthan; my mother, Kandiah Rajapushpam; my brothers, Ayinkaran, Achuthan, Rageeprasath, and Kokulan; my nephew Arikaran; and my sisters-in-law, Sarmini and Rajitha. Even across distance, they remained part of my everyday life and support system. Through every high and low, every doubt and small success, I shared my days with them, and their constant presence, patience, and love carried me forward more than words can express. Finally, to my husband, Dr. Kuddithamby Gunaalan, who has been my strongest pillar throughout this journey, thank you. Your understanding, patience, and support carried me through the most difficult times. You believed in me when I struggled to believe in myself, and your presence, even from afar, gave me the strength to keep going. This achievement is as much yours as it is mine.

Looking back, this PhD was more than a research project; it was a lesson in resilience, perseverance, and personal growth. It taught me that courage is not the absence of doubt, but the determination to keep moving forward despite it. Despite all the challenges, it is a journey I would choose again.

Abstract

Over recent decades, per- and polyfluoroalkyl substances (PFAS) have emerged as pervasive contaminants, with documented presence even in remote regions such as the Arctic and Antarctica, and far-reaching consequences for human health and ecosystem functioning. In particular, the widespread distribution of PFAS raises concerns about their effects on foundational organisms in food webs, such as diatoms, a major group of phytoplankton that regulate biogeochemical cycles by contributing 20% of global primary production. In this context, the aim of this thesis was to examine the effects of PFAS on two ecologically distinct marine diatom species, the pelagic *Thalassiosira pseudonana* and the benthic *Cylindrotheca closterium*, and to assess the consequences for their physiology, molecular responses, and associated microbial communities.

Cultures of both species were exposed to individual long-chain PFAS and a replacement compound across a concentration gradient in short-term assays, followed by a chronic exposure to an environmentally relevant PFAS mixture. Physiological traits related to growth, photosynthesis, oxidative stress, and cellular composition were quantified, and these responses were integrated with gene expression and targeted endometabolome analysis of diatoms and diatom-associated bacterial community changes.

Short-term exposure caused pronounced growth inhibition in both species at high (100 mg/L) and mid (1mg/L) PFAS concentrations, with mixtures exerting stronger effects than individual compounds. Responses were species specific: *C. closterium* was more sensitive to PFCAs (C8-C12), whereas *T. pseudonana* was more strongly affected by PFAS chains longer than C11. PFAS exposure reduced photosynthetic efficiency and chlorophyll and protein contents, and increased stress markers such as proline and total antioxidant activity. Under long-term exposure to a PFAS mixture (0.9 ng/L), growth rates recovered to control levels after 14 days, indicating potential compensatory or acclimatory responses.

At the molecular level, *T. pseudonana* showed a broad, multi-pathway reconfiguration of core housekeeping metabolism, whereas *C. closterium* exhibited a more focused response dominated by ABC transporter-mediated efflux and changes in central carbon metabolism. *T. pseudonana* metabolites and gene expression changes showed a shift from a growth-oriented, high nitrogen demand state toward a stress-acclimated phenotype that prioritized redox homeostasis, membrane repair, and the synthesis of protective, secondary metabolite-rich survival traits over continued growth. PFAS exposure also restructured the diatom-associated bacterial communities in a host-dependent manner, but little change in overall alpha diversity, consistent with community reorganization rather than collapse. These results show PFAS mixtures can substantially alter diatom physiology, metabolism, and community structure, impacting marine primary producers' resilience and biogeochemical stability in contaminated environments.

Ágrip

Á undanförnum áratugum hafa fjölflúorsetin alkýlefni (PFAS) komið fram sem útbreidd mengunarefni, sem hafa greinst jafnvel á afskekktum svæðum á borð við Norðurskautið og Suðurskautslandið, með víðtæk áhrif á heilsu manna og vistkerfa. Sérstakar áhyggjur hafa vaknað vegna útbreiðslu PFAS og mögulegra áhrifa þeirra á lykillífverur í fæðuvefjum, svo sem kísilþörunga, sem eru stór hópur svifþörunga og gegna lykilhlutverki í lífefnafræðilegum hringrásum með því að standa undir um 20% af frumframleiðslu jarðar. Markmið þessarar ritgerðar var að rannsaka áhrif PFAS á tvær vistfræðilega ólíkar tegundir sjávar-kísilþörunga, uppsjávartegundina *Thalassiosira pseudonana* og botnlægu tegundina *Cylindrotheca closterium*, og meta áhrif þeirra á lífeðlisfræði þörunganna, genatjáningu þeirra og á sambýlisörverur þeirra.

Báðar tegundirnar voru ræktaðar í viðurvist langkeðja PFAS efnasambanda yfir styrkhallanda í skammtímatilraunum, auk langvarandi snertingar við PFAS-blöndu í styrk áþekkum þeim sem mælist í sjó á Norðurslóðum. Mældir voru lífeðlisfræðilegir þættir tengdir vexti, ljóstillífun, oxunarálagi og frumuefnasamsetningu. Þessar niðurstöður voru síðan samþættar greiningum á genatjáningu, markvissri efnaskiptagreiningu innan frumna (endometabolome) og breytingum á bakteríusamfélögum tengdum kísilþörungunum.

Skammtímatilraunirnar sýndu marktæka vaxtarhömlun hjá báðum tegundum við háa (100 mg/L) og miðlungs (1 mg/L) PFAS-styrki, þar sem blöndur höfðu sterkari áhrif en einstök efni. Viðbrögðin voru þó tegundasértæk. *C. closterium* reyndist næmari fyrir perflúoraðri karboxýlsýrum (PFCAs; C8-C12), en *T. pseudonana* varð fyrir meiri áhrifum af PFAS-efnum með kolefniskeðjur lengri en C11. PFAS-útsetning dró úr ljóstillífunarvirkni, blaðgrænumagni og próteininnihaldi, en jók á sama tíma streituvísa eins og prólín og heildarvirkni andoxunarkerfa. Við langvarandi útsetningu fyrir PFAS-blöndu (0,9 ng/L) náðu vaxtarhraðar sér aftur á strik eftir 14 daga og urðu sambærilegir við samanburðarhópa, sem bendir til mögulegra aðlögunar- eða uppbótarviðbragða.

Á sameindastigi sýndi *T. pseudonana* víðtæk áhrif PFAS á marga grunnefnaskiptaferla, en svörun *C. closterium* var markvissari og einkenndist einkum af aukinni virkni ABC-flutningspróteina og breytingum í miðlægum kolefnaefnaskiptum. Breytingar í efnaskiptum og genatjáningu hjá *T. pseudonana* bentu til tilfærslu frá vaxtarhvetjandi ástandi með mikla köfnunarefnisþörf yfir í streituaðlagaða svipgerð sem lagði meiri áherslu á viðhald oxunar-jafnvægis, viðgerð frumuhimna og myndun verndandi afleiddra efnasambanda fremur en áframhaldandi vöxt. PFAS-útsetning leiddi einnig til endurskipulagningar bakteríusamfélaga tengdra kísilþörungunum á hýsilháðan hátt, þó án verulegra breytinga á alfa-fjölbreytni, sem bendir til breytinga á samfélagsgerð frekar en hruns samfélaganna.

Niðurstöðurnar sýna að PFAS-blöndur geta haft veruleg áhrif á lífeðlisfræði, efnaskipti og samfélagsgerð kísilþörunga. Slíkar breytingar geta haft áhrif á seiglu frumframleiðenda sjávar og stöðugleika lífefnafræðilegra hringrása í menguðum vistkerfum.

Contents

List of abbreviations

AFFF: Aqueous Film-Forming Foam
PSII: photosystem II
Fv: Variable Fluorescence
Fm: Maximum Fluorescence
Fv/Fm: Maximum Quantum Yield of Photosystem II
PFAS: Per- and Polyfluoroalkyl Substances
PFCA: Perfluorocarboxylic acid
PFAA: Perfluoroalkyl acid
PFSA: Perfluoroalkane Sulfonic Acid
PFOA: Perfluorooctanoic acid
PFOS: Perfluorooctanesulfonic acid
FTOH: fluorotelomer alcohols
PFNA: Perfluorononanoic acid
PFHxA: Perfluorohexanoic Acid
PFBS: Perfluorobutane Sulfonate
PFSA: Perfluoroalkane Sulfonic Acid
PFDA: Perfluorodecanoic acid
PFDoA: Perfluorodecanoic acid
PFTrDA: Perfluorotridecanoic Acid
PFUnDA: Perfluoroundecanoic Acid
PFTeDA: Perfluorotetradecanoic Acid
PFECHS: Perfluoroethylcyclohexane Sulfonate
PCBs: polychlorinated biphenyls
PDBE: polybrominated diphenyl ethers
GenX/HFPO-DA: Hexafluoropropylene Oxide Dimer Acid
MPs: Microplastics
GSH: Reduced Glutathione
GSSG: Oxidized Glutathione
TCA: Tricarboxylic Acid Cycle
ESFA: European Food Safety Authority
EC50: Half-Maximal Effective Concentration
NOEC: No Observed Effect Concentration
TAC: Total Antioxidant Capacity/activity
OECD: Organization for Economic Co-operation and Development
LC-MS/MS: Liquid Chromatography–Tandem Mass Spectrometry
GC-MS/MS: Gas Chromatography–Tandem Mass Spectrometry
HILIC: Hydrophilic interaction liquid chromatography
UPLC-qTOF-MS: ultra-performance liquid chromatography coupled with quadrupole time-of-flight mass spectrometry

List of figures

List of tables

Overview of original articles

This thesis is based on the following four Articles. Hereafter, they will be referred to by their numbers as follows:

I. Arulananthan, A., Vilhelmsson, O., Karsten, U., Grossart, H.-P., Sigurbjornsdottir, A., Rolfsson, Ó., Joerss, H., & Scholz, B. (2025). Per- and polyfluoroalkyl substances (PFAS) in the Cryosphere -Occurrence, organismic accumulation, ecotoxicological impacts, transformation, and management strategies. *Frontiers in Environmental Science*, *13*. https://doi.org/10.3389/fenvs.2025.1559941 (Published)

II. Arulananthan, A., Scholz, B., Karsten, U., Grossart, H.-P., Sigurbjörnsdóttir, A., Rolfsson, Ó., Joerss, H., Duarte, B., & Vilhelmsson, O. Þ. (2025). Arctic and sub-Arctic marine diatom responses to PFAS exposure: Understanding physiological changes and resilience. *Aquatic Toxicology*, *289*, 107562. https://doi.org/10.1016/j.aquatox.2025.107562 (Published)

III. Arulananthan, A., Vilhelmsson, O. Þ., Rolfsson, Ó., Grossart, H.-P., Sigurbjörnsdóttir, A., Karsten, U., Wünsch, M., Ebinghaus, R., Joerss, H., Duarte, B., Jónsson, Z. O., & Scholz, B. (2026). PFAS at environmental concentration alters metabolic and gene expression patterns in two model marine diatoms: Decoding survival and acclimation mechanisms (Under Review).

IV. Arulananthan, A., Vilhelmsson, O., Sigurbjornsdottir, A., Grossart, H.-P., Karsten, U., Scholz, B. (2026). The phycosphere microbiomes of marine diatoms show indirect resistance to PFAS at environmentally relevant concentrations (Under review)

Declaration of Contribution to the thesis

The following authors have contributed to the main Articles and manuscripts for this thesis: Ashani Arulananthan (AA), Oddur Þór Vilhelmsson (OV), Bettina Scholz (BS), Auður Sigurbjörnsdóttir (AS), Óttar Rolfsson (OR), Hans-Peter Grossart (HP), Ulf Karsten (UK), Hanna Joerss (HJ), Bernardo Duarte (BD), Ralf Ebinghaus (RE), Zophonías O. Jónsson (ZJ), and Marie Wünsch (MW).

Article I:
AA: Conceptualization, Writing, Investigation, Methodology, Visualization, Formal Analysis. OV: Conceptualization, Funding acquisition, review and editing; UK: Conceptualization, Review and editing, Methodology. HP: Conceptualization, Data curation, Visualization, Review and editing; AS: Review and editing. ÓR: Review and editing, Methodology; HJ: Data curation, Review and editing, Investigation, Validation. BS: Conceptualization, Methodology, Review and editing.

Article II:
AA: Writing-original draft, Visualization, Methodology, Investigation, Formal analysis, Conceptualization; BS: Review & editing, Validation, Resources, Investigation, Funding acquisition, Data curation, Conceptualization. UK: Review & editing, Data curation, Conceptualization. HP: Review & editing, Conceptualization; AS: Review & editing, Resources; OR: Review & editing, Resources, Conceptualization; HJ: Review & editing, Visualization, Validation, Conceptualization; BD: Review & editing, Validation, Conceptualization; OV: Review & editing, Resources, Resources, Conceptualization.

Article III:
AA: Conceptualization, Writing, Investigation, Methodology, Visualization, Formal Analysis. OV: Review & editing, Resources, Conceptualization; ÓR: Review and editing, Methodology; HP: Conceptualization, Data curation, Visualization, Rreview and editing; AS: Review and editing, Conceptualization; UK: Review & editing, Data curation, Conceptualization; MW: Methodology; RE: Review and editing, Conceptualization; HJ: Review and editing; BD: Review and editing, Conceptualization; ZJ: Review and editing, Conceptualization; BS: Conceptualization, Review and editing.

Article IV:
AA: Writing, Investigation, Methodology, Visualization, Formal Analysis; OV: Review & editing, Resources, Conceptualization; AS: Review and editing, Conceptualization; HP: Review and editing, Conceptualization; UH: Review and editing; BS: Review & editing, Resources, Funding acquisition.

1 Introduction

1.1 Primary Producers Rule the Oceanic Earth - Diatoms

Diatoms (class Bacillariophyceae) are stramenopile protists and are among the most successful and influential organisms on Earth, quietly shaping life in the oceans for millions of years (Armbrust, 2009). These unicellular, photosynthetic eukaryotes are responsible for nearly 20% of global photosynthesis, producing a substantial fraction of the oxygen we breathe while simultaneously fixing carbon dioxide (CO_2) into organic matter (Falkowski, 2012; Field et al., 1998; Geider et al., 2001) (**Figure 1**). Given that oceans cover nearly 70% of the Earth‘s surface, diatoms form the foundation of marine food webs, including in polar environments, supporting organisms from grazers to higher trophic levels, and ecological influence extends across biogeochemical cycles (Falciatore & Mock, 2022; Karsten et al., 2012).

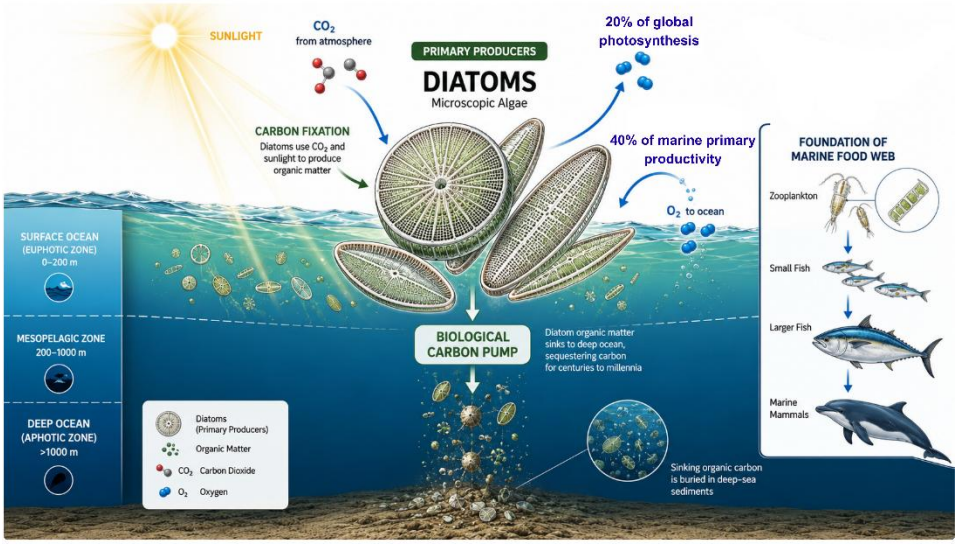

Figure 1: *Ecological and biogeochemical importance of marine diatoms.*

Schematic illustration of the central role of diatoms as primary producers in marine ecosystems. Through photosynthesis, diatoms utilize sunlight and atmospheric CO_2 to fix carbon into organic matter and release oxygen, contributing to global oxygen production. As the foundation of marine food webs, diatoms support higher trophic levels, including zooplankton, fish, and marine mammals. A portion of the organic matter produced by diatoms sinks through the water column, transporting carbon from the surface ocean to deep-sea sediments via the biological carbon pump, thereby contributing to long-term carbon sequestration. The figure also highlights the distribution of diatoms within the oceanic water column, from the sunlit euphotic zone to deeper waters, and their dual role

in sustaining marine productivity and regulating global biogeochemical cycles. *Note*. Graphical design (elements) assisted by ChatGPT plus 5.5 (OpenAI, 2026) using author-provided scientific content and prompt; reviewed by the author for accuracy.

Encased in intricately patterned silica shells known as frustules, diatoms possess a unique structural feature, which not only provides structural protection but also influences their ecological function (Armbrust, 2009; Round et al., 1990). When they die, these dense silica structures facilitate rapid sinking from the euphotic zone to deeper waters, effectively exporting fixed organic carbon to the ocean interior. This process, known as the biological carbon pump, is a major pathway for long-term carbon sequestration (Tréguer et al., 2018). Diatoms are estimated to contribute up to 40% of marine primary productivity and a substantial proportion of particulate carbon export, underscoring their importance in regulating atmospheric CO_2 levels (Behrenfeld et al., 2021; Tréguer et al., 2018) (**Figure 1**). In parallel, they influence cycling of essential elements such as nitrogen, carbon, silicon, and iron, thereby shaping the composition and productivity of marine microbial communities (Behrenfeld et al., 2021).

1.2 The Phycosphere: A Microscale Interface Structuring Diatom-Algae Interaction

Over the past decades, researchers have increasingly highlighted that diatoms function not as isolated organisms but as components of complex microbial consortia. Central to this perspective is the concept of the phycosphere- a microscale diffusive boundary layer surrounding diatom cells enriched in dissolved organic matter (DOM) (Cole, 1982; Di Costanzo et al., 2023; Seymour et al., 2017). This microenvironment facilitates interaction between diatoms and heterotrophic bacteria, which utilize diatom-derived metabolites as carbon and energy sources. In return, bacteria provide essential nutrients and cofactors, including vitamins and bioavailable iron, that are often limiting in marine systems (Grossart, 1999; Seymour et al., 2017). These reciprocal exchanges form tightly coupled symbiotic relationships that are now recognized as fundamental to diatom physiology, ecological success, and adaptation to environmental variability (Daly et al., 2023; F. Liu et al., 2022). This matters for carbon cycling because bacterial identity can determine whether diatom-derived carbon is exported as aggregates and marine snow or retained in the surface microbial loop through polymer degradation and respiration (Gärdes et al., 2011a; Teeling et al., 2012).

Over evolutionary time, such proximity has fostered intimate metabolic and genetic interdependencies between diatoms and bacteria (Armbrust, 2009; Bowler et al., 2008). Comparative genomics has revealed that diatoms harbor numerous genes of bacterial origin, many of which are involved in nitrogen and carbon metabolism, cell wall processes, and other core cellular functions, highlighting the

long evolutionary co-adaptation of these lineages (Behrenfeld et al., 2021; Falciatore & Mock, 2022; Tirichine et al., 2017). Experimental studies demonstrate that exposure of phytoplankton to their natural microbial consortia can trigger major transcriptional and metabolic reprogramming, including the release of specialized secondary metabolites that selectively promote symbionts and suppress non-beneficial or competing bacteria (Amin et al., 2015a; Buchan et al., 2014; Falciatore et al., 2020).

Emerging evidence suggests that per- and polyfluoroalkyl substances (PFAS) contamination can also reshape microbial community composition. In natural microbial communities, PFAS exposure has been associated with the depletion of Cyanobacteria and favored Bacteroidia, Gammaproteobacteria, and Alphaproteobacteria, accompanied by reductions in microbial diversity and evenness (Davis et al., 2024). Similarly, in algae-bacteria mesocosms, PFAS partitioned into the phycosphere, which acted as a measurable PFAS reservoir, while longer-chain PFAS showed stronger associations with biosphere distribution and community succession (J.-Y. Wu et al., 2022).

For diatom-bacteria interactions, this creates a plausible feedback loop. PFAS stress changes diatom photosynthesis and metabolite allocation; diatoms change extracellular polymeric substances (EPS) and exudate chemistry; bacteria respond to the new substrate and contaminant regime; and altered bacterial functions then feedback on vitamin supply, nutrient remineralization, reactive oxygen species (ROS) buffering, aggregation, or algicidal pressure. This loop is still under-tested experimentally, but it follows directly from the established sensitivity of extracellular polymeric substances (EPS) mediated diatom-bacteria interactions and the demonstrated PFAS effects on EPS and community structure (Daly et al., 2023; L. Li et al., 2026).

1.3 PFAS in Arctic and Polar Regions: A Silent Ecological Threat

As key drivers of ocean ecology and biogeochemistry, diatom-bacteria partnerships exist in an ocean increasingly altered by anthropogenic stressors. Among the most persistent and globally distributed contaminants are PFAS, commonly dubbed as “forever chemicals” due to their persistence nature, have emerged as a pervasive contaminant even in the world’s most remote polar ecosystems and biota (Alfaro Garcia et al., 2022; Bargagli & Rota, 2024; Casal, Zhang, et al., 2017; Evenset et al., 2016; Garnett et al., 2022; Hartz et al., 2024; Munoz et al., 2017; Trilla-Prieto et al., 2025).

Comprising a fluorocarbon backbone attached to various functional groups, PFAS shows a unique due to their hydrophobic and oleophobic properties that gives them soluble in both aqueous and non-polar media, supporting their

widespread industrial and household applications including waterproof fabrics, cookware, surfactants, detergents, pesticides, semiconductors, food packaging materials, and non-stick makeup products (**Figure 2**) (ECHA, 2024; A. Y.-C. Lin et al., 2009; Okazoe, 2009; Renfrew & Pearson, 2021). Their detection across Arctic air, drinking water, snow, glaciers, sea ice, and biota, far away from any point of manufacture, draws attention to the magnitude of long-range contamination (Casal, Zhang, et al., 2017; Garnett, Halsall, Thomas, et al., 2021; Grung et al., 2024; Hartz et al., 2024; Lohmann et al., 2024).

Reported Arctic marine concentrations vary by orders of magnitude across environmental matrices. Surface seawater studies documented ~ 0.5 ng/L ∑PFCA (perfluorocarboxylic acid) in the Arctic Ocean in one North Pacific to Arctic transect, European High Arctic under-ice seawater reached ~ 2.7ng/L ∑PFAA (perfluoroalkyl acid) at 0.5 m near the Barents Sea shelf break, Bering-to-western Arctic surface sediments contained 0.06 -1.73 ng/g dry weight ∑PFAS, and global synthesis reported Arctic Ocean plankton around 5.7 ng/g with perfluorooctanesulfonic acid (PFOS) as the key perfluoroalkane sulfonic acid (PFSA) (Cai et al., 2012; Garnett, Halsall, Vader, et al., 2021; Khan et al., 2023; Y. Lin et al., 2020). Direct Arctic marine-snow PFAS data remains scarce, while current evidence supports particle-associated transfer and sinking-particle removal mainly for long-chain PFAAs; however, the lack of research with definite data on Arctic marine-snow concentration series (Hartz et al., 2024; Savvidou et al., 2023)

1.3.1 Pathways to Arctic Marine Systems

PFAS distribution in Arctic environments shows multiple long- range transport mechanisms, as described in Article I, among atmospheric and oceanic pathways, significant contributions are made by multiple PFAS dominating seawater, snow, and sea-ice (**Figure 2**). Volatile PFAS processors such as fluorotelomer alcohols (FTOH), undergo photochemical degradation in the upper troposphere and are deposited as stable perfluoroalkyl acids (PFCAs) via snowfall and dry deposition (X. Li et al., 2026). The Arctic cold amplifies this process through "cold condensation," whereby PFAS with lower boiling points condense preferentially in frigid environments. Oceanic circulation, including the Norwegian Sea current, a key PFAS corridor, delivers long-chain compounds such as perfluorooctanoic acid (PFOA) and PFOS into Arctic waters over decadal timescales (Joerss et al., 2019). Additionally, accelerating glacial meltwater and river discharge increasingly mobilize previously deposited PFAS into coastal marine systems (MacInnis et al., 2022). Similar patterns have been documented in Antarctica, where both polar regions show comparable temporal trends in PFAS accumulation since the 1990s (Cabrerizo et al., 2013; X. Li et al., 2026; Scheringer et al., 2024).

On the other hand, not only long-range transport, but also local sources were identified as having higher PFAS loads, including PFAS alternatives, in samples analyzed from firefighting training stations (365 ng/L) and landfill areas (643 ng/L) in Svalbard (Ali et al., 2021). Despite the regulatory phase-out of legacy compounds such as PFOS and PFOA, the continual introduction of fluorinated substitutes means that new PFAS variants are regularly detected in Arctic environments, underscoring the urgent need for comprehensive regulatory action.

1.3.2 PFAS Build Up in Arctic Marine Food Web: Plankton to Higher Trophic Levels

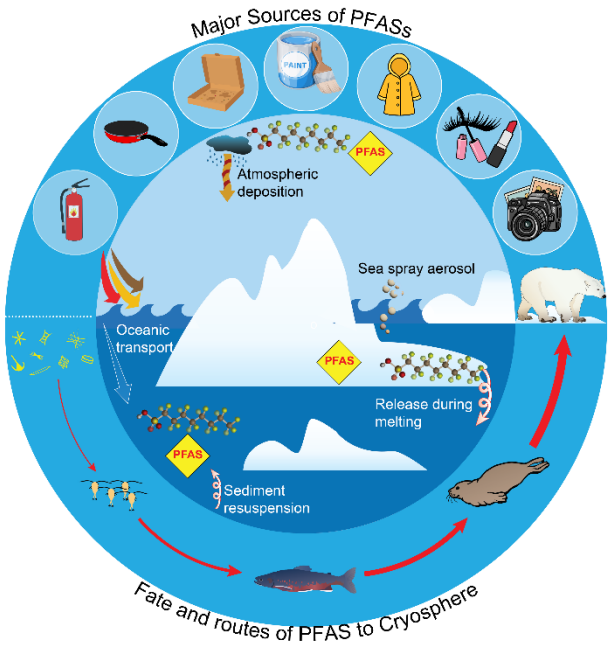

Figure 2: *Sources of PFAS, transport, and fate in the marine environmental food web*

Once PFAS enter Arctic waters, they come into contact with the base of the marine food web. Phytoplankton and zooplankton absorb PFAS directly from the water column, with PFOS being the dominant compound detected in oceanic plankton (Casal, González-Gaya, et al., 2017; Ma et al., 2022; X. Zhang et al., 2019). As energy transfers upward through the trophic levels (**Figure 2**), from phytoplankton to zooplankton to fish, seabirds, and marine mammals, PFAS concentrations intensify through biomagnification, with meta-analysis revealing that PFAS concentrations approximately double with each trophic level on average (Ricolfi et al., 2025). Arctic ocean plankton contained ∑PFAS 5.7 ng/g

with PFOS as the key compound (Khan et al., 2023). At the same time, it is vital to note that datasets on direct PFAS concentration and effect analyses remain much thinner than those for Arctic phytoplankton on wildlife. However, the documented PFAS in Arctic waters indicates exposure at the base of the marine food web, and the most important Arctic-specific exposure mechanism for primary producers is seasonal snow and sea-ice melt, which indeed releases PFAAs into near-surface and under-ice waters used by ice algae and early season phytoplankton (Garnett, Halsall, Thomas, et al., 2021; Garnett, Halsall, Vader, et al., 2021; Thomas et al., 2023).

Arctic apex predators are among the most severely affected. In polar bears, PFAS concentrations are roughly ten times those detected in local human populations, with PFOS and perfluorononanoic acids (PFNA) being the most prevalent compounds and continuing to rise across the bear and seal populations (Sonne et al., 2023; Tartu et al., 2017). High PFAS burdens have also been documented in the eggs of seabirds, including herring gulls, common eiders, and thick-billed murres (Haque et al., 2023; Munoz et al., 2017; Sun et al., 2023). Further, research on Arctic marine webs in Svalbard confirms that emerging PFAS substitutes such as 6:2 FTS and PFBS were also identified in invertebrates and benthic organisms (Ali et al., 2021).

Thereby, intrusion of PFAS into Arctic food webs poses cascading threats to ecosystem integrity as the disruptions start at the foundational planktonic level, affecting photosynthesis, growth, and community balance, and can propagate upward, destabilizing the biodiversity and ecosystems functioning of the entire Arctic ecosystem (Cara et al., 2022; Kelly et al., 2009) (**Figure 2**).

PFAS do not behave like polychlorinated biphenyls (PCBs) or polybrominated diphenyl ethers (PBDEs) because many PFAS bind or partition into proteins and phospholipids, and do not partition into neural lipids, so lipid -normalized bioaccumulation concepts can be misleading when applied without quantification (Burkhard & Votava, 2023; Kelly et al., 2009). Several long-chain PFAS were also found in tissues of protein-rich tissues in wildlife and at high trophic levels, such as the liver, kidney, blood, eggs, and other organs (Cai et al., 2012; Garnett, Halsall, Vader, et al., 2021; Kelly et al., 2009; Khalid et al., 2024). This property complicates the interpretation of biota-sediment bioaccumulation factors (BSAFs) because equilibrium partitioning assumptions based on lipid-organic-carbon affinity often fail for PFAS. A BSAF meta-analysis concluded that lipid normalization has limited utility for PFAS, that protein normalization may be conceptually relevant but was not statistically predictive across available data, and that PFAS residues are influenced by active transport plus binding to proteins and phospholipids (Burkhard & Votava, 2023).

For apex predators, modelled serum PFOS concentrations in several polar bear subpopulations already exceeded the established immunotoxic thresholds of the European Food Safety Authority (EFSA)(Sonne et al., 2023). Since several coastal

people, including the indigenous in the Arctic, relying on traditional marine fish and marine mammal (seals and polar bears) diets, face disproportionately elevated PFAS exposure, raising serious concerns for reproductive health, immune function, and food sovereignty (Lohmann et al., 2024; Sonne et al., 2025).

1.4 Cellular Toxicity and Photosynthetic Impairment Caused by PFAS

PFAS effects in phytoplankton and microalgae commonly include growth inhibition, chlorophyll reduction, altered photosynthetic efficiency, oxidative stress, and membrane effects (Table 1). A review of aquatic invertebrates, plankton, and microorganisms reported phytoplankton toxicity endpoints, including *Scenedesmus obliquus* PFOA 96 h EC50 of 139.23 mg/L, *Isochrysis galbana* PFOS acute EC50 of 37.5 mg/L, *Isochrysis galbana* PFOA acute EC50 of 163.6 mg/L, *Chlorella vulgaris* PFOS growth no observed effect concentration (NOEC) of 8.2 mg/L, and *Selenastrum capricornutum* PFOS autotroph growth NOEC of 5.3 mg/L (Boudreau et al., 2003; Ma et al., 2022).

The same review reported that PFAS exposure altered chlorophyll and chloroplast structure in *C. vulgaris*, decreased chlorophyll *a* and soluble protein in *Chlorella pyrenoidosa*, and altered superoxide dismutase (SOD), catalase (CAT), reactive oxygen species (ROS), and malondialdehyde (MDA) responses in *S. obliquus* and *C. vulgaris* (Ma et al., 2022). These endpoints map directly onto photosynthetic electron transport, redox homeostasis, membrane integrity, and protein biosynthesis, which are key processes for diatom productivity under Arctic light and nutrient stress.

Experimental and literature studies (Table 1) have shown that PFAS can disrupt cellular homeostasis in organisms by partitioning with lipid membranes, destabilizing membrane structure, leading to lipid peroxidation, and interfering with organelles such as chloroplasts (Ahrens & Bundschuh, 2014; Ankley et al., 2021; Boltes et al., 2012; Hagenaars et al., 2013; Latała et al., 2009; Y. Li et al., 2021; Liao et al., 2024; W. Liu et al., 2008b; Mahoney et al., 2023). In microalgae and other primary producers, PFAS exposure has been associated with reduced growth rates, affecting photosynthetic efficiency, increased oxidative stress, and broad biochemical alterations in antioxidant systems and metabolic pathways (Davis et al., 2024; Latała et al., 2009; Y. Li et al., 2021; Liao, Huang, et al., 2025a; Okpanachi et al., 2025) . However, most existing research has focused on single-species responses, with limited attention given to how PFAS exposure influences the integrated diatom-bacteria system (Table 1).

Such cellular disruptions have clear implications for diatoms. Impairment of photosystem II activity, increased production of reactive oxygen species, and damage to chloroplast membranes can compromise photosynthetic efficiency and

energy balance, ultimately affecting growth, carbon fixation, and the capacity to contribute to the biological pump (Davis et al., 2024).

Because diatoms are intimately connected to heterotrophic bacteria in the phycosphere, perturbations to diatom physiology are likely to cascade to their associated microbiomes (Johansson et al., 2019; Seymour et al., 2017). PFAS can directly or indirectly alter bacterial community structures and function, favouring resistant or tolerant taxa while reducing sensitive lineages, thereby reshaping the composition and metabolic potential of diatom-associated bacterial communities (Cerro-Gálvez et al., 2020; J. Wu et al., 2022). Yet the combined response of diatoms and their microbiomes to PFAS remains poorly constrained, particularly for environmentally realistic exposure regimes and for species occupying contrasting ecological niches such as pelagic and benthic habitats.

1.5 Knowledge Gaps in PFAS Responses of Diatom Physiology and Microbiome Assemblages

Despite growing evidence of widespread PFAS contamination in marine and even polar environments, the responses of key marine primary producers such as diatoms remain poorly characterized. Most of the existing PFAS ecotoxicology studies have focused on vertebrates and higher trophic levels, often using single compounds at concentrations far above those measured in Arctic surface waters, and have provided only a partial view of how PFAS interfere with cellular metabolism, stress responses, and longer-term acclimation in microalgae (Kelly et al., 2009; Y. Li et al., 2023; Liao, Huang, et al., 2025b; Ricolfi et al., 2025; Zhou et al., 2024).

The physiological endpoints documented so far, growth inhibition, PSII impairment, ROS accumulation, altered protein and lipid content, imply disruption of light harvesting, electron transport, carbon fixation, membrane integrity, and antioxidant capacity, but the molecular mechanisms underlying these responses remain insufficiently resolved (Table 1) (Flynn et al., 2025; P. Li et al., 2020; Liao, Huang, et al., 2025a; Xue et al., 2022). Transcriptomic and metabolomic data from PFAS-exposed marine diatoms are particularly scarce, so pathway-level inference has, until recently, largely relied on physiological and biochemical proxies rather than direct molecular evidence.

An additional complexity arises from the ecological diversity of diatoms. Pelagic diatoms dominate open-water primary production and are key contributors to export fluxes via fast-sinking aggregates and fecal pellets (Turner, 2015), whereas benthic diatoms colonize sediments and surfaces, supporting coastal productivity and mediating sediment biogeochemistry (Battin et al., 2007; Underwood & Kromkamp, 1999). These contrasting habitats differ in light penetration, hydrodynamics, nutrient regimes, and contaminant exposure patterns,

potentially shaping diatom physiology, cellular defenses, and associated bacterial communities in distinct ways (Gärdes et al., 2011b; Litchman et al., 2007; Simon et al., 2002). The benthic diatoms may experience sediment-associated and porewater exposure, whereas pelagic diatoms more directly track dissolved water-column pulses (Y. Lin et al., 2020), yet comparative studies that explicitly contrast PFAS impacts between these two ecological guilds remain lacking.

Finally, the consequences of PFAS exposure for phycosphere-associated bacterial communities, and how microbiome restructuring may feedback on host physiology and biogeochemical functioning, remain virtually unexplored. While some studies have measured diatom physiology, EPS dynamics, or community-level shifts under PFAS stress, none have yet resolved whether specific bacterial partners buffer or amplify PFAS toxicity in the host (Davis et al., 2024; L. Li et al., 2026).

1.5.1 Rationale and Research Aims

My thesis aims to provide insights to address these gaps by integrating physiological, transcriptomic, metabolomic, and microbiome analyses to characterize how environmentally relevant PFAS mixtures affect two ecologically distinct marine diatoms, *Cylindrotheca closterium* (benthic, pennate) and *Thalassiosira pseudonana* (pelagic, centric). For Arctic primary producers, the most relevant exposure scenario is not simply constant seawater concentration but episodic under-ice and meltwater exposure during biologically sensitive windows. This involves chronic, low-level exposure to a mixture, including short-chain PFAAs that dominate sea ice and snow, alongside longer-chain legacy compounds elevated in near-surface under-ice water, rather than acute single-compound conditions. Arctic plankton also already shows measurable PFAS burdens (Khan et al., 2023; Lohmann et al., 2024).

By combining short-term PFAS exposures at different concentrations and long-term PFAS mixture exposure at environmentally relevant concentrations, this research investigates how PFAS affect both diatom physiology and their associated bacterial communities. By linking changes in cellular function to shifts in microbiome composition, the study aims to elucidate the mechanisms by which PFAS disrupt diatom-bacteria interactions and overall diatom performance (**Figure 3**).

This knowledge is important for understanding how increasing PFAS contamination may affect key marine ecosystem processes such as carbon fixation, nutrient cycling, and the biological carbon pump. It will also provide much-needed data on Arctic marine primary producers to support future environmental risk assessments, regulatory decisions, and mitigation strategies.

***Table 1**: Summary of reported effects of per- and polyfluoroalkyl substances (PFAS) on freshwater and marine microalgae, highlighting tested compounds, exposure conditions, measured physiological and molecular endpoints, and the major biological responses observed across studies.*

Organism	**PFAS tested**	**Concentration/exposure**	**Endpoints measured**	**Overall impact**
Chlorella pyrenoidosa (Y. Li et al., 2021)	PFOA, GenX / HFPO-DA	100 ng/L and 100 µg/L, 12 d chronic	Growth, cell density inhibition rates, changes in photosynthetic pigment chlorophyll *a* & chl *b,* photosynthetic activity, Fv/Fm, transcriptomics	Growth inhibited after day 6; at day 12, inhibition was 3.81–6.76% at 100 ng/L and 14.4–15.4% at 100 µg/L. Chlorophyll and photosynthesis declined; photosynthesis-related genes were altered.
Marine *Chlorella* sp. (W. Mao et al., 2023)	PFOA, PFOS	PFOA 0,5,10,20,40,80,160,320 mg/L, PFOS 0,5,10,20,40,80,160mg/L, 7 d(growth), PFOA 0,5,10,20,40,80 mg/l, PFOS 0,5,10,20,40 96h (chlrophyll fluroscence)	Growth (measured using cell density), reproduction, cell membrane integrity, growth inhibition rate, esterase activity, Chlorophyll *a* fluorescence, Fv/Fm, rETR, ROS, SOD, CAT, GSH, uptake/BCF, gene expression	Low dose hormesis: PFOA <40 mg/L and PFOS <20 mg/L stimulated reproduction; higher doses inhibited growth. PFOS caused stronger membrane damage, photosynthetic disruption, ROS increase and bioaccumulation than PFOA.

Chlorella vulgaris, *Skeletonema marinoi*, *Geitlerinema amphibium* (Latała et al., 2009)	Linear PFCAs C6–C9(PFHxA, PFHpA, PFOA, and PFNA)	72 h acute; chemical concentration range from 50 mM to 0.000005 mM.	Ec50, Growth inhibition / algal population growth	Toxicity increased with carbon chain length; about twofold higher per added $–CF_2–$ group. Diatom/cyanobacterium was generally more sensitive than green algae
Chlorella vulgaris (Xu et al., 2017)	PFOS	Reported as 96 h, approx. 0,40,80,120,160,200 mg/L in secondary summaries	Chlorophyll concentration, cell permeability, antioxidant defense (SOD, CAT), ROS, MDA, chloroplast damage	PFOS decreased membrane permeability/integrity, damaged photosynthesis, increased ROS and MDA, altered antioxidant responses, and chloroplast structure.
Chlamydomonas reinhardtii, *Scenedesmus obliquus* (C. Hu et al., 2014)	PFOA	96 h acute, PFOA 0, 1, 3.16, 10, 31.6, 100, 316, and 1000 mg/l, EC50 measured	Growth inhibition test, EC50, physiological responses, lipid peroxidation (MDA contents), uptake, proline content	PFOA caused acute growth toxicity and increased lipid peroxidation; algal cell uptake was quantified.
Scenedesmus obliquus (Xue et al., 2022)	PFOS, PFBS	7 d; reported EC50: PFOS about 0, 25, 50, 75, 100, 150, and 200 mg/L, PFBS 0, 300, 600, 1200, and 1800 mg/L in summaries	Growth, E50, photosynthetic characteristics (Fv/Fm, ETR, oxidative damage, transcriptome, Antioxidant activity (SOD, MDA, CAT)	PFOS was much more toxic than PFBS; effects included growth inhibition, photosynthetic impairment, oxidative damage, and transcriptomic changes.

Marine microbial / phytoplankton community (Davis et al., 2024)	PFAS mixture, especially PFOS-focused impacts	Exposure details not fully visible in abstract (4days PFOS- 0,2.5, 5, 10, 20, and 30 mg/L ,6:2 FTS- 0,5, 10, 20, 40, and 80 mg/L)	Photosynthesis, cellular exudates, nutrient cycling, community composition	PFAS altered phytoplankton photosynthesis, exudate release, nutrient cycling and microbial community composition.
Cyanobacterium *Microcystis aeruginosa* (Liao et al., 2024)	PFCA, PFSA	PFOS effects apparent >5 µg/L under environmental stressors (7 days, 25 different PFAS compounds, 100ng/l)	Growth, oxidative damage, cellular responses under heatwave/nutrient stress	PFOS suppressed algal growth and induced oxidative damage; environmental stress modified toxicity.
Microcystis aeruginosa (Liao, Huang, et al., 2025a)	PFOS / PFAS	Environmentally relevant to higher concentrations; exact range not visible in abstract	Growth, photosynthesis, oxidative stress, metabolomics, microcystin-related responses	Higher PFOS suppressed bloom formation by reducing growth/photosynthesis and inducing oxidative stress; environmentally relevant PFAS levels could promote cyanobacterial growth/photosynthesis
Chlorella sorokiniana (Zhao et al., 2023)	PFOA, alone and with polystyrene microplastics	PFOA 0.05,0.5,5 mg/l PS-MP 10mg/l PS-MPs + 0.05 mg/L PFOA PS-MPs + 0.5 mg/L PFOA PS-MPs + 5 mg/L PFOA PS-MPs + 0.5 mg/L PFOA PS-MPs + 5 mg/L PFOA	Growth, inhibition rate, photosynthetic pigment determination, Fv/Fm, oxidative stress (Contents of GSH, MDA, GSSG, CAT, SOD, T-GSH, EPS, antioxidant system, lipid peroxidation	PFOA stress affected photosynthesis, oxidative balance, extracellular polymeric substances and antioxidant defenses; microplastics modified the response.

Chlorella vulgaris (Z. Liu et al., 2025)	PFBA	96 h PFBA 10-2560 mg/L	Growth, growth inhibition rate, toxicity mechanism, Fv/Fm, rETR, ROS, cell membrane integrity, physiological/biochemical endpoints	Short-chain PFBA still caused measurable algal toxicity, though generally less potent than longer-chain PFAS. (ScienceDirect)
Thalassiosira minima (Zheng et al., 2026)	PFOS	14 days 1–100 µg/L	Growth, BMAA-related protein and transcriptomics (TCA, AA, CysK)	Hormetic growth: high-dose PSII and BMAA protein inhibition
Chlorella vulgaris; Scenedesmus obliquus (Mojiri, Nazari Vishkaei, et al., 2023)	PFOA + PFOS (mixture)	Up to 7 days 0–10 mg/L	Growth, Cell viability, pigment content, protein content, molecular docking, and enzymatic interaction	Increasing dose and duration decrease viability, chl, and protein; species-specific sensitivity: *Scenedesmus* is more sensitive than Chlorella
Chlorella vulgaris, Microcystis aeruginosa (L. Zhang et al., 2023)	PFOS, PFBS, 6:2 FTS	4 days to 12 days 0.01,1,10,50,100,250,500 mg/L)	Growth, photosynthesis efficiency, pigment content, toxicity, and ecological risk	mixtures synergistic in cyanobacteria but antagonistic in green algae
Chlorella minutissima (James et al., 2026)	7 PFAS compounds (varied chain length and structure, PFOS, PFNA, PFOA, PFHpA, PFHxA, PFHxS, PFDA)	14 days 1 mg/L	Growth, photosynthesis efficiency, pigments content, Biochemical composition, fatty acid profile, antioxidant defense	Compound-specific physiological and biochemical responses; chain length modulates toxicity

2 Objectives

This thesis set out to explore how pelagic and benthic marine diatoms and their associated bacterial communities respond to exposure to different PFAS types and concentrations at the physiological, metabolic, and molecular levels (**Figure 3**). This was addressed through the following objectives positioned to address their respective hypotheses:

Objective 1: **Assess how different PFAS compounds and concentrations affect the physiological traits of *Cylindrotheca closterium* and *Thalassiosira pseudonana.***
Hypothesis: Exposure to PFAS will negatively affect the physiological performance of marine diatoms in a concentration- and compound-dependent manner.

Objective 2: **Resolve PFAS-driven molecular and metabolic responses using metabolomics and transcriptomics**
Hypothesis: Exposure to an environmentally relevant low-concentration PFAS mixture will induce measurable metabolic and transcriptomic alterations in marine diatoms associated with stress tolerance, detoxification, and adaptive survival mechanisms.

Objective 3: **Characterize PFAS-driven changes in diatoms' phycosphere bacterial communities**
Hypothesis: PFAS exposure will alter the composition and diversity of diatom-associated phycosphere bacterial communities.

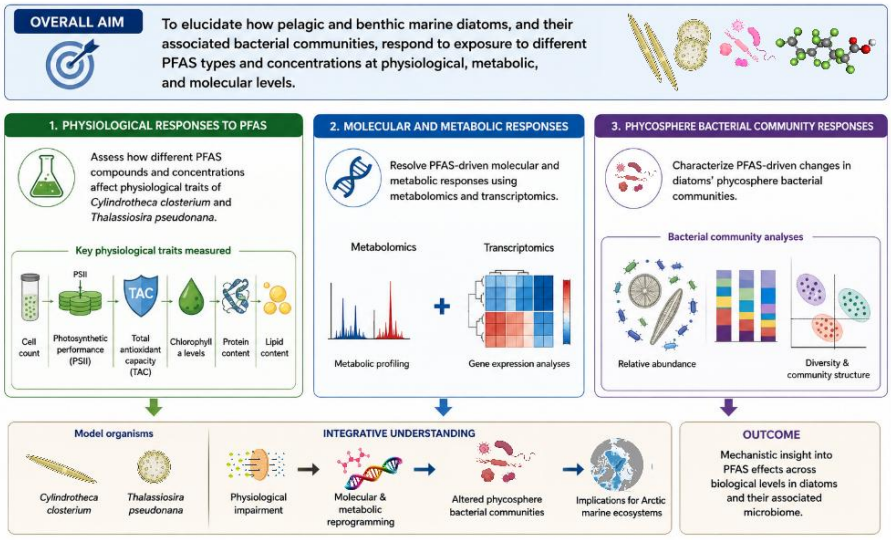

Figure 3*: Overall aim and main objectives studied are outlined as 1, 2, and 3.*

Note. Graphical design (elements) assisted by ChatGPT plus 5.5 (OpenAI, 2026) using author-provided scientific content and prompt; reviewed by the author for accuracy.

Scientific articles addressing these hypotheses form the basis of the PhD thesis:

Article I: A literature review was conducted to understand the environmental case of PFAS in the Arctic Cryosphere: Transport, Trophic Transfer, and the Imperative to Study Primary Producers. The review provided a contextual foundation for further work.

Article II: Investigated how exposure to differnt PFAS compounds and concentrations affects key physiological traits in diatoms, by measuring their cell count, photosynthetic performance (PSII), total antioxidant capacity (TAC), chlorophyll *a* levels, protein, and lipid content.

Article III: Explored how *C. closterium* and *T. pseudonana* responded to low concentrations (900 pg/L) of a mixture of PFAS exposure at the molecular level by combining targeted endometabolome profiling and gene expression analyses, with a focus on identifying pathways involved in stress responses, adaptations, and survival.

Article IV: Determined how PFAS exposure altered bacterial community structure and relative abundance patterns associated with both *C. closterium* and *T. pseudonana*.

3 Materials and Methods

3.1 PFAS in the Cryosphere and Their Ecological Footprints (Article I)

Literature Search and Study Selection

This review was conducted through a systematic search of peer-reviewed scientific literature, grey literature, and regulatory documents pertaining to per- and polyfluoroalkyl substances (PFAS) in cryospheric environments. Relevant literature was identified through searches of major scientific databases, including Web of Science, Scopus, and Google Scholar, using keyword combinations such as "PFAS", "perfluoroalkyl", "polyfluoroalkyl", "cryosphere", "Arctic", "Antarctic", "glaciers", "permafrost", "sea ice", "bioaccumulation", "biomagnification", "bioremediation", and "transformation." No explicit date range restriction was applied, though the review prioritized publications from the past two decades, reflecting the period of greatest scientific attention to PFAS in polar environments, with the earliest references dating to the mid-20th century to provide historical context on PFAS production and chemistry

Inclusion and Exclusion Criteria

Studies were included if they reported on: (1) the occurrence, concentration, or distribution of PFAS in cryosphere matrices including snow, glacial ice, sea ice, permafrost, meltwater, and sediments; (2) bioaccumulation or biomagnification of PFAS in organisms inhabiting polar or cold environments; (3) physicochemical properties governing PFAS environmental fate and transformation in cold environments; (4) ecotoxicological effects of PFAS on cryosphere-associated biota; (5) microbial degradation and bioremediation potential for PFAS; and (6) regulatory frameworks and management strategies relevant to PFAS in polar regions. Studies were excluded if they reported solely on PFAS in temperate or tropical environments and were not relevant to cold-environment dynamics, or if data quality was insufficient for meaningful synthesis.

Data Extraction and Synthesis

Thereby, data in Article I were extracted from eligible studies and compiled into structured summary tables. Concentration data extracted for the figures of Article I were digitized and organized by cryosphere compartment (snow, glacier, seawater, and sediment) and geographic location, allowing visual comparison of PFAS burden across diverse polar and mountain environments. The number of PFAS compounds analyzed in each study was encoded to reflect the scope of chemical profiling at each sampling location (Article I).

Thematic Organization

The synthesized literature was organized thematically to address: (1) PFAS chemical nature and physicochemical properties; (2) phase behavior and transformation pathways; (3) transport and distribution mechanisms, including atmospheric, oceanic, and cryospheric vectors; (4) bioaccumulation and biomagnification across trophic levels; (5) regulatory history and phase-out trajectories; and (6) microbial degradation and bioremediation prospects. Transformation and degradation pathways were also synthesized into schematic diagrams to illustrate key reaction mechanisms and environmental processes that affect PFAS fate in cold environments (Article I).

3.2 Setting Up the Stage

Diatom Culture Conditions

Two xenic marine diatom species representing contrasting ecological habitats were selected for this study: *Cylindrotheca clostrium* and the pelagic species *Thalassiosira pseudonana. C. closterium* was isolated from Arctic marine samples collected in Svalbard (from sediment samples), whereas *T. pseudonana* (strain DCG 0682) was obtained from the Belgian Coordinated Collections of Microorganisms (BCCM/DCG, Ghent University, Belgium) through the BioPol Marine Biotechnology Centre.

Cultures were maintained in 2 L Erlenmeyer flasks containing artificial seawater prepared from distilled water and commercial sea salt (35 g L^{-1}; Tropic Marin Bio-Actif). The medium was enriched with f/2 nutrients according to Guillard, 1975 adjusted to a salinity of 30 and pH 8.0. All cultures were grown under controlled laboratory conditions at 16 ± 0.5 °C with a 12 h light:12 h dark photoperiod and a light intensity of approximately 100 μmol photons m^{-2} s^{-1}.

3.3 PFAS Exposure and Physiological Assessment (Article II)

The effects of PFAS on marine diatoms were investigated using both short-term and long-term exposure experiments. The short-term experiment was designed to evaluate physiological and biochemical responses during the exponential growth phase, whereas the long-term experiment assessed the effects of prolonged exposure to environmentally relevant PFAS concentrations and the potential for acclimation over time. Both species were first exposed to eight types of long-chain PFAS and a replacement compound at three broader environmental concentrations, 100 mg/L, 1 mg/L, and 0.9 ng/L, for 10 days to capture short-term responses across a gradient from relatively high to ultra-low levels **(Figure 4)**. The details of PFAS used, and their chemical properties and applications are shown in Table 2.

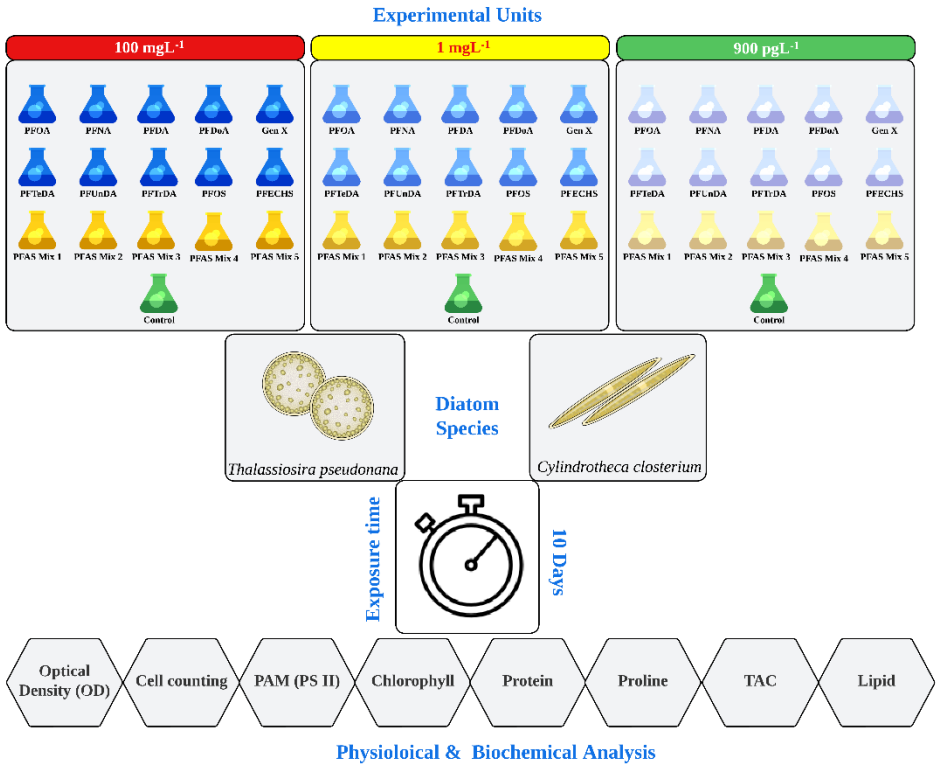

Figure 4: *Experimental design of the short-term PFAS exposure study.*

Two marine diatom species, *Thalassiosira pseudonana* and *Cylindrotheca closterium*, were exposed for 10 days to ten individual PFAS compounds (PFOA, PFNA, PFDA, PFDoA, PFUnDA, PFTrDA, PFTeDA, PFOS, GenX, and PFECHS) and five PFAS mixtures (Mix 1–Mix 5) at three concentrations (100 mg L^{-1}, 1 mg L^{-1}, and 0.9 ng L^{-1}), alongside untreated controls. Physiological and biochemical endpoints measured included optical density, cell density, photosynthetic efficiency (Fv/Fm), chlorophyll, protein, proline, total antioxidant capacity, and lipid content

These selected PFAS concentrations were selected to encompass environmentally relevant background exposure levels as well as highly contaminated scenarios reported in aquatic systems. Elevated PFAS concentrations are frequently associated with point-source environments such as landfill leachates, wastewater discharge outlets, and firefighting training areas, where concentrations can reach mg/L levels (Ahrens et al., 2011; X. C. Hu et al., 2016; Sabba et al., 2025; Tolaymat et al., 2023). In a study on the ultrasonic remediation of AFFF-derived wastewater (FC-600), (Vecitis et al., 2010) measured substantial PFAS concentrations, particularly PFOS (3,650 ± 710 mg/L). Furthermore, concentrations within this range have been used in experimental PFAS toxicity studies on microalgae and diatoms without causing immediate lethality, thereby enabling assessment of sublethal physiological and molecular responses s (Latała

et al., 2009). Further, algal studies have similarly reported physiological and oxidative stress responses at mg/L concentrations of PFOS and PFOA (Liao, Huang, et al., 2025a; W. Liu et al., 2008a; X. Liu et al., 2022).
Arctic environments, including drinking water sources and biota samples, showed concentrations ranging from ng to pg per liter (Grung et al., 2024; Sabba et al., 2025). Consequently, the 0.9 ng/L treatment was included to determine whether environmentally realistic PFAS burdens, already present in current marine systems, are sufficient to elicit detectable physiological or metabolic responses in diatoms, even when far below conventional toxicity thresholds.

Table 2: *Overview of the PFAS compounds used in this study.*

Name	Structure & molecular weight (MW)	Products	Reference
Perfluorooctanoic acid (PFOA) $C_7F_{15}COOH$	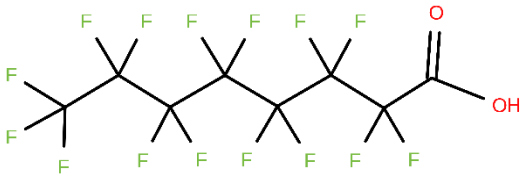 MW: 414.07	carpets, water proof textiles, food packaging, Flame retardants, Gore-Tex and Teflon	(Louisse et al., 2020; Mojiri, Zhou, et al., 2023)
Perfluorononanoic acid (PFNA) $C_8F_{17}COOH$	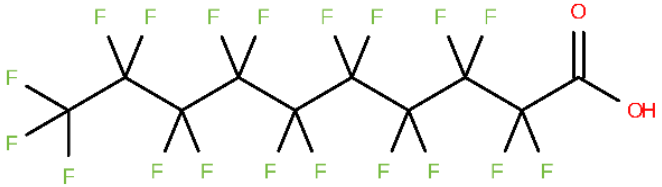 MW: 464.08	Surfactants, fluoropolymer processing, AFFF	(US EPA, 2022)
Perfluorodecanoic acid (PFDA) $C_9F_{19}COOH$	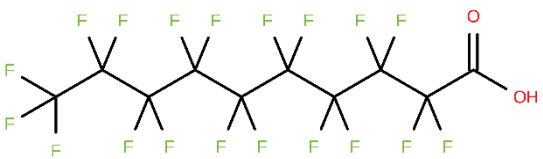 MW: 564.09	Stain and grease-proof coatings on food packaging, Ski wax, cosmetics	(Ivantsova et al., 2025; NTP et al., 2022)

Perfluorododecanoic acid (PFDoA) $C_{11}F_{19}COOH$	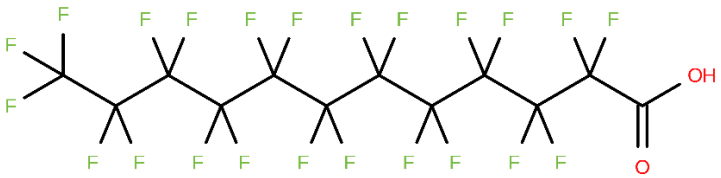 MW:614.1	Food packaging materials, firefighters	(OECD, 2022)
Hexafluoropropylene oxide dimer acid (GenX) $C_3F_7OCF(CF_3)COOH$	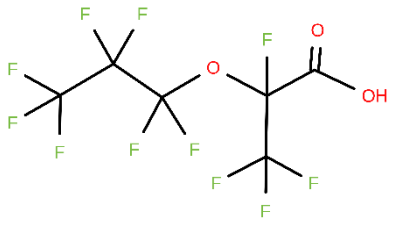 MW: 330.05	PTFE/Fluoropolymer polymerization aid (PFOA replacement)	(OECD, 2022)
Perfluorotetradecanoic acid (PFTeDA) $C_{13}F_{27}COOH$	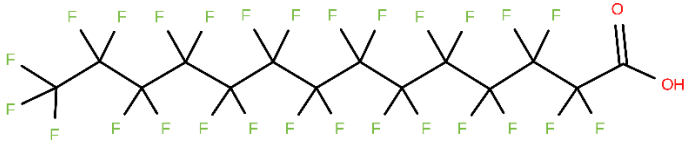 MW: 714.11	Firefighting foams, detergents, photographic films, food containers	(Chiesa et al., 2018)

Perfluorotridecanoic acid (PFTrDA) $C_{12}F_{25}COOH$	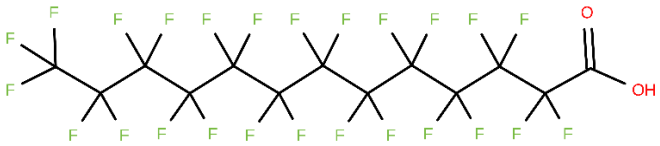 MW: 664.10	Food packaging, fluorinated surface treatments	(OECD, 2022)
Perfluoroundecanoic acid (PFUnDA) $C_9F_{19}COOH$	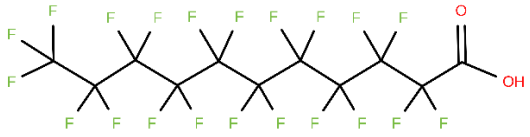 MW: 514.08	Breakdown product of stain/grease proof coatings on food food packaging product	(Ivantsova et al., 2025)
Perfluorooctanesulfonic acid (PFOs) $C_8HF_{17}O_3S$	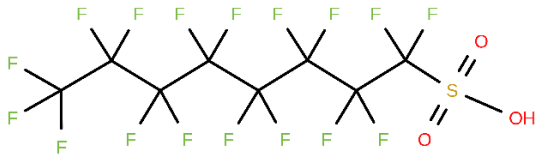 MW: 500.13	AFFF foams, semiconductors, photolithography	(Gaines, 2023)
Potassium perfluoro-4-ethylcyclohexane sulfonate (PFECHS) $C_8F_{15}KO_3S$	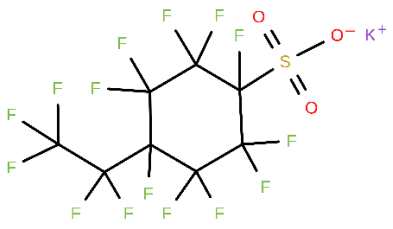 MW: 500.22	Aircraft hydraulic fluid erosion inhibitor (PFOS replacement)	(Stefanac et al., 2018)

3.3.1 Measures of Key Physiological Traits

Following PFAS exposures, key physiological traits were measured, including growth, photosystem II activity, total antioxidant capacity (TAC), total protein content, crude lipid content, and chlorophyll concentration, providing an integrated view of photosynthetic performance, oxidative stress, and cellular resource allocation (Article II, materials and methods section). These physiological endpoints were selected on the basis of OECD 201 guideline (Moorthy et al., 2022; OECD, 2011), pollutant-induced stress in phytoplankton manifests simultaneously across multiple cellular systems, and no single parameter adequately captures the full scope of toxicological impact.

Growth rate is the most ecologically integrative endpoint, as it reflects the cumulative effects of all cellular processes on the net biomass accumulation. In ecotoxicology, growth inhibition is a standardized regulatory endpoint as per OECD 201, and provides a direct measure of population-level changes (OECD, 2011).

Photosystem II maximum quantum efficiency (Fv/Fm) is a non-invasive, highly sensitive fluorometric indicator of photosynthetic capacity and PSII integrity (Maxwell & Johnson, 2000). It is useful because it detects photosynthetic stress before it shows as a visible growth effect, thereby serving as an early-warning molecular proxy of photosystem damage. High concentrations of PFAS have been reported to inhibit chlorophyll synthesis and destroy the cell structure, with PFAS exposure leading to the accumulation of reactive oxygen species, inducing lipid peroxidation and oxidative damage (Z. Liu et al., 2025; Shi et al., 2024). Since primary photosynthesis is both the energy foundation for all downstream biosynthetic activity and a key ecosystem service provided by marine diatoms, any impairment in Fv/Fm signals disruption of the entire cellular energy budget and has cascading implications for carbon fixation and trophic energy transfer.

Proline concentration was measured as an indicator of cellular stress acclimation and metabolic adjustment. Proline is a multifunctional amino acid that accumulates in many microalgae and plants under environmental stress conditions, where it acts as a compatible osmolyte, ROS scavenger, membrane stabilizer, and reservoir of carbon and nitrogen (Szabados & Savouré, 2010) . In diatoms, enhanced proline synthesis is often associated with oxidative stress and metabolic reprogramming, reflecting a shift from growth-oriented metabolism toward cellular protection and homeostasis.

Total antioxidant capacity (TAC) was measured as an integrated indicator of the cell's oxidative stress defence status. PFAS compounds are known to induce reactive oxygen species (ROS) overproduction in microalgae, disrupting the redox balance and triggering antioxidant responses (Soares et al., 2025). Measuring TAC rather than individual antioxidant enzymes (e.g., SOD, CAT, GPx separately) provides a holistic assessment of the total scavenging capacity of the cell, capturing the combined contribution of both enzymatic and non-enzymatic defences (Silvestrini et al., 2023). This is particularly informative when comparing two phylogenetically distant diatom species, which may employ different antioxidant strategies in response to the same stressor.

Total protein content was used as a proxy for cellular nitrogen metabolism, biosynthetic capacity, and nutritional status, since proteins represent the major nitrogen-containing macromolecular fraction in microalgal biomass and largely determine their nutritional value. Protein biosynthesis and turnover are energetically expensive processes tightly coupled to carbon and nitrogen assimilation; consequently, changes in total protein under stress reflect metabolic reallocation between growth and stress responses (McCain et al., 2021). PFAS exposure has been shown to alter the growth dynamics and physiological performance of microalgae (James et al., 2026; Liao, Lu, et al., 2025). Hence, PFAS-induced shifts in total protein content provide a sensitive and discriminatory endpoint to distinguish compound-specific effects of individual PFAS and their mixture

Crude lipid content was included because lipids occupy a central position in diatom stress physiology, serving as both primary energy reserves and structural components of membranes. Long-chain PFAS are known to interact with lipid bilayers and disrupt fatty acid metabolism, and the accumulation of neutral lipids, particularly triacylglycerols, is a well-characterized stress response in diatoms under nutrient or chemical stress (Levitan et al., 2015). Long-chain PFDA induced the highest lipid accumulation along with the lowest protein content, indicating compound-specific disruption of macromolecular resource allocation in microalgae (James et al., 2026). Measuring bulk lipid content, therefore, directly links to the metabolomic findings on fatty acid metabolism and phospholipid remodeling observed in the targeted endometabolome analysis.

Chlorophyll *a* concentration provides an independent, quantitative measure of photosynthetic pigment content, complementing Fv/Fm by quantifying the absolute pigment pool rather than just its functional efficiency. Changes in chlorophyll *a* can reflect photoinhibition, pigment degradation, or altered thylakoid membrane integrity. Importantly, the appearance of pheophytin *a,* chlorophyll degradation product detected in the metabolomic analysis, would be

preceded and accompanied by a measurable decline in intact chlorophyll *a*, providing cross-validation between the physiological and metabolomic dataset (H. Wu et al., 2025).

3.3.2 Long-term PFAS exposure

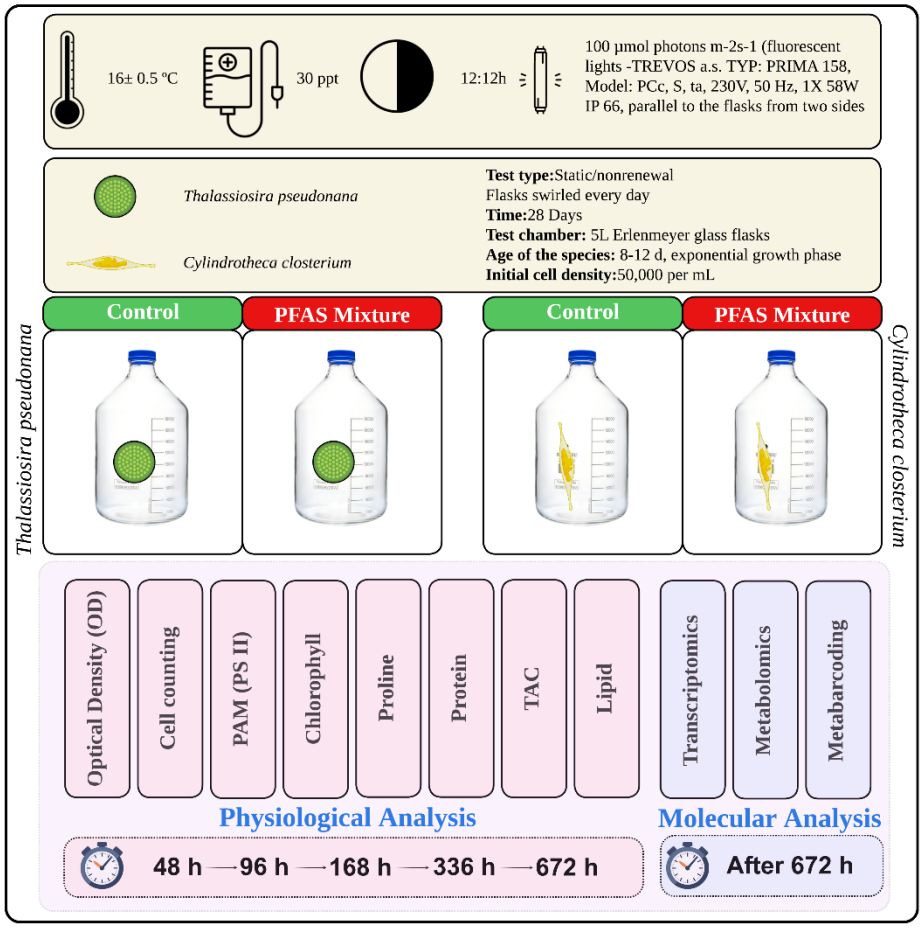

Figure 5*: Schematic overview of the 28-day chronic PFAS mixture exposure experiment.*

The marine *diatoms Thalassiosira pseudonana* and *Cylindrotheca closterium* were cultured in 5 L Erlenmeyer flasks and exposed for 28 days to a low-concentration PFAS mixture (900 pg L^{-1} per compound) under controlled laboratory conditions (16 ± 0.5 °C, salinity 30 ppt, 12:12 h light: dark photoperiod, and 100 µmol photons m^{-2} s^{-1} irradiance). Cultures were initiated at an approximate cell density of 5 × 10^4 cells mL^{-1} using exponentially growing inocula (8–12 days old) and maintained under static, non-renewal conditions with daily manual mixing. Physiological and biochemical responses, including optical density (OD), cell abundance, photosystem II maximum quantum efficiency (PAM fluorometry; Fv/Fm), chlorophyll, proline, protein, total antioxidant capacity (TAC), and lipid content, were monitored at 48, 96, 168, 336, and 672 h. Following 672 h of exposure, samples were harvested for integrative molecular analyses, including transcriptomics, metabolomics, and metabarcoding (From Supplementary Table M1: Article III).

Building on these results, five individual long-chain PFAS that elicited pronounced responses were selected along with a replacement compound, GenX, and combined into a mixture of each at 0.9 ng/L, which was then applied for 28 days to simulate chronic, low-level exposure more representative of environmental conditions (**Figure 5**). At the end of this long-term exposure, diatom physiological responses were assessed and complemented with molecular and biochemical analyses to capture changes in gene expression and metabolism.

Transcriptome sequencing was used to characterize global shifts in gene expression associated with PFAS exposure, while targeted endometabolomic analysis (**Figure 6**) provided insights into alterations in key metabolic pathways (Paper III, Supplementary Doc 1). In parallel, diatom-associated bacterial communities were profiled by amplicon sequencing targeting 16S rRNA V4 region (**Figure 7**) to determine how PFAS influence microbiome composition and the potential restructuring of diatom-bacteria symbioses. By integrating physiological, transcriptomic, metabolomic, and microbiome data, this work aims to provide a comprehensive and mechanistic understanding of how PFAS mixtures affect pelagic and benthic diatoms and their associated bacterial partners, and aims to situate these findings within broader questions about the stability and adaptability of marine biogeochemical processes in the Anthropocene epoch in oceans.

3.3.3 Metabolite Extraction and Analysis

Intracellular metabolites were extracted from wet diatom pellets using repeated cold 70% methanol washes, which effectively quench enzymatic activity upon cell disruption (**Figure 6**), thereby preserving the metabolic snapshot at the time of sampling. Samples were spiked with internal standards prior to drying to enable normalization and analytical quality control.

Metabolic profiling was performed using ultra-performance liquid chromatography coupled with quadrupole time-of-flight mass spectrometry (UPLC-qTOF-MS) operated in both positive and negative electrospray ionization modes. Hydrophilic interaction liquid chromatography (HILIC) separation was employed to improve retention and detection of polar intracellular metabolites.

Targeted metabolite annotation was performed by matching accurate mass and retention time to an in-house spectral library, with annotation confidence assigned in accordance with established metabolomics reporting guidelines. Differentially expressed metabolites were identified using fold-change and statistical significance thresholds through MetaboAnalyst 6.0.

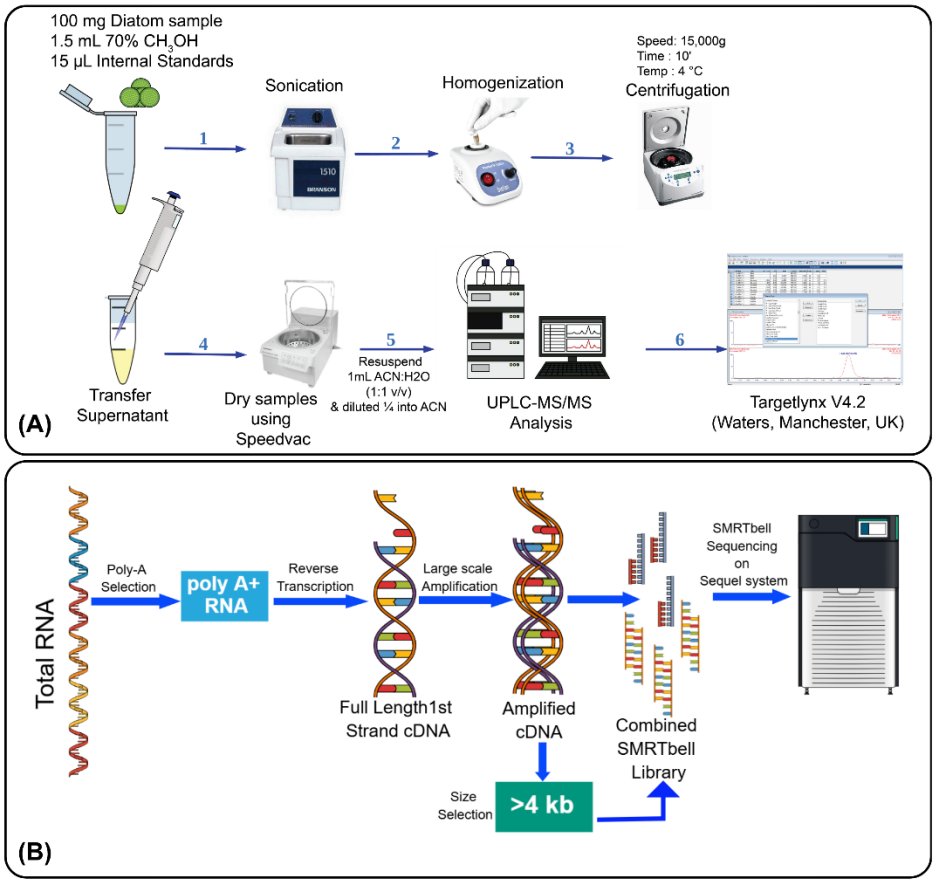

***Figure 6**: Overview of the targeted endometabolite analysis workflow. A) PacBio ISO sequencing process for the transcriptome analysis, B) detailed methods and sequence analysis described in Article III, supplementary sections.*

3.3.4 Metabolomic Profiling of Intracellular Metabolites in Response to PFAS Long-Term Exposure

A targeted endometabolomics approach was selected to enable sensitive, accurate, and reproducible quantification of intracellular metabolites associated with stress physiology, energy metabolism, membrane regulation, and antioxidant responses in diatoms exposed to PFAS. Since PFAS are known to interfere with cellular homeostasis, oxidative balance, and lipid metabolism, targeted metabolomics allowed focused investigation of biologically relevant metabolic pathways potentially involved in PFAS toxicity and adaptation. As the study plainly aimed to understand the responses and stress-related pathways rather than to conduct broad metabolite discovery, targeted endometabolomics was chosen over untargeted profiling. A targeted approach provides more reliable detection of low-abundance intracellular metabolites and minimizes false annotations, which is

especially important when working with marine diatoms, as their metabolomes are still not fully characterized in public databases.

Furthermore, the use of an in-house reference library of authenticated standards enabled accurate metabolite identification through retention-time and exact-mass matching, thereby increasing confidence in pathway-level interpretation. This approach was particularly suitable for detecting subtle metabolic perturbations induced by environmentally relevant concentrations of PFAS (10 ng/L).

3.3.5 Metabarcoding

Bacterial community profiling was conducted using amplicon sequencing of the V4 hypervariable region of the 16S rRNA gene, using the primer pair 515 F and 806R (Article IV) (**Figure 7**) and the standard adopted by the Earth Microbiome Project (EMP) for global marine microbiome characterization (Caporaso et al., 2023). In addition, within the V4-targeting primer options, the specific 515F/806R combination is the most extensively validated primer pair for marine bacterial communities; its adoption by the EMP also ensures direct comparability of the microbiome data generated in this study with the growing body of global marine microbiome datasets (Lee et al., 2023).

Besides, the V4 region (~253 bp amplicon) is appropriate for Illumina paired-end sequencing because it falls within the read length capacity of the MiSeq platform, enabling full amplicon coverage with substantial read overlap, thereby improving base-call accuracy and chimera detection (L. Lin & Ju, 2023). Comparative studies of primer pairs show that the 515F/806R combination recovers more ASVs and provides better resolution across taxonomic levels in bacterial communities, thereby yielding greater bacterial coverage than alternative primer sets (Ghyselinck et al., 2013). This is particularly important when characterizing the diverse and often understudied bacterial communities associated with marine diatom phycospheres, where taxonomic resolution at the genus and species level is needed to detect ecologically meaningful shifts in community composition under PFAS stress.

On the other side, the choice of Amplicon Sequence Variants (ASVs) rather than the traditional Operational Taxonomic Units (OTUs). OTUs are generated by clustering sequences sharing ≥97% similarity, a threshold that can arbitrarily group distinct bacterial species or strains into a single unit, masking ecologically and functionally relevant microbial diversity. Recent advances have made it possible to analyze high-throughput marker-gene sequencing data by resolving ASVs precisely, down to single-nucleotide differences across the sequenced gene region, with ASVs representing consistent labels with fundamental biological meaning that are identified independently of any reference database (Callahan et

al., 2017). This is a key advantage in ecotoxicological studies, where detecting subtle but ecologically meaningful shifts in closely related bacterial taxa, such as the gain or loss of a specific symbiont or opportunist, in response to PFAS exposure demands finer resolution than OTU-level clustering provides. ASVs identify sequence variations at the single-nucleotide level, allowing researchers to distinguish between microbial strains that differ by only a few bases, whereas OTUs might group several similar bacterial species; ASVs can separate them into distinct entities, revealing finer ecological patterns. Additionally, because ASVs represent exact, error-corrected biological sequences produced by denoising algorithms such as DADA2 (Callahan et al., 2016), they are fully reproducible and comparable across studies and datasets, a property that OTU-based analyses lack due to their dependence on arbitrary and variable clustering thresholds. This reproducibility is particularly important here, as it allows future studies of PFAS-affected diatom microbiomes to directly compare ASV profiles with those generated in this thesis.

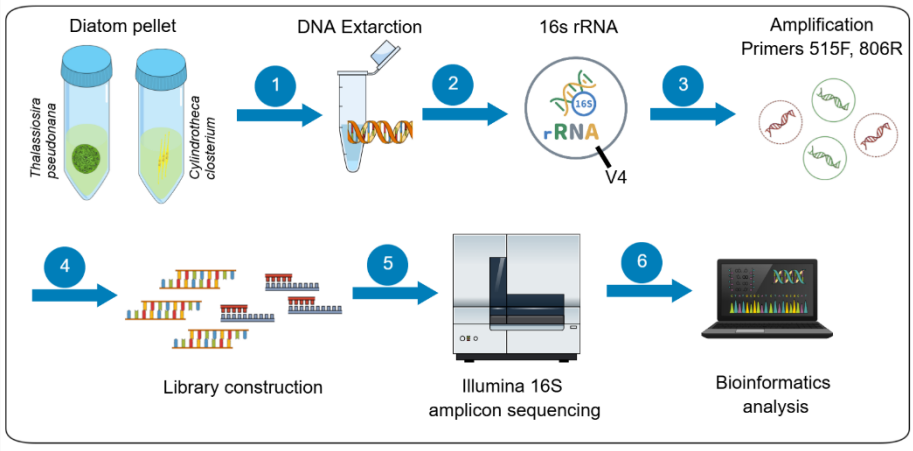

***Figure 7**: Workflow of DNA extraction and subsequent V4 region of 16S rRNA gene sequencing and analysis process.*

Note: The pathway diagram was created in https://BioRender.com

3.3.6 Integrative Multi-Omic Framework

The integration of physiological, transcriptomic, metabolomic, and microbiome data across two ecologically distinct diatom species and a gradient of PFAS concentrations and exposure durations was designed to provide a mechanistic, multi-level understanding of PFAS toxicity that no single analytical approach could achieve alone. Physiological endpoints capture the emergent, fitness-level consequences of PFAS exposure (Article II); transcriptomics reveals the genome-wide gene regulatory responses; metabolomics translates these transcriptional

signals into biochemical pathway activity (Article III, detailed transcriptomic methods and sequence analysis (page 112 -117) described along with the supplementary details in page 145-160); and microbiome profiling contextualises these responses within the broader microbial phycosphere associated with the diatom cell (Article IV). This framework places the observed molecular and cellular findings in the context of how PFAS contamination could impact the stability and resilience of marine biogeochemical processes that are driven by phytoplankton communities

4 Research Findings and General Discussion

The three main Articles (II-IV) comprising this thesis were designed to address a recognized knowledge gap concerning the effects of PFAS on marine diatoms- a taxonomic group that anchors polar marine food webs and contributes disproportionately to global carbon cycling (Falkowski, 2012; Hopkinson et al., 2011). Although ecotoxicology of PFAS has progressed significantly in freshwater and terrestrial environments, the effects of PFAS exposure on key marine primary producers, in the context of complex mixture scenarios and environmental concentrations found in Arctic and Sub-Arctic coastal systems, have remained largely unclear (Davis et al., 2024) (Article I). This thesis addresses that gap through a graduated experimental framework, short-term physiological toxicity assessment across ten individual PFAS and five mixtures at three concentrations (Article II); an integrated transcriptomic metabolomic investigation of this chronic molecular acclamation at environmentally relevant mixture concentration; (Article III); and a 16S rRNA amplicon-based characterization of how the same chronic exposure restructures the diatoms' phycosphere-associated bacterial microbiome (Article IV). Together, these three lab experiments and the literature studies provide insights in multi-scale portrait of PFAS toxicity from the cellular to the community level, using two ecologically contrasting model diatoms, the benthic *Cylindrotheca clsoterium* and the pelagic *Thalassiosira pseudonana*.

4.1 Establishing the Environmental Case for Studying PFAS-Diatom Interactions (Article I)

The review Article that opens this thesis (Article I: (Arulananthan et al., 2025) constructed the environmental and scientific rationale upon which the three experimental investigations were built. By synthesizing the physical, chemical, and biological dimensions of PFAS contamination across cryosphere compartments, it established that a critical knowledge gap existed at the base of the Arctic food web and that closing it required the organism-specific, multi-scale experimental approach that Articles II–IV subsequently presented in the following sections (**Figure 8**).

Persistent Exposure and the Experimental Design Rationale

Article I demonstrated that PFAS contamination of the Arctic cryosphere is structurally sustained rather than episodic. The convergence of long-range atmospheric deposition of volatile precursors, oceanic advection of long-chain legacy compounds through the Fram Strait, sea ice concentration and seasonal melt-pulse dynamics, and permafrost thaw releasing historically deposited contamination collectively indicates chronic multi-compound exposure for Arctic

marine organisms regardless of proximity to emission sources (Garnett, Halsall, Vader, et al., 2021; Hartz et al., 2023a; Joerss et al., 2020; MacInnis et al., 2022). This environmental reality directly justified the long-term, mixture-based, environmentally relevant exposure design of Articles II–IV, a departure from the dominant paradigm of acute, single-compound, high-concentration laboratory exposures that characterised most prior algal PFAS research. Article I also described that GenX (HFPO-DA) is already detectable in Arctic surface waters and that regulatory phase-out of legacy compounds has accelerated environmental loading of replacement compounds with similarly concerning ecological hazard profiles, the so-called,‘‘regrettable substitution problem (Guo et al., 2024; Hamid et al., 2024; Joerss et al., 2020). This is one of the reasons for testing GenX alongside PFOS and long-chain PFCAs in the experimental mixture used throughout this thesis.

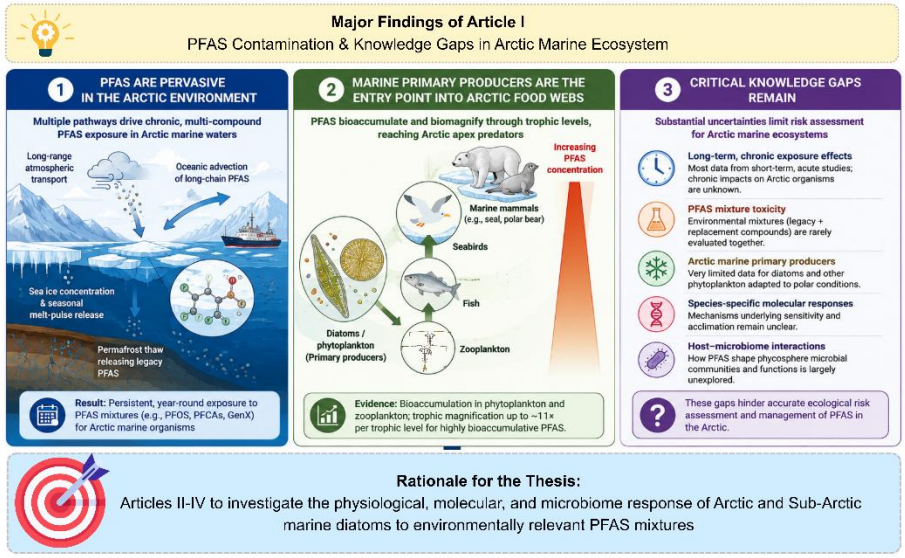

Figure 8*: Major findings of Article I and their role in shaping the experimental framework of this thesis.*

The review identified three key conclusions regarding PFAS contamination in Arctic marine ecosystems. First, PFAS contamination is pervasive and sustained in the Arctic through multiple pathways, including long-range atmospheric transport, oceanic advection, sea-ice accumulation and seasonal melt release, and permafrost thaw, resulting in chronic exposure of marine organisms to complex PFAS mixtures. Second, marine diatoms and other phytoplankton serve as the primary entry point for PFAS into Arctic food webs, facilitating bioaccumulation and trophic transfer to higher consumers, including fish, seabirds, and marine mammals. Third, significant knowledge gaps remain regarding the long-term effects of environmentally relevant PFAS mixtures on Arctic marine primary producers, species-specific physiological and molecular responses, and the role of host-associated microbiomes in contaminant tolerance and ecosystem functioning. Collectively, these knowledge gaps provided the scientific rationale for Articles II–IV.
Note. Graphical design (elements) assisted by ChatGPT plus 5.5 (OpenAI, 2026) using author-provided scientific content and prompt; reviewed by the author for accuracy.

4.1.1 Bioaccumulation Chain: Positioning Diatoms Within the Arctic Marine Food Web

A critical contribution of Article I was to embeded the diatom studies within a food-web context, thereby extending their ecological significance far beyond the organisms themselves. The review synthesized evidence that PFAS concentrations increase systematically from seawater through phytoplankton and zooplankton to fish, seabirds, and marine mammals, with trophic magnification factors reported up to eleven per trophic level for the most bioaccumulative congeners (Kelly et al., 2009; Ricolfi et al., 2025). Both phytoplankton and zooplankton readily accumulate PFAS from seawater (Casal, González-Gaya, et al., 2017; X. Zhang et al., 2019), confirming that bioavailability at the primary producer level is the entry point for a contamination cascade whose endpoints extending to various systems, such as reproductive failure, hormonal disruption, and immunosuppression in Arctic apex predators (Ask et al., 2021; Dietz et al., 2019; Jouanneau et al., 2023), are already documented. This framing turns sublethal physiological and molecular impairments from Articles II–IV into ecologically impactful events that affect the food web, highlighting why understanding diatom responses to PFAS is important.

4.1.2 Bioremediation Perspective and Connection to the Phycosphere Findings

Article I further reviewed the potential of polar microbial communities for PFAS bioremediation, identifying Sphingomonadales and Planctomycetota as lineages with structural or metabolic features potentially conferring tolerance to organofluorine compounds, while acknowledging that complete biological mineralization of perfluorinated chains under natural conditions remains unachieved (Huang et al., 2024; Jin et al., 2023; J. Wu et al., 2022). This assessment showed its worth by predicting what would happen. In Article IV, and in the phycosphere investigation of this thesis tried to identify those groups and more on, Sphingomonadales (Parasphingorhabdus) and SM1A02 (Planctomycetota), across both host diatom species under PFAS exposure. The convergence between candidate taxa identified in the literature in Article I and those empirically selected under PFAS pressure in Article IV strengthens the biological plausibility of both the review's predictions and the experimental community ecology findings, and positions the phycosphere as a relevant natural context for investigating microbial PFAS tolerance and potential biotransformation.

4.1.3 Regulatory Context and the Evidence Gap

Article I synthesized information from the Stockholm Convention, REACH restriction proposals, the US EPA PFAS Strategic Roadmap, and Arctic Council

assessments, highlighting important knowledge gaps regarding the ecological effects of PFAS in Arctic marine environments. In particular, much of the ecotoxicological information currently available for PFAS risk assessment is derived from acute studies on temperate freshwater organisms, whereas chronic effects on Arctic marine primary producers remain comparatively understudied.

Against this background, Articles II–IV investigated the physiological, molecular, and microbiome responses of marine diatoms exposed to environmentally relevant PFAS concentrations. Although these studies do not provide the breadth of evidence required for regulatory decision-making, they contribute new data on selected PFAS compounds and mixtures in ecologically relevant marine microorganisms. Collectively, these findings help address some of the knowledge gaps identified in Article I and provide a foundation for future research to improve understanding of PFAS impacts in Arctic marine ecosystems. In this way, Article I provided a scientific rationale for subsequent experimental studies by identifying key areas where additional ecotoxicological information was needed.

4.2 PFAS as a Multi-Scale Stressor: A Graduated and Sustained Disruption (Article II)

One of the most important overarching findings of this thesis is that PFAS interfere with diatom biology across multiple levels. This disruption ranges from rapid biochemical changes detectable within days to extensive molecular reprogramming unfolding over weeks to selective restructuring of the host-associated microbial community. This graduated, multi-scale disruption calls into question the adequacy of any single-endpoint, single-timepoint assessment for characterizing PFAS risk to marine primary producers.

Short-term exposure revealed that PFAS impair the most fundamental aspects of diatom physiology with high sensitivity: photosynthetic efficiency (PSII) declined before growth inhibition became manifest, indicating that energy capture is compromised before cellular multiplication is visibly affected (Article II). Thus, a major early response was the reduction in photosystem II (PSII) photochemical efficiency (Fv/Fm), indicating impairment of photosynthetic machinery (**Figure 9**). Decreased Fv/Fm is widely recognized as one of the most sensitive indicators of environmental stress in phytoplankton because it reflects damage to PSII reaction centers before visible growth inhibition occurs. The observed decline suggests that PFAS interfered with electron transport processes and energy conversion efficiency, likely through interactions with membrane-associated photosynthetic complexes. Similar PFAS-induced reductions in photosynthetic performance have been reported in marine and freshwater microalgae, where PFAS exposure altered chloroplast structure, disrupted pigment composition, and

impaired electron transport chains (James et al., 2026; Y. Li et al., 2021; W. Mao et al., 2023). This sequence, photosynthetic dysfunction preceding growth inhibition, is consistent with a broader principle in phytoplankton ecotoxicology whereby sublethal stress is encoded in the energetic budget of the cell before it is expressed in demographic terms (van Kooten & Snel, 1990; Xue et al., 2022).

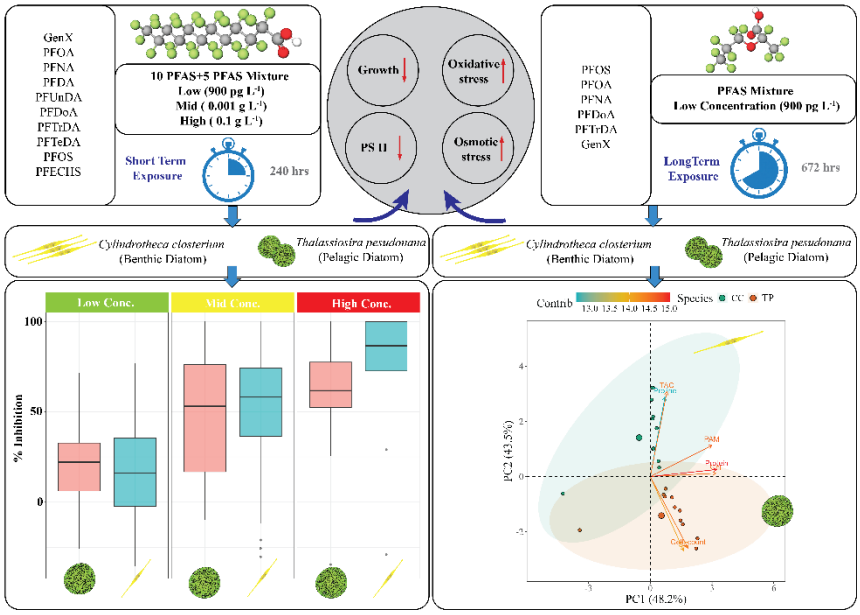

***Figure 9**: Summary of short- and long-term physiological responses of marine diatoms to PFAS exposure.*

During short-term exposure (240 h), PFAS mixtures caused concentration-dependent inhibition of growth in both the benthic diatom Cylindrotheca closterium and the pelagic diatom Thalassiosira pseudonana, with toxicity increasing from low to high concentrations. In contrast, long-term exposure (672 h) to an environmentally relevant PFAS mixture (900 ng L^{-1}) triggered species-specific physiological reorganization involving growth, photosynthetic performance, oxidative stress, and osmotic regulation, suggesting adaptive acclimation mechanisms under chronic PFAS stress.

The early activation of proline biosynthesis and antioxidant defense systems, observed across all compounds and species in short-term exposure, further confirmed that oxidative and osmotic stress represent the first lines of PFAS disruption, a conclusion corroborated by numerous studies where algae exposed to individual long-chain PFAS (Y. Li et al., 2021; Liao, Huang, et al., 2025a; X. Liu et al., 2022), but demonstrated here under a mixture of both long-chain and short-chain PFAS compounds, including the replacement compound at environmentally Arctic-relevant concentrations in cold-adapted marine diatoms.

Elevated proline concentrations and increased total antioxidant capacity (TAC) were observed in both species (**Figure 9**), demonstrating activation of osmoprotective and antioxidant defense systems. Proline accumulation is commonly associated with oxidative and osmotic stress and functions as both a reactive oxygen species (ROS) scavenger and a compatible solute (Szabados & Savouré, 2010) . Similarly, increased TAC further indicates activation of cellular antioxidant networks to counteract ROS generated during PFAS exposure (Article II). Oxidative stress has been repeatedly identified as a key mechanism of PFAS toxicity across a range of organisms, including algae (C. Hu et al., 2014; Koletti et al., 2025; Liao, Lu, et al., 2025; Z. Liu et al., 2025; Zhao et al., 2023, 2024). Therefore, the coordinated increase in proline and TAC observed here suggests that oxidative stress is an important component of the cellular response of marine diatoms to chronic PFAS exposure.

This multi-scale pattern carries an important methodological implication: growth rate, the standard endpoint in regulatory algal toxicity testing (OECD, 2011). It is demonstrably inadequate for characterizing chronic, sub-lethal PFAS risk in marine diatoms. Corresponding disputes between growth normalization and persistent molecular disruption have been reported under other persistent organic pollutants (Y. Mao et al., 2024).

Concentration-dependent physiological changes were clearly observed with the mixtures, which often exerted greater impacts than individual compounds, indicating additive or synergistic interactions among PFAS constituents (**Figure 9**) (Article II). These findings are consistent with previous studies demonstrating that PFAS mixtures frequently produce stronger biological effects than single compounds because organisms experience simultaneous disruption of multiple cellular targets (Davis et al., 2024; Latała et al., 2009; Liao, Huang, et al., 2025a).

4.2.1 Mixture Complexity and Environmental Realism: A Persistent Signal

A consistent finding across all three articles (Article II-IV) was that PFAS mixture exposures produced stronger or qualitatively different biological responses than individual compound exposures at equivalent concentrations. In the short-term experiment, mixtures consistently exceeded the inhibitory effects of their component compounds, with evidence of both additive and synergistic interactions depending on the endpoint and species examined (Article II). This pattern is not unexpected from a mechanistic perspective: PFAS compounds with different chain lengths, functional groups, and physicochemical properties disrupt multiple cellular targets simultaneously, including membrane fluidity, protein binding, electron transport chains, and antioxidant systems, such that their

combined action on overlapping targets likely amplifies damage beyond what any single compound achieves alone (Dale et al., 2022; X. Liu et al., 2022).

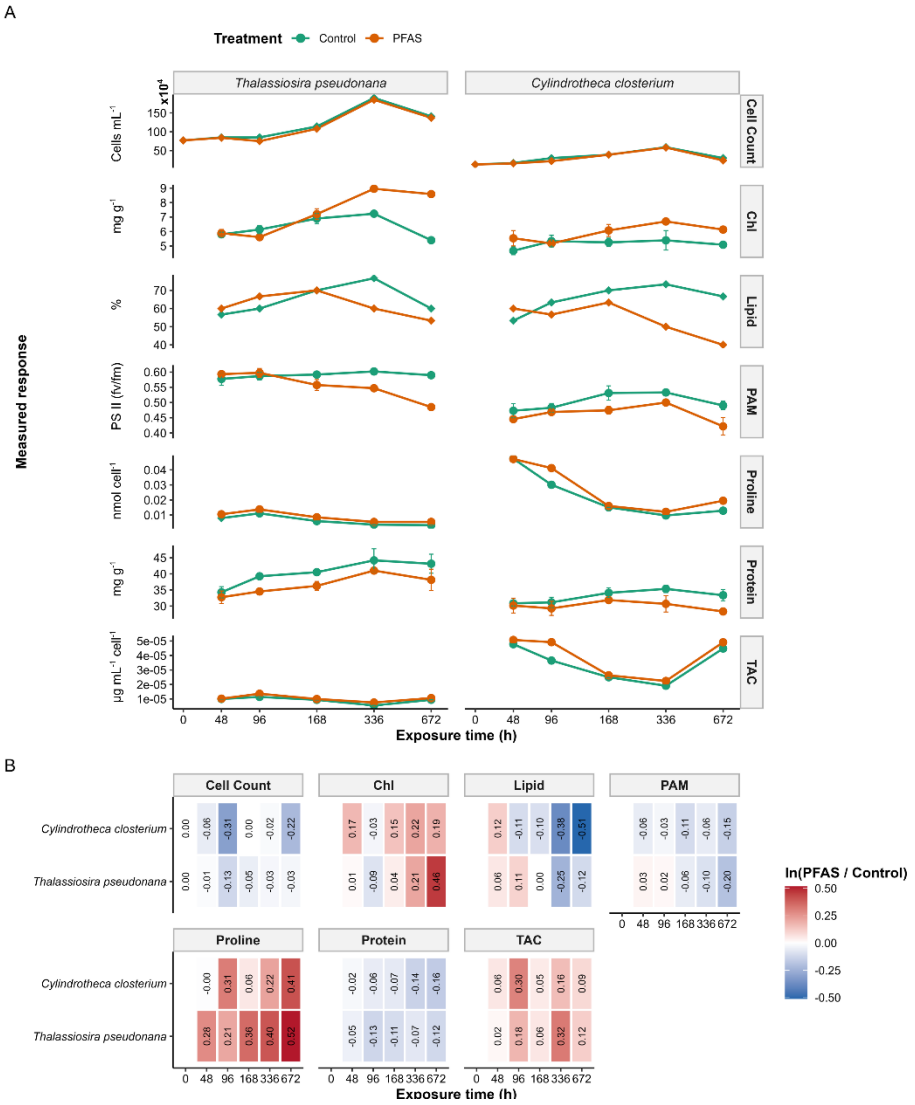

***Figure 10**: Long-term PFAS exposure responses in terms of diatoms' physiological changes.*

Temporal responses of *Thalassiosira pseudonana* and *Cylindrotheca closterium* exposed to a PFAS mixture (900 pg L^{-1}) over 28 days. (A) Changes in cell abundance, chlorophyll *a* (Chl), total lipid content, photosystem II efficiency (Fv/Fm; PAM), proline, protein, and total antioxidant capacity (TAC) were measured at 0, 48, 96, 168, 336, and 672 h under control and PFAS treatments. Values represent mean ± SD (n = 3). (B) Heatmap showing the natural logarithm of the PFAS-to-control response ratio [ln(PFAS/Control)] for each physiological and biochemical parameter across

exposure times, where positive values (red) indicate increases and negative values (blue) indicate decreases relative to the corresponding control (Article III, Supplementary Figure 5).

The mixture used in the long-term molecular experiments was selected in part on the basis of its weak short-term physiological signal, ensuring that the documented molecular responses in Articles III and IV reflect genuine chronic sublethal effects rather than overwhelming acute toxicity. Interestingly, despite significant physiological impairment during the exponential growth phase, the long-term experiment demonstrated that growth inhibition became less pronounced after approximately two weeks of exposure (**Figure 10**). This pattern suggests that while PFAS initially reduce cellular fitness, surviving populations can activate compensatory mechanisms that partially restore growth under prolonged exposure. Such responses are consistent with acclimation rather than complete recovery, because biochemical and molecular stress markers remained elevated despite normalized growth trajectories (**Figure 9**).

The fact that even this moderate-effect mixture elicited thousands of differentially expressed genes and pervasive metabolite reorganization in *T. pseudonana*, and restructured the phycosphere microbiome of both species, testifies to the biological potency of environmentally representative PFAS mixtures at concentrations actually encountered in Arctic surface waters and sea ice (Ali et al., 2021; Dai et al., 2025; Hartz et al., 2023a, 2024; MacInnis et al., 2022).

The mixture complexity issue has important regulatory implications that this thesis helps to understand. Current environmental risk assessments for PFAS predominantly rely on single-compound studies and fail to account for the synergistic or additive potency of the complex mixtures to which real organisms are exposed (Guo et al., 2024; H. Wu et al., 2025; J. Wu et al., 2022). The present findings support growing calls in the ecotoxicological literature for mixture-based regulation, the so-called "mixture assessment factor" approach advocated by the European Chemicals Agency (ECHA, 2024), and provide a mechanistic ground for why mixture toxicity consistently exceeds that of individual constituents in photosynthetic marine microorganisms.

Moreover, the inclusion of GenX (HFPO-DA) alongside legacy long-chain PFCAs and PFOS in the tested mixture ensured that the experimental design reflected the contemporary contamination reality in many marine environments, where regulatory pressure on legacy compounds has accelerated the transition to short-chain and ether-based replacements whose ecotoxicological profiles are far less characterized (Guo et al., 2024; Hamid et al., 2024; Joerss et al., 2020; Letcher et al., 2018; Munoz et al., 2019).

4.3 Species-Specific Vulnerability and Acclimation: Ecological Niche Shapes Molecular Resilience (Article III)

The most scientifically distinctive contribution of this thesis is the systematic, multi-level demonstration that *C. closterium* and *T. pseudonana* respond to identical PFAS conditions through fundamentally different molecular strategies (Article III). This divergence, observed consistently across physiological, metabolomic, transcriptomic, and microbiome levels, reflects deeper differences in cellular architecture, ecological niche, and evolutionary history that have practical implications for how PFAS risk is assessed and how diatom community composition may shift under contamination.

The benthic diatom *C. closterium* exhibited widespread depletion of metabolite pools. Amino acids, soluble sugars, nucleotides, osmolytes, and several cofactors were substantially reduced under PFAS exposure. Decreased concentrations of glucose, fructose, trehalose, nucleotide precursors, folate, riboflavin, carnitine, and acetyl-carnitine suggest impaired biosynthetic capacity, altered energy homeostasis, and disruption of one-carbon metabolism. Simultaneously, the accumulation of phosphocholine indicated membrane degradation and active recycling of membrane components (**Figure 11**).

Transcriptomic responses were comparatively modest, involving mainly upregulation of ABC transporters and alterations in the pentose phosphate pathway. ABC transporters are frequently associated with xenobiotic detoxification and membrane transport processes and likely represent an important defense mechanism against PFAS accumulation. Enhanced pentose phosphate pathway activity may help sustain NADPH production required for antioxidant regeneration and maintenance of redox homeostasis. Collectively, these responses indicate a conservative stress strategy in which cellular resources are conserved through metabolic downscaling, while detoxification and redox-protection mechanisms remain active.

In contrast, the pelagic diatom *T. pseudonana* displayed a far more dynamic response characterized by extensive transcriptional reprogramming and selective metabolite accumulation. *T. pseudonana* deployed an active, membrane-centered acclimation: coordinated photosystem repair, carbon flux rerouting toward NADPH generation via the pentose phosphate pathway, suppression of energetically costly external nitrogen assimilation in favor of internal recycling, extensive membrane lipid remodeling through peroxisomal β-oxidation, and broad secondary metabolite synthesis for ROS scavenging (**Figure 12**).

The breadth of this transcriptional response, spanning thousands of genes across more than a dozen functional categories, reflects high metabolic plasticity consistent with a pelagic lifestyle requiring rapid adjustment to fluctuating

conditions (Bowler et al., 2008; Falciatore & Mock, 2022). One of the most striking responses was the activation of photosystem repair machinery. Upregulation of PsbA, PsbO, Psb27, Psb28, fucoxanthin-chlorophyll proteins, and photoprotective LHCSR proteins indicates active replacement of damaged PSII components rather than photosynthetic shutdown (**Figure 12**). This contrasts with responses reported in several green algae where PFAS exposure causes broad suppression of photosynthetic genes (Y. Li et al., 2021; Z. Liu et al., 2025). Thus, *T. pseudonana* appears capable of maintaining energy production through continuous repair and restructuring of photosynthetic systems under chronic PFAS stress (Kim et al., 2023).

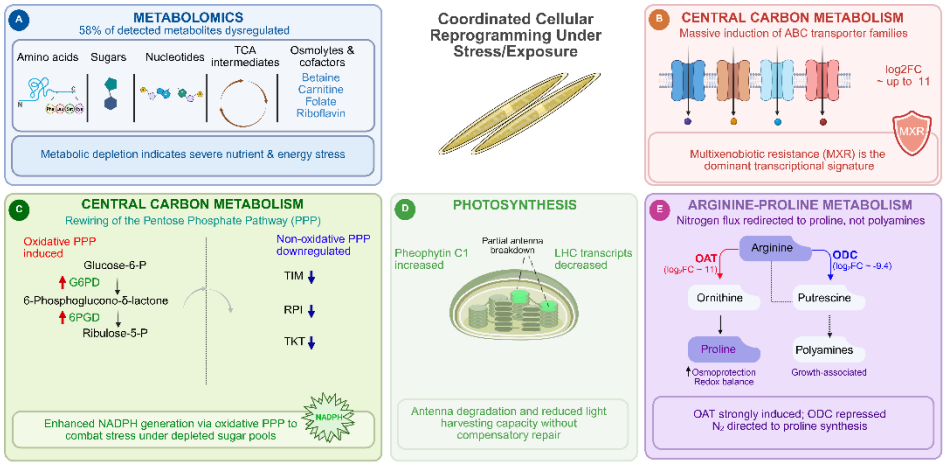

Figure 11: *Integrated metabolomic and transcriptomic model of PFAS-induced cellular reprogramming in Cylindrotheca closterium.*

Chronic PFAS exposure triggered coordinated metabolic and transcriptional responses characterized by (A) widespread depletion of metabolites involved in amino acid, sugar, nucleotide, TCA-cycle intermediate, and cofactor metabolism, indicative of nutrient and energy stress; (B) strong induction of ABC transporters and multidrug resistance-associated proteins (MXR), suggesting activation of xenobiotic defence mechanisms; (C) extensive rewiring of central carbon metabolism, including activation of the oxidative pentose phosphate pathway (PPP) to enhance NADPH production; (D) photosynthetic adjustments marked by increased pheophytin C1 accumulation and reduced light-harvesting complex (LHC) transcripts, consistent with antenna remodelling and compensatory repair; and (E) redirection of nitrogen metabolism towards proline biosynthesis through induction of ornithine aminotransferase (OAT) and repression of ornithine decarboxylase (ODC). Collectively, these responses indicate a shift from growth and biosynthesis towards stress tolerance, redox homeostasis, osmoprotection, and cellular defence under PFAS exposure. Abbreviations are in the Article III supplementary details, page 145. The pathway diagram was created in https://BioRender.com

Article III describes in detail how carbon metabolism was similarly reorganized. Strong induction of transketolase (TKT), pyruvate phosphate dikinase (PPDK), GAPDH, and related enzymes indicates rerouting of carbon

through the pentose phosphate pathway to maximize NADPH generation. The resulting reducing power supports antioxidant defense and biosynthetic repair processes. Although acetyl-CoA pools declined, suggesting a bottleneck in carbon utilization, enhanced carbon flux through glycolysis and PPP likely compensates by supplying energy and reducing equivalents for stress management.

Nitrogen metabolism underwent particularly extensive reprogramming. Near-complete repression of nitrate transporters, nitrate reductase, and nitrite reductase suggests suppression of external nitrogen acquisition (Article III). Concurrent upregulation of glutamate dehydrogenase, ornithine aminotransferase, cysteine biosynthesis pathways, and proline metabolism indicates a shift toward internal nitrogen recycling and conservation. This response resembles the molecular signature of nitrogen limitation and suggests that PFAS exposure induces a quasi-nitrogen stress state despite nutrient availability (**Figure 12**).

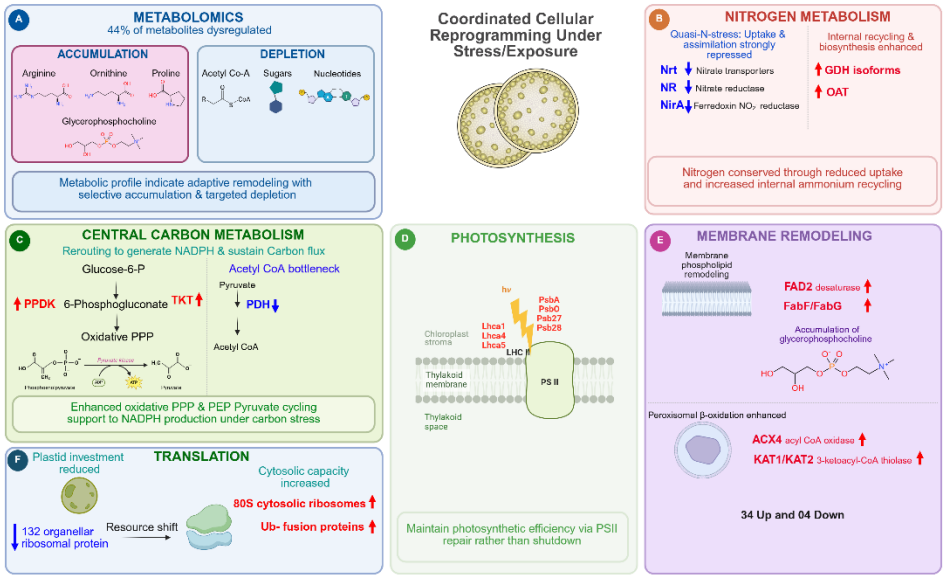

***Figure 12**: Integrated metabolomic and transcriptomic model of PFAS-induced cellular reprogramming in Thalassiosira pseudonana.*

(A) Metabolomic profiling revealed selective accumulation of compatible solutes and amino acids, including arginine, ornithine, proline, and glycerophosphocholine, alongside depletion of acetyl-CoA, sugars, and nucleotides, indicating adaptive metabolic remodeling. (B) Induced a quasi-nitrogen stress response characterized by repression of nitrate uptake and assimilation genes (Nrt, NR, and NirA) and concomitant upregulation of GDH isoforms and ornithine aminotransferase (OAT), promoting internal nitrogen recycling and amino acid biosynthesis. (C) Central carbon metabolism was reprogrammed through induction of pyruvate phosphate dikinase (PPDK) and transketolase (TKT), enhancing oxidative pentose phosphate pathway activity and phosphoenolpyruvate-pyruvate cycling to support NADPH generation, while pyruvate dehydrogenase (PDH) repression indicated an acetyl-CoA bottleneck. (D) Photosynthetic machinery remained functional through enhanced photosystem II (PSII) repair and maintenance, supported by increased expression of PSII core proteins and light-harvesting complex genes. (E) Membrane

homeostasis was preserved through phospholipid remodeling, glycerophosphocholine accumulation, induction of fatty acid desaturases (FAD2), elongation enzymes (FabF/FabG), and activation of peroxisomal β-oxidation pathways (ACX4, KAT1/KAT2). (F) Simultaneously, translation capacity shifted from plastids to the cytosol, as reflected by the repression of organellar ribosomal proteins and the induction of cytosolic 80S ribosomes and ubiquitin-fusion proteins. Collectively, these responses indicate that T. pseudonana maintains photosynthetic performance and cellular homeostasis under PFAS stress through coordinated metabolic rewiring, nitrogen conservation, membrane remodeling, and prioritization of cytosolic protein synthesis. The pathway diagram was created in https://BioRender.com

C. closterium pervasive depletion of central metabolite pools with a circumscribed transcriptional response centred on ABC transporter-mediated xenobiotic efflux, a conservative, transporter-based defence strategy (**Figure 11**) more consistent with benthic life in EPS-rich, chemically buffered sediment environments (Lauritano et al., 2015). While this more limited reprogramming may reflect genuine biological conservatism in a benthic species adapted to the relative physicochemical stability of sediment-surface environments, it may also partially reflect the less complete genome annotation available for *C. closterium* relative to the fully sequenced *T. pseudonana* genome, a methodological caveat acknowledged in Article III.

These contrasting strategies have a coherent evolutionary logic. Benthic diatoms such as *C. closterium* survive in microenvironments enriched in organic matter and biofilm matrices where EPS-mediated buffering of chemical stress and multixenobiotic resistance transporters represent well-established defenses (Lauritano et al., 2015; Vingiani et al., 2022). Pelagic diatoms such as *T. pseudonana*, by contrast, cannot rely on biofilm chemistry or sediment organic matter to buffer pollutant bioavailability; instead, they must mount intracellular responses capable of managing PFAS that readily partition into their lipid membranes (Fitzgerald et al., 2018). The activation of peroxisomal β-oxidation and fatty acid desaturation pathways in *T. pseudonana*, the "membrane remodeling" hallmark of its PFAS response, directly addresses the surfactant-like membrane disruption that PFAS impose, replacing peroxidized polyunsaturated fatty acids with newly synthesized membrane lipids to restore bilayer integrity and photosynthetic functionality (Li-Beisson et al., 2019; Vasilev et al., 2022). That *C. closterium* instead accumulated phosphocholine, a degradation product of membrane phospholipids, while *T. pseudonana* accumulated glycerophosphocholine, a membrane-repair precursor, encapsulates the fundamental contrast in a single metabolic biomarker pair: one species is losing membrane integrity while the other is repairing it (Article III), (**Figure 12**).

The broader significance of this species divergence extends beyond the two organisms studied. Marine diatom communities are taxonomically diverse, spanning thousands of species with vastly different ecophysiological traits, and the assumption that a single model organism can represent this diversity in risk assessments is clearly untenable (Debenest et al., 2013). My thesis provides direct

experimental evidence that the direction and magnitude of PFAS responses depend on species-level traits in ways that cannot be predicted from physicochemical properties of the compounds alone. This has practical implications: standard algal ecotoxicity testing protocols (OECD, 2011), rely on single freshwater green algae (Raphidocelis subcapitata, Chlorella spp.) under short-term acute exposure conditions that are poorly representative of the diversity, exposure duration, and contamination complexity encountered by Arctic marine diatom communities. Regulatory risk assessments based on such data will systematically underestimate the vulnerability of some ecologically critical species while overestimating that of others.

4.4 Phycosphere:An Overlooked Risk Dimension (Article IV)

The phycosphere investigation introduced a biological dimension largely absent from current PFAS risk assessment frameworks: indirect contamination effects mediated through disruption of the diatom's associated bacterial community (**Figure 13**). This dimension is not merely an ecological curiosity; it directly bears on the fitness of the host diatom and on the biogeochemical functioning of diatom-dominated systems.

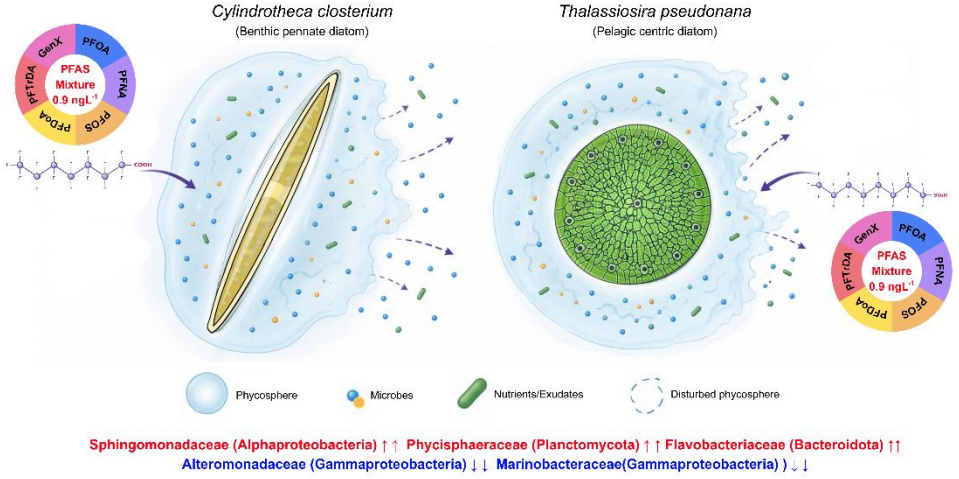

***Figure 13**: Conceptual illustration of PFAS-induced restructuring of diatom-associated microbial communities in the phycosphere.*

Exposure to an environmentally relevant PFAS mixture (0.9 ng L^{-1}; PFOA, PFNA, PFDA, PFTrDA, PFOS, and GenX) altered bacterial communities inhabiting the diatom phycosphere. In *C. closterium*, PFAS exposure was associated with increased relative abundances of Sphingomonadaceae (Alphaproteobacteria) and Physisphaeraceae (Planctomycetota), whereas in the *T. pseudonana*, Flavobacteriaceae (Bacteroidota) increased markedly.
Note. Graphical design (elements) assisted by ChatGPT plus 5.5 (OpenAI, 2026) using author-provided scientific content and prompt; reviewed by the author for accuracy.

The phycosphere bacteria of marine diatoms supply essential growth factors, including vitamin B_{12}, iron-chelating compounds, and amino acids; in return, they depend on diatom-derived dissolved organic matter and EPS for carbon and energy (Amin et al., 2015b; Daly et al., 2023; Seymour et al., 2017). Disruption of this mutualism, even without direct killing of the host, may reduce diatom fitness and alter organic matter cycling in ways invisible to standard toxicity endpoints.

A central finding of Article IV was that host diatom species identity, rather than PFAS exposure per se, was the primary determinant of phycosphere community structure. This result is consistent with the broader phycosphere literature demonstrating that host-derived exudate chemistry, the unique cocktail of polysaccharides, organic acids, vitamins, and signaling compounds released by each diatom species, acts as a chemical template for bacterial community assembly (Grossart et al., 2005; Johansson et al., 2019).

However, PFAS exposure selectively restructured this template-defined community by enriching PFAS-tolerant taxa and depleting PFAS-sensitive ones, particularly from the *T. pseudonana* phycosphere, where copiotrophic Gammaproteobacteria suffered disproportionate losses (**Figure 14**). The interpretation that this depletion was partially mediated by PFAS-induced modification of host exudate chemistry, specifically the disruption of sulfonated metabolite release that *T. pseudonana* normally uses to recruit specialist Gammaproteobacterial partners (Seymour et al., 2017; Zhu et al., 2024), represents an indirect-effect pathway that warrants attention in the risk assessment literature. This pattern suggests a shift from copiotrophic Gammaproteobacteria to stress-tolerant Alphaproteobacteria, which are commonly associated with nutrient scavenging and environmental stress mitigation (Cernava et al., 2017; Sigurbjörnsdóttir et al., 2014, 2015). If PFAS alter what a diatom releases into its phycosphere, the consequences for the associated bacterial community composition flow not only from direct bacterial toxicity but also from a chemically mediated disruption of host-microbe communication.

Host diatom identity, rather than PFAS treatment, remained the primary determinant of overall community structure, but the functional guild analysis revealed ecologically meaningful shifts: xenobiotic-degrader guilds declined while oligotrophic guilds expanded, indicating reduced organic matter turnover capacity even where bulk diversity appeared stable (Article II, Figure 4). The cross-species enrichment of SM1A02 and Sphingomonadales, lineages with documented membrane structural resistance to amphiphilic compounds and partial halogenated compound transformation potential (Huang et al., 2024; Huang & Jaffé, 2019; Jin et al., 2023; J. Wu et al., 2022; Yin et al., 2019), identifies these groups as candidate bioindicators of PFAS exposure in marine phytoplankton microbiomes. Importantly, the depletion of copiotrophic recyclers

from the *T. pseudonana* phycosphere suggests that current environmental PFAS levels may impair microbial loop efficiency in pelagic systems, with consequences for dissolved organic carbon turnover and nutrient regeneration that extend well beyond what host-centric toxicological assessments can detect (W. Lin et al., 2025).

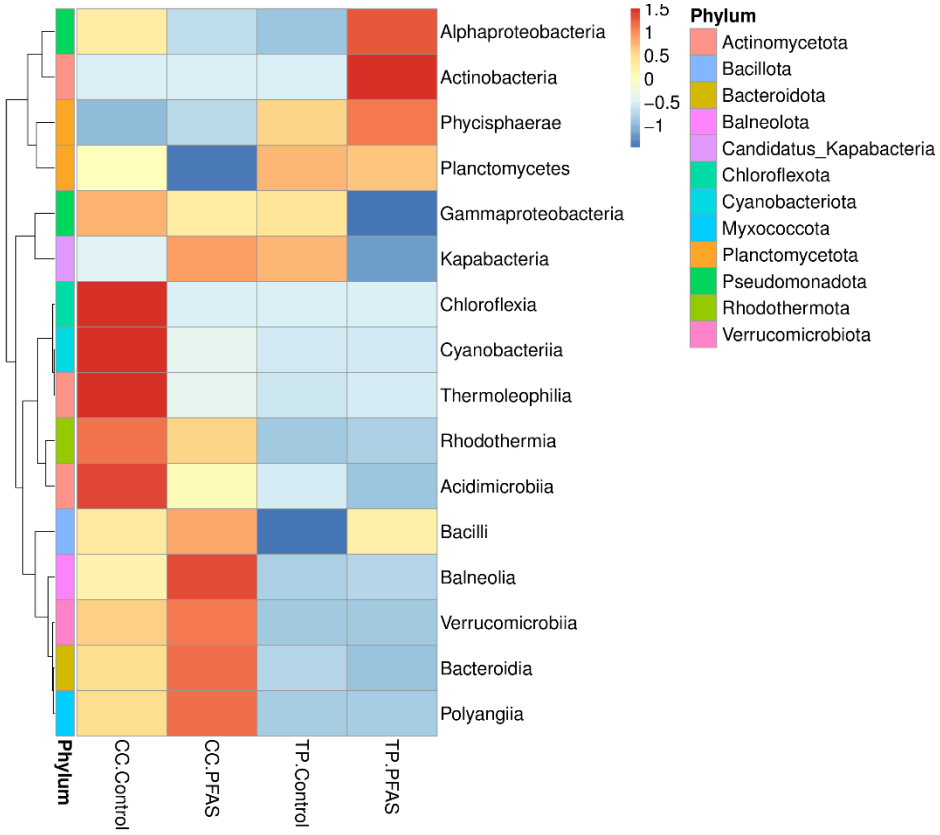

***Figure 14**: Heatmap showing standardized relative abundances of the dominant bacterial classes associated with diatoms.*

Cylindrotheca closterium (CC) and *Thalassiosira pseudonana* (TP) under control and PFAS treatments. Rows represent bacterial classes and columns represent treatment groups. Colors indicate relative abundance patterns, with red denoting enrichment and blue indicating depletion relative to the dataset mean. The dendrogram illustrates hierarchical clustering of bacterial classes based on abundance profiles. The colored sidebar indicates the corresponding bacterial phyla. PFAS exposure altered the composition of several major bacterial groups, including members of the Proteobacteria (Alpha- and Gammaproteobacteria), Bacteroidota (Bacteroidia), Verrucomicrobiota (Verrucomicrobiia), Chloroflexota (Chloroflexia), Cyanobacteriota (Cyanobacteriia), and Planctomycetota (Planctomycetes), with species-specific responses observed between the benthic diatom *C. closterium* and the pelagic diatom *T. pseudonana.*

The functional guild analysis in Article IV- showing that PFAS drove convergent loss of xenobiotic-degrader guilds and enrichment of oligotrophic guilds across both hosts despite their divergent taxonomic restructuring- introduces an important nuance. Functional community composition may be a more meaningful indicator of ecosystem-level PFAS impacts than taxonomic diversity metrics, which remained largely unchanged across treatments. This aligns with emerging perspectives in microbial ecology arguing that ecosystem functions are embedded in guilds rather than species, and that contaminant-driven guild shifts can alter biogeochemical cycling even when bulk diversity appears stable (Cerro-Gálvez et al., 2020; W. Lin et al., 2025). The demonstrated loss of copiotrophic DOM-remineralizers from the *T. pseudonana* phycosphere under PFAS exposure is precisely the kind of functional change that would not be captured by standard diversity metrics but could meaningfully reduce dissolved organic carbon turnover and nutrient regeneration in pelagic marine environments.

4.5 Ecological Significance, Limitations, and Future Directions

The cumulative ecological significance of the findings reported in this thesis can be assessed at least three levels: individual diatom fitness, diatom community composition, and broader ecosystem processes, including the biological carbon pump. At the individual fitness level, the most important conclusion is that PFAS imposes a chronic metabolic tax on diatom cells even at concentrations within the range measured in Arctic and sub-Arctic surface waters and sea ice (Hartz et al., 2023b, 2024). This tax is not primarily expressed as mortality or even visible growth inhibition, but rather as a diversion of cellular resources, fixed carbon, reducing equivalents, and synthesized amino acids from growth and reproduction toward maintenance, repair, and detoxification. Because primary production per unit of biomass and the efficiency with which fixed carbon is converted to particulate organic matter available to grazers are functions of this cellular resource budget, chronic PFAS exposure may reduce diatom ecological effectiveness without reducing cell counts. Models of Arctic carbon export efficiency that do not account for sublethal metabolic reallocation under contaminant stress may therefore overestimate the productivity contribution of PFAS-exposed diatom populations.

At the community composition level, the species-specific differences in PFAS tolerance documented here suggest that chronic PFAS contamination may selectively favor *T. pseudonana*-like pelagic species with high metabolic plasticity over *C. closterium*-like benthic species, whose more limited capacity for acclimation leads to net metabolic depletion under prolonged exposure. Given that benthic diatoms play key roles in sediment stabilization, ice-associated

productivity, and benthic-pelagic carbon coupling in Arctic systems (Karsten et al., 2012), a PFAS-driven shift in diatom community composition toward pelagic dominance could alter the spatial and temporal distribution of primary production in ways that cascade through the Arctic food web. This concern is heightened by the co-occurrence of PFAS contamination with other Arctic change drivers, sea ice loss, warming, and freshwater input from melting ice, which independently favor pelagic over sea-ice and benthic diatom communities (de Wit et al., 2019). The potential for synergistic ecological shifts under compound environmental pressures deserves specific attention in Arctic ecosystem monitoring frameworks.

Scaling the cellular and community findings to the ecosystem level, the most consequential outcome of chronic PFAS exposure may be the quasi-nitrogen stress state documented in *T. pseudonana*: the near-complete transcriptional suppression of nitrate acquisition despite ambient nutrient availability. Because nitrate assimilation underpins the Redfield-ratio coupling of carbon fixation to nitrogen drawdown that drives export production in diatom-dominated systems (Hopkinson et al., 2011), PFAS-induced disruption of this coupling could reduce biological carbon pump efficiency in Arctic surface waters, a consequence invisible to standard growth-rate endpoints but with global biogeochemical implications. Combined with the trophic magnification documented by (Ricolfi et al., 2025), even modest reductions in diatom primary production efficiency at current Arctic PFAS concentrations may propagate into detectable consequences at higher trophic levels.

Methodological limitations qualify the findings. PFAS concentrations were not analytically verified, and sorption to dissolved organic carbon and EPS in xenic cultures may have reduced freely dissolved concentrations below nominal values. Thereby, observed effects may reflect even lower effective thresholds than reported, reinforcing rather than undermining their ecological significance. Dissolved nutrient concentrations were not monitored during long-term exposures, introducing uncertainty in attributing nitrogen-conservation signatures to PFAS-induced energetic stress versus incidental medium drawdown. The PFAS mixture design, while environmentally representative, precludes compound-specific attribution of molecular responses, and the modest sample size of the phycosphere dataset limits statistical confidence in treatment effects.

The imitations define the priorities for future research: analytically verified, concentration-structured single-compound and sub-mixture long-term exposures to resolve compound-specific molecular mechanisms; metatranscriptomic profiling of phycosphere functional gene expression to determine whether the guild-level shifts observed translate into measurable changes in nutrient cycling; Arctic mesocosm and field validation using natural phytoplankton assemblages across PFAS contamination gradients; and investigation of interactive effects

between PFAS and co-occurring Arctic stressors, warming, acidification, and sea ice loss, that may synergistically amplify diatom vulnerability in ways not predictable from either stressor alone.

5 Concluding Remarks

My thesis aimed to analyze how marine diatoms respond to PFAS exposure at three biologically related levels: physiological performance, molecular acclimation, and host-associated microbial communities. By integrating these aspects, the work provides new insight into how environmentally relevant PFAS mixtures influence marine primary producers beyond conventional growth-based toxicity assessments.

First, the results indicate that environmentally relevant PFAS exposures can induce sustained physiological and metabolic adjustments in marine diatoms, even when clear effects on growth are limited or absent. The observed biochemical, transcriptomic, and metabolomic responses suggest that long-term exposure may alter cellular resource allocation and acclimation processes, highlighting the importance of considering sublethal endpoints when evaluating contaminant effects on phytoplankton.

Second, the study demonstrates substantial species-specific variation in PFAS responses. Benthic and pelagic diatoms exposed to identical PFAS mixtures exhibited distinct physiological and molecular response patterns, indicating that ecological strategy and cellular characteristics may influence sensitivity and acclimation capacity. These findings emphasize the need to broaden investigations beyond a small number of model species to better capture the diversity of responses within natural diatom communities.

Third, my thesis experimental results show that PFAS exposure can be associated with shifts in the phycosphere bacterial community composition. Changes in the relative abundance of specific bacterial taxa suggest that exposure to contaminants may influence not only the diatom host but also its associated microbiome. Although the functional implications of these community changes remain to be resolved, the results support growing recognition that host-microbiome interactions represent an important component of phytoplankton responses to environmental stressors.

Although the exposure concentrations studied here are similar to those documented in Arctic surface waters, the controlled laboratory setting inevitably simplifies the complex dynamics of natural coastal environments. Therefore, translating these findings to field settings will require careful consideration of how salinity gradients, seasonal temperature variation, and tidal mixing govern PFAS bioavailability and shape phycosphere chemistry. Finally, by combining physiological analysis, microbial community profiling, transcriptomics, and metabolomics under long-term exposure conditions, my thesis demonstrates the value of integrative approaches for understanding contaminant responses in marine microorganisms. Such approaches reveal acclimation processes and mechanistic drivers of species-specific PFAS responses that growth measurements alone cannot capture.

References

Ahrens, L., & Bundschuh, M. (2014). Fate and effects of poly- and perfluoroalkyl substances in the aquatic environment: A review. *Environmental Toxicology and Chemistry*, *33*(9), 1921–1929. https://doi.org/10.1002/etc.2663

Ahrens, L., Shoeib, M., Harner, T., Lee, S. C., Guo, R., & Reiner, E. J. (2011). Wastewater Treatment Plant and Landfills as Sources of Polyfluoroalkyl Compounds to the Atmosphere. *Environmental Science & Technology*, *45*(19), 8098–8105. https://doi.org/10.1021/es1036173

Alfaro Garcia, L. A., Descamps, S., Herzke, D., Chastel, O., Carravieri, A., Cherel, Y., Labadie, P., Budzinski, H., Munoz, G., Bustamante, P., Polder, A., Gabrielsen, G. W., Bustnes, J. O., & Borgå, K. (2022). Bioaccumulation of Per and Polyfluoroalkyl Substances in Antarctic Breeding South Polar Skuas (Catharacta maccormicki) and Their Prey. *Frontiers in Marine Science*, *9*. https://doi.org/10.3389/fmars.2022.819525

Ali, A. M., Langberg, H. A., Hale, S. E., Kallenborn, R., Hartz, W. F., Mortensen, Å.-K., Ciesielski, T. M., McDonough, C. A., Jenssen, B. M., & Breedveld, G. D. (2021). The fate of poly- and perfluoroalkyl substances in a marine food web influenced by land-based sources in the Norwegian Arctic. *Environmental Science: Processes & Impacts*, *23*(4), 588–604. https://doi.org/10.1039/D0EM00510J

Amin, S. A., Hmelo, L. R., van Tol, H. M., Durham, B. P., Carlson, L. T., Heal, K. R., Morales, R. L., Berthiaume, C. T., Parker, M. S., Djunaedi, B., Ingalls, A. E., Parsek, M. R., Moran, M. A., & Armbrust, E. V. (2015a). Interaction and signalling between a cosmopolitan phytoplankton and associated bacteria. *Nature*, *522*(7554), 98–101. https://doi.org/10.1038/nature14488

Amin, S. A., Hmelo, L. R., van Tol, H. M., Durham, B. P., Carlson, L. T., Heal, K. R., Morales, R. L., Berthiaume, C. T., Parker, M. S., Djunaedi, B., Ingalls, A. E., Parsek, M. R., Moran, M. A., & Armbrust, E. V. (2015b). Interaction and signalling between a cosmopolitan phytoplankton and associated bacteria. *Nature*, *522*(7554), 98–101. https://doi.org/10.1038/nature14488

Ankley, G. T., Cureton, P., Hoke, R. A., Houde, M., Kumar, A., Kurias, J., Lanno, R., McCarthy, C., Newsted, J., Salice, C. J., Sample, B. E., Sepúlveda, M. S., Steevens, J., & Valsecchi, S. (2021). Assessing the Ecological Risks of Per- and Polyfluoroalkyl Substances: Current State-of-the Science and a Proposed Path Forward. *Environmental Toxicology and Chemistry*, *40*(3), 564–605. https://doi.org/10.1002/etc.4869

Armbrust, E. V. (2009). The life of diatoms in the world's oceans. *Nature*, *459*(7244), 185–192. https://doi.org/10.1038/nature08057

Arulananthan, A., Vilhelmsson, O., Karsten, U., Grossart, H.-P., Sigurbjornsdottir, A., Rolfsson, Ó., Joerss, H., & Scholz, B. (2025). Per- and polyfluoroalkyl substances (PFAS) in the Cryosphere -Occurrence, organismic accumulation, ecotoxicological impacts, transformation, and

management strategies. *Frontiers in Environmental Science*, *13*. https://doi.org/10.3389/fenvs.2025.1559941

Ask, A. V., Jenssen, B. M., Tartu, S., Angelier, F., Chastel, O., & Gabrielsen, G. W. (2021). Per- and Polyfluoroalkyl Substances Are Positively Associated with Thyroid Hormones in an Arctic Seabird. *Environmental Toxicology and Chemistry*, *40*(3), 820–831. https://doi.org/10.1002/etc.4978

Bargagli, R., & Rota, E. (2024). Environmental contamination and climate change in Antarctic ecosystems: An updated overview. *Environmental Science: Advances*, *3*(4), 543–560. https://doi.org/10.1039/D3VA00113J

Battin, T. J., Sloan, W. T., Kjelleberg, S., Daims, H., Head, I. M., Curtis, T. P., & Eberl, L. (2007). Microbial landscapes: New paths to biofilm research. *Nature Reviews Microbiology*, *5*(1), 76–81. https://doi.org/10.1038/nrmicro1556

Behrenfeld, M. J., Halsey, K. H., Boss, E., Karp-Boss, L., Milligan, A. J., & Peers, G. (2021). Thoughts on the evolution and ecological niche of diatoms. *Ecological Monographs*, *91*(3), e01457. https://doi.org/10.1002/ecm.1457

Boltes, K., Rosal, R., & García-Calvo, E. (2012). Toxicity of mixtures of perfluorooctane sulphonic acid with chlorinated chemicals and lipid regulators. *Chemosphere*, *86*(1), 24–29. https://doi.org/10.1016/j.chemosphere.2011.08.041

Boudreau, T. M., Sibley, P. K., Mabury, S. A., Muir, D. G. C., & Solomon, K. R. (2003). Laboratory evaluation of the toxicity of Perfluorooctane Sulfonate (PFOS) on Selenastrum capricornutum, Chlorella vulgaris, Lemna gibba, Daphnia magna, and Daphnia pulicaria. *Archives of Environmental Contamination and Toxicology*, *44*(3), 307–313. https://doi.org/10.1007/s00244-002-2102-6

Bowler, C., Allen, A. E., Badger, J. H., Grimwood, J., Jabbari, K., Kuo, A., Maheswari, U., Martens, C., Maumus, F., Otillar, R. P., Rayko, E., Salamov, A., Vandepoele, K., Beszteri, B., Gruber, A., Heijde, M., Katinka, M., Mock, T., Valentin, K., … Grigoriev, I. V. (2008). The Phaeodactylum genome reveals the evolutionary history of diatom genomes. *Nature*, *456*(7219), 239–244. https://doi.org/10.1038/nature07410

Buchan, A., LeCleir, G. R., Gulvik, C. A., & González, J. M. (2014). Master recyclers: Features and functions of bacteria associated with phytoplankton blooms. *Nature Reviews Microbiology*, *12*(10), 686–698. https://doi.org/10.1038/nrmicro3326

Burkhard, L. P., & Votava, L. K. (2023). Biota-Sediment Accumulation Factors for Per- and Polyfluoroalkyl Substances. *Environmental Toxicology and Chemistry*, *42*(2), 277–295. https://doi.org/10.1002/etc.5526

Cabrerizo, A., Dachs, J., Barceló, D., & Jones, K. C. (2013). Climatic and Biogeochemical Controls on the Remobilization and Reservoirs of Persistent Organic Pollutants in Antarctica. *Environmental Science & Technology*, *47*(9), 4299–4306. https://doi.org/10.1021/es400471c

Cai, M., Zhao, Z., Yin, Z., Ahrens, L., Huang, P., Cai, M., Yang, H., He, J., Sturm, R., Ebinghaus, R., & Xie, Z. (2012). Occurrence of Perfluoroalkyl Compounds in Surface Waters from the North Pacific to the Arctic Ocean. *Environmental Science & Technology*, *46*(2), 661–668. https://doi.org/10.1021/es2026278

Callahan, B. J., McMurdie, P. J., & Holmes, S. P. (2017). Exact sequence variants should replace operational taxonomic units in marker-gene data analysis. *The ISME Journal*, *11*(12), 2639–2643. https://doi.org/10.1038/ismej.2017.119

Callahan, B. J., McMurdie, P. J., Rosen, M. J., Han, A. W., Johnson, A. J. A., & Holmes, S. P. (2016). DADA2: High-resolution sample inference from Illumina amplicon data. *Nature Methods*, *13*(7), 581–583. https://doi.org/10.1038/nmeth.3869

Caporaso, J. G., Ackermann, G., Apprill, A., Bauer, M., Berg-Lyons, D., Betley, J., Fierer, N., Fraser, L., Fuhrman, J. A., Gilbert, J. A., Gormley, N., Humphrey, G., Huntley, J., Jansson, J. K., Knight, R., Lauber, C. L., Lozupone, C. A., McNally, S., Needham, D. M., … Weber, L. (2023). *EMP 16S Illumina Amplicon Protocol V.2*. https://www.protocols.io/view/emp-16s-illumina-amplicon-protocol-kqdg3dzzl25z/v2

Cara, B., Lies, T., Thimo, G., Robin, L., & Lieven, B. (2022). Bioaccumulation and trophic transfer of perfluorinated alkyl substances (PFAS) in marine biota from the Belgian North Sea: Distribution and human health risk implications. *Environmental Pollution*, *311*, 119907. https://doi.org/10.1016/j.envpol.2022.119907

Casal, P., González-Gaya, B., Zhang, Y., Reardon, A. J. F., Martin, J. W., Jiménez, B., & Dachs, J. (2017). Accumulation of Perfluoroalkylated Substances in Oceanic Plankton. *Environmental Science & Technology*, *51*(5), 2766–2775. https://doi.org/10.1021/acs.est.6b05821

Casal, P., Zhang, Y., Martin, J. W., Pizarro, M., Jiménez, B., & Dachs, J. (2017). Role of Snow Deposition of Perfluoroalkylated Substances at Coastal Livingston Island (Maritime Antarctica). *Environmental Science & Technology*, *51*(15), 8460–8470. https://doi.org/10.1021/acs.est.7b02521

Cernava, T., Erlacher, A., Aschenbrenner, I. A., Krug, L., Lassek, C., Riedel, K., Grube, M., & Berg, G. (2017). Deciphering functional diversification within the lichen microbiota by meta-omics. *Microbiome*, *5*(1), 82. https://doi.org/10.1186/s40168-017-0303-5

Cerro-Gálvez, E., Roscales, J. L., Jiménez, B., Sala, M. M., Dachs, J., & Vila-Costa, M. (2020). Microbial responses to perfluoroalkyl substances and perfluorooctanesulfonate (PFOS) desulfurization in the Antarctic marine environment. *Water Research*, *171*, 115434. https://doi.org/10.1016/j.watres.2019.115434

Chiesa, L. M., Nobile, M., Pasquale, E., Balzaretti, C., Cagnardi, P., Tedesco, D., Panseri, S., & Arioli, F. (2018). Detection of perfluoroalkyl acids and sulphonates in Italian eel samples by HPLC-HRMS Orbitrap. *Chemosphere*, *193*, 358–364. https://doi.org/10.1016/j.chemosphere.2017.10.082

Cole, J. J. (1982). Interactions Between Bacteria and Algae in Aquatic Ecosystems. *Annual Review of Ecology, Evolution, and Systematics*, *13*(Volume 13, 1982), 291–314. https://doi.org/10.1146/annurev.es.13.110182.001451

Dai, S., Zhang, G., Dong, C., Yang, R., Pei, Z., Li, Y., Li, A., Zhang, Q., & Jiang, G. (2025). Occurrence, bioaccumulation and trophodynamics of per- and polyfluoroalkyl substances (PFAS) in terrestrial and marine ecosystems of Svalbard, Arctic. *Water Research*, *271*, 122979. https://doi.org/10.1016/j.watres.2024.122979

Dale, K., Yadetie, F., Horvli, T., Zhang, X., Frøysa, H. G., Karlsen, O. A., & Goksøyr, A. (2022). Single PFAS and PFAS mixtures affect nuclear receptor- and oxidative stress-related pathways in precision-cut liver slices of Atlantic cod (*Gadus morhua*). *Science of The Total Environment*, *814*, 152732. https://doi.org/10.1016/j.scitotenv.2021.152732

Daly, G., Decorosi, F., Viti, C., & Adessi, A. (2023). Shaping the phycosphere: Analysis of the EPS in diatom-bacterial co-cultures. *Journal of Phycology*, *59*(4), 791–797. https://doi.org/10.1111/jpy.13361

Davis, S. N., Klumker, S. M., Mitchell, A. A., Coppage, M. A., Labonté, J. M., & Quigg, A. (2024). Life in the PFAS lane: The impact of perfluoroalkyl substances on photosynthesis, cellular exudates, nutrient cycling, and composition of a marine microbial community. *Science of The Total Environment*, *927*, 171977. https://doi.org/10.1016/j.scitotenv.2024.171977

de Wit, C. A., Balmer, J., Muir, D. C. G., Vorkamp, K., & Wilson, S. (2019). Chemicals of Emerging Arctic Concern: Preface. *Emerging Contaminants*, *5*, 1–3. https://doi.org/10.1016/j.emcon.2018.12.001

Debenest, T., Silvestre, J., & Pinelli, E. (2013). Diatoms in Ecotoxicology. In J.-F. Férard & C. Blaise (Eds.), *Encyclopedia of Aquatic Ecotoxicology* (pp. 295–304). Springer Netherlands. https://doi.org/10.1007/978-94-007-5704-2_29

Di Costanzo, F., Di Dato, V., & Romano, G. (2023). Diatom–Bacteria Interactions in the Marine Environment: Complexity, Heterogeneity, and Potential for Biotechnological Applications. *Microorganisms*, *11*(12), 2967. https://doi.org/10.3390/microorganisms11122967

Dietz, R., Letcher, R. J., Desforges, J.-P., Eulaers, I., Sonne, C., Wilson, S., Andersen-Ranberg, E., Basu, N., Barst, B. D., Bustnes, J. O., Bytingsvik, J., Ciesielski, T. M., Drevnick, P. E., Gabrielsen, G. W., Haarr, A., Hylland, K., Jenssen, B. M., Levin, M., McKinney, M. A., … Víkingsson, G. (2019). Current state of knowledge on biological effects from contaminants on arctic wildlife and fish. *Science of The Total Environment*, *696*, 133792. https://doi.org/10.1016/j.scitotenv.2019.133792

ECHA. (2024). *Per- and polyfluoroalkyl substances (PFAS)—ECHA*. https://echa.europa.eu/hot-topics/perfluoroalkyl-chemicals-pfas

Evenset, A., Hallanger, I. G., Tessmann, M., Warner, N., Ruus, A., Borgå, K., Gabrielsen, G. W., Christensen, G., & Renaud, P. E. (2016). Seasonal

variation in accumulation of persistent organic pollutants in an Arctic marine benthic food web. *The Science of the Total Environment*, *542*(Pt A), 108–120. https://doi.org/10.1016/j.scitotenv.2015.10.092

Falciatore, A., Jaubert, M., Bouly, J.-P., Bailleul, B., & Mock, T. (2020). Diatom Molecular Research Comes of Age: Model Species for Studying Phytoplankton Biology and Diversity[OPEN]. *The Plant Cell*, *32*(3), 547–572. https://doi.org/10.1105/tpc.19.00158

Falciatore, A., & Mock, T. (Eds.). (2022). *The Molecular Life of Diatoms*. Springer International Publishing. https://doi.org/10.1007/978-3-030-92499-7

Falkowski, P. (2012). *Do tiny floating microorganisms in the ocean's surface waters play a massive role in controlling the global climate?*

Fitzgerald, N. J. M., Wargenau, A., Sorenson, C., Pedersen, J., Tufenkji, N., Novak, P. J., & Simcik, M. F. (2018). Partitioning and Accumulation of Perfluoroalkyl Substances in Model Lipid Bilayers and Bacteria. *Environmental Science & Technology*, *52*(18), 10433–10440. https://doi.org/10.1021/acs.est.8b02912

Flynn, K. M., Bush, K., Cavallin, J., Hazemi, M., Kasparek, A., Schumann, P., & Villeneuve, D. L. (2025). Transcriptomic response of an algal species (Raphidocelis subcapitata) exposed to 22 per- and polyfluoroalkyl substances. *Environmental Toxicology and Chemistry*, *44*(4), 995–1006. https://doi.org/10.1093/etojnl/vgaf022

Gaines, L. G. T. (2023). Historical and current usage of per- and polyfluoroalkyl substances (PFAS): A literature review. *American Journal of Industrial Medicine*, *66*(5), 353–378. https://doi.org/10.1002/ajim.23362

Gärdes, A., Iversen, M. H., Grossart, H.-P., Passow, U., & Ullrich, M. S. (2011a). Diatom-associated bacteria are required for aggregation of Thalassiosira weissflogii. *The ISME Journal*, *5*(3), 436–445. https://doi.org/10.1038/ismej.2010.145

Gärdes, A., Iversen, M. H., Grossart, H.-P., Passow, U., & Ullrich, M. S. (2011b). Diatom-associated bacteria are required for aggregation of Thalassiosira weissflogii. *The ISME Journal*, *5*(3), 436–445. https://doi.org/10.1038/ismej.2010.145

Garnett, J., Halsall, C., Thomas, M., Crabeck, O., France, J., Joerss, H., Ebinghaus, R., Kaiser, J., Leeson, A., & Wynn, P. M. (2021). Investigating the Uptake and Fate of Poly- and Perfluoroalkylated Substances (PFAS) in Sea Ice Using an Experimental Sea Ice Chamber. *Environmental Science & Technology*, *55*(14), 9601–9608. https://doi.org/10.1021/acs.est.1c01645

Garnett, J., Halsall, C., Vader, A., Joerss, H., Ebinghaus, R., Leeson, A., & Wynn, P. M. (2021). High Concentrations of Perfluoroalkyl Acids in Arctic Seawater Driven by Early Thawing Sea Ice. *Environmental Science & Technology*, *55*(16), 11049–11059. https://doi.org/10.1021/acs.est.1c01676

Garnett, J., Halsall, C., Winton, H., Joerss, H., Mulvaney, R., Ebinghaus, R., Frey, M., Jones, A., Leeson, A., & Wynn, P. (2022). Increasing Accumulation of Perfluorocarboxylate Contaminants Revealed in an

Antarctic Firn Core (1958–2017). *Environmental Science & Technology*, *56*(16), 11246–11255. https://doi.org/10.1021/acs.est.2c02592
Ghyselinck, J., Pfeiffer, S., Heylen, K., Sessitsch, A., & De Vos, P. (2013). The Effect of Primer Choice and Short Read Sequences on the Outcome of 16S rRNA Gene Based Diversity Studies. *PLoS ONE*, *8*(8), e71360. https://doi.org/10.1371/journal.pone.0071360
Grossart, H.-P. (1999). Interactions between marine bacteria and axenic diatoms (Cylindrotheca fusiformis, Nitzschia laevis, and Thalassiosira weissflogii) incubated under various conditions in the lab. *Aquatic Microbial Ecology*, *19*, 1–11. https://doi.org/10.3354/ame019001
Grossart, H.-P., Levold, F., Allgaier, M., Simon, M., & Brinkhoff, T. (2005). Marine diatom species harbour distinct bacterial communities. *Environmental Microbiology*, *7*(6), 860–873. https://doi.org/10.1111/j.1462-2920.2005.00759.x
Grung, M., Hjermann, D. Ø., Rundberget, T., Bæk, K., Thomsen, C., Knutsen, H. K., & Haug, L. S. (2024). Low levels of per- and polyfluoroalkyl substances (PFAS) detected in drinking water in Norway, but elevated concentrations found near known sources. *Science of The Total Environment*, *947*, 174550. https://doi.org/10.1016/j.scitotenv.2024.174550
Guillard, R. R. L. (1975). Culture of Phytoplankton for Feeding Marine Invertebrates. In W. L. Smith & M. H. Chanley (Eds.), *Culture of Marine Invertebrate Animals: Proceedings—1st Conference on Culture of Marine Invertebrate Animals Greenport* (pp. 29–60). Springer US. https://doi.org/10.1007/978-1-4615-8714-9_3
Guo, W., Hao, W., & Xiao, W. (2024). Emerging Perfluorinated Chemical GenX: Environmental and Biological Fates and Risks. *Environment & Health*. https://doi.org/10.1021/envhealth.4c00164
Hagenaars, A., Vergauwen, L., Benoot, D., Laukens, K., & Knapen, D. (2013). Mechanistic toxicity study of perfluorooctanoic acid in zebrafish suggests mitochondrial dysfunction to play a key role in PFOA toxicity. *Chemosphere*, *91*(6), 844–856. https://doi.org/10.1016/j.chemosphere.2013.01.056
Hamid, N., Junaid, M., Sultan, M., Yoganandham, S. T., & Chuan, O. M. (2024). The untold story of PFAS alternatives: Insights into the occurrence, ecotoxicological impacts, and removal strategies in the aquatic environment. *Water Research*, *250*, 121044. https://doi.org/10.1016/j.watres.2023.121044
Haque, F., L. Soerensen, A., Sköld, M., Awad, R., M. Spaan, K., Z. Lauria, M., M. Plassmann, M., & P. Benskin, J. (2023). Per- and polyfluoroalkyl substances (PFAS) in white-tailed sea eagle eggs from Sweden: Temporal trends (1969–2021), spatial variations, fluorine mass balance, and suspect screening. *Environmental Science: Processes & Impacts*, *25*(9), 1549–1563. https://doi.org/10.1039/D3EM00141E
Hartz, W. F., Björnsdotter, M. K., Yeung, L. W. Y., Hodson, A., Thomas, E. R., Humby, J. D., Day, C., Jogsten, I. E., Kärrman, A., & Kallenborn, R. (2023a). Levels and distribution profiles of Per- and Polyfluoroalkyl

Substances (PFAS) in a high Arctic Svalbard ice core. *Science of The Total Environment*, *871*, 161830. https://doi.org/10.1016/j.scitotenv.2023.161830

Hartz, W. F., Björnsdotter, M. K., Yeung, L. W. Y., Hodson, A., Thomas, E. R., Humby, J. D., Day, C., Jogsten, I. E., Kärrman, A., & Kallenborn, R. (2023b). Levels and distribution profiles of Per- and Polyfluoroalkyl Substances (PFAS) in a high Arctic Svalbard ice core. *Science of The Total Environment*, *871*, 161830. https://doi.org/10.1016/j.scitotenv.2023.161830

Hartz, W. F., Björnsdotter, M. K., Yeung, L. W. Y., Humby, J. D., Eckhardt, S., Evangeliou, N., Ericson Jogsten, I., Kärrman, A., & Kallenborn, R. (2024). Sources and Seasonal Variations of Per- and Polyfluoroalkyl Substances (PFAS) in Surface Snow in the Arctic. *Environmental Science & Technology*, *58*(49), 21817–21828. https://doi.org/10.1021/acs.est.4c08854

Hopkinson, B. M., Dupont, C. L., Allen, A. E., & Morel, F. M. M. (2011). Efficiency of the CO2-concentrating mechanism of diatoms. *Proceedings of the National Academy of Sciences*, *108*(10), 3830–3837. https://doi.org/10.1073/pnas.1018062108

Hu, C., Luo, Q., & Huang, Q. (2014). Ecotoxicological effects of perfluorooctanoic acid on freshwater microalgae Chlamydomonas reinhardtii and Scenedesmus obliquus. *Environmental Toxicology and Chemistry*, *33*(5), 1129–1134. https://doi.org/10.1002/etc.2532

Hu, X. C., Andrews, D. Q., Lindstrom, A. B., Bruton, T. A., Schaider, L. A., Grandjean, P., Lohmann, R., Carignan, C. C., Blum, A., Balan, S. A., Higgins, C. P., & Sunderland, E. M. (2016). Detection of Poly- and Perfluoroalkyl Substances (PFASs) in U.S. Drinking Water Linked to Industrial Sites, Military Fire Training Areas, and Wastewater Treatment Plants. *Environmental Science & Technology Letters*, *3*(10), 344–350. https://doi.org/10.1021/acs.estlett.6b00260

Huang, S., & Jaffé, P. R. (2019). Defluorination of Perfluorooctanoic Acid (PFOA) and Perfluorooctane Sulfonate (PFOS) by Acidimicrobium sp. Strain A6. *Environmental Science & Technology*, *53*(19), 11410–11419. https://doi.org/10.1021/acs.est.9b04047

Huang, S., Pilloni, G., Key, T. A., & Jaffé, P. R. (2024). Defluorination of various perfluoro alkyl acids and selected PFOA and PFOS monomers by *Acidimicrobium* sp. Strain A6 enrichment cultures. *Journal of Hazardous Materials*, *480*, 136426. https://doi.org/10.1016/j.jhazmat.2024.136426

Ivantsova, E., Sultan, A., & Martyniuk, C. J. (2025). Occurrence and Toxicity Mechanisms of Perfluorononanoic Acid, Perfluorodecanoic Acid, and Perfluoroundecanoic Acid in Fish: A Review. *Toxics*, *13*(6), 436. https://doi.org/10.3390/toxics13060436

James, J., Bisht, B., Dmitriev, A. A., Nanda, M., Hussain, A., Vlaskin, M. S., Verma, M., Kim, H., Chauhan, P. K., & Kumar, V. (2026). Impact of PFAS compounds on microalgal growth, biochemical composition, and

metabolism in *Chlorella minutissima*. *Chemical Engineering Journal*, *536*, 175970. https://doi.org/10.1016/j.cej.2026.175970

Jin, B., Liu, H., Che, S., Gao, J., Yu, Y., Liu, J., & Men, Y. (2023). Substantial defluorination of polychlorofluorocarboxylic acids triggered by anaerobic microbial hydrolytic dechlorination. *Nature Water*, *1*(5), 451–461. https://doi.org/10.1038/s44221-023-00077-6

Joerss, H., Apel, C., & Ebinghaus, R. (2019). Emerging per- and polyfluoroalkyl substances (PFASs) in surface water and sediment of the North and Baltic Seas. *Science of The Total Environment*, *686*, 360–369. https://doi.org/10.1016/j.scitotenv.2019.05.363

Joerss, H., Xie, Z., Wagner, C. C., von Appen, W.-J., Sunderland, E. M., & Ebinghaus, R. (2020). Transport of Legacy Perfluoroalkyl Substances and the Replacement Compound HFPO-DA through the Atlantic Gateway to the Arctic Ocean—Is the Arctic a Sink or a Source? *Environmental Science & Technology*, *54*(16), 9958–9967. https://doi.org/10.1021/acs.est.0c00228

Johansson, O. N., Pinder, M. I. M., Ohlsson, F., Egardt, J., Töpel, M., & Clarke, A. K. (2019). Friends With Benefits: Exploring the Phycosphere of the Marine Diatom Skeletonema marinoi. *Frontiers in Microbiology*, *10*, 1828. https://doi.org/10.3389/fmicb.2019.01828

Jouanneau, W., Léandri-Breton, D.-J., Herzke, D., Moe, B., Nikiforov, V. A., Pallud, M., Parenteau, C., Gabrielsen, G. W., & Chastel, O. (2023). Does contaminant exposure disrupt maternal hormones deposition? A study on per- and polyfluoroalkyl substances in an Arctic seabird. *The Science of the Total Environment*, *868*, 161413. https://doi.org/10.1016/j.scitotenv.2023.161413

Karsten, U., Schlie, C., Woelfel, J., & Becker, B. (2012). Benthic Diatoms in Arctic Seas – Ecological Functions and Adaptations. *Polarforschung 81, 77-84.*, 77–84.

Kelly, B. C., Ikonomou, M. G., Blair, J. D., Surridge, B., Hoover, D., Grace, R., & Gobas, F. A. P. C. (2009). Perfluoroalkyl Contaminants in an Arctic Marine Food Web: Trophic Magnification and Wildlife Exposure. *Environmental Science & Technology*, *43*(11), 4037–4043. https://doi.org/10.1021/es9003894

Khalid, N. K., Le Calvez, M., Lemire, M., Dinh, Q. T., Fontaine, J., Lair, S., & Sauvé, S. (2024). Occurrence of 80 per and polyfluorinated alkyl substances (PFAS) in muscle and liver tissues of marine mammals of the St. Lawrence Estuary and Gulf, Quebec, Canada. *Frontiers in Environmental Chemistry*, *5*. https://doi.org/10.3389/fenvc.2024.1403728

Khan, B., Burgess, R. M., & Cantwell, M. G. (2023). Occurrence and Bioaccumulation Patterns of Per- and Polyfluoroalkyl Substances (PFAS) in the Marine Environment. *ACS ES&T Water*, *3*(5), 1243–1259. https://doi.org/10.1021/acsestwater.2c00296

Kim, J. H., Ahn, J. W., Park, E.-J., & Choi, J. (2023). *Overexpression of S-Adenosylmethionine Synthetase in Recombinant Chlamydomonas for*

Enhanced Lipid Production. *33*(3), 310–318. https://doi.org/10.4014/jmb.2212.12009
Koletti, A., Skliros, D., Dervisi, I., Roussis, A., & Flemetakis, E. (2025). Oxidative Stress Responses in Microalgae: Modern Insights into an Old Topic. *Applied Microbiology*, *5*(2), 37. https://doi.org/10.3390/applmicrobiol5020037
Latała, A., Nędzi, M., & Stepnowski, P. (2009). Acute toxicity assessment of perfluorinated carboxylic acids towards the Baltic microalgae. *Environmental Toxicology and Pharmacology*, *28*(2), 167–171. https://doi.org/10.1016/j.etap.2009.03.010
Lauritano, C., Orefice, I., Procaccini, G., Romano, G., & Ianora, A. (2015). Key genes as stress indicators in the ubiquitous diatom Skeletonema marinoi. *BMC Genomics*, *16*(1), 411. https://doi.org/10.1186/s12864-015-1574-5
Lee, H. B., Jeong, D. H., Cho, B. C., & Park, J. S. (2023). Comparative analyses of eight primer sets commonly used to target the bacterial 16S rRNA gene for marine metabarcoding-based studies. *Frontiers in Marine Science*, *10*. https://doi.org/10.3389/fmars.2023.1199116
Letcher, R. J., Morris, A. D., Dyck, M., Sverko, E., Reiner, E. J., Blair, D. A. D., Chu, S. G., & Shen, L. (2018). Legacy and new halogenated persistent organic pollutants in polar bears from a contamination hotspot in the Arctic, Hudson Bay Canada. *Science of The Total Environment*, *610–611*, 121–136. https://doi.org/10.1016/j.scitotenv.2017.08.035
Li, L., Ding, R., Liu, L., Liu, Z., Han, T., Li, B., Tang, X., & Zhao, Y. (2026). Higher toxicity and bioaccumulation of PFOA and HFPO-DA mixture than individuals on the marine model diatom *Thalassiosira pseudonana*. *Journal of Hazardous Materials*, *504*, 141217. https://doi.org/10.1016/j.jhazmat.2026.141217
Li, P., Oyang, X., Xie, X., Li, Z., Yang, H., Xi, J., Guo, Y., Tian, X., Liu, B., Li, J., & Xiao, Z. (2020). Phytotoxicity induced by perfluorooctanoic acid and perfluorooctane sulfonate via metabolomics. *Journal of Hazardous Materials*, *389*, 121852. https://doi.org/10.1016/j.jhazmat.2019.121852
Li, X., Hou, M., Jiang, S., Cousins, I. T., Li, P., Shi, Y., Cai, Y., & Jiang, G. (2026). Atmospheric transport and deposition of PFAS in East Antarctica: Evidence from snow transect measurements and a multidecadal record. *Science Advances*, *12*(12), eadz4749. https://doi.org/10.1126/sciadv.adz4749
Li, Y., Liu, X., Zheng, X., Yang, M., Gao, X., Huang, J., Zhang, L., & Fan, Z. (2021). Toxic effects and mechanisms of PFOA and its substitute GenX on the photosynthesis of *Chlorella pyrenoidosa*. *Science of The Total Environment*, *765*, 144431. https://doi.org/10.1016/j.scitotenv.2020.144431
Li, Y., Yao, J., Pan, Y., Dai, J., & Tang, J. (2023). Trophic behaviors of PFOA and its alternatives perfluoroalkyl ether carboxylic acids (PFECAs) in a coastal food web. *Journal of Hazardous Materials*, *452*, 131353. https://doi.org/10.1016/j.jhazmat.2023.131353
Liao, J., Huang, L., Liu, Y., Sun, B., Zhang, K., Wang, C., Lei, H., Cao, Z., & Lu, Y. (2025a). Metabolomic analysis reveals contrasting effects of

PFOS and PFAS on cyanobacterial bloom and metabolic pathways in eutrophic water. *Environmental Pollution*, *375*, 126340. https://doi.org/10.1016/j.envpol.2025.126340

Liao, J., Huang, L., Liu, Y., Sun, B., Zhang, K., Wang, C., Lei, H., Cao, Z., & Lu, Y. (2025b). Metabolomic analysis reveals contrasting effects of PFOS and PFAS on cyanobacterial bloom and metabolic pathways in eutrophic water. *Environmental Pollution*, *375*, 126340. https://doi.org/10.1016/j.envpol.2025.126340

Liao, J., Lu, Y., Liu, Y., Sun, B., Zhang, K., Wang, C., Lei, H., & Cao, Z. (2025). How heatwaves impact microalgae in the presence of environmentally relevant PFAS concentration: Metabolic shifts and challenges posed. *Journal of Hazardous Materials*, *484*, 136640. https://doi.org/10.1016/j.jhazmat.2024.136640

Liao, J., Sun, B., Wang, C., Cao, Z., Wu, Z., An, X., Liang, Z., Huang, X., & Lu, Y. (2024). Uptake and cellular responses of *Microcystis aeruginosa* to PFOS in various environmental conditions. *Ecotoxicology and Environmental Safety*, *272*, 116041. https://doi.org/10.1016/j.ecoenv.2024.116041

Li-Beisson, Y., Thelen, J. J., Fedosejevs, E., & Harwood, J. L. (2019). The lipid biochemistry of eukaryotic algae. *Progress in Lipid Research*, *74*, 31–68. https://doi.org/10.1016/j.plipres.2019.01.003

Lin, A. Y.-C., Panchangam, S. C., & Lo, C.-C. (2009). The impact of semiconductor, electronics and optoelectronic industries on downstream perfluorinated chemical contamination in Taiwanese rivers. *Environmental Pollution*, *157*(4), 1365–1372. https://doi.org/10.1016/j.envpol.2008.11.033

Lin, L., & Ju, F. (2023). Evaluation of different 16S rRNA gene hypervariable regions and reference databases for profiling engineered microbiota structure and functional guilds in a swine wastewater treatment plant. *Interface Focus*, *13*(4), 20230012. https://doi.org/10.1098/rsfs.2023.0012

Lin, W., Zhao, J., Wu, X., Jiang, J., Zhou, C., Zheng, J., Zhang, C., Guo, Y., Wang, L., Ng, H. Y., Li, S., & Wang, S. (2025). The effects of perfluoroalkyl substance pollution on microbial community and key metabolic pathways in the Pearl River Estuary. *Ecotoxicology and Environmental Safety*, *298*, 118293. https://doi.org/10.1016/j.ecoenv.2025.118293

Lin, Y., Jiang, J.-J., Rodenburg, L. A., Cai, M., Wu, Z., Ke, H., & Chitsaz, M. (2020). Perfluoroalkyl substances in sediments from the Bering Sea to the western Arctic: Source and pathway analysis. *Environment International*, *139*, 105699. https://doi.org/10.1016/j.envint.2020.105699

Litchman, E., Klausmeier, C. A., Schofield, O. M., & Falkowski, P. G. (2007). The role of functional traits and trade-offs in structuring phytoplankton communities: Scaling from cellular to ecosystem level. *Ecology Letters*, *10*(12), 1170–1181. https://doi.org/10.1111/j.1461-0248.2007.01117.x

Liu, F., Gledhill, M., Tan, Q.-G., Zhu, K., Zhang, Q., Salaün, P., Tagliabue, A., Zhang, Y., Weiss, D., Achterberg, E. P., & Korchev, Y. (2022). Phycosphere pH of unicellular nano- and micro- phytoplankton cells and consequences for iron speciation. *The ISME Journal*, *16*(10), 2329–2336. https://doi.org/10.1038/s41396-022-01280-1

Liu, W., Chen, S., Quan, X., & Jin, Y. (2008a). Toxic effect of serial perfluorosulfonic and perfluorocarboxylic acids on the membrane system of a freshwater alga measured by flow cytometry. *Environmental Toxicology and Chemistry*, *27*(7), 1597–1604. https://doi.org/10.1897/07-459.1

Liu, W., Chen, S., Quan, X., & Jin, Y.-H. (2008b). Toxic effect of serial perfluorosulfonic and perfluorocarboxylic acids on the membrane system of a freshwater alga measured by flow cytometry. *Environmental Toxicology and Chemistry*, *27*(7), 1597–1604. https://doi.org/10.1897/07-459.1

Liu, X., Zheng, X., Zhang, L., Li, J., Li, Y., Huang, H., & Fan, Z. (2022). Joint toxicity mechanisms of binary emerging PFAS mixture on algae (*Chlorella pyrenoidosa*) at environmental concentration. *Journal of Hazardous Materials*, *437*, 129355. https://doi.org/10.1016/j.jhazmat.2022.129355

Liu, Z., Cao, X., Wu, M., Huang, W., Dong, X., Chen, X., & Zhang, C. (2025). Mechanisms of PFBA toxicity in *Chlorella vulgaris*: Photosynthesis, oxidative stress, and antioxidant impairment. *Environmental Research*, *273*, 121228. https://doi.org/10.1016/j.envres.2025.121228

Lohmann, R., Abass, K., Bonefeld-Jørgensen, E. C., Bossi, R., Dietz, R., Ferguson, S., Fernie, K. J., Grandjean, P., Herzke, D., Houde, M., Lemire, M., Letcher, R. J., Muir, D., De Silva, A. O., Ostertag, S. K., Rand, A. A., Søndergaard, J., Sonne, C., Sunderland, E. M., … Weihe, P. (2024). Cross-cutting studies of per- and polyfluorinated alkyl substances (PFAS) in Arctic wildlife and humans. *Science of The Total Environment*, *954*, 176274. https://doi.org/10.1016/j.scitotenv.2024.176274

Louisse, J., Rijkers, D., Stoopen, G., Janssen, A., Staats, M., Hoogenboom, R., Kersten, S., & Peijnenburg, A. (2020). Perfluorooctanoic acid (PFOA), perfluorooctane sulfonic acid (PFOS), and perfluorononanoic acid (PFNA) increase triglyceride levels and decrease cholesterogenic gene expression in human HepaRG liver cells. *Archives of Toxicology*, *94*(9), 3137–3155. https://doi.org/10.1007/s00204-020-02808-0

Ma, T., Ye, C., Wang, T., Li, X., & Luo, Y. (2022). Toxicity of Per- and Polyfluoroalkyl Substances to Aquatic Invertebrates, Planktons, and Microorganisms. *International Journal of Environmental Research and Public Health*, *19*(24), Article 24. https://doi.org/10.3390/ijerph192416729

MacInnis, J., Silva, A. O. D., Lehnherr, I., G. Muir, D. C., Pierre, K. A. S., Louis, V. L. S., & Spencer, C. (2022). Investigation of perfluoroalkyl substances in proglacial rivers and permafrost seep in a high Arctic

watershed. *Environmental Science: Processes & Impacts*, *24*(1), 42–51. https://doi.org/10.1039/D1EM00349F

Mahoney, H., Cantin, J., Xie, Y., Brinkmann, M., & Giesy, J. P. (2023). Perfluoroethylcyclohexane sulphonate, an emerging perfluoroalkyl substance, disrupts mitochondrial membranes and the expression of key molecular targets *in vitro*. *Aquatic Toxicology*, *257*, 106453. https://doi.org/10.1016/j.aquatox.2023.106453

Mao, W., Li, M., Xue, X., Cao, W., Wang, X., Xu, F., & Jiang, W. (2023). Bioaccumulation and toxicity of perfluorooctanoic acid and perfluorooctane sulfonate in marine algae *Chlorella sp. Science of The Total Environment*, *870*, 161882. https://doi.org/10.1016/j.scitotenv.2023.161882

Mao, Y., Ye, K., Yang, S., Salam, M., Yu, W., He, Q., He, R., & Li, H. (2024). Repeated Exposure Enhanced Toxicity of Clarithromycin on Microcystis aeruginosa Versus Single Exposure through Photosynthesis, Oxidative Stress, and Energy Metabolism Shift. *Environmental Science & Technology*, *58*(9), 4070–4082. https://doi.org/10.1021/acs.est.3c07008

Maxwell, K., & Johnson, G. N. (2000). Chlorophyll fluorescence—A practical guide. *Journal of Experimental Botany*, *51*(345), 659–668. https://doi.org/10.1093/jexbot/51.345.659

McCain, J. S. P., Tagliabue, A., Susko, E., Achterberg, E. P., Allen, A. E., & Bertrand, E. M. (2021). Cellular costs underpin micronutrient limitation in phytoplankton. *Science Advances*, *7*(32), eabg6501. https://doi.org/10.1126/sciadv.abg6501

Mojiri, A., Nazari Vishkaei, M., Ansari, H. K., Vakili, M., Farraji, H., & Kasmuri, N. (2023). Toxicity Effects of Perfluorooctanoic Acid (PFOA) and Perfluorooctane Sulfonate (PFOS) on Two Green Microalgae Species. *International Journal of Molecular Sciences*, *24*(3), 2446. https://doi.org/10.3390/ijms24032446

Mojiri, A., Zhou, J. L., Ozaki, N., KarimiDermani, B., Razmi, E., & Kasmuri, N. (2023). Occurrence of per- and polyfluoroalkyl substances in aquatic environments and their removal by advanced oxidation processes. *Chemosphere*, *330*, 138666. https://doi.org/10.1016/j.chemosphere.2023.138666

Moorthy, A. K., Shukla, S. P., Govindarajan, R. B., Kumar, K., & Bharti, V. S. (2022). Application of Microalgal Physiological Response as Biomarker for Evaluating the Toxicity of the Textile Dye Alizarin Red S. *Bulletin of Environmental Contamination and Toxicology*, *109*(2), 401–408. https://doi.org/10.1007/s00128-022-03525-3

Munoz, G., Labadie, P., Geneste, E., Pardon, P., Tartu, S., Chastel, O., & Budzinski, H. (2017). Biomonitoring of fluoroalkylated substances in Antarctica seabird plasma: Development and validation of a fast and rugged method using on-line concentration liquid chromatography tandem mass spectrometry. *Journal of Chromatography A*, *1513*, 107–117. https://doi.org/10.1016/j.chroma.2017.07.024

Munoz, G., Liu, J., Vo Duy, S., & Sauvé, S. (2019). Analysis of F-53B, Gen-X, ADONA, and emerging fluoroalkylether substances in environmental

and biomonitoring samples: A review. *Trends in Environmental Analytical Chemistry*, *23*, e00066. https://doi.org/10.1016/j.teac.2019.e00066

NTP, N. T., Program, N. T., Dzierlenga, A. L., Blystone, C. R., Herbert, R. A., Janardhan, K. S., Bouknight, S. A., Buccellato, M. A., Cora, M. C., Cristy, T. A., Cunny, H. C., DeVito, M. J., Fostel, J. M., Gerken, D. K., Graves, S. W., Hejtmancik, M. R., Hooth, M. J., King-Herbert, A. P., Kooistra, L. H., … Zmarowski, A. (2022). *NTP Technical Report on the Toxicity Studies of Perfluoroalkyl Carboxylates (Perfluorohexanoic Acid, Perfluorooctanoic Acid, Perfluorononanoic Acid, and Perfluorodecanoic Acid) Administered by Gavage to Sprague Dawley (Hsd:Sprague Dawley SD) Rats (Revised)*. National Toxicology Program.

OECD. (2011). Test No. 201: Freshwater Alga and Cyanobacteria, Growth Inhibition Test. *OECD Guidelines for the Testing of Chemicals, Section 2*. https://doi.org/10.1787/9789264069923-en

OECD. (2022). *Fact Cards of Major Groups of Per- and Polyfluoroalkyl Substances (PFASs)*. OECD. https://doi.org/10.1787/59e7ffc6-en

Okazoe, T. (2009). Overview on the history of organofluorine chemistry from the viewpoint of material industry. *Proceedings of the Japan Academy. Series B, Physical and Biological Sciences*, *85*(8), 276–289. https://doi.org/10.2183/pjab.85.276

Okpanachi, I. Y., Gotan, Y. S., Dauda, S., Otogo, R. A., Samuel, S. A., Iortsuum, D. N., & Chia, M. A. (2025). Combined effect of PFOS and PFOA on phytoplankton interactions and overall community health. *Journal of Plankton Research*, *47*(5), fbaf044. https://doi.org/10.1093/plankt/fbaf044

Renfrew, D., & Pearson, T. W. (2021). *The Social Life of the "Forever Chemical."* https://doi.org/10.3167/ares.2021.120109

Ricolfi, L., Yang, Y., Pottier, P., Morrison, K., Williams, C., Pollo, P., Hesselson, D., Neely, G. G., Taylor, M. D., Nakagawa, S., & Lagisz, M. (2025). Unravelling the magnitude and drivers of PFAS trophic magnification: A meta-analysis. *Nature Communications*, *16*(1), 10720. https://doi.org/10.1038/s41467-025-65746-4

Round, F. E., Crawford, R. M., & Mann, D. G. (1990). *Diatoms: Biology and Morphology of the Genera*. Cambridge University Press.

Sabba, F., Kassar, C., Zeng, T., Mallick, S. P., Downing, L., & McNamara, P. (2025). PFAS in landfill leachate: Practical considerations for treatment and characterization. *Journal of Hazardous Materials*, *481*, 136685. https://doi.org/10.1016/j.jhazmat.2024.136685

Savvidou, E. K., Sha, B., Salter, M. E., Cousins, I. T., & Johansson, J. H. (2023). Horizontal and Vertical Distribution of Perfluoroalkyl Acids (PFAAs) in the Water Column of the Atlantic Ocean. *Environmental Science & Technology Letters*, *10*(5), 418–424. https://doi.org/10.1021/acs.estlett.3c00119

Scheringer, M., Cousins, I. T., & Goldenman, G. (2024). Is a Seismic Shift in the Landscape of PFAS Uses Occurring? *Environmental Science & Technology*, *58*(16), 6843–6845. https://doi.org/10.1021/acs.est.4c01947

Seymour, J. R., Amin, S. A., Raina, J.-B., & Stocker, R. (2017). Zooming in on the phycosphere: The ecological interface for phytoplankton–bacteria relationships. *Nature Microbiology*, *2*(7), 17065. https://doi.org/10.1038/nmicrobiol.2017.65

Shi, J., Hu, M., Xia, Z., Zhang, J., Wang, Z., Li, L., & Zhao, Y. (2024). Influence of perfluoroalkyl substances, with focus on perfluorobutanoic acid on the responding characteristics and molecular mechanisms of *Thalassiosira pseudonana*. *Ecotoxicology and Environmental Safety*, *285*, 117048. https://doi.org/10.1016/j.ecoenv.2024.117048

Sigurbjörnsdóttir, M. A., Andrésson, Ó. S., & Vilhelmsson, O. (2015). Analysis of the Peltigera membranacea metagenome indicates that lichen-associated bacteria are involved in phosphate solubilization. *Microbiology*, *161*(5), 989–996. https://doi.org/10.1099/mic.0.000069

Sigurbjörnsdóttir, M. A., Heiðmarsson, S., Jónsdóttir, A. R., & Vilhelmsson, O. (2014). Novel bacteria associated with Arctic seashore lichens have potential roles in nutrient scavenging. *Canadian Journal of Microbiology*, *60*(5), 307–317. https://doi.org/10.1139/cjm-2013-0888

Silvestrini, A., Meucci, E., Ricerca, B. M., & Mancini, A. (2023). Total Antioxidant Capacity: Biochemical Aspects and Clinical Significance. *International Journal of Molecular Sciences*, *24*(13), 10978. https://doi.org/10.3390/ijms241310978

Simon, M., Grossart, H.-P., Schweitzer, B., & Ploug, H. (2002). Microbial ecology of organic aggregates in aquatic ecosystems. *Aquatic Microbial Ecology*, *28*, 175–211. https://doi.org/10.3354/ame028175

Soares, L. O. S., de Araujo, G. F., Gomes, T. B., Júnior, S. F. S., Cuprys, A. K., Soares, R. M., & Saggioro, E. M. (2025). Antioxidant system alterations and oxidative stress caused by polyfluoroalkyl substances (PFAS) in exposed biota: A review. *Science of The Total Environment*, *977*, 179395. https://doi.org/10.1016/j.scitotenv.2025.179395

Sonne, C., Desforges, J.-P., Gustavson, K., Bossi, R., Bonefeld-Jørgensen, E. C., Long, M., Rigét, F. F., & Dietz, R. (2023). Assessment of exposure to perfluorinated industrial substances and risk of immune suppression in Greenland and its global context: A mixed-methods study. *The Lancet Planetary Health*, *7*(7), e570–e579. https://doi.org/10.1016/S2542-5196(23)00106-7

Sonne, C., Gustavson, K., Bossi, R., Søndergaard, J., Desforges, J.-P., Bonefeld-Jørgensen, E. C., & Dietz, R. (2025). Ubiquitous global use of persistent PFAS threatens Arctic Indigenous peoples for decades to come. *Cell Reports Sustainability*, *2*(3). https://doi.org/10.1016/j.crsus.2025.100341

Stefanac, T., McCrindle, R., McAlees, A. J., Riddell, N., Brazeau, A. L., & Chittim, B. C. (2018). Characterization of Nine Isomers in Commercial Samples of Perfluoroethylcyclohexanesulfonate and of Some Minor Components Including PFOS Isomers. *Environmental Science & Technology*, *52*(17), 9937–9945. https://doi.org/10.1021/acs.est.8b02369

Sun, J., Xing, L., & Chu, J. (2023). Global ocean contamination of per- and polyfluoroalkyl substances: A review of seabird exposure. *Chemosphere*, *330*, 138721. https://doi.org/10.1016/j.chemosphere.2023.138721

Szabados, L., & Savouré, A. (2010). Proline: A multifunctional amino acid. *Trends in Plant Science*, *15*(2), 89–97. https://doi.org/10.1016/j.tplants.2009.11.009

Tartu, S., Bourgeon, S., Aars, J., Andersen, M., Polder, A., Thiemann, G. W., Welker, J. M., & Routti, H. (2017). Sea ice-associated decline in body condition leads to increased concentrations of lipophilic pollutants in polar bears (*Ursus maritimus*) from Svalbard, Norway. *Science of The Total Environment*, *576*, 409–419. https://doi.org/10.1016/j.scitotenv.2016.10.132

Teeling, H., Fuchs, B. M., Becher, D., Klockow, C., Gardebrecht, A., Bennke, C. M., Kassabgy, M., Huang, S., Mann, A. J., Waldmann, J., Weber, M., Klindworth, A., Otto, A., Lange, J., Bernhardt, J., Reinsch, C., Hecker, M., Peplies, J., Bockelmann, F. D., … Amann, R. (2012). Substrate-Controlled Succession of Marine Bacterioplankton Populations Induced by a Phytoplankton Bloom. *Science*, *336*(6081), 608–611. https://doi.org/10.1126/science.1218344

Thomas, M., Cate, B., Garnett, J., Smith, I. J., Vancoppenolle, M., & Halsall, C. (2023). The effect of partial dissolution on sea-ice chemical transport: A combined model–observational study using poly- and perfluoroalkylated substances (PFASs). *The Cryosphere*, *17*(8), 3193–3201. https://doi.org/10.5194/tc-17-3193-2023

Tirichine, L., Rastogi, A., & Bowler, C. (2017). Recent progress in diatom genomics and epigenomics. *Current Opinion in Plant Biology, 36 Genome Studies and Molecular Genetics*, *36*, 46–55. https://doi.org/10.1016/j.pbi.2017.02.001

Tolaymat, T., Robey, N., Krause, M., Larson, J., Weitz, K., Parvathikar, S., Phelps, L., Linak, W., Burden, S., Speth, T., & Krug, J. (2023). A critical review of perfluoroalkyl and polyfluoroalkyl substances (PFAS) landfill disposal in the United States. *The Science of the Total Environment*, *905*, 167185. https://doi.org/10.1016/j.scitotenv.2023.167185

Tréguer, P., Bowler, C., Moriceau, B., Dutkiewicz, S., Gehlen, M., Aumont, O., Bittner, L., Dugdale, R., Finkel, Z., Iudicone, D., Jahn, O., Guidi, L., Lasbleiz, M., Leblanc, K., Levy, M., & Pondaven, P. (2018). Influence of diatom diversity on the ocean biological carbon pump. *Nature Geoscience*, *11*(1), 27–37. https://doi.org/10.1038/s41561-017-0028-x

Trilla-Prieto, N., Dachs, J., Iriarte, J., Berrojalbiz, N., Colomer-Vidal, P., Casas, G., Garcia-Garin, O., Vila-Costa, M., & Jiménez, B. (2025). Accumulation of perfluoroalkyl acids as forever chemicals in Antarctic waters. *Communications Earth & Environment*, *6*(1), 545. https://doi.org/10.1038/s43247-025-02535-3

Turner, J. T. (2015). Zooplankton fecal pellets, marine snow, phytodetritus and the ocean's biological pump. *Progress in Oceanography*, *130*, 205–248. https://doi.org/10.1016/j.pocean.2014.08.005

Underwood, G. J. C., & Kromkamp, J. (1999). Primary Production by Phytoplankton and Microphytobenthos in Estuaries. In *Advances in Ecological Research* (Vol. 29, pp. 93–153). Academic Press. https://doi.org/10.1016/S0065-2504(08)60192-0

US EPA, C. F. P. H. & E. A. (2022, August 6). *IRIS Toxicological Review of Perfluorononanoic Acid (PFNA) and Related Salts (Public Comment and External Review Draft)* [Reports and Assessments]. US EPA. https://iris.epa.gov/document/&deid%3D355409

van Kooten, O., & Snel, J. F. H. (1990). The use of chlorophyll fluorescence nomenclature in plant stress physiology. *Photosynthesis Research*, *25*(3), 147–150. https://doi.org/10.1007/BF00033156

Vasilev, J., Mix, A.-K., Heimerl, T., Maier, U. G., & Moog, D. (2022). Inferred Subcellular Localization of Peroxisomal Matrix Proteins of Guillardia theta Suggests an Important Role of Peroxisomes in Cryptophytes. *Frontiers in Plant Science*, *13*. https://doi.org/10.3389/fpls.2022.889662

Vecitis, C. D., Wang, Y., Cheng, J., Park, H., Mader, B. T., & Hoffmann, M. R. (2010). Sonochemical Degradation of Perfluorooctanesulfonate in Aqueous Film-Forming Foams. *Environmental Science & Technology*, *44*(1), 432–438. https://doi.org/10.1021/es902444r

Vingiani, G. M., Leone, S., De Luca, D., Borra, M., Dobson, A. D. W., Ianora, A., De Luca, P., & Lauritano, C. (2022). First identification and characterization of detoxifying plastic-degrading DBP hydrolases in the marine diatom *Cylindrotheca closterium*. *Science of The Total Environment*, *812*, 152535. https://doi.org/10.1016/j.scitotenv.2021.152535

Wu, H., Huang, X., Duan, X., Lao, A., & Zheng, Z. (2025). Meta-analysis evaluates toxicity of PFAS to microalgae: Mechanisms and ecological risks. *Journal of Hazardous Materials*, *496*, 139328. https://doi.org/10.1016/j.jhazmat.2025.139328

Wu, J., Hua, Z., & Gu, L. (2022). Per-, poly-fluoroalkyl substances (PFASs) and planktonic microbiomes: Identification of biotic and abiotic regulations in community coalescence and food webs. *Environmental Pollution*, *302*, 119078. https://doi.org/10.1016/j.envpol.2022.119078

Wu, J.-Y., Gu, L., Hua, Z.-L., Wang, D.-W., Xu, R.-Y., Ge, X.-Y., & Chu, K.-J. (2022). Removal of Per-, Poly-fluoroalkyl substances (PFASs) and multi-biosphere community dynamics in a bacteria-algae symbiotic aquatic ecosystem. *Environmental Pollution*, *314*, 120266. https://doi.org/10.1016/j.envpol.2022.120266

Xu, D., Chen, X., & Shao, B. (2017). Oxidative Damage and Cytotoxicity of Perfluorooctane Sulfonate on Chlorella vulgaris. *Bulletin of Environmental Contamination and Toxicology*, *98*(1), 127–132. https://doi.org/10.1007/s00128-016-1957-6

Xue, X., Gao, N., & Xu, F. (2022). Toxicity of perfluooctane sulfonate (PFOS) and perfluorobutane sulfonate (PFBS) to *Scenedesmus obliquus*: Photosynthetic characteristics, oxidative damage and transcriptome analysis. *Environmental Pollution*, *315*, 120397. https://doi.org/10.1016/j.envpol.2022.120397

Yin, T., Tran, N. H., Huiting, C., He, Y., & Gin, K. Y.-H. (2019). Biotransformation of polyfluoroalkyl substances by microbial consortia from constructed wetlands under aerobic and anoxic conditions. *Chemosphere*, *233*, 101–109. https://doi.org/10.1016/j.chemosphere.2019.05.227

Zhang, L., Zheng, X., Liu, X., Li, J., Li, Y., Wang, Z., Zheng, N., Wang, X., & Fan, Z. (2023). Toxic effects of three perfluorinated or polyfluorinated compounds (PFCs) on two strains of freshwater algae: Implications for ecological risk assessments. *Journal of Environmental Sciences*, *131*, 48–58. https://doi.org/10.1016/j.jes.2022.10.042

Zhang, X., Lohmann, R., & Sunderland, E. M. (2019). Poly- and Perfluoroalkyl Substances in Seawater and Plankton from the Northwestern Atlantic Margin. *Environmental Science & Technology*, *53*(21), 12348–12356. https://doi.org/10.1021/acs.est.9b03230

Zhao, Z., Zheng, X., Han, Z., Li, Y., He, H., Lin, T., & Xu, H. (2024). Polystyrene microplastics enhanced the effect of PFOA on *Chlorella sorokiniana*: Perspective from the cellular and molecular levels. *Journal of Hazardous Materials*, *465*, 133455. https://doi.org/10.1016/j.jhazmat.2024.133455

Zhao, Z., Zheng, X., Han, Z., Yang, S., Zhang, H., Lin, T., & Zhou, C. (2023). Response mechanisms of *Chlorella sorokiniana* to microplastics and PFOA stress: Photosynthesis, oxidative stress, extracellular polymeric substances and antioxidant system. *Chemosphere*, *323*, 138256. https://doi.org/10.1016/j.chemosphere.2023.138256

Zheng, X., Qiu, J., & Li, A. (2026). Effects of perfluorooctanesulfonic acid on *Thalassiosira minima*: Insights from growth, photosynthesis, oxidative stress, and toxin biosynthesis. *Journal of Hazardous Materials*, *508*, 141960. https://doi.org/10.1016/j.jhazmat.2026.141960

Zhou, Y., Wang, X., Wang, C., Ji, Z., Niu, X., & Dong, H. (2024). Fate of 'forever chemicals' in the global cryosphere. *Earth-Science Reviews*, *259*, 104973. https://doi.org/10.1016/j.earscirev.2024.104973

Zhu, J., Yu, Z., He, L., Cao, X., Wang, W., & Song, X. (2024). Phycosphere bacterial composition and function in colony and solitary *Phaeocystis globosa* strains providing novel insights into the algal blooms. *Marine Pollution Bulletin*, *206*, 116700. https://doi.org/10.1016/j.marpolbul.2024.116700

Peer-reviewed articles

Article I

Per- and polyfluoroalkyl substances (PFAS) in the cryosphere – occurrence, organismic accumulation, ecotoxicological impacts, transformation, and management strategies.

Graphical Abstract

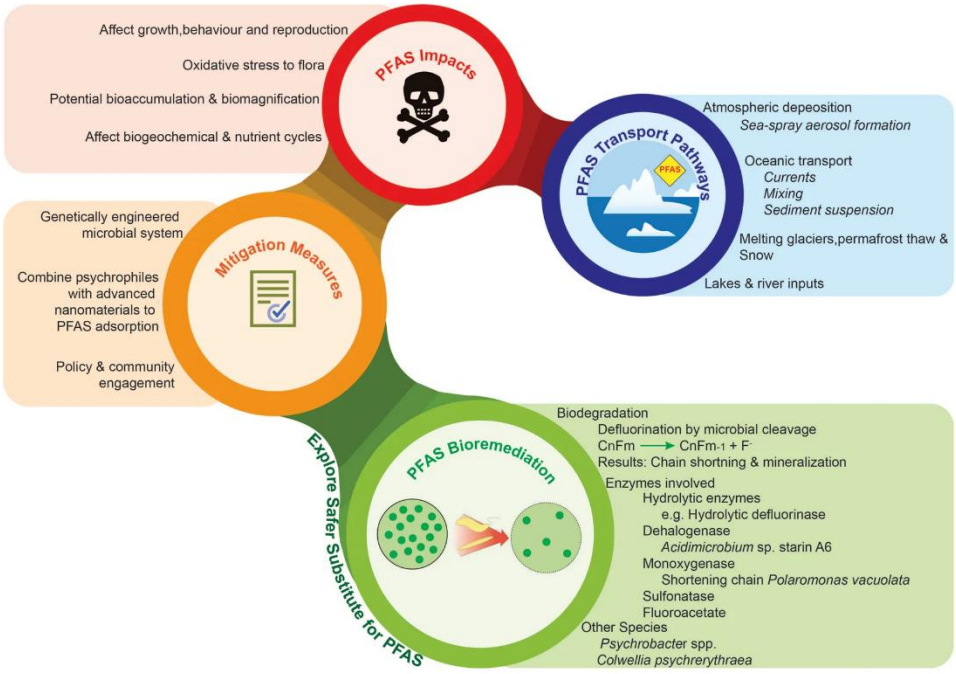

frontiers | Frontiers in Environmental Science

TYPE Review
PUBLISHED 08 April 2025
DOI 10.3389/fenvs.2025.1559941

OPEN ACCESS

EDITED BY
Nsikak U. Benson,
Topfaith University, Nigeria

REVIEWED BY
Manavi Yadav,
New Jersey Institute of Technology,
United States
Duwage Charitha Perera,
New Jersey Institute of Technology,
United States

*CORRESPONDENCE
Ashani Arulananthan,
ashani@unak.is
Bettina Scholz,
bettina@biopol.is

RECEIVED 13 January 2025
ACCEPTED 17 March 2025
PUBLISHED 08 April 2025

CITATION
Arulananthan A, Vilhelmsson OÞ, Karsten U, Grossart H-P, Sigurbjörnsdóttir A, Rolfsson Ó, Joerss H and Scholz B (2025) Per- and polyfluoroalkyl substances (PFAS) in the cryosphere – occurrence, organismic accumulation, ecotoxicological impacts, transformation, and management strategies. *Front. Environ. Sci.* 13:1559941. doi: 10.3389/fenvs.2025.1559941

Per- and polyfluoroalkyl substances (PFAS) in the cryosphere – occurrence, organismic accumulation, ecotoxicological impacts, transformation, and management strategies

Ashani Arulananthan[1,2]*, Oddur Þór Vilhelmsson[1], Ulf Karsten[3], Hans-Peter Grossart[4,5], Auður Sigurbjörnsdóttir[1], Óttar Rolfsson[6], Hanna Joerss[7] and Bettina Scholz[2]*

[1]Faculty of Natural Resource Sciences, University of Akureyri, Akureyri, Iceland, [2]BioPol ehf. Marine Biotechnology, Skagaströnd, Iceland, [3]Institute of Biological Sciences, University of Rostock, Rostock, Germany, [4]Plankton and Microbial Ecology, Leibniz-Institute of Freshwater Ecology and Inland Fisheries, Berlin, Germany, [5]Institute of Biochemistry and Biology, Potsdam University, Potsdam, Germany, [6]Department of Biochemistry and Molecular Biology, Faculty of Medicine, University of Iceland, Reykjavik, Iceland, [7]Institute of Coastal Environmental Chemistry, Helmholtz-Zentrum Hereon, Geesthacht, Germany

The cryosphere faces increasing threats from anthropogenic pollutants, including per- and polyfluoroalkyl substances (PFAS), a class of synthetic chemicals produced in significant quantities and released into the environment for over seven decades. PFAS are widely utilized for their water- and grease-resistant properties in numerous industrial, household, personal care, and medical products. Despite their widespread applications, all PFAS or their degradation and transformation products are environmentally persistent and pose health risks to humans. PFAS are detected ubiquitously, even in remote regions like the Arctic and Antarctica, and they bioaccumulate within polar trophic food chains. The primary transport and transmission mechanisms for PFAS involve atmospheric transport through volatile precursors, atmospheric oxidation, ocean currents, and the formation of sea spray aerosols. Additionally, contamination of surface snow, post-deposition processes in snow, and sediment interactions significantly contribute to PFAS transport. The physical and chemical properties, including density, melting points (Tm), boiling points (Tb), solubility, vapor pressure, electronegativity, low polarizability, chemical stability, and thermal stability, play key roles in determining their environmental fate and transformation. The toxicity of certain PFAS has raised concerns, prompting bans and efforts to develop safer alternatives. Despite increasing public awareness and regulations to limit the production of legacy PFAS, their long-term environmental impacts remain unclear. As global warming accelerates cryosphere shrinkage, which releases PFAS with meltwater, cold-adapted ecosystems and associated biota face unprecedented challenges and uncertainties, particularly regarding the accumulation of non-degradable materials. This situation underscores the urgent need to comprehensively understand the fate of PFAS and adopt

effective management strategies for polar systems. This review summarizes current literature on the transport, distribution, and legacy of PFAS, along with their known ecological impacts, bioremediation potential, and other management options in the cryosphere.

KEYWORDS

PFAS, cryosphere, bioaccumulation, biomagnification, bioremediation, PFAS-phaseout, transformation

1 The cryosphere

The cryosphere, derived from the Greek word "κρῦος" meaning icy cold, encompasses the planet's frozen (solid) water systems found across marine and terrestrial environments. This includes snow, glaciers, lake and river ice, frozen ground and permafrost, the Antarctic and Greenland Ice Sheets, mountain ice caps, ice shelves and icebergs, and sea ice. These environments form a vital part of our planet´s ecosystems and influence Earth´s albedo, surface energy, and moisture fluxes, that in turn impact atmospheric and oceanic circulation patterns (Ásmundsdóttir and Scholz, 2021; NOAA, 2024). These intricate dynamics are increasingly offset by environmental pollutants, alongside the pervasive effects of climate change (Borgå et al., 2022; Bargagli and Rota, 2024; Zhou et al., 2024b).

In the Anthropocene epoch, the Earth's systems have been significantly impacted by rapid industrialization, population growth, deforestation, pollution, and climate change (Zalasiewicz et al., 2019). Global warming, ocean acidification, melting glaciers, and thawing permafrost disrupt cryosphere ecosystems (Sonne et al., 2023; Bargagli and Rota, 2024). Compounding this challenge is environmental pollution that disrupts these fragile systems by altering the long-range transport, remobilization, bioavailability, and fate of persistent contaminants, as this frozen region acts as a storage of various pollutants. When the different forms of the cryosphere melt due to warming, the trapped contaminants are released into the environment and become bioavailable for organisms (Codling et al., 2014; Chen et al., 2019; McGovern et al., 2022; Zhou et al., 2024a). These chemical changes could threaten the survival of cold-adapted organisms and compromise their vital biogeochemical functions in polar ecosystems (Bargagli and Rota, 2024). Per-and polyfluoroalkyl substances (PFAS) are a group of emerging contaminants that raise significant concerns among scientists due to their widespread presence. Their

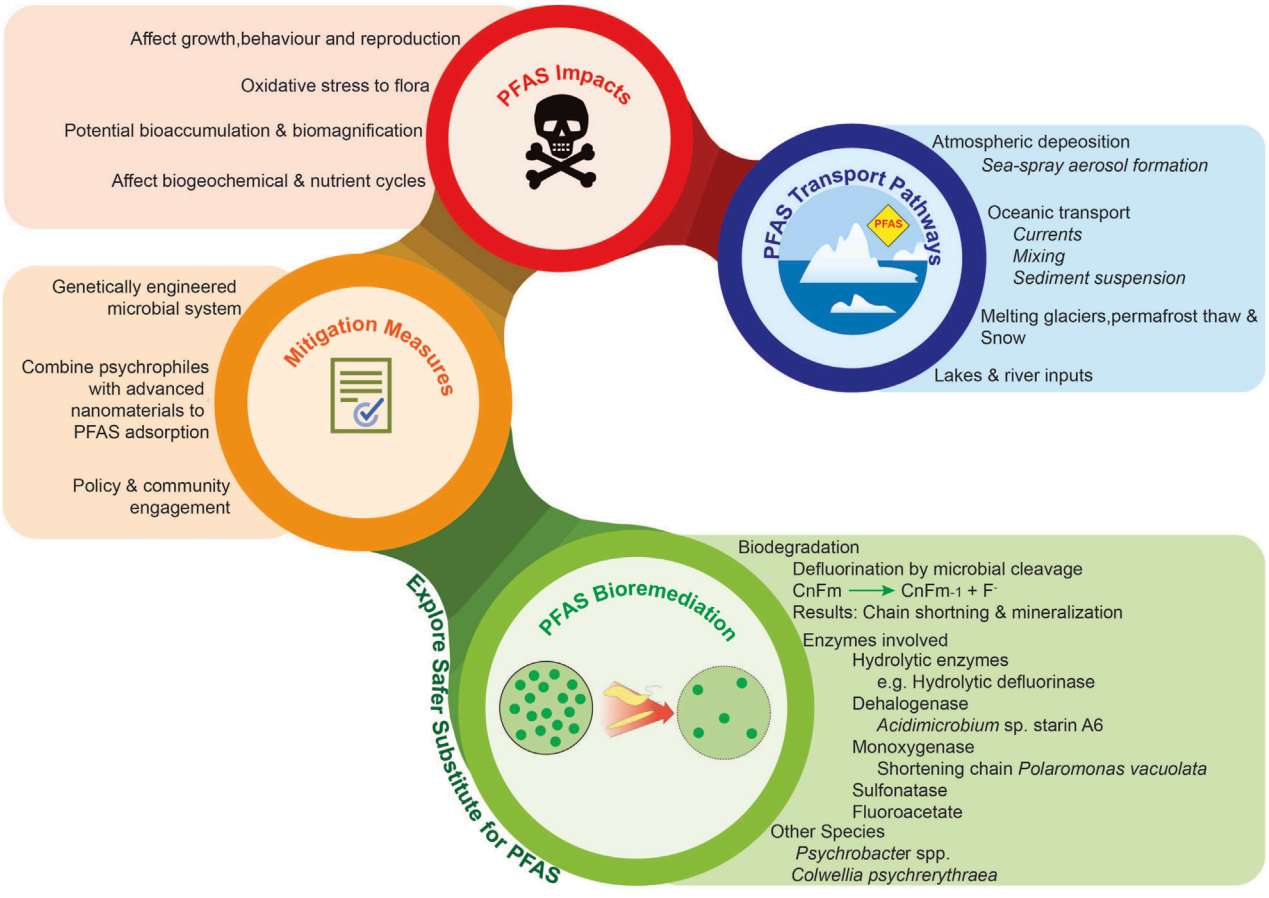

GRAPHICAL ABSTRACT

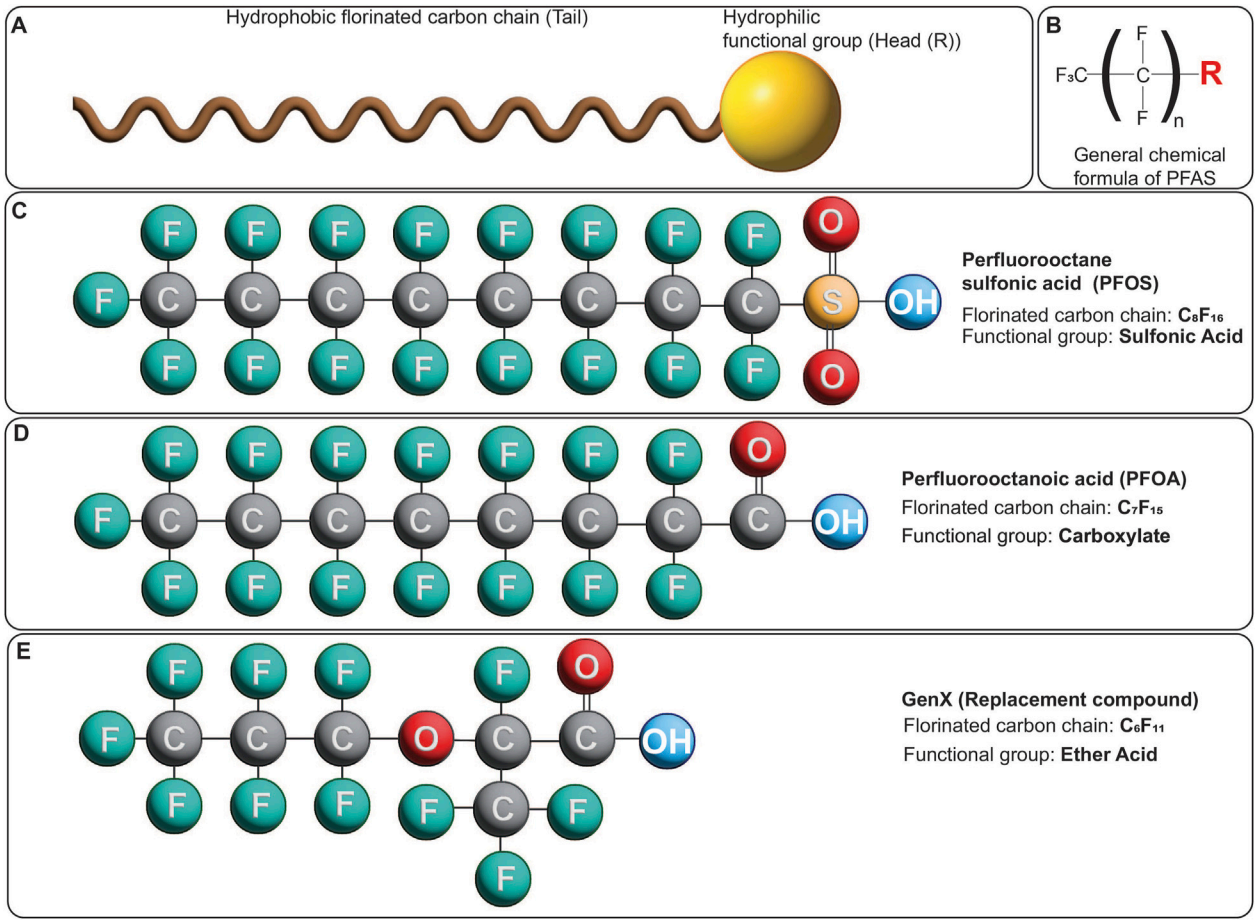

FIGURE 1
(A) Diagram representing the dual chemical nature of PFAS, showing the hydrophilic functional "head" group and the hydrophobic fluorinated carbon chain "tail." **(B)** The basic framework of PFAS is where $C_n F_{2n+1}$ denotes the perfluoroalkyl chain length, and "R" represents the functional group. **(C)** Shown are the example examples of general chemical structures of a fully fluorinated compound and the perfluoroalkane sulfonic acid (PFSA) with the functional group of (SO_3^-) (e.g., PFOS), and **(D)** is the illustration of the chemical structure of a fully fluorinated perfluoroalkyl carboxylic acids (PFCAs) with a functional group of (-COOH) (e.g., PFOA), and **(E)** represents an example of a short chain replacement compound hexafluoropropylene oxide dimer acid (GenX), often used as an alternative to long-chain PFOS and PFOA.

detection in remote regions, from Mount Everest to the Arctic and Antarctic ice cores, demonstrates their long-range transport (Miner et al., 2021; Shan et al., 2021; Ahrens et al., 2023). As such, the integrity of these cold ecosystems is at considerable risk, emphasizing the urgent need for comprehensive measures to mitigate their impacts and protect the integrity of these vulnerable environments.

2 PFAS in the cryosphere: chemical nature, transformation, transport, distribution and occurrence

2.1 PFAS chemical nature and significance

Production of perfluorocarbons can be traced back to the late 19th century, with the synthesis of carbon tetrafluoride, recognized as the simplest perfluorocarbon, being produced in 1886 (Banks and Tatlow, 1986; Okazoe, 2009; Gaines, 2023). Synthesis of PFAS with various functional groups started in the mid-20th century, wherein the application of PFAS was applied as fluoropolymer coatings and materials designed to withstand heat, repel oil, resist stains, and provide protection against grease and water (Meegoda et al., 2020; Hamid et al., 2024). DuPont introduced the first commercial fluoropolymer, polytetrafluoroethylene (PTFE), branded as 'Teflon,' in 1948 (Okazoe, 2009). Shortly after World War II, the Minnesota Mining and Manufacturing Company (3M) began using electrochemical fluorination, leading to the commercial production of fluorocarbons in 1951. This expansion included fluorocarbon derivatives with functional groups like perfluoroethers, perfluoroacyl fluorides, perfluoroalkanesulfonyl fluorides, and perfluorinated amines. These derivatives have played a vital role for corporations, including DuPont, 3M, and W. L. Gore and Associates, which still use them to produce well-known products such as Teflon and Gore-Tex. Subsequently, during the 1960s, DuPont advanced partially-fluorinated polymers, including poly (vinylidene fluoride) (PVDF) and its modified form, polyvinyl fluoride (PVF) (Okazoe, 2009).

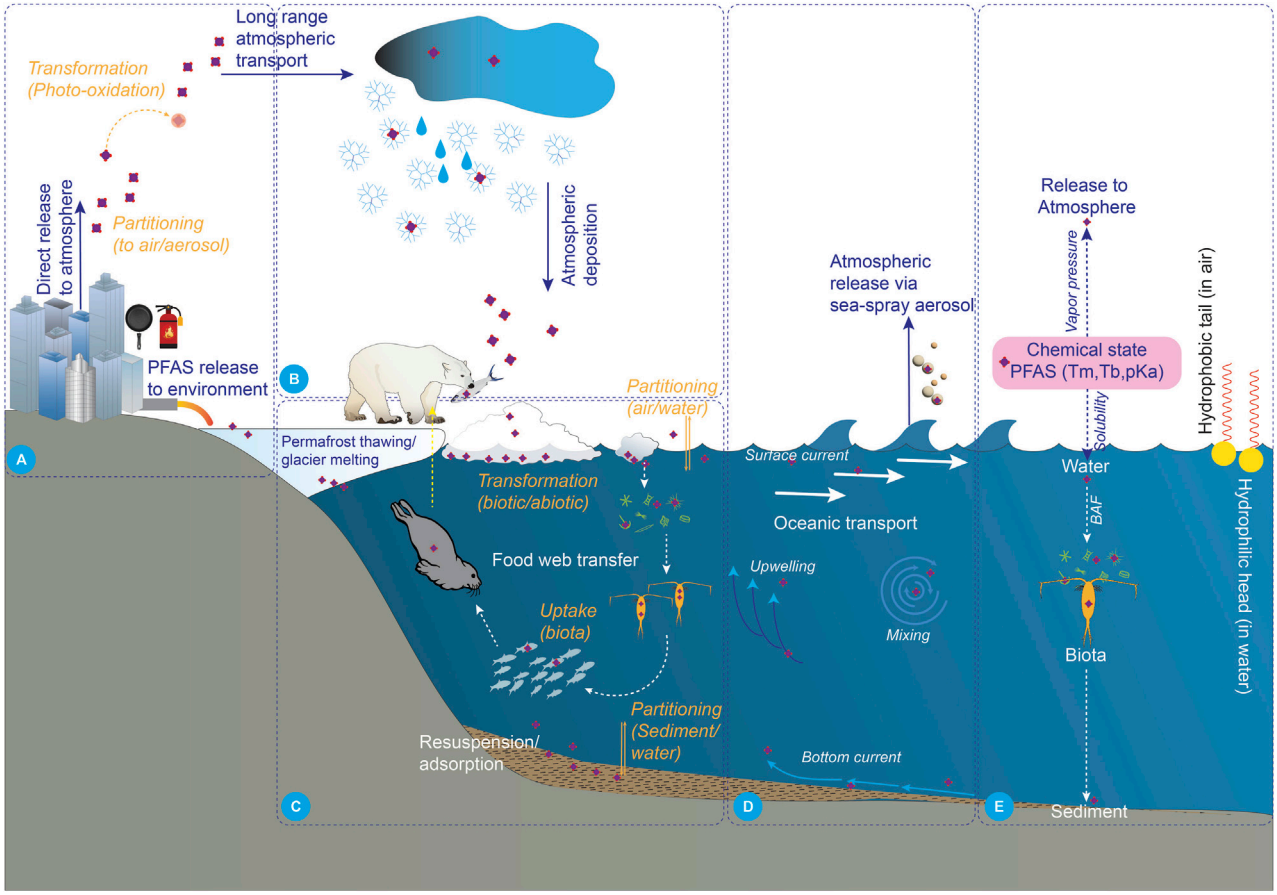

FIGURE 2
Schematic illustration of compound environmental processes influencing the PFAS transformation, fate, transport, and distribution of PFAS in the cryosphere. In the cryosphere, organisms are exposed to PFAS through contaminated water (sea, ice, snow, or glacier meltwater), sediment, and prey, leading to their transfer and magnification through the polar food web. BAF- bioaccumulation factor, the accumulation of PFAS in organisms from both seawater and their diet. **(A)** various sources of PFAS entering the environment., **(B)** Atmospheric transport of PFAS through snow, air, and rain., **(C)** potential entry points of PFAS to the food chain and biomagnification., **(D)** Oceanic transport routes of PFAS., and **(E)** PFAS chemical states influenced by factors, i.e., T_m- melting point, T_b- boiling point, pK_a- acid dissociation constant.

The commercial production of PFAS began in the 1970s with the advent of telomerization, marking the inception of these widely used anthropogenic chemicals (Okazoe, 2009). Due to their persistence, PFAS are often described as "forever chemicals" (Miner et al., 2021; Renfrew and Pearson, 2021; Manojkumar et al., 2023). They are a group of synthetic organofluorine compounds with a fluorocarbon backbone attached to a functional group (Figure 1). PFAS are defined by the presence of at least one fully fluorinated methyl ($-CF_3$) or methylene ($-CF_2$) group, with no hydrogen, chlorine, bromine, or iodine atoms attached to these carbon atoms (Wang Z. et al., 2021).

Polyfluoroalkyl substances are composed of a fluorinated aliphatic backbone, and compared to their hydrocarbon analogs, several hydrogen atoms are replaced by fluorine atoms (Buck et al., 2011). The corresponding perfluoroalkyl substances maintain the same structural configuration, with the distinction being that the chain is completely saturated with fluorine atoms, resulting in a more compact and electronegative demeanor (Buck et al., 2011).

PFAS are amphipathic and, as such, have emulsifying properties, making them excellent surface-active compounds as they interact with water and nonpolar substances (Figure 1). Owing to these attributes, PFAS are extensively utilized in various household products and industrial applications (Gaines, 2023), including waterproof clothing, carpets, furniture, paper, food packaging, heat-resistant non-stick cooking surfaces, and electrical wire insulation. Due to their broad applications, PFAS-based products enter the environment through multiple pathways, such as waste and rainwater, atmospheric deposition, water currents, etc., (Jansson, 2019; Ahrens et al., 2023). They spread globally, even reaching the most remote regions like the Arctic and Antarctica. PFAS have received significant attention due to their ability to travel long distances and documented bioaccumulation from the base of the food chain to apex predators, including polar bears (Khan et al., 2023; Figures 2A–D).

2.2 PFAS phase behavior and transformation

The unique physicochemical properties influence the PFAS' environmental fate and transformation. Key factors such as density, melting points (T_m), boiling points (T_b), solubility, vapor pressure, electronegativity, low polarizability, chemical stability, and

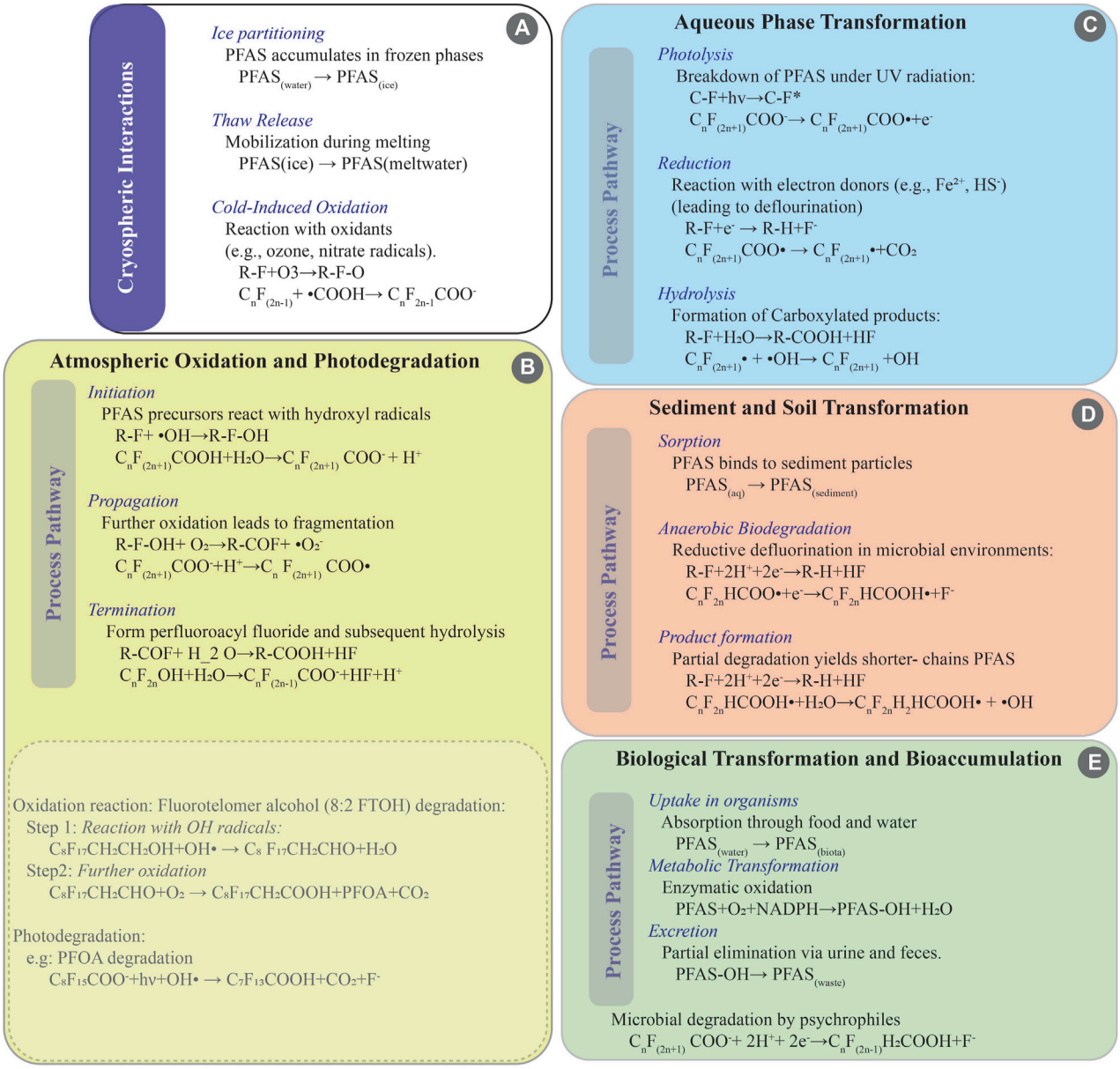

FIGURE 3
Possible transformation and degradation pathways of PFAS in cold environments. The diagram outlines key equations and processes affecting PFAS, i.e., fate and mobilization **(A)**, atmospheric oxidation and photodegradation **(B)**, aqueous phase transformation **(C)**, sediment and soil transformation **(D)**, and biological transformation and bioaccumulation **(E)**. These processes collectively determine PFAS degradation/transformation, distribution, persistence, and potential environmental impacts of PFAS in the cryosphere.

thermal stability dictate their mobility and persistence (Figure 2E; Interstate Technology and Regulatory Council, 2023). Additionally, PFAS can partition into mobile colloids, facilitating their transport across different environmental matrices, a phenomenon relevant in cryosphere environments undergoing freeze-thaw cycles (Garnett et al., 2019; Garnett et al. 2021b; Sherman-Bertinetti et al., 2024).

PFAS mobility can be affected by salinity, pH, organic carbon content, and the presence of polyvalent cations (Nguyen et al., 2020). Cold environments often have unique geochemical conditions, such as acidic soils, permafrost, and glacial sediments, further impacting PFAS behavior. PFAS tend to associate the air-water interface with organic matter hydrophobically and form an electrostatic connection with charged surfaces (Interstate Technology and Regulatory Council, 2023). This is relevant in cold environments where organic matter is preserved in permafrost, thereby PFAS potentially affecting its mobility (Figure 2E).

PFAS density influences their behavior as dense, non-aqueous phase liquids or remain dissolved in water (Figures 2E, 3A). High-density PFAS, like 4:2 Fluorotelomer alcohol (FTOH) (1.59 g/cm^3), can sink downward through the water column, potentially accumulating in deep-sea sediments. Volatile precursors undergo oxidation, converting into persistent perfluorooctanoic acid (PFOA) and perfluorooctanesulfonic acid (PFOS), leading to secondary contamination (Figures 3B–D; Ellis et al., 2004; Interstate

Technology and Regulatory Council, 2023). Their higher vapor pressure allows them to exist in the gases, increasing their potential for long-range atmospheric transport (Hartz et al., 2023). The breakdown of 8:2 FTOH in the atmosphere has been linked to PFOA in Arctic summers due to increased photochemical activity (Van de Vijver et al., 2003). This illustrates the role of atmospheric degradation of FTOH into persistent PFCAs, including PFOA and PFNA (Figure 3B).

Sea ice formation concentrates long-chain (C8-C12) PFAS in surface layers, enriching them up to threefold compared to short-chain (C4-C7) and sodium chloride (NaCl). As seawater freezes, expelled salts create brine channels that concentrate with PFAS. This partitioning process plays a key role in PFAS accumulation (Garnett et al., 2021a).) While some PFAS can form floating separate-phase layers, this behavior is primarily due to their surface activity rather than density alone (Figure 3A). This can enhance PFAS deposition in polar snowpacks and ice layers (Hartz et al., 2024). Factors like melting ice and snow, temperature changes, and sunlight durations also significantly affect the PFAS incorporation into air, water, and sediment (MacInnis et al., 2019b). For hexafluoropropylene oxide dimer acid (HFPO-DA: GenX), deposition in surface snow was notably higher during periods of continuous daylight, suggesting that sunlight-driven atmospheric degradation processes play a significant role in their formation and deposition (Hartz et al., 2024).

Cold condensation effects allow PFAS with low boiling points to volatilize and undergo long-range atmospheric transport before condensing in colder regions, known as global distillation. This is evidenced with the presence of short-chain PFAS and volatile precursors like FTOH in Arctic and Antarctic environments (Garnett et al., 2022). Moreover, PFAS with high melting points for long-chain PFAS, such as perfluortetradecanoic acid (PFTeDA), melting at 130°C–135°C, and chlorinated polyfluorinatedether sulfonic acid (Cl-PFESA), tend to sorb onto ice and snow, delaying the release until thawing occurs. This results in seasonal (summer) pulses of PFAS contamination into Arctic waters (Garnett et al., 2021b).

Acid dissociation constants (pK_a) influence PFAS'sPFAS solubility and bioavailability (Interstate Technology and Regulatory Council, 2023). Low pK_a PFAS, such as perfluorobutanoic acid (PFBA), perfluorohexanoic acid (PFHxA), and PFTeDA, exist almost entirely in their ionic form, increasing their mobility in Arctic waters and, leading to uptake by marine organisms (Joerss et al., 2020). PFBA (T_m is −17°C) has been detected at high concentrations (53% of total PFAS measured) in Svalbard meltwater, indicating a potential risk for polar biota (Ahrens et al., 2023). Neutral or weakly acidic PFAS such as polyfluorinated alkyl phosphoric acid esters (PAP) and FTOH cross the cell membranes before undergoing transformation and bioaccumulation (Wang et al., 2015b; Xie et al., 2015). They also partition into organic matter and lipid-rich marine organisms, thereby increasing long-term exposure (Gebbink et al., 2016; Xie and Kallenborn, 2023; Feng et al., 2024).

2.3 PFAS transport and distribution

PFAS concentrations vary geographically and are influenced by human population density and proximity to urbanized regions and landfills (Wee and Aris, 2023). These spatial differences suggest that PFAS distribution results from biological and geographical factors, as the latter alone do not fully account for concentration variations.

Their environmental fate, such as bioavailability, potential entry into the marine food web (Figure 2), and broader dispersal, is shaped by Arctic ocean surface conditions, air and water circulation patterns, and temperature-dependent physical-chemical characteristics like vapor pressure and partitioning coefficients (Lamon et al., 2009). While horizontal transport via surface currents is the primary mechanism for most PFAS, certain compounds- such as perfluorodecanoic acid (PFDA) and PFOS precursors, exhibit notable vertical fluxes through sediment resuspension, upwelling, and mixing, underscoring the need to consider multiple transport processes when assessing the distribution of PFAS (Figure 2D; Zhang et al., 2017).

2.3.1 Currents of contamination: PFAS in oceanic pathways

Ocean currents serve as a slow but significant pathway for the long-range transport of PFAS, gradually moving these pollutants from industrial areas to remote Arctic regions over decades (Joerss et al., 2020). This process contributes to the steady accumulation of PFAS, particularly long-chain compounds in the cryosphere regions (Ahrens et al., 2023; Hartz et al., 2023). Oceanic transport of PFAS to the Arctic cryosphere is substantial, with significant mass flows reported through key gateways like the Fram Strait (Joerss et al., 2020).

Global ocean models, such as the Berkeley-Trent Global Model (BETR), have shown that ocean currents are the primary transport route for PFOA-like long-chain PFCAs to enter polar waters (Armitage, 2009; Stemmler and Lammel, 2010). For example, the Norwegian Sea is a major PFAS pathway, particularly for PFOA, which moves northward into the Arctic (Stemmler and Lammel, 2010). Similarly, in the Mid-Atlantic, PFAS concentrations remain highest in surface waters, as isolation from deeper layers creates a long residence time in warmer surface currents like the Gulf Stream and North Atlantic drift. In contrast, PFAS levels in the South Pacific Ocean are low from surface to depth, reflecting limited inputs and influence from older, deep currents (Stemmler and Lammel, 2010).

2.3.2 Oceanic transport and impact on PFAS storage in the cryosphere

The cryosphere serves as both a PFAS reservoir and a secondary contamination source. Less volatile PFAS are deposited via aerosols, accumulating in water bodies, sediments, marine ice, and vegetation through cold trapping (Bengtson Nash et al., 2010; Wild et al., 2015; Sha et al., 2022; Egas et al., 2023; Xie and Kallenborn, 2023). Increased melting glaciers due to climate change may release previously trapped PFAS into the Arctic waters. This contamination effect is compounded by the weakening of the Atlantic Meridional Overturning Circulation (AMOC), which alters the distributional dynamics of PFAS in the oceans (Zhang et al., 2017).

The Arctic Ocean is predicted to become a significant PFOS reservoir, potentially storing between 63 and 180 t in the future (Yeung et al., 2017). Moreover, long-chain and emerging short-chain PFAS show significant temporal changes and are transported by ocean currents, resulting in consistent exposure over time within

environmental matrices (Ahrens et al., 2023). The shift from long-chain to short-chain PFAS production in recent years has altered the types of PFAS reaching the Arctic. With rapid atmospheric responses to industrial changes, the Arctic is experiencing higher concentrations of short-chain PFAS alongside legacy compounds like PFOA and PFOS, despite their phase-out in 2020 and 2009 (ECHA, 2024). Although certain PFAS precursors have decreased due to reduced production, recent studies indicate that PFAS levels have stabilized since around 2009–2010, suggesting ongoing exposure through ocean currents (Routti et al., 2017).

2.3.3 Atmospheric transport

Due to their persistent nature and capacity for long-range atmospheric travel, PFAS depositions occur in remote Arctic regions. This process may occur over days to weeks, making it a relatively rapid mechanism for distributing PFAS, particularly for short-chain PFAS and their volatile precursors (Wania, 2007; Blévin et al., 2017). Volatile precursors of PFAS, such as FTOH, are known to travel considerable distances before degrading into stable compounds like PFCAs (Van de Vijver et al., 2003).

In Antarctica, the atmospheric delivery of FTOH-derived ionic PFAS is influenced by wind patterns and the rate of FTOH oxidation, which has a modest yield of stable PFAS (3%–10%) (Wania, 2007). Estimates suggest that about 40% of North American FTOH production has been linked to ionic PFAS contamination in Canadian Arctic ice caps, emphasizing atmospheric pathways as primary sources of PFAS in these regions (Young et al., 2007). Casas et al. (2023) reported a higher concentration of per- and polyfluoroalkyl acids (PFAA) in snow, emphasizing the role of atmospheric deposition in introducing PFAA to Antarctica, as demonstrated by their presence in aerosols, rain, snow, and small lakes.

Laboratory and modeling studies highlight that sea spray aerosols (SSA) are a significant source of PFAS in the atmosphere and are capable of long-range transport (Reth et al., 2011; Johansson et al., 2019; Casas et al., 2020). While SSA formation and organic matter enrichment are understood, field data on PFAS concentrations in marine sea surface microlayers, crucial for aerosol formation, is limited. More field measurements are needed to enhance our understanding of PFAS emission and transport dynamics through SSA-mediated processes (Ju et al., 2008; Figure 2).

Seasonal variations in PFAS concentrations of PFAS indicate that atmospheric oxidation is a critical contributor to Arctic contamination (Young et al., 2007). High levels in winter are likely linked to increased deposition events that gather PFAS on glaciers, frozen lakes, and streams (Muir et al., 2019). Snow pit samples from the high Arctic ice caps further confirm these atmospheric deposition patterns (Hartz et al., 2023).

2.3.4 Snow, glacial meltwater, and permafrost thaw as PFAS transport vectors

Snow and glacial melt water are crucial pathways for contaminant transport in cryosphere regions. As an effective scavenger, snow captures PFAS from atmospheric deposition, leading to contamination even in remote polar, the Tibetan Plateau, and the Alps regions (Benskin et al., 2011; Wang et al., 2014; Pickard et al., 2018; Casal et al., 2019; Chen et al., 2019; Skaar et al., 2019; Wang et al., 2019). The interplay of atmospheric deposition, meltwater mixing, and permafrost thaw accelerates the spread of PFAS (Vonk et al., 2015; Gruber et al., 2017; Jones et al., 2022). The Antarctic "snow amplification effect" demonstrates how snow scavenges persistent organic pollutants (POP), including PFAS, from the atmosphere, which are later released into seawater during snowmelt (Casal et al., 2019; Casas et al., 2020; Casas et al., 2023).

Warming-induced snow and glacier melt contribute to remobilizing both recently deposited and legacy PFAS, leading to increased contamination of freshwater and marine environments. Elevated PFAS concentrations have been documented in soils, permafrost layers, and lake sediments downstream from glaciers (Chen et al., 2019; MacInnis et al., 2019b; Zhou et al., 2024a). Recent studies indicate that freshly deposited snow in Antarctica contained higher concentrations of PFCA compared to coastal seawater, with a concentration ratio ranging from one to over 30 ratios, increasing with the alkylated chain length of PFAS (Casal et al., 2017a; Casas et al., 2023; Bargagli and Rota, 2024). Similarly, in the Lake Hazen watershed, Canada, higher PFAS concentrations were detected upstream, indicating snowmelt as the primary transport mechanism integrating inputs from atmospheric sources and permafrost thaw (MacInnis et al., 2022; Figures 2B, D).

Recent studies have also detected novel PFAS compounds in the Arctic and Antarctica, such as HFPO-DA and fluorotelomer sulfonates (6:2 and 8:2 FTS). These compounds were substitutes for traditional PFAS like PFOS and PFOA (Zhou et al., 2024a). In Antarctica, 16 PFAS were measured in snow samples collected at the Dome C ice core drilling station (French/Italian Station Dome Concordia, Wilkes Land, East Antarctica) in the summer of 2016, with PFOA identified as the dominant compound, followed by perfluoroheptanoic acid (PFHpA), perfluorohexanoic acid (PFHxA), and perfluoropentanoic acid (PFPeA). Long-chain PFCA (C9-C14) represented 10% of the total PFCA content, while PFOS, perfluorobutane sulfonate (PFBS), and PFHxS were the predominant PFSA. Notably, HFPO-DA (4.7–13.0 pg/L) was detected in Antarctic snow for the first time (Xie et al., 2015). In high-Arctic ice cores, PFOA (66 pg/L) detected in ice cores during 1977–2015 have been regarded as the background levels, likely resulting from atmospheric deposition (Pickard et al., 2018; Joerss et al., 2020).

2.3.5 PFAS trapped in sea ice and released when it melts

Sea ice is a critical reservoir and transport vector for PFAS and POP. During winter, sea ice acts as a seasonal "sink," accumulating PFAS and other contaminants. Early models predicted that the decline of sea ice and subsequent increases in open water would enhance the exchange of chemicals between the atmosphere and ocean surface waters, raising exposure levels in marine environments (Stemmler and Lammel, 2010; Dunn et al., 2024). However, recent research revealed that PFAS behavior in sea ice involves complex interactions between contaminant retention, seasonal ice dynamics, and environmental release processes (Yeung et al., 2017; Hartz et al., 2023).

Various types of PFAS have been detected in ice and water samples at different concentrations from the cryosphere (Figure 4). For instance, PFBA was the dominant PFAS in the ice of Canadian

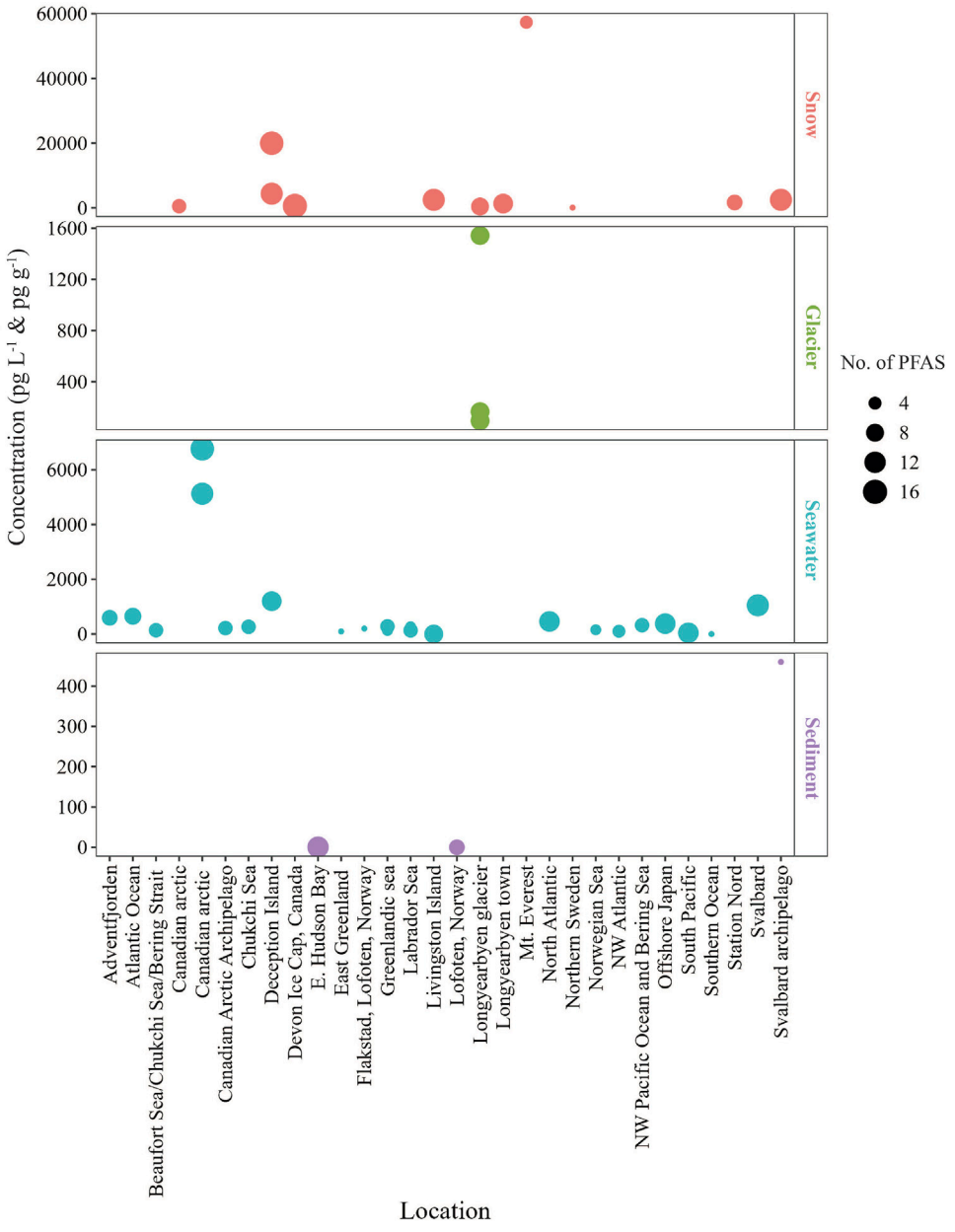

FIGURE 4
PFAS levels in distinct cryosphere compartments across diverse geographic regions summarized based on the literature (Young et al., 2007; Yamashita et al., 2008; Benskin et al., 2012; Zhao et al., 2012; Kwok et al., 2013; Codling et al., 2014; Pickard et al., 2018; MacInnis et al., 2019a; Muir et al., 2019; Skaar et al., 2019; Miner et al., 2021; Ahrens et al., 2023; Casas et al., 2023). The right-side legend shows the number of PFAS analyzed in each sampling location (Supplementary Table S1).

Lake Hazen in 2013 and 2014, followed by PFNA, PFOA, and PFDA (MacInnis et al., 2019a). Recently, a large number of PFAS were detected in an ice core from the Lomonosovfonna ice cap on Svalbard in the Arctic, where short-chain PFAS, such as trifluoroacetic acid (TFA), perfluoropropionic acid (PFPrA) and PFBA dominated atmospheric deposition fluxes. These findings align with similar results from Canada's High Arctic (Pickard et al., 2018; Hartz et al., 2023). Interestingly, the occurrence of long-chain PFAS, like perfluorododecanoic acid (PFDoDA) and perfluorotridecanoic acid (PFTrDA), was substantially higher in the Lomonosovfonna ice core (82%) compared to the Devon Ice Cap core, Canada (13%) (von Appen, 2018). Additionally, in both polar regions, glacier melting and sea ice retreat serve as secondary sources of PFAS, releasing previously deposited contaminants back into the environment as ice and snow thaw (Xie and Kallenborn, 2023).

2.3.6 Regional dynamics and barriers in PFAS oceanic distribution

PFAS concentrations reported from various studies show notable variations influenced by oceanic circulation. For instance, PFAS levels decreased from high-emission zones in Northern

TABLE 1 Compiled studies of documented PFAS contamination profiles in cryosphere environments.

No.	Habitat/location	PFAS type	PFAS concentrations	Sample matrices	Detection method	Reference
1	Ny-Ålesund, Svalbard	12 neutral PFAS	Arctic atmosphere: ΣnPFAS 6.7–39 pg m^{-3} (mean: 17 pg m^{-3}) Snow: ΣnPFAS 334–692 pg/L with an average value of 523 pg/L	air and fresh snow	GC-MS/MS	Xie et al. (2015)
2	Coastal Livingston Island (Maritime Antarctica)	8 types of PFSAs and 14 types of PFCAs	Freshly deposited snow: 760–3,600 pg/L (∑PFAS) Background surface snow: 82–430 pg/L (∑PFAS) Seawater: 94–420 pg/L (∑PFAS) Plankton: 3.1–16 ng/g dw (∑PFAS)	fresh snow deposition, surface snow, streams from melted snow, coastal seawater, and plankton samples	LC-MS/MS	Casal et al. (2017b)
3	Antarctica Deception Island and Livingston Island	several PFAAs	PFAA: 240–2,100 pg/L, PFOS: 1,1–30 pg/L	Snow and coastal water surfaces	LC-MS/MS	Casas et al. (2023)
4	Larsemann Hills, East Antarctica	15 types of PFAS	∑PFAS was 193 pg/L, dominant was PFOA (mean 55.7 pg/L)	Surface waters (ice-melting lakes)	LC-MS/MS	Shan et al. (2021)
5	Livingston Island, South Shetland Islands, Antarctica	12 types of PFAS	∑PFAS in SW averaged 313 pg/L, ranging from 185 pg/L to 509 pg/L. SML- 447 pg/L, SSA-0,67 pG/L	Surface seawater (SW), sea-surface microlayer (SML), sea-spray aerosol (SSA)	LC-MS/MS	Casas et al. (2020)
6	North Sea to Southern Arctic Ocean	PFOS, PFOA, PFNA, PFDA, PFHxA, PFHpA, PFUnDA, PFTrDA, PFDoA	Σ9PFAS on average and up to 4.4 μg/kg dry weight	Sediment top layer	LC-MS/MS	Boitsov et al. (2024)
7	Greenland Sea, the East Atlantic Ocean, and the Southern Ocean	15 types of PFAS including C4–C10 PFSAs, and C5, C6, and C8–C16	ΣPFAS in the North Atlantic Ocean 130–650 pg/L. Greenland Sea, the ΣPFAS from 45 to 280 pg/L	Marine surface water samples	LC-MS/MS	Zhao et al. (2012)
8	Qiangyong Lake and Pumoyong Lake, on the Tibetan Plateau	PFOA, PFOS, PFBS, PFBA and other PFAS	ΣPFAS 421–665 pg/g dry weight	Proglacial river sediment	LC-MS/MS	Zhou et al. (2024a)
9	Nyainqȇntanglha Mountain Range, a central part of the Tibetan Plateau	PFBA, PFBS, PFPeA, PFOA, PFHpA, PFNA, PFDA	Concentration of PFAAs in snow PFBA > PFBS > PFPeA ≈ PFOA PFAA: 1,413 pg/L in glacial ice 1,277 pg/L in meltwater runoff 980 pg/L for lake water, and 616 pg/L for rain	glacial snow/ice, glacial runoff, nonglacial runoff, precipitation, and lake water	LC-MS/MS	Chen et al. (2019)
10	High and Low Arctic Lakes, Canada	PFOA, PFDA, PFBS, PFOS, PFNA, PFHpA, PFUnDA, PFECHS	ΣPFAS 0.006–0.161 ng/g	Lake sediment points receive glacial meltwater inputs, surface runoff, and thaw (i.e.,,permafrost)	LC-MS/MS	MacInnis et al. (2019b)
11	Mt.Everest	PFOS, PFOA, PFHxA	Snow samples PFAS, 26.14 ng/L, Meltwater ranged from 0.64 ng/L to 4 ng/L	Mt.Everest snow and glacier meltwater	LC-MS/MS	Miner et al. (2021)
12	Arctic Svalbard Ice core	26 types of PFAS	PFCA: 2.5–8,200 ng m^{-2} $years^{-1}$ (9.51–16,500 pg L^{-1})	Svalbard ice cores	SFC - MS/MS and LC-MS/MS	Hartz et al. (2023)
13	Arctic Fjords, Svalbard	PFOA at six different locations	Ranged between 0.14 ng/g to 6.54 ng/g	Sediment samples	LC-MS/MS	Saritha et al. (2023)
14	Arctic Svalbard, Norway	PFBA, PFHxA, PFHpA, PFOA, PFNA, PFDA, PFDoDA, PFUnDA, PFBS	5–6 ng/L in seawater, 4 ng/L in meltwater, PFOS was dominant	Seawater, meltwater run-off, surface snow, and coastal sediment samples	LC-MS/MS	Skaar et al. (2019)
15	Arctic regions Greenland Sea North Sea Norwegian Sea	11 PFAS types HFPO-DA, C6 to C12 PFCAs, PFBS, PFBHxS, L-PFOS/Br-PFOS	PFAS ranged from Greenland Sea-140 pg/L to North Sea-340pg/L	Surface seawater	LC-MS/MS	Joerss et al. (2020)
16	West China	16 types of PFAS	ΣPFAS ranged from 879 to 3,974 pg/L	Surface snow	LC-MS/MS	Wang et al. (2019)

(Continued on following page)

TABLE 1 (*Continued*) Compiled studies of documented PFAS contamination profiles in cryosphere environments.

No.	Habitat/location	PFAS type	PFAS concentrations	Sample matrices	Detection method	Reference
17	Antarctic ice core	12 types of PFAS (C5-C14 PFCA, C6/C8 PFSA	0.5–100 ng/L	Waters samples	LC-MS/MS	Shi et al. (2015)
18	Svalbard west coast of Spitsbergen in the Svalbard archipelago, Arctic	22 Types of PFAS. Dominant types: PFBA in freshwater; PFCAs in snow and surface water; PFSA and 6:2 FTSA in water and soil	ΣPFAS in meltwater 6.5 ± 1.4 ng/L, surface snow 2.5 ± 1.7 ng/L, freshwater 2.3 ± 1.1 ng/L, seawater 1.05 ± 0.64 ng/L, lake sediments 0.084 ± 0.038 ng/g	Water, snow, sediment, and soil samples	LC-MS/MS	Ahrens et al. (2023)
19	Adventfjorden, Svalbard, Arctic	15 types of PFAS, most common were PFOA, PFNA, PFDA, PFUnDA, L-PFOS, PFHxA, PFUnDA	ΣPFAS in snow: 18.70 ng/L	Ice core, glacier, melted glacier, surface snow	LC-MS/MS	Ali et al. (2021)
20	Svalbard, Arctic	PFOA, PFNA, PFBA, PFUnDA, PFOS, PFPeA, FHxSA	Σ20PFAS in Arctic soil: 0.12–4.84 ng/g, sediment: 0.15–0.93 ng/g, biota: 0.0049–2.62 ng/g	Arctic soil, sediment, biota	LC-MS/MS	Dai et al. (2025)
21	Lomonosovfonna, Svalbard, Arctic	26 types of PFAS	ΣPFCA 9.51–16500 pg/L, PFOS: 195 pg/L, PFHxS: 28.3 pg/L, PFBS: 28.4 pg/L, 6:2 FTSA: 14.1 pg/L	Ice cores	LC-MS/MS	Hartz et al. (2023)
22	Mt.Oreles, Alps, Italy	12 types of PFAS	ΣPFAS ranged from 1 ng/L to 5.8 ng/L, abundant PFAS., PFOA: 0.1–0.9 ng/L, PFBA: 0.3–1.7 ng/L, PFNA: 2.1 ng/L	Glacier firn core	GC-MS	Kirchgeorg et al. (2016)
23	Klippitztorl, Austria	16 types of PFAS	ΣPFAS ranged <1.7 bg/L to 143 ng/L in snow melt, <0.62–5.35 ng/g in soil, <1.89 and 874 ± 240 ng/g in ski wax	Ski wax, snowmelts, and snow from skiing sites	LC-MS/MS	Müller et al. (2023)
24	Mt.Oxford, Ellesmere Island, Canada	15 types of PFAS and GenX	PFCA: up to 316 ng/m^2/area, PFOA From the detected high < 2.33 ng/L, similar amount of PFNA, PFDA > PFPeA, PFHpA > PFHxA > PFUnDA > PFDoA, GenX below the detection limit. PFSA: average 13 ng/m^2/area, but elevated levels of PFOS and PFBS up to 471 ng/m^2/area in pre-1990s samples	Ice core	LC-MS/MS	Persaud et al. (2024)

GC-MS/MS: gas chromatography-tandem mass spectrometry, LC-MS/MS: liquid chromatography-tandem mass spectrometry, SFC-MS/MS- supercritical fluid chromatography-tandem mass spectrometry.

Europe toward the South Atlantic due to dilution and circulation effects (Joerss et al., 2020; Ahrens et al., 2010).

Regional studies underscore the impact of ocean currents on PFAS distribution in polar regions, where the Arctic experiences higher PFAS accumulation than Antarctica. Concentrations declined from the North Sea continental shelf toward the Norwegian Sea, and only PFOS was detected in the Antarctic circumpolar current zone (Bengtson Nash et al., 2010). However, several studies reported the presence of PFAS in remote regions of Antarctica (Figure 4; Table 1) (Bengtson Nash et al., 2010; Wild et al., 2015; Shan et al., 2021; Casas et al., 2023). Though oceanic currents mainly facilitate the transport of PFAS on a global scale, the Antarctic circumpolar currents act as a barrier, limiting the influx of PFAS from northern marine regions to the Southern Ocean (Bengtson Nash et al., 2010; Stemmler and Lammel, 2010; Benskin et al., 2012). Quantitative estimates suggested that approximately 123 t of PFAS flow annually into the Arctic Ocean from the North Atlantic, with 110 t returning to the Atlantic (Dunn et al., 2024). This pattern highlights an extensive and ongoing circulation of PFAS within northern waters, impacting surface and deeper ocean layers (Sha et al., 2022).

2.4 PFAS transformation and degradation pathways in the cryosphere

2.4.1 Atmospheric oxidation and photodegradation

PFAS, particularly volatile PFAS precursors, such as FTOH and perfluoroalkyl sulfonamides (FASA), undergo oxidative transformation in the atmosphere. These reactions are primarily driven by hydroxyl radicals ($^{\bullet}$OH) and photochemical processes, particularly during the polar summer when sunlight exposure is prolonged (Garnett et al., 2019; Hartz et al., 2024; Figure 3B). Oxidation leads to the formation of PFCAs, such as PFOA and PFNA, which are more persistent and water-soluble, facilitating their deposition in cold environments. The yield of long-chain

PFCA is higher in remote areas due to low NOx conditions, which are typical for cold areas (Sulbaek Andersen et al., 2005; Young et al., 2007).

PFOA undergoes degradation via photochemical oxidation initiated by UV radiation. This process is enhanced by high snow reflectivity (albedo)) of snow, increasing UV penetration during the Arctic summer, and the presence of ice-induced reactive species ($OH^{\cdot}$, $HO^{\cdot}_2$). The secondary products of FTOH oxidation, such as PFOA, PFNA, and PFDA, can enter seawater via wet and dry deposition and subsequently undergo sea spray aerosol (SSA), acting) which act as a re-emission pathway for these PFAS into the atmosphere. However, FTOH atmospheric oxidation is a chemical transformation process, while SSA is a physical process of PFAS from seawater to the atmosphere via bubble bursting and wave action (Figure 2).

2.4.2 Aqueous phase transformation

In cold environments, PFAS transformation exhibits slow reaction kinetics as it can be influenced by unique low temperatures and more prolonged UV exposure in summer. These factors affect the rates and pathways of PFAS degradation (Figure 3C). PFAS can undergo direct photolysis when exposed to UV radiation, leading to cleavage of carbon-fluorine bonds (C-F) (Xin et al., 2023). Therefore, the photolysis rate and its extent are influenced by the molar absorptivity of particular PFAS compounds.

The reduction process involves reactions where PFAS molecules gain electrons, leading to fluorination. In cold environments, the presence of electron donors such as ferrous ions (Fe^{2+}) or bisulfide (HS^{-}) can facilitate such chemical reactions. Exposure to artificial UV-C can induce PFAS degradation of PFAS, by generating hydrated electrons that can attack PFAS molecules, resulting in the cleavage of C-F bonds with subsequent defluorination (Yin and Villagrán, 2022).

Hydrolysis involves the reaction of PFAS with water, leading to the formation of carboxylated products. While PFAS are generally resistant to hydrolysis due to the strength of the C-F bonds, certain precursor compounds can undergo hydrolytic transformation under specific environmental conditions. For example, perfluorooctane sulfonyl fluoride (POSF) can hydrolyze to produce PFOS. The hydrolysis reactions can be influenced by temperature, pH, and the presence of catalysts (Interstate Technology and Regulatory Council, 2023).

2.4.3 Sediment and soil transformation

Permafrost thaw significantly influences the transport of PFAS in Arctic freshwater systems and soils (Schuur et al., 2015). Mostly, permafrost acts as a reservoir for airborne PFAS, and climate-induced thawing now transforms these frozen aquatic systems into a source of PFAS pollution (Gruber et al., 2017; MacInnis et al., 2022).

The release of PFAS from thawing permafrost induced by local pollution sources, such as sewage and landfills, creates a complex interaction of multiple contamination pathways (Garcia-Barrios et al., 2021; Alfaro Garcia et al., 2022). Warming accelerates freeze-thaw cycles, which alter PFAS mobilization, particularly affecting the distribution and chemical behavior of short-chain PFAS, which persist in deeper soil layers (Brendel et al., 2018). The efficiency of PFAS transport depends on the composition of thawed organic matter, the morphology of lakes and streams, and landscape characteristics, such as topography, soil type, and ground ice content (Vonk et al., 2015). Thawing permafrost further deepens the active soil and releases dissolved organic carbon and other nutrients that tend to change the water chemistry of nearby lakes and rivers, consequently impacting hydrological pathways (Roberts et al., 2017). Furthermore, releasing carbon-rich organic matter may increase the bioavailability of POP, amplifying their ecological risks (MacInnis et al., 2019a; MacInnis et al., 2022). This complex interplay shows how PFAS may be redistributed across the cryosphere.

PFAS binds to organic matter and mineral surfaces like clay, and iron oxide and manganese oxide act as sorbents, affecting PFAS mobility and degradation. Iron. Iron oxides in sediments enhance PFAS adsorption and influence degradation kinetics under reducing conditions (Figure 3D; Interstate Technology and Regulatory Council, 2023). Anoxic conditions in sediments favor reductive fluorination. This is usually effective when coupled with microbial degradation by sulfite-reducing bacteria (e.g., *Desulfovibrio* spp.), which enhances PFAS breakdown in aquatic sediments (Douna and Yousefi, 2023; Jin et al., 2023).

2.4.4 Biological transformation

The biological transformation of PFAS can be facilitated by microbes and their metabolic activities mediated by cold-adapted enzymes at low temperatures (Figure 3E). Enzymes like peroxidases or cytochrome P450 enhance defluorination (Beškoski et al., 2018; Huang and Jaffé, 2019). *Pseudomonas* and Dehalococcoides species have been detected in Arctic environments, where they use PFAS as terminal electron acceptors under anoxic conditions (Huang and Jaffé, 2019; Zhang Z. et al., 2022). *Acidomicrobium* species have been identified in diverse habitats, including cold environments such as soils and sediments, and they defluorinated PFOA and PFOS under Feammox conditions (where ammonium is oxidized while iron is reduced) (Huang and Jaffé, 2019).

3 Bioaccumulation and biomagnification impacts

3.1 PFAS far-reaching overall impacts on cryosphere

The environmental transport of PFAS inevitably leads to their accumulation in the cryosphere. PFAS concentrations are notably high in the cryosphere, with unique bioaccumulation patterns compared to other regions (Khan et al., 2023) with several studies documenting a range of compounds including long-chain PFAA, such as PFDA and PFOS, and newer replacement PFAS across multiple marine taxa (Table 2; Casal et al., 2017b; Alfaro Garcia et al., 2022; Khan et al., 2023; Zhang et al., 2023). These compounds accumulate in individual species and are also biomagnifying along the food chain, heightening exposure risks for top predators (Figures 2C, E). Recent toxicological research showed that PFAS exposure

TABLE 2 PFAS documented in various tissues and organisms around the cryosphere regions (If there are more than eight types of PFAS studied in a particular location, the most abundant type, and their concentration are given; otherwise, the sum of all identified PFAS is provided).

Biota and tissue types	PFAS type and concentration	Location	Reference
Amphipods, barnacles, Atlantic cod, seaweed	Σ20 types of PFAS: 0.049–2.62 ng/g (mean 8.84 ng/g). Amphipods: 22.6–26.2 ng/g, barnacles: 3.16–7.02 ng/g, Atlantic cod 2.31–4.44 ng/g, seaweed 0.049–3.29 ng/g	Svalbard, Norway	Dai et al. (2025)
Polar bear (*Ursus maritimus*) liver samples	ΣPFAS, ≈ 60% was PFOS	Hudson Bay Canada	Letcher et al. (2018)
Polar bear (*Ursus maritimus*) plasma samples	PFOS > PFNA > PFHxS > PFUnDA > PFDA > PFTrDA > PFOA > PFDoDA)	Svalbard, Norway	Tartu et al. (2017)
Greenland polar bears (*Ursus maritimus*) - liver, blood, muscle, adipose, and brain tissue samples	C6 -C11 PFCAs C13- C15 PFCAs and PFOS were in higher concentration in liver > blood > muscle ≈ adipose	Scoresby Sound, Central East Greenland	Greaves et al. (2012)
Ringed seals (*Phoca hispida*) liver sample	PFOS>>> PFUnDA > PFNA > PFDA	Greenland	Rigét et al. (2013)
Polar bear (*Ursus maritimus*) liver sample	PFOS>>> PFNA > PFDA > PFUnDA	Greenland	Rigét et al. (2013)
Killer whales' liver sample	14 types of PFAS ∑PFAS- 269 ± 90 ng/g	Greenland	Gebbink et al. (2016)
Ringed seals liver sample	14 types of PFAS ∑PFAS- 138 ± 7 ng/g	Greenland	Gebbink et al. (2016)
Polar bear (*Ursus maritimus*) liver sample	14 types of PFAS ∑PFAS- 2,336 ± 263 ng/g	Greenland	Gebbink et al. (2016)
North Atlantic pilot whale *Globicephala melas*	15 types of PFAS ∑PFAS in 1998: 31 ng/g, in 2013: 21 ng/g	Faroe Islands	Dassuncao et al. (2017)
Arctic seabird, black-legged kittiwakes (*Rissa tridactyla*), blood samples	Short chain (C9-C12) PFCAs and long chain (C13-C14) PFCAs	Svalbard, Norway	Léandri-Breton et al. (2024)
Arctic foxes (*Vulpes lagopus*): liver, blood, kidney, adipose, muscle samples	∑PFCA and PFSA were higher in lean foxes than fat ones ∑PFSA > PFCA in all tissues PFOS > PFNA > PFUnDA > PFTrDA	Svalbard, Norway	Aas et al. (2014)
North American river otters (*Lontra canadensis*)	Liver: 931 ng/g wet wt (highest tissue specific concentration), (∑all PFAS): 1580 μg across the entire body, PFSA:58%–75%, PFCA: 21%–35%	West Virginia, United States	Li et al. (2024)
Zooplankton, polychaetes, spider crab, sculpin and wolffish, glaucous gull	∑PFAS, in zooplankton: 1.1 ± 0.32 μg/kg, polychaetes 2.8 ± 0.80 μg/kg, Spider crab: 2.9 ± 0.70 μg, fish liver: 5.4 ± 0.87 μg/kg, gull liver samples 62.2 ± 11.2 μg/kg	Arctic Fjord, Svalbard, Norway	Ali et al. (2021)
Zooplankton, clams, glaucous gulls	Calms: 0.28 ± 0.09 ng/g (we weight, whole body), gulls: 20.2 ± 3.9 (liver), zooplankton: ± 2.6 ± 0.3 ng/g (wet weigh)	Various Arctic regions	Tomy et al. (2004)
Polar bear	Livre: PFOS 1735.67 ng/g, adipose tissue: PFHxS 2.2 ng/g	Arctic region	Khan et al. (2023)
Seabird,black-legged kittiwakes (*Rissa tridactyla*)	PFOS 0.00704 ng/mL, PFNA 0.000409 ng/mL, PFDcA 0.000619 ng/mL, PFUnA 0.00083 ng/mL, PFDoA 0.00109 ng/mL, PFTrA 0.00360 ng/mL	Kongsfjorden, Svalbard	Blévin et al. (2017)
White whales *Delphinapterus leucas*, plasma samples of whales	PFOS 22.8 ng/mL, sum of PFCAs 13.7 ng/mL: PFOA, PFNA, PFDA, PFUnDA, PFDoDA, PFTrDA, PFTeDA, sum of PFSAs 24,6 ng/mL:PFHxS, PFHpS., FOSA 2.61 ng/mL	Svalbard, Norway	Villanger et al. (2020)
Marine mammals (Polar bear, grey seal, trout fish)	PFECHS, PFHxA, HFPO-DA, PFSA, PFPA, PFPiA, PFCA precursors. polar bear liver samples (*Ursus maritimus*) from Greenland PFAS sum of 1,426–1890 ng/g, 35.1 ng/g in grey seal, 140 ng/g in white-beaked dolphin	Nordic environment	Kärrman et al. (2019)
Cod livers (200 Codfish) (*Boreogadus saida*)	PFOS, PFUdA, PFTrDA, PFDA, PFOSA, PFDoDA, PFOA, PFNA, and PFOS were the predominant, 1.5 μg kg/wet weight in 72% of the samples	Cod livers (200 Codfish)	Valdersnes et al. (2017)

Note: 9Cl-PF_3ONS: 9-Chloroperfluuoro-3-oxanesulfonic acid, PFOES: perfluorooctane ethyl sulfonate, 6:2 FTSA: 6:2 fluorotelomer sulfonic acid, 6:2 FTCA: 6:2 fluorotelomer carboxylic acid, 11Cl-PF3OUdS: 11-chloroperfluoro-3-oxaundecane sulfonic acid.

affects growth, behavior, reproduction, physiology, and genetic characteristics across various species (Zhao et al., 2012; Jouanneau et al., 2023; Manojkumar et al., 2023). PFAS contamination has been documented not only in wildlife but also in drinking water, groundwater, and even rain, underscoring their widespread environmental health risks (Boiteux et al., 2012; Table 1; Kim and Kannan, 2007; Schwanz et al., 2016; Kim et al., 2023; Olney et al., 2023; Sonne et al., 2023). Consequently, PFAS poses a complex threat to cryosphere ecosystems by affecting organisms across different trophic levels (Figure 2C; Tomy et al., 2004; Muir et al., 2019; Ali et al., 2021).

3.2 Bioaccumulation in apex predators and marine mammals

Apex predators in cryosphere ecosystems, including seals, whales, and polar bears, are exposed to significant challenges from PFAS contamination (Table 2; Alfaro Garcia et al., 2022; Chen et al., 2023; Lu et al., 2024). Despite regulatory phase-outs of C8-based PFAS, recent studies have shown that PFOS and C_9 - C_{11} PFCA generally persist in tissue samples from polar bears (*Ursus maritimus*) (liver) and ringed seals (*Phoca hispida*) in regions like Greenland (Figure 2; Rigét et al., 2013; Gebbink et al., 2016; Dietz et al., 2019) and Hudson Bay (Routti et al., 2017; Letcher et al., 2018). Furthermore, elevated PFSA (C_4, C_6, C_8, and C_{10}) levels in the liver samples of higher trophic level species, such as East Greenland polar bears, with concentrations reaching 2,611 ± 202 ng/g wet weight, predominantly consisting of PFOS were also reported (Boutet et al., 2023). The mean $\sum_4$ PFSA in seal liver was 111 ± 5 ng/g wet weight with 98% PFOS. This concentration was three orders of magnitude higher than in seal blubber, which had a concentration of 0.05 ± 0.01 ng/g ww, consisting entirely of PFHxS. Biomagnification factors (BMFs) were significantly higher for PFHxS and C9 to C13 PFCA when comparing polar bear liver to seal liver. BMFs decreased as chain length increased, like PFCA (C9 to C13) (Kärrman et al., 2019; Boutet et al., 2023). Therefore, BMF comparison between seal blubber and bear liver more accurately reflects the dietary exposure of PFAS from seals to bears (Boutet et al., 2023). Specifically, the exposure of polar bears to PFAS has been associated with a range of health issues, such as hormonal imbalances and immune system impairment (Miner et al., 2017; Dietz et al., 2019). A risk assessment study over three decades (1983–2013) indicated that the reproductive, immunotoxic, and carcinogenic effects of PFOS in East Greenland polar bears were significant during this period, with only a slight decline over the years (Dietz et al., 2019; Xie and Kallenborn, 2023).

In addition, PFAS biomagnification is particularly pronounced in air-breathing animals, likely due to their protein-affinity (proteinophilic nature) and respiratory differences compared to aquatic species (Chen et al., 2023; Kelly et al., 2009; Khan et al., 2023). For instance, studies on beluga calves in Hudson Bay indicate that PFOS and PFCA (C7-C14) levels exceed recommended exposure limits, with trophic magnification factors (TMFs) ranging from 2 to 11, suggesting potential health risks for Arctic marine life (Kelly et al., 2009). In addition, the research emphasizes that cetaceans, unlike other mammals, cannot convert precursor perfluorooctane sulfonamide (FOSA) into PFOS, which leads to different tissue burdens of both compounds (Dassuncao et al., 2017). FOSA accounted for many PFAS in North Atlantic pilot whales in 2000 but has significantly declined in recent years, while PFOS and other long-chain PFAS (C9-C13) have increased. This change is linked to shifts in atmospheric inputs of FOSA, especially after 2000, which have reduced PFOS exposure in species that metabolize FOSA, such as whales and seafood-consuming humans (Dassuncao et al., 2017). These findings stress the importance of considering PFAS precursors when studying bioaccumulation and environmental impacts.

3.3 Bioaccumulation in birds

Arctic seabirds, so far studied, always exhibited high PFAS concentrations in their tissues, leading to reduced reproductive success and impaired chick development (Ask et al., 2021; Jouanneau et al., 2023). Long-chain PFAS such as PFUnDA (C11) and PFTrDA (C13) are highly bioaccumulative, often exceeding PFOS levels in Arctic seabirds (Khan et al., 2023). These long-chain PFCA often exceed or are comparable to PFOS levels, as seen in species like northern fulmar (*Fulmarus* glacialis) and thick-billed murre (*Uria lomvia*). Although long-chain PFCA is increasingly dominant, PFOS remains a major fluorinated contaminant in Arctic bird species. For instance, extreme cases of PFOS concentrations have been reported in white-tailed eagle eggs (*Haliaeetus albicilla*) (1,514 ng/g wet weight) (Khan et al., 2023). Perfluoroundecanoic acid (PFUnA) concentrations in the blood of Arctic birds, such as glaucous gulls (*Larus hyperboreus*), have reached 74.4 ng/g wet weight. In contrast, egg concentrations of PFOA in Audouin gulls (*Larus audouinii*) were recorded at 23.53 ng/g, indicating significant PFAS burdens in these species.

In Antarctica, PFAS have been identified in the south polar skua (*Catharacta maccormicki*), highlighting biomagnification levels that vary between different colonies (Garcia-Barrios et al., 2021; Alfaro Garcia et al., 2022). Seven of the 22 PFAS analyzed were commonly found, with increasing concentrations from prey to skuas. Notably, PFOS levels were higher in skuas at Dumont d'Úrville (French research station, Antarctica) compared to other colonies, indicating complex source pathways and bioaccumulation trends (Alfaro Garcia et al., 2022). The findings emphasize the importance of diet and location in determining PFAS levels in cryosphere species.

3.4 Bioaccumulation in lower trophic levels

Sea ice facilitates the uptake of atmospherically deposited contaminants into marine ecosystems and is then released into the aquatic food web as the ice melts (Khan et al., 2023). This process supports phytoplankton blooms and subsequently increases zooplankton biomass, marking the start of a bioaccumulation chain that can extend up to higher trophic levels (Miner et al., 2018). Food web analysis revealed that bioaccumulation patterns in marine plankton are complex. Certain PFCA and PFOS exhibited higher-than-expected bioaccumulation factors (BAFs) in Arctic waters (Zhang et al., 2019). PFAS have been identified in both phytoplankton (Zhang Y. et al., 2022; Davis et al., 2024; Ma et al., 2022) and zooplankton (Miner et al., 2017), indicating their bioavailability at the base of the marine food chain (Rigét et al., 2013).

Zooplankton, vital for energy transfer in marine ecosystems, also showed significant PFAS accumulation. PFAS can disrupt reproductive and developmental processes, leading to population declines and altered food web dynamics (Ali et al., 2021). Changes in zooplankton populations can affect fish species that depend on them as food sources, causing ripple effects across the food web and affecting the entire ecosystem (Ren et al., 2022; Munoz et al., 2019). As larger organisms consume contaminated prey, PFAS

concentrations increase with each trophic level, known as biomagnification, which raises significant ecological Ma et al., 2022 concerns since primary producers and consumers form the foundation of every ecosystem.

4 PFAS regulation and phase-out: progress and challenges

4.1 Forever chemicals in focus

The chemical structure of PFAS contributes to their high stability and low degradability, posing a significant environmental challenge (Kannan et al., 2001). PFOS, PFOA, and other long-chain PFAA are often referred to as "legacy contaminants," i.e., they are recognized to continue impacting ecosystems and human health long after their use has been reduced or even banned because of their persistence in the environment, tendency to bioaccumulate, and potential toxic effects (Chen et al., 2023). Among legacy compounds like polychlorinated biphenyls (PCB), dichlorodiphenyltrichloroethane (DDT), chlorofluorocarbons (CFC), and heavy metals, some long-chain PFAS are currently under regulation.

In contrast, replacement chemicals that are not yet regulated or included in routine monitoring programs are termed "contaminants of emerging concern" or "emerging contaminants" (Gaden et al., 2012). They can consist of either newly introduced compounds and their metabolites or molecules with previously unrecognized adverse effects on wildlife. PFAS has emerged as a growing concern in the past two decades as more than 5,000 varieties of synthetic highly fluorinated organofluoride substances were developed in this relatively short time frame (OECD, 2021; Gaines, 2023). This is mainly driven by the rising demand for products and their intriguing characteristics mentioned above (EU, 2019, 2021; OECD, 2021), as well as the result of the phase-out of some of the long-chain PFAS, leading to the use of replacement compounds like short-chain and ether-based PFAS (e.g., hexafluoropropylene oxide dimer acid: HFPO-DA, on the market as its ammonium salt GenX) (ECHA, 2024).

4.2 Historical efforts and global regulation

Several regulatory bodies and international agreements are currently addressing the management and regulation of PFAS in the Arctic and globally. The Stockholm Convention on Persistent Organic Pollutants is a global treaty that aims to eliminate or restrict the production of POPs, including certain PFAS. Only a comparatively small number of PFAS have been listed under the Stockholm Convention, i.e., PFOA and perfluorohexanoic sulfonic acid (PFHxS), their salts and related substances are included in Annex A, and PFOS and its salts are included in Annex B to regulate and control their production and application (UNEP, 2023; Davis et al., 2024; Hamid et al., 2024).

ECHA, operating under the European Union, has been instrumental in proposing restrictions and evaluating risks associated with various PFAS compounds to protect human health and the environment. The European Registration, Evaluation, Authorization and Restriction of Chemicals (REACH) Regulation aims to identify and restrict the use of substances of very high concern, including many PFAS with long-chain fluorinated carbon (C9-C14) atoms (Teymourian et al., 2021; ECHA, 2024). Temporal trends, like those observed in Sweden, show declining concentrations of certain PFAS, indicating the effectiveness of such regulatory measures (Haque et al., 2023). Recently, it has been proposed to restrict the entire group of PFAS unless a specific use is proven essential for society under REACH (ECHA, 2024).

Individual European countries have implemented bans on specific PFAS, citing their toxicological effects according to the European Food Safety Authority (EFSA), European Human Biomonitoring Initiative (HBM4EU) and the inadequacy of replacement PFAS (Schrenk et al., 2020). Advocacy groups and responsible companies call for immediate eradication of PFAS through enhanced regulatory frameworks, such as United Kingdom REACH and global conventions (Fernández, 2024; REACH, 2024). Many of these efforts are being carried out in European and North American regions where environmental concerns and consumer pressures often drive businesses to adopt more sustainable practices ahead of regulatory requirements (Magazine, 2024).

Arctic Council working groups, like the Arctic monitoring and assessment programme (AMAP) and the Arctic contaminants action program (ACAP), are addressing PFAS contamination in the Arctic regions (ACAP, 2021). AMAP conducts scientific pollution assessments of pollution, including PFAS, and provides policy-relevant advice to protect Arctic ecosystems and communities from these harmful contaminants (Arctic Council, 2024). ACAP focuses on preventing and reducing pollutants and provides policy recommendations to nations to implement actions that mitigate environmental health risks associated with contaminants (AFFF, 2021).

The US EPA addresses PFAS contamination through comprehensive strategies and regulatory actions. Step vice series of action plans from October 2021, the agency announced a Strategic Roadmap outlining plans to confront PFAS pollution, including developing national drinking water standards for PFOA, PFOS, and PFBS (US EPA, 2024). Recently, they have been expanding the list of PFAS that are subject to reporting under the Toxics Release Inventory (TRI) as mandated by the National Defense Authorization Act (NDAA). This act provides a framework for the annual addition of PFAS to the TRI list (US EPAO, 2019; US EPAO, 2025).

Environmental and Climate Change Canada (ECCC) is considering a class-based approach to address PFAS under the Canadian Environmental Protection Act, 1999 (CEPA), moving beyond individual substance assessments (ECCC, 2024). The latest ECCC draft report includes fluoropolymers, acknowledging their distinct exposure and hazard profiles. This class-based approach addresses the potential cumulative effects of exposure to PFAS mixtures and prevents the substitution of regulated PFAS with unregulated ones that may have similar hazardous properties. This strategy aligns with international efforts, as other jurisdictions, such as the European Union and certain U.S. states, are also exploring class-based approaches to PFAS regulation (ECCC, 2024).

TABLE 3 Most common PFAS alternatives identified in cold environments and their environmental fate and potential transformation (Wang et al., 2015a; US EPA, 2021; Hamid et al., 2024).

Replacement compounds	Water solubility	Volatility	Bioaccumulation potential	Persistence	Reference
PFECA (e.g., GenX, ADONA)	High	Moderate (volatilization from water possible)	Low to moderate	High	Sun et al. (2016), Joerss et al. (2020), Feng et al. (2024)
PFESA (e.g., 9Cl-PF_3ONS, PFOES)	Moderate to low	low	High	Very high	Guo et al. (2024)
C6 fluorotelomer-based compounds (e.g., 6:2 FTSA, 6:2 FTCA	Moderate	Low	Moderate (degrades into PFHxA)	Moderate to high	Ali et al. (2021), Xie and Kallenborn (2023), Lohmann et al. (2024)
PFPrOPrA	High	Moderate	Low	High	Sun et al. (2016)
PAP (e.g., diPAP, monoPAP)	Moderate	Low	Low (but degrades into PFOA)	Low to moderate	Gebbink et al. (2016)
6:2 Cl-PFESA (e.g., 9Cl-PF_3ONS, 11Cl-PF_3OUdS	Low	Low	Very high	Extremely high	Gebbink et al. (2016), Wang et al. (2021a)

4.3 Transition to alternatives and challenges

Despite being introduced as "safer" PFAS alternatives, many of these molecules share similar negative characteristics with legacy PFAS in terms of their persistence, broader mobility, and toxicity with varying degrees of environmental harm (Wang et al., 2015a). PFAS alternatives from PFCAs were perfluroethercarboxylic acids (PFECAs), perfluoroalkylethersulfonic acids (PFESAs), C6 fluorotelomer-based compounds, polyfluorinated alkyl phosphoric acid esters (PAPs) and chlorinated polyfluorinated ether sulfonic acids (Cl-PFESAs) are the currently common PFAS replacement compounds marketed, and they have been identified with potential accumulation and health effects (OECD, 2022; Feng et al., 2024; Table 3).

Cl-PFESAs, such as 6:2 Cl-PFESAs, are highly persistent in the environment due to their higher thermal and chemical stability, high toxicity, and more bioaccumulative than PFOS, raising serious health risks. They have been identified as bioaccumulated substances in various marine organisms, including gastropods, bivalves, crabs, shrimps, cephalopods, and fish. These compounds tend to magnify along the food chain, raising severe concerns about their health impacts (Feng et al., 2024).

C6 fluorotelomer-based compounds like FTOHs can transform into PFCA in the environment, and due to their moderate solubility and low volatility, they exhibit a higher persistence and bioaccumulation potential in cold environments (MacInnis et al., 2019b; Munoz et al., 2019). Studies have detected Cl-PFPECAs in vegetation and subsoils, indicating their environmental persistence and tendency to accumulate in vegetation, indicating potential for atmospheric transport and deposition (Davis et al., 2023). PAP, used in food packaging and paper coating, can degrade into PFOA and other PFCAs (OECD, 2022; Feng et al., 2024).

Of the PFECAs, GenX as an alternative for PFOA was recorded in Arctic waters, especially in the Fram Strait between Greenland and Svalbard, highlighting their persistence and ability to travel long distances from their source (Joerss et al., 2020). In addition to GenX, ADONA (4,8-dioxa-3-H-perfluorononanoic acid) also shares similar properties of GenX as it is resistant to hydrolysis, photolysis, and biodegradation (Haque et al., 2023).

The EPA' toxicity assessment mentioned that GenX exhibits significant persistence and is more mobile than longer-chain PFAS, increasing their contamination risks through water and air. GenX is highly water soluble and exhibits mobility in aquatic environments, as well as transformation pathways like volatilization, allowing atmospheric transport and potential redistribution (U.S. EPA, 2022). Because of these characteristics, they are highly bioaccumulate and have an increasing trend of presence in different environmental matrices and organisms; the transition from legacy PFAS to GenX raises concerns as a "regrettable substitution," albeit being increased application and environmentally benign, and poses a severe risk than even PFOA (EEA, 2023).

Since GenX and other replacement compounds, intended as a safer alternative, are identified with similar environmental and health risks to the compound they are replacing, their toxicity and regulatory scrutiny highlight the need for continued research and precautionary policies to assess the long-term exposure effects, mainly when they are present as a mixture with other contaminant scenarios. Thus, future restrictions or phase-outs are urgently needed for safer alternative fluoropolymer production without any persistent nature, hopefully becoming the next major industrial focus.

4.4 Voluntary measures

The voluntary commitments by manufacturers to cease the production and sale of PFAS-containing food contact substances reflect industry recognition of the need to address safety concerns. However, challenges remain in ensuring the complete elimination of PFAS exposure and mitigating the environmental legacy of their past use. Voluntary measures by industry players play a significant role in reducing PFAS emissions. Although some companies, such as Páramo and Finisterre, have phased out PFAS or pledged to do so by 2025, nearly half of the assessed brands lack plans to stop their use (REACH, 2024).

Several companies and retailers, such as IKEA, Lindex, H&M, COOP in Denmark, L´Oreal in Europe, Jack Wolfskin, Fjallraven, and Houdini Sportswear, have come forward to phase out PFAS from their supply chains (Magazine, 2024). However, it is not as successful as they had proposed; in particular, many outdoor clothes (various brands) still contain PFAS. Further, by January 2025, under

the California Safer Clothes and Textiles Act (AB 1817), US-based outdoor apparel and equipment brands, along with major industry suppliers, are expected to eliminate PFAS from some product lines and supply chains following 10 years of advocacy by Green Science Policy Institute (ECHA, 2024). These initiatives reduce PFAS usage and put pressure on chemical manufacturers to develop safer alternatives. Moreover, these voluntary measures can serve as case studies for regulators, demonstrating that functional alternatives are visible and encouraging broader regulatory action.

4.5 PFAS management- future directions

Phaseout of PFAS and adopting safer alternatives are imperative for protecting the environment and public health. Through structured assessments of alternatives, robust regulatory measures using a class-based approach, and proactive industry initiatives, the transition away from PFAS could be effectively managed, paving the way for a safer and more sustainable future. Moreover, PFAS management by harmonizing measurement methods, enhancing supply chain transparency, industrial discharge control, introducing extended producer responsibility to shift remediation costs, and balancing regulations with essential PFAS uses (Feng et al., 2024) Besides, more funding is needed for research on PFAS alternatives and removal technologies, along with establishing best practices for safe PFAS concentrate management to prevent environmental re-contamination.

At the same time, a comprehensive assessment of PFAS alternatives is crucial due to significant data gaps in exposure ways, transport routes, environmental and biological fate, and long-term-health effects. Limited research on PFAS alternatives, both long and short-chain PFAS transformation or degradation mechanisms, lifecycle, production, and used impurities raise concerns about their long-term impact despite indications of a reduced hazard profile (Fernández, 2024). The OECD report highlights this regard, making it essential to address these uncertainties to ensure effective management and regulation of PFAS alternatives (OECD, 2024).

5 Coupling microbial degradation for PFAS management

5.1 Current methods and limitations

Due to the widespread presence of PFAS in remote regions of the Arctic and Antarctica, the challenges associated with these contaminants have sparked interest in whether microbial degradation could provide a viable remediation strategy that would complement existing physical and chemical techniques. These include photocatalytic reactions utilizing boron nitride and titanium dioxide, as well as non-photocatalytic methods using dimethylsulfoxide (DMSO) which lead to the mineralization of certain PFAS (Mahinroosta and Senevirathna, 2020; Senevirathna et al., 2022; Garg et al., 2023; Kang et al., 2023; Antonopoulou et al., 2024). Other physicochemical methods such as adsorption using colloidal activated carbon, pyrolysis, reduction methods using iodide, sulfite, and dithionite, thermal treatments like incineration and microwave-hydrothermal processing, ion exchange, electrochemical oxidation, and some other treatment processes like ball milling have also been investigated for PFAS treatment (Merino et al., 2016; Mahinroosta and Senevirathna, 2020). While these methods have shown effectiveness in PFAS mineralization, they often require significant energy inputs or specialized equipment.

In contrast, microbial degradation offers a potential alternative, often cheaper approach by utilizing microorganisms' natural capacity to degrade pollutants, even though traditional microbial treatment or remediation techniques that effectively degrade other organic pollutants have mainly proven ineffective against PFAS (Ross et al., 2018). Some studies indicate that PFAS, particularly PFOA and PFOS, resist biodegradation under various environmental conditions (Liou et al., 2010).

Despite these challenges, recent research has identified specific microbial species capable of degrading particular PFAS compounds under controlled conditions, such as mixed cultures (Huang and Jaffé, 2019; Chiavola et al., 2020; Choi and Kan, 2024). This suggests that microbial degradation, although challenging, may be possible with further advancements. Success in microbial degradation depends on the ′biodegradation triangle′- the interplay between the structural complexity of the PFAS compounds, microbial community composition, and environmental conditions (Zhang Z. et al., 2022).

5.2 Potential of polar microorganisms for PFAS bioremediation

Polar microorganisms, particularly those adapted to extreme cold (psychrophiles), show a unique potential for PFAS bioremediation due to their resilience and metabolic versatility (Egas et al., 2023). Psychrophiles are adapted to thrive at temperatures between −20°C and 20°C and have developed mechanisms to maintain cellular function in cold environments, such as enhanced membrane fluidity, cold-shock protein synthesis, and accumulation of cryoprotectants like mannitol (Feller and Gerday, 2003; Baraúna et al., 2017; Clarke et al., 2013).

Several studies identified the potential biodegrading capacity of polycyclic aromatic hydrocarbons (PAH) from polar microbes (Egas et al., 2023). Polar environments have been studied in this context, often focusing on bioprospecting for psychrophiles and polyextremophiles (Orellana et al., 2018; Pearce 2012; Thomas and Dickmann, 2002; Cavicchioli et al., 2002; Nizovoy et al., 2021).

Psychrophiles isolated from Antarctic regions, for instance, contain enzymes capable of degrading hydrocarbons at sub-zero temperatures, a function attributed to enzymes like alkane hydroxylases (Fuentes et al., 2014, Figure 3E; Bowman and Deming, 2014). Beyond hydrocarbon degradation, some Antarctic bacterial communities have demonstrated the capacity to reduce PFOS (Cerro-Gálvez et al., 2020). While not achieving complete degradation, this process promoted the growth of certain bacterial groups, such as Gammaproteobacteria, Roseobacter, and Flavobacteria. These observations signal microbial involvement in modifying PFAS compounds, albeit not entirely breaking them down Orellana et al., 2018; Pearce 2012; Thomas and Dickmann, 2002; Cavicchioli et al., 2002 (MacInnis et al., 2019b).

Besides, environmental toxicity of PFAS studies found that *Pseudomonas* lineages have the potential to break down PFOA (Yi et al., 2019), PFOS (Chetverikov et al., 2017), and other PFAA (Zhang Z. et al., 2022; Smorada et al., 2024). Specific bacterial genera like *Rhodanobacter* and *Chujaibacter* were dominant in PFAS-contaminated soils (Senevirathna et al., 2022). Their growth and degradation of PFAS-enriched materials showed potential bioremediation insights under varying physio-chemical conditions (Smorada et al., 2024). However, despite established links between biodegradation, bacterial communities, and gene expression in laboratory settings, there remains a significant knowledge gap in our understanding of PFAS biodegradation, particularly in natural environments.

5.3 Biotechnological insights and research directions

The metabolic pathways used by cold-adapted microorganisms for organic pollutant degradation, such as those for PCBs and PAHs, could serve as models for PFAS degradation (Bamforth and Singleton, 2005; Crisafi et al., 2016; Gran-Scheuch et al., 2017; Papale et al., 2017). Strains of *Salinibacter, Arthrobacter,* and *Pusillimonas* from Svalbard possess biphenyl dioxygenase (*bphA*) and have the potential to metabolize PCB mixtures at low temperatures (Papale et al., 2017; Papale et al., 2022). These findings suggest that similar microbial mechanisms, e.g., dehalogenation oxidation by members of the Actinobacteria and Gammaproteobacteria, may likely occur for PFAS degradation in Arctic habitats.

Enzymatic analyses of polar microbes have revealed potential for degrading SVOCs, particularly several PAHs like anthracene, naphthalene, phenanthrene, PCBs, and PFOS (Egas et al., 2023). Genes encoding enzymes for sulfur metabolism in polar microbes, such as sulfonate and alkanesulfonate monooxygenases, could facilitate the degradation of PFAS, especially PFOS (Cerro-Gálvez et al., 2020). Several studies have documented polar microbes, mainly from Antarctica and the Arctic marine environment, that can potentially degrade SVOCs (Egas et al., 2023).

Laboratory studies have also indicated that Arctic marine bacteria possess phosphoesterases capable of hydrolyzing phosphate ester bonds in organophosphates, pointing to another potential pathway for PFAS degradation (Martinez-Varela et al., 2021). Additional studies identified various species of bacteria as well as fungi from polar regions, such as bacterial *Sphingobium xenophagum*, *Burkholderia glathei*, *Paeniglutamicibacter* sp., *Psychrobacter* spp., *Pseudomonas* sp., *Rhodococcus* sp., *Polaromonas* sp., and *Pseudoalteromonas* sp., as well as fungal *Penicillium* sp. and *Aspergillus* sp., exhibit diverse genetic and enzymatic machineries capable of degrading complex organic pollutants, suggesting a yet untapped potential for PFAS degradation (Gran-Scheuch et al., 2017; Singh et al., 2023).

In this context, the high stability of PFAS compounds suggests that complete microbial degradation is unlikely without significant advances in biotechnology and the discovery of new microbes or microbial pathways. Non-biological methods such as hydrolysis, pyrolysis, and chemical oxidation remain the most effective for breaking down these resilient chemicals (Garg et al., 2023). Nonetheless, continued exploration of microbial degradation pathways could lead to breakthroughs in mitigating the environmental impacts of PFAS. Despite the harsh conditions of cryosphere environments, psychrophiles' metabolic versatility and resilience make them promising candidates for bioremediation efforts. They offer a cost-effective and environmentally friendly solution to mitigate PFAS pollution in polar and other cold environments. Further research is crucial to fully elucidate the underlying mechanisms and refine bioremediation strategies for effective PFAS degradation.

5.4 Synthetic solutions through genetically engineered microbes

Bioremediation of PFAS is a significant research area, focusing on developing efficient ways to improve the biodegradation capabilities of microorganisms and their enzymes, including using genetically engineered microbes (GEM) (Berhanu et al., 2023). The typical PFAS breakdown process involves three key steps: defluorination, carbon-fluorine chain shortening, and mineralization, resulting in harmless fragments or by-products. Studies identified certain microbial groups and their enzymes have greater potential, making them ideal candidates for GEM applications (Huang and Jaffé, 2019; Wackett and Robinson, 2020; Yu et al., 2020).

Relevant enzymes identified for their potential C-F bond cleavage can be further studied and incorporated into psychrophilic bacteria capable of rapid evolutionary adaptation to enhance their PFAS degradation. For example, hydrolytic defluorinase from *Streptomyces* spp has been shown to metabolize fluoroacetate to glycolate (Berhanu et al., 2023), showing the breaking mechanism of PFAS. In addition, oxygenases such as alkane monooxygenases can shorten the chain by adding hydroxyl groups into carbon atoms, completing the activity of hydrolytic enzymes in breaking C-F bonds (Huang and Jaffé, 2019).

Cold-adapted bacteria like *Polaromonas vacuolate,* host dehalogenases that can be used alongside hydrolytic enzymes to enhance defluorination capabilities (Martinez Alvarez et al., 2022). Similarly, dehalogenases from the *Acidimicrobium* sp. Strain A6 facilitates PFAS reduction through defluorination (Huang and Jaffé, 2019; Wackett and Robinson, 2020). Other psychrophiles, including *Polaromonas* spp., *Psychrobacter* spp., *Colwellia psychreythraea,* are also promising candidates for defluorination due to their hydrolytic enzyme systems (Bakermans et al., 2006; Bowman and Deming, 2014; Papale et al., 2017; Martinez Alvarez et al., 2022).

Biotechnological tools can be employed to improve enzyme activity and substrate specificity for PFAS to explore the potential of using the above microbes. Genetic modifications can induce synthetic pathway networks that promote oxidation and reduction, generating reactive intermediates for further breakdown or adding harmless by-products. Additionally, specific regulatory pathways can be engineered to activate PFAS-degrading enzymes when fluorinated compounds are accessible for further breakdown. Developing a GEM that integrates these competencies can provide a robust platform for PFAS remediation, supporting

ongoing efforts to mitigate contaminants in the cryosphere and other diverse environments.

6 Conclusion: implications and urgent research needs

The dual abiotic pressures of rising temperatures and melting sea ice significantly foster the release of stored PFAS from ice and increase exposure through atmospheric deposition and ocean currents. However, the different physicochemical properties of PFAS, their accumulation in ice, their movements via marine and atmospheric pathways, and their transformation into persistent contaminants necessitate further studies to comprehend the specific underlying mechanisms in cold environments. Additionally, assessing long-term environmental risks in cryosphere regions and implementing regulatory measures for PFAS management is urgently needed. This requires comprehensive monitoring of PFAS levels, their physiological effects on critical species, and their cascading impact on ecosystem functioning.

On the other hand, addressing the existing PFAS in the vulnerable cryosphere environment necessitates reliable remediation techniques. Bioremediation presents a potential sustainable solution for PFAS removal. Psychrophiles play a unique and crucial role in cold-environment biogeochemical cycles, and some show promising PFAS degradation capabilities. Genetic engineering may enable the development of modified microbes by optimizing key enzymes to enhance defluorination efficiency. Therefore, future efforts should concentrate on bioremediation approaches utilizing genetically engineered microbial consortia adapted to cryosphere conditions. These strategies must be scalable, cost-effective, and environmentally friendly. At the same time, identifying and developing new, safer chemical alternatives, along with robust environmental management strategies and stringent regulatory frameworks, are essential for addressing the impact of PFAS.

Author contributions

AA: Conceptualization, Writing–original draft, Investigation, Methodology, Visualization, Formal Analysis. OV: Conceptualization, Funding acquisition, Resources, Supervision, Writing–review and editing, Data curation. UK: Data curation, Supervision, Writing–review and editing, Methodology. H-PG: Conceptualization, Data curation, Visualization, Writing–review and editing, Supervision. AS: Supervision, Writing–review and editing. ÓR: Supervision, Writing–review and editing, Resources, Methodology. HJ: Data curation, Writing–review and editing, Investigation, Validation. BS: Conceptualization, Funding acquisition, Methodology, Project administration, Supervision, Writing–review and editing.

Funding

The author(s) declare that financial support was received for the research and/or publication of this article. The Icelandic Research Fund has supported the work in the frame of the project "Per- and poly-fluoroalkyl substances (PFAS) meet Arctic and sub-Arctic marine diatoms and their associated symbionts" (RANNIS ID: 239548-051).

Acknowledgments

The authors gratefully acknowledge the support of the Icelandic Research Fund in the frame of the project "Per- and poly-fluoroalkyl substances (PFAS) meet Arctic and sub-Arctic marine diatoms and their associated symbionts" (RANNIS ID: 239548-051).

Conflict of interest

The authors declare that the research was conducted in the absence of any commercial or financial relationships that could be construed as a potential conflict of interest.

Generative AI statement

The author(s) declare that Generative AI was used in the creation of this manuscript. ChatGPT, a language model developed by OpenAI for language improvement, was used for stylistic polishing, but the authors completed the final writing and revisions in their own voice.

Publisher's note

Supplementary material

The Supplementary Material for this article can be found online at: https://www.frontiersin.org/articles/10.3389/fenvs.2025.1559941/full#supplementary-material

References

Aas, C. B., Fuglei, E., Herzke, D., Yoccoz, N. G., and Routti, H. (2014). Effect of body condition on tissue distribution of perfluoroalkyl substances (PFASs) in arctic fox (Vulpes lagopus). *Environ. Sci. Technol.* 48, 11654–11661. doi:10.1021/es503147n

ACAP (2021). Aqueous film-forming foam (AFFF) Phaseout in the Arctic factsheet (Fact Sheet). Arctic. Council. Available online at: http://hdl.handle.net/11374/2737.

AFFF (2021). Aqueous film-forming foam (AFFF) Phaseout in the Arctic factsheet. Available online at: https://oaarchive.arctic-council.org/items/670868f4-d8bc-4cd3-ac4e-feb995bc29a0 (Accessed February 24, 2025).

Ahrens, L., Rakovic, J., Ekdahl, S., and Kallenborn, R. (2023). Environmental distribution of per- and polyfluoroalkyl substances (PFAS) on Svalbard: local sources and long-range transport to the Arctic. *Chemosphere* 345, 140463. doi:10.1016/j.chemosphere.2023.140463

Ahrens, L., Xie, Z., and Ebinghaus, R. (2010). Distribution of perfluoroalkyl compounds in seawater from northern Europe, atlantic ocean, and Southern Ocean. *Chemosphere* 78, 1011–1016. doi:10.1016/j.chemosphere.2009.11.038

Alfaro Garcia, L. A., Descamps, S., Herzke, D., Chastel, O., Carravieri, A., Cherel, Y., et al. (2022). Bioaccumulation of per and polyfluoroalkyl substances in antarctic breeding south polar skuas (Catharacta maccormicki) and their prey. *Front. Mar. Sci.* 9. doi:10.3389/fmars.2022.819525

Ali, A. M., Langberg, H. A., Hale, S. E., Kallenborn, R., Hartz, W. F., Mortensen, Å.-K., et al. (2021). The fate of poly- and perfluoroalkyl substances in a marine food web influenced by land-based sources in the Norwegian Arctic. *Environ. Sci. Process. Impacts* 23, 588–604. doi:10.1039/D0EM00510J

Antonopoulou, M., Spyrou, A., Tzamaria, A., Efthimiou, I., and Triantafyllidis, V. (2024). Current state of knowledge of environmental occurrence, toxic effects, and advanced treatment of PFOS and PFOA. *Sci. Total Environ.* 913, 169332. doi:10.1016/j.scitotenv.2023.169332

Arctic Council (2024). 6 facts about PFAS and Arctic Council efforts to address threats posed by them. Available online at: https://arctic-council.org/news/6-facts-about-pfas-and-arctic-councils-efforts-to-address-threats-posed-by-them/(Accessed February 24, 2025).

Armitage, J. M. (2009). Modeling the global fate and transport of perfluoroalkylated substances (PFAS). Available online at: https://urn.kb.se/resolve?urn=urn:nbn:se:su:diva-8571 (Accessed September 10, 2024).

Ask, A. V., Jenssen, B. M., Tartu, S., Angelier, F., Chastel, O., and Gabrielsen, G. W. (2021). Per- and polyfluoroalkyl substances are positively associated with thyroid hormones in an arctic seabird. *Environ. Toxicol. Chem.* 40, 820–831. doi:10.1002/etc.4978

Ásmundsdóttir, Á. M., and Scholz, B. (2021). "Effects of microplastics in the cryosphere," in *Handbook of microplastics in the environment*. Editors T. Rocha-Santos, M. Costa, and C. Mouneyrac (Cham: Springer International Publishing), 1–46.

Bakermans, C., Ayala-Del-Río, H. L., Ponder, M. A., Vishnivetskaya, T., Gilichinsky, D., Thomashow, M. F., et al. (2006). Psychrobacter cryohalolentis sp. nov. and Psychrobacter arcticus sp. nov., isolated from Siberian permafrost. *Int. J. Syst. Evol. Microbiol.* 56, 1285–1291. doi:10.1099/ijs.0.64043-0

Bamforth, S. M., and Singleton, I. (2005). Bioremediation of polycyclic aromatic hydrocarbons: current knowledge and future directions. *J. Chem. Technol. and Biotechnol.* 80, 723–736. doi:10.1002/jctb.1276

Banks, R. E., and Tatlow, J. C. (1986). Synthesis of CF bonds: the pioneering years, 1835 – 1940. *J. Fluor. Chem.* 33, 71–108. doi:10.1016/S0022-1139(00)85272-0

Baraúna, R. A., Freitas, D. Y., Pinheiro, J. C., Folador, A. R. C., and Silva, A. (2017). A proteomic perspective on the bacterial adaptation to cold: integrating OMICs data of the psychrotrophic bacterium exiguobacterium antarcticum B7. *Proteomes* 5, 9. doi:10.3390/proteomes5010009

Bargagli, R., and Rota, E. (2024). Environmental contamination and climate change in Antarctic ecosystems: an updated overview. *Environ. Sci. Adv.* 3, 543–560. doi:10.1039/D3VA00113J

Bengtson Nash, S., Rintoul, S. R., Kawaguchi, S., Staniland, I., Hoff, J. v. d., Tierney, M., et al. (2010). Perfluorinated compounds in the Antarctic region: ocean circulation provides prolonged protection from distant sources. *Environ. Pollut.* 158, 2985–2991. doi:10.1016/j.envpol.2010.05.024

Benskin, J. P., Muir, D. C. G., Scott, B. F., Spencer, C., De Silva, A. O., Kylin, H., et al. (2012). Perfluoroalkyl acids in the atlantic and Canadian arctic oceans. *Environ. Sci. Technol.* 46, 5815–5823. doi:10.1021/es300578x

Benskin, J. P., Phillips, V., St. Louis, V. L., and Martin, J. W. (2011). Source elucidation of perfluorinated carboxylic acids in remote alpine lake sediment cores. *Environ. Sci. Technol.* 45, 7188–7194. doi:10.1021/es2011176

Berhanu, A., Mutanda, I., Taolin, J., Qaria, M. A., Yang, B., and Zhu, D. (2023). A review of microbial degradation of per- and polyfluoroalkyl substances (PFAS): biotransformation routes and enzymes. *Sci. Total Environ.* 859, 160010. doi:10.1016/j.scitotenv.2022.160010

Beškoski, V. P., Yamamoto, A., Nakano, T., Yamamoto, K., Matsumura, C., Motegi, M., et al. (2018). Defluorination of perfluoroalkyl acids is followed by production of monofluorinated fatty acids. *Sci. Total Environ.* 636, 355–359. doi:10.1016/j.scitotenv.2018.04.243

Blévin, P., Angelier, F., Tartu, S., Bustamante, P., Herzke, D., Moe, B., et al. (2017). Perfluorinated substances and telomeres in an Arctic seabird: cross-sectional and longitudinal approaches. *Environ. Pollut.* 230, 360–367. doi:10.1016/j.envpol.2017.06.060

Boiteux, V., Dauchy, X., Rosin, C., and Munoz, J.-F. (2012). National screening study on 10 perfluorinated compounds in raw and treated tap water in France. *Arch. Environ. Contam. Toxicol.* 63, 1–12. doi:10.1007/s00244-012-9754-7

Boitsov, S., Bruvold, A., Hanssen, L., Jensen, H. K. B., and Ali, A. (2024). Per- and polyfluoroalkyl substances (PFAS) in surface sediments of the North-east Atlantic Ocean: a non-natural PFAS background. *Environ. Adv.* 16, 100545. doi:10.1016/j.envadv.2024.100545

Borgå, K., McKinney, M. A., Routti, H., Fernie, K. J., Giebichenstein, J., Hallanger, I., et al. (2022). The influence of global climate change on accumulation and toxicity of persistent organic pollutants and chemicals of emerging concern in Arctic food webs. *Environ. Sci. Process. Impacts* 24, 1544–1576. doi:10.1039/D1EM00469G

Boutet, V., Dominique, M., Eccles, K., Branigan, M., Dyck, M., van Coeverden de Groot, P., et al. (2023). An exploratory spatial contaminant assessment for polar bear (*Ursus maritimus*) liver, fat, and muscle from northern Canada. *Environ. Pollut.* 316, 120663. doi:10.1016/j.envpol.2022.120663

Bowman, J. S., and Deming, J. W. (2014). Alkane hydroxylase genes in psychrophile genomes and the potential for cold active catalysis. *BMC Genomics* 15, 1120. doi:10.1186/1471-2164-15-1120

Brendel, S., Fetter, É., Staude, C., Vierke, L., and Biegel-Engler, A. (2018). Short-chain perfluoroalkyl acids: environmental concerns and a regulatory strategy under REACH. *Environ. Sci. Eur.* 30, 9. doi:10.1186/s12302-018-0134-4

Buck, R. C., Franklin, J., Berger, U., Conder, J. M., Cousins, I. T., de Voogt, P., et al. (2011). Perfluoroalkyl and polyfluoroalkyl substances in the environment: terminology, classification, and origins. *Integr. Environ. Assess. Manag.* 7, 513–541. doi:10.1002/ieam.258

Casal, P., Casas, G., Vila-Costa, M., Cabrerizo, A., Pizarro, M., Jiménez, B., et al. (2019). Snow amplification of persistent organic pollutants at coastal Antarctica. *Environ. Sci. Technol.* 53, 8872–8882. doi:10.1021/acs.est.9b03006

Casal, P., González-Gaya, B., Zhang, Y., Reardon, A. J. F., Martin, J. W., Jiménez, B., et al. (2017a). Accumulation of perfluoroalkylated substances in oceanic plankton. *Environ. Sci. Technol.* 51, 2766–2775. doi:10.1021/acs.est.6b05821

Casal, P., Zhang, Y., Martin, J. W., Pizarro, M., Jiménez, B., and Dachs, J. (2017b). Role of snow deposition of perfluoroalkylated substances at coastal livingston island (maritime Antarctica). *Environ. Sci. Technol.* 51, 8460–8470. doi:10.1021/acs.est.7b02521

Casas, G., Iriarte, J., D'Agostino, L. A., Roscales, J. L., Martinez-Varela, A., Vila-Costa, M., et al. (2023). Inputs, amplification and sinks of perfluoroalkyl substances at coastal Antarctica. *Environ. Pollut.* 338, 122608. doi:10.1016/j.envpol.2023.122608

Casas, G., Martínez-Varela, A., Roscales, J. L., Vila-Costa, M., Dachs, J., and Jiménez, B. (2020). Enrichment of perfluoroalkyl substances in the sea-surface microlayer and sea-spray aerosols in the Southern Ocean. *Environ. Pollut.* 267, 115512. doi:10.1016/j.envpol.2020.115512

Cavicchioli, R., Siddiqui, K. S., Andrews, D., and Sowers, K. R. (2002). Low-temperature extremophiles and their applications. *Curr. Opin. Biotechnol.* 13, 253–261. doi:10.1016/s0958-1669(02)00317-8

Cerro-Gálvez, E., Roscales, J. L., Jiménez, B., Sala, M. M., Dachs, J., and Vila-Costa, M. (2020). Microbial responses to perfluoroalkyl substances and perfluorooctanesulfonate (PFOS) desulfurization in the Antarctic marine environment. *Water Res.* 171, 115434. doi:10.1016/j.watres.2019.115434

Chen, M., Wang, C., Wang, X., Fu, J., Gong, P., Yan, J., et al. (2019). Release of perfluoroalkyl substances from melting glacier of the Tibetan plateau: insights into the impact of global warming on the cycling of emerging pollutants. *J. Geophys. Res. Atmos.* 124, 7442–7456. doi:10.1029/2019JD030566

Chen, Z., zhan, X., Zhang, J., Diao, J., Su, C., Sun, Q., et al. (2023). Bioaccumulation and risk mitigation of legacy and novel perfluoroalkyl substances in seafood: insights from trophic transfer and cooking method. *Environ. Int.* 177, 108023. doi:10.1016/j.envint.2023.108023

Chetverikov, S. P., Sharipov, D. A., Korshunova, T.Y., and Loginov, O. N. (2017). Degradation of perfluorooctanyl sulfonate by strain Pseudomonas plecoglossicida 2.4-D. *Appl. Biochem. Microbiol.* 53, 533–538. doi:10.1134/S0003683817050027

Chiavola, A., Di Marcantonio, C., Boni, M. R., Biagioli, S., Frugis, A., and Cecchini, G. (2020). "PFOA and PFOS removal processes in activated sludge reactor at laboratory scale," in *Frontiers in water-energy-nexus—nature-based solutions, advanced technologies and best practices for environmental sustainability*. Editors V. Naddeo, M. Balakrishnan, and K.-H. Choo (Cham: Springer International Publishing), 375–377.

Choi, G., and Kan, E. (2024). Effects of perfluorooctanoic acid and perfluorooctane sulfonic acid on microbial community structure during anaerobic digestion. *Bioresour. Technol.* 393, 129999. doi:10.1016/j.biortech.2023.129999

Clarke, A., Morris, G. J., Fonseca, F., Murray, B. J., Acton, E., and Price, H. C. (2013). A low temperature limit for life on Earth. *PLOS ONE* 8, e66207. doi:10.1371/journal.pone.0066207

Codling, G., Halsall, C., Ahrens, L., Del Vento, S., Wiberg, K., Bergknut, M., et al. (2014). The fate of per- and polyfluoroalkyl substances within a melting snowpack of a boreal forest. *Environ. Pollut.* 191, 190–198. doi:10.1016/j.envpol.2014.04.032

Crisafi, F., Giuliano, L., Yakimov, M. M., Azzaro, M., and Denaro, R. (2016). Isolation and degradation potential of a cold-adapted oil/PAH-degrading marine bacterial consortium from Kongsfjorden (Arctic region). *Rend. Fis. Acc. Lincei* 27, 261–270. doi:10.1007/s12210-016-0550-6

Dai, S., Zhang, G., Dong, C., Yang, R., Pei, Z., Li, Y., et al. (2025). Occurrence, bioaccumulation and trophodynamics of per- and polyfluoroalkyl substances (PFAS) in terrestrial and marine ecosystems of Svalbard, Arctic. *Water Res.* 271, 122979. doi:10.1016/j.watres.2024.122979

Dassuncao, C., Hu, X. C., Zhang, X., Bossi, R., Dam, M., Mikkelsen, B., et al. (2017). Temporal shifts in poly- and perfluoroalkyl substances (PFASs) in North Atlantic pilot whales indicate large contribution of atmospheric precursors. *Environ. Sci. Technol.* 51, 4512–4521. doi:10.1021/acs.est.7b00293

Davis, M. J. B., Evich, M. G., Goodrow, S. M., and Washington, J. W. (2023). Environmental fate of Cl-PFPECAs: accumulation of novel and legacy perfluoroalkyl compounds in real-world vegetation and subsoils. *Environ. Sci. Technol.* 57, 8994–9004. doi:10.1021/acs.est.3c00665

Davis, S. N., Klumker, S. M., Mitchell, A. A., Coppage, M. A., Labonté, J. M., and Quigg, A. (2024). Life in the PFAS lane: the impact of perfluoroalkyl substances on photosynthesis, cellular exudates, nutrient cycling, and composition of a marine microbial community. *Sci. Total Environ.* 927, 171977. doi:10.1016/j.scitotenv.2024.171977

Dietz, R., Letcher, R. J., Desforges, J.-P., Eulaers, I., Sonne, C., Wilson, S., et al. (2019). Current state of knowledge on biological effects from contaminants on arctic wildlife and fish. *Sci. Total Environ.* 696, 133792. doi:10.1016/j.scitotenv.2019.133792

Douna, B. K., and Yousefi, H. (2023). Removal of PFAS by biological methods. *Asian Pac. J. Environ. Cancer* 6, 53–68. doi:10.31557/apjec.2023.6.1.53-68

Dunn, M., Vojta, S., Soltwedel, T., Von Appen, W.-J., and Lohmann, R. (2024). Passive sampler derived profiles and mass flows of perfluorinated alkyl substances (PFASs) across the Fram Strait in the North Atlantic. *Environ. Sci. Technol. Lett.* 11, 166–171. doi:10.1021/acs.estlett.3c00835

ECCC (2024). Updated draft state of per- and polyfluoroalkyl substances (PFAS) report. Available online at: https://www.canada.ca/en/environment-climate-change/services/evaluating-existing-substances/updated-draft-state-per-polyfluoroalkyl-substances-report.html (Accessed February 24, 2025).

ECHA (2024). Per- and polyfluoroalkyl substances (PFAS) - ECHA. Available online at: https://echa.europa.eu/hot-topics/perfluoroalkyl-chemicals-pfas (Accessed November 18, 2024).

EEA (2023). Cross-cutting story 3: PFAS — European environment agency. Available online at: https://www.eea.europa.eu/publications/zero-pollution/cross-cutting-stories/pfas (Accessed May 18, 2024).

Egas, C., Galbán-Malagón, C., Castro-Nallar, E., and Molina-Montenegro, M. A. (2023). Role of Microbes in the degradation of organic semivolatile compounds in polar ecosystems: a review. *Sci. Total Environ.* 879, 163046. doi:10.1016/j.scitotenv.2023.163046

Ellis, D. A., Martin, J. W., De Silva, A. O., Mabury, S. A., Hurley, M. D., Sulbaek Andersen, M. P., et al. (2004). Degradation of fluorotelomer alcohols: a likely atmospheric source of perfluorinated carboxylic acids. *Environ. Sci. Technol.* 38, 3316–3321. doi:10.1021/es049860w

Feller, G., and Gerday, C. (2003). Psychrophilic enzymes: hot topics in cold adaptation. *Nat. Rev. Microbiol.* 1, 200–208. doi:10.1038/nrmicro773

Feng, S., Lu, X., Ouyang, K., Su, G., Li, Q., Shi, B., et al. (2024). Environmental occurrence, bioaccumulation and human risks of emerging fluoroalkylether substances: insight into security of alternatives. *Sci. Total Environ.* 922, 171151. doi:10.1016/j.scitotenv.2024.171151

Fernández, S. G. (2024). Proactive approaches towards the phase-out of the PFAS family: The PFAS Movement status and a multi-national automotive enterprise towards hazardous chemicals phase-out. Sweden: University of Lund. Available online at: https://lup.lub.lu.se/student-papers/search/publication/9171566

Fuentes, S., Méndez, V., Aguila, P., and Seeger, M. (2014). Bioremediation of petroleum hydrocarbons: catabolic genes, microbial communities, and applications. *Appl. Microbiol. Biotechnol.* 98, 4781–4794. doi:10.1007/s00253-014-5684-9

Gaden, A., Ferguson, S. H., Harwood, L., Melling, H., Alikamik, J., and Stern, G. A. (2012). Western Canadian arctic ringed seal organic contaminant trends in relation to sea ice break-up. *Environ. Sci. Technol.* 46, 4427–4433. doi:10.1021/es204127j

Gaines, L. G. T. (2023). Historical and current usage of per- and polyfluoroalkyl substances (PFAS): a literature review. *Am. J. Industrial Med.* 66, 353–378. doi:10.1002/ajim.23362

Garcia-Barrios, J., Drysdale, M., Ratelle, M., Gaudreau, É., LeBlanc, A., Gamberg, M., et al. (2021). Biomarkers of poly- and perfluoroalkyl substances (PFAS) in Sub-Arctic and Arctic communities in Canada. *Int. J. Hyg. Environ. Health* 235, 113754. doi:10.1016/j.ijheh.2021.113754

Garg, A., Shetti, N. P., Basu, S., Nadagouda, M. N., and Aminabhavi, T. M. (2023). Treatment technologies for removal of per- and polyfluoroalkyl substances (PFAS) in biosolids. *Chem. Eng. J.* 453, 139964. doi:10.1016/j.cej.2022.139964

Garnett, J., Halsall, C., Thomas, M., Crabeck, O., France, J., Joerss, H., et al. (2021a). Investigating the uptake and fate of poly- and perfluoroalkylated substances (PFAS) in sea ice using an experimental sea ice chamber. *Environ. Sci. Technol.* 55, 9601–9608. doi:10.1021/acs.est.1c01645

Garnett, J., Halsall, C., Thomas, M., France, J., Kaiser, J., Graf, C., et al. (2019). Mechanistic insight into the uptake and fate of persistent organic pollutants in sea ice. *Environ. Sci. Technol.* 53, 6757–6764. doi:10.1021/acs.est.9b00967

Garnett, J., Halsall, C., Vader, A., Joerss, H., Ebinghaus, R., Leeson, A., et al. (2021b). High concentrations of perfluoroalkyl acids in arctic seawater driven by early thawing sea ice. *Environ. Sci. Technol.* 55, 11049–11059. doi:10.1021/acs.est.1c01676

Garnett, J., Halsall, C., Winton, H., Joerss, H., Mulvaney, R., Ebinghaus, R., et al. (2022). Increasing accumulation of perfluorocarboxylate contaminants revealed in an antarctic firn core (1958–2017). *Environ. Sci. Technol.* 56, 11246–11255. doi:10.1021/acs.est.2c02592

Gebbink, W. A., Bossi, R., Rigét, F. F., Rosing-Asvid, A., Sonne, C., and Dietz, R. (2016). Observation of emerging per- and polyfluoroalkyl substances (PFASs) in Greenland marine mammals. *Chemosphere* 144, 2384–2391. doi:10.1016/j.chemosphere.2015.10.116

Gran-Scheuch, A., Fuentes, E., Bravo, D. M., Jiménez, J. C., and Pérez-Donoso, J. M. (2017). Isolation and characterization of phenanthrene degrading bacteria from diesel fuel-contaminated antarctic soils. *Front. Microbiol.* 8, 1634. doi:10.3389/fmicb.2017.01634

Greaves, A. K., Letcher, R. J., Sonne, C., Dietz, R., and Born, E. W. (2012). Tissue-specific concentrations and patterns of perfluoroalkyl carboxylates and sulfonates in East Greenland polar bears. *Environ. Sci. Technol.* 46, 11575–11583. doi:10.1021/es303400f

Gruber, S., Fleiner, R., Guegan, E., Panday, P., Schmid, M.-O., Stumm, D., et al. (2017). Review article: inferring permafrost and permafrost thaw in the mountains of the Hindu Kush Himalaya region. *Cryosphere* 11, 81–99. doi:10.5194/tc-11-81-2017

Guo, W., Hao, W., and Xiao, W. (2024). Emerging perfluorinated chemical GenX: environmental and biological fates and risks. *Environ. Health*. doi:10.1021/envhealth.4c00164

Hamid, N., Junaid, M., Sultan, M., Yoganandham, S. T., and Chuan, O. M. (2024). The untold story of PFAS alternatives: insights into the occurrence, ecotoxicological impacts, and removal strategies in the aquatic environment. *Water Res.* 250, 121044. doi:10.1016/j.watres.2023.121044

Haque, F. L., Soerensen, A., Sköld, M., Awad, R., Spaan, M., Lauria, Z., et al. (2023). Per- and polyfluoroalkyl substances (PFAS) in white-tailed sea eagle eggs from Sweden: temporal trends (1969–2021), spatial variations, fluorine mass balance, and suspect screening. *Environ. Sci. Process. and Impacts* 25, 1549–1563. doi:10.1039/D3EM00141E

Hartz, W. F., Björnsdotter, M. K., Yeung, L. W. Y., Hodson, A., Thomas, E. R., Humby, J. D., et al. (2023). Levels and distribution profiles of per- and polyfluoroalkyl substances (PFAS) in a high arctic svalbard ice core. *Sci. Total Environ.* 871, 161830. doi:10.1016/j.scitotenv.2023.161830

Hartz, W. F., Björnsdotter, M. K., Yeung, L. W. Y., Humby, J. D., Eckhardt, S., Evangeliou, N., et al. (2024). Sources and seasonal variations of per- and polyfluoroalkyl substances (PFAS) in surface snow in the arctic. *Environ. Sci. Technol.* 58, 21817–21828. doi:10.1021/acs.est.4c08854

Huang, S., and Jaffé, P. R. (2019). Defluorination of perfluorooctanoic acid (PFOA) and perfluorooctane sulfonate (PFOS) by Acidimicrobium sp. strain A6. *Environ. Sci. Technol.* 53, 11410–11419. doi:10.1021/acs.est.9b04047

Interstate Technology and Regulatory Council (ITRC) (2023). Per- and Polyfluoroalkyl Substances (PFAS) technical and regulatory guidance document. Available online at: https://itrcweb.org/pfas-guidance/ (Accessed February 24, 2025).

Jansson, F. (2019). Occurrence of per- and polyfluorinated alkyl substances (PFAS), including ultra-short-chain compounds. Seasonal variation in rainwater from the Swedish west coast. Available online at: https://urn.kb.se/resolve?urn=urn:nbn:se:oru:diva-76989 (Accessed May 2, 2024).

Jin, B., Liu, H., Che, S., Gao, J., Yu, Y., Liu, J., et al. (2023). Substantial defluorination of polychlorofluorocarboxylic acids triggered by anaerobic microbial hydrolytic dechlorination. *Nat. Water* 1, 451–461. doi:10.1038/s44221-023-00077-6

Joerss, H., Xie, Z., Wagner, C. C., Von Appen, W.-J., Sunderland, E. M., and Ebinghaus, R. (2020). Transport of legacy perfluoroalkyl substances and the replacement compound HFPO-da through the atlantic gateway to the Arctic Ocean—is the arctic a sink or a source? *Environ. Sci. Technol.* 54, 9958–9967. doi:10.1021/acs.est.0c00228

Johansson, J. H., Salter, M. E., Acosta Navarro, J. C., Leck, C., Nilsson, E. D., and Cousins, I. T. (2019). Global transport of perfluoroalkyl acids via sea spray aerosol. *Environ. Sci. Process. Impacts* 21, 635–649. doi:10.1039/c8em00525g

Jones, B. M., Grosse, G., Farquharson, L. M., Roy-Léveillée, P., Veremeeva, A., Kanevskiy, M. Z., et al. (2022). Lake and drained lake basin systems in lowland permafrost regions. *Nat. Rev. Earth Environ.* 3, 85–98. doi:10.1038/s43017-021-00238-9

Jouanneau, W., Léandri-Breton, D.-J., Herzke, D., Moe, B., Nikiforov, V. A., Pallud, M., et al. (2023). Does contaminant exposure disrupt maternal hormones deposition? A study on per- and polyfluoroalkyl substances in an Arctic seabird. *Sci. Total Environ.* 868, 161413. doi:10.1016/j.scitotenv.2023.161413

Ju, X., Jin, Y., Sasaki, K., and Saito, N. (2008). Perfluorinated surfactants in surface, subsurface water and microlayer from Dalian coastal waters in China. *Environ. Sci. Technol.* 42, 3538–3542. doi:10.1021/es703006d

Kang, S. B., Wang, Z., Zhang, W., Kim, K.-Y., and Won, S. W. (2023). Removal of short- and long-chain PFAS from aquatic systems using electrostatic attraction of polyethylenimine-polyvinyl chloride electrospun nanofiber adsorbent. *Sep. Purif. Technol.* 326, 124853. doi:10.1016/j.seppur.2023.124853

Kannan, K., Koistinen, J., Beckmen, K., Evans, T., Gorzelany, J. F., Hansen, K. J., et al. (2001). Accumulation of perfluorooctane sulfonate in marine mammals. *Environ. Sci. Technol.* 35, 1593–1598. doi:10.1021/es001873w

Kärrman, A., Wang, T., Kallenborn, R., Langseter, A. M., Ræder, E. M., Lyche, J. L., et al. (2019). *PFASs in the Nordic environment*. Copenhagen: Nordic Council of Ministers, 515.

Kelly, B. C., Ikonomou, M. G., Blair, J. D., Surridge, B., Hoover, D., Grace, R., et al. (2009). Perfluoroalkyl contaminants in an arctic marine food web: trophic magnification and wildlife exposure. *Environ. Sci. Technol.* 43, 4037–4043. doi:10.1021/es9003894

European Union (2019). Regulation (EU) 2019/1021 of the European Parliament and of the council of 20 June 2019 on persistent organic Pollutants (consolidated version: 22 February 2021). Available online at: https://eur-lex.europa.eu/legal-content/EN/TXT/PDF/?uri=CELEX:02019R1021-20210222 (Accessed March 25, 2025).

Khan, B., Burgess, R. M., and Cantwell, M. G. (2023). Occurrence and bioaccumulation patterns of per- and polyfluoroalkyl substances (PFAS) in the marine environment. *ACS Est. Water* 3, 1243–1259. doi:10.1021/acsestwater.2c00296

Kim, S.-K., and Kannan, K. (2007). Perfluorinated acids in air, rain, snow, surface runoff, and lakes: relative importance of pathways to contamination of urban lakes. *Environ. Sci. Technol.* 41, 8328–8334. doi:10.1021/es072107t

Kim, Y., Pike, A., Gray, R., Faust, J., and Edmiston, P. (2023). Non-targeted identification and semi-quantitation of emerging per- and polyfluoroalkyl substances (PFAS) in US rainwater. *Environ. Sci. Process. and Impacts* 25, 1771–1787. doi:10.1039/D2EM00349J

Kirchgeorg, T., Dreyer, A., Gabrielli, P., Gabrieli, J., Thompson, L. G., Barbante, C., et al. (2016). Seasonal accumulation of persistent organic pollutants on a high altitude glacier in the Eastern Alps. *Environ. Pollut.* 218, 804–812. doi:10.1016/j.envpol.2016.08.004

Kwok, K. Y., Yamazaki, E., Yamashita, N., Taniyasu, S., Murphy, M. B., Horii, Y., et al. (2013). Transport of Perfluoroalkyl substances (PFAS) from an arctic glacier to downstream locations: implications for sources. *Sci. Total Environ.* 447, 46–55. doi:10.1016/j.scitotenv.2012.10.091

Lamon, L., von Waldow, H., MacLeod, M., Scheringer, M., Marcomini, A., and Hungerbühler, K. (2009). Modeling the global levels and distribution of polychlorinated biphenyls in air under a climate change scenario. *Environ. Sci. Technol.* 43, 5818–5824. doi:10.1021/es900438j

Léandri-Breton, D.-J., Jouanneau, W., Legagneux, P., Tarroux, A., Moe, B., Angelier, F., et al. (2024). Winter tracking data suggest that migratory seabirds transport per- and polyfluoroalkyl substances to their arctic nesting site. *Environ. Sci. Technol.* 58, 12909–12920. doi:10.1021/acs.est.4c02661

Letcher, R. J., Morris, A. D., Dyck, M., Sverko, E., Reiner, E. J., Blair, D. A. D., et al. (2018). Legacy and new halogenated persistent organic pollutants in polar bears from a contamination hotspot in the Arctic, Hudson Bay Canada. *Sci. Total Environ.* 610–611, 121–136. doi:10.1016/j.scitotenv.2017.08.035

Li, Z.-M., Roos, A., Serfass, T. L., Lee, C., and Kannan, K. (2024). Concentrations of 45 per- and polyfluoroalkyl substances in North American river otters (lontra canadensis) from West Virginia, USA. *Environ. Sci. Technol.* 58, 2089–2101. doi:10.1021/acs.est.3c09467

Liou, J. S.-C., Szostek, B., DeRito, C. M., and Madsen, E. L. (2010). Investigating the biodegradability of perfluorooctanoic acid. *Chemosphere* 80, 176–183. doi:10.1016/j.chemosphere.2010.03.009

Lohmann, R., Abass, K., Bonefeld-Jørgensen, E. C., Bossi, R., Dietz, R., Ferguson, S., et al. (2024). Cross-cutting studies of per- and polyfluorinated alkyl substances (PFAS) in Arctic wildlife and humans. *Sci. Total Environ.* 954, 176274. doi:10.1016/j.scitotenv.2024.176274

Lu, X., Ouyang, K., Su, G., Li, Q., Shi, B., Meng, J., et al. (2024). Environmental occurrence, bioaccumulation and human risks of emerging fluoroalkylether substances: insight into security of alternatives. *Sci. Total Environ.* 922, 171151. doi:10.1016/j.scitotenv.2024.171151

Ma, T., Ye, C., Wang, T., Li, X., and Luo, Y. (2022). Toxicity of per- and polyfluoroalkyl substances to aquatic invertebrates, planktons, and microorganisms. *Int. J. Environ. Res. Public Health* 19, 16729. doi:10.3390/ijerph192416729

MacInnis, J., Silva, A. O. D., Lehnherr, I., G. Muir, D. C., Pierre, K. A. S., Louis, V. L. S., et al. (2022). Investigation of perfluoroalkyl substances in proglacial rivers and permafrost seep in a high Arctic watershed. *Environ. Sci. Process. and Impacts* 24, 42–51. doi:10.1039/D1EM00349F

MacInnis, J. J., Lehnherr, I., Muir, D. C. G., Quinlan, R., and De Silva, A. O. (2019a). Characterization of perfluoroalkyl substances in sediment cores from High and Low Arctic lakes in Canada. *Sci. Total Environ.* 666, 414–422. doi:10.1016/j.scitotenv.2019.02.210

MacInnis, J. J., Lehnherr, I., Muir, D. C. G., St. Pierre, K. A., St. Louis, V. L., Spencer, C., et al. (2019b). Fate and transport of perfluoroalkyl substances from snowpacks into a lake in the high arctic of Canada. *Environ. Sci. Technol.* 53, 10753–10762. doi:10.1021/acs.est.9b03372

Magazine, S. (2024). PFAS legislation or not, brands must phase out "forever chemicals.". Available online at: https://sustonmagazine.com/2024/04/03/pfas-legislation-or-not-brands-must-phase-out-forever-chemicals/(Accessed June 7, 2024).

Mahinroosta, R., and Senevirathna, L. (2020). A review of the emerging treatment technologies for PFAS contaminated soils. *J. Environ. Manag.* 255, 109896. doi:10.1016/j.jenvman.2019.109896

Manojkumar, Y., Pilli, S., Rao, P. V., and Tyagi, R. D. (2023). Sources, occurrence and toxic effects of emerging per- and polyfluoroalkyl substances (PFAS). *Neurotoxicology Teratol.* 97, 107174. doi:10.1016/j.ntt.2023.107174

Martinez Alvarez, L., Bolhuis, H., Mau, G. K., Kok-Gan, C., Sing, C. C., Mac Cormack, W., et al. (2022). Identification of key bacterial players during successful full-scale soil field bioremediation in Antarctica. *Int. Biodeterior. and Biodegrad.* 168, 105354. doi:10.1016/j.ibiod.2021.105354

Martinez-Varela, A., Cerro-Gálvez, E., Auladell, A., Sharma, S., Moran, M. A., Kiene, R. P., et al. (2021). Bacterial responses to background organic pollutants in the northeast subarctic Pacific Ocean. *Environ. Microbiol.* 23, 4532–4546. doi:10.1111/1462-2920.15646

McGovern, M., Warner, N. A., Borgå, K., Evenset, A., Carlsson, P., Skogsberg, E., et al. (2022). Is glacial meltwater a secondary source of legacy contaminants to arctic coastal food webs? *Environ. Sci. Technol.* 56, 6337–6348. doi:10.1021/acs.est.1c07062

Meegoda, J. N., Kewalramani, J. A., Li, B., and Marsh, R. W. (2020). A review of the applications, environmental release, and remediation technologies of per- and polyfluoroalkyl substances. *Int. J. Environ. Res. Public Health* 17, 8117. doi:10.3390/ijerph17218117

Merino, N., Qu, Y., Rula, A., Mahendra, S., and Hoffmann, M. R. (2016). Degradation and removal methods for perfluoroalkyl and polyfluoroalkyl substances in water. *Environ. Eng. Sci.* 33, 615–649. Available online at: https://home.liebertpub.com/ees. doi:10.1089/ees.2016.0233

Miner, K. R., Blais, J., Bogdal, C., Villa, S., Schwikowski, M., Pavlova, P., et al. (2017). Legacy organochlorine pollutants in glacial watersheds: a review. *Environ. Sci. Process. Impacts* 19, 1474–1483. doi:10.1039/C7EM00393E

Miner, K. R., Campbell, S., Gerbi, C., Liljedahl, A., Anderson, T., Perkins, L. B., et al. (2018). Organochlorine pollutants within a polythermal glacier in the interior eastern Alaska range. *Water* 10, 1157. doi:10.3390/w10091157

Miner, K. R., Clifford, H., Taruscio, T., Potocki, M., Solomon, G., Ritari, M., et al. (2021). Deposition of PFAS 'forever chemicals' on Mt. Everest. *Sci. Total Environ.* 759, 144421. doi:10.1016/j.scitotenv.2020.144421

Muir, D., Bossi, R., Carlsson, P., Evans, M., De Silva, A., Halsall, C., et al. (2019). Levels and trends of poly- and perfluoroalkyl substances in the Arctic environment – an update. *Emerg. Contam.* 5, 240–271. doi:10.1016/j.emcon.2019.06.002

Müller, V., Costa, L. C. A., Rondan, F. S., Matic, E., Mesko, M. F., Kindness, A., et al. (2023). Per and polyfluoroalkylated substances (PFAS) target and EOF analyses in ski wax, snowmelts, and soil from skiing areas. *Environ. Sci. Process. Impacts* 25, 1926–1936. doi:10.1039/D3EM00375B

Munoz, G., Budzinski, H., Babut, M., Lobry, J., Selleslagh, J., Tapie, N., et al. (2019). Temporal variations of perfluoroalkyl substances partitioning between surface water, suspended sediment, and biota in a macrotidal estuary. *Chemosphere* 233, 319–326. doi:10.1016/j.chemosphere.2019.05.281

Nguyen, T. M. H., Bräunig, J., Thompson, K., Thompson, J., Kabiri, S., Navarro, D. A., et al. (2020). Influences of chemical properties, soil properties, and solution pH on soil–water partitioning coefficients of per- and polyfluoroalkyl substances (PFASs). *Environ. Sci. Technol.* 54, 15883–15892. doi:10.1021/acs.est.0c05705

Nizovoy, P., Bellora, N., Haridas, S., Sun, H., Daum, C., Barry, K., et al. (2021). Unique genomic traits for cold adaptation in Naganishia vishniacii, a polyextremophile yeast isolated from Antarctica. *FEMS Yeast Res.* 21, foaa056. doi:10.1093/femsyr/foaa056

NOAA (2024). What is the cryosphere? Available online at: https://oceanservice.noaa.gov/facts/cryosphere.html (Accessed May 3, 2024).

OECD (2021). *Reconciling terminology of the universe of per- and polyfluoroalkyl substances: recommendations and practical guidance*. OECD Environment Health and Safety Publications.

OECD (2022). *Synthesis report on understanding side-chain fluorinated polymers and their life cycle*. OECD.

OECD (2024). *Synthesis report on understanding Perfluoropolyethers (PFPEs) and their life cycle*. OECD. Available online at: https://www.oecd.org/en/publications/synthesis-report-on-understanding-perfluoropolyethers-pfpes-and-their-life-cycle_99ee2d3e-en.html (Accessed February 21, 2025).

Okazoe, T. (2009). Overview on the history of organofluorine chemistry from the viewpoint of material industry. *Proc. Jpn. Acad. Ser. B Phys. Biol. Sci.* 85, 276–289. doi:10.2183/pjab.85.276

Olney, S., Jones, M., Rockwell, C., Collins, R. D., Bryant, J. D., and Occhialini, J. (2023). Influence of convective and stratiform precipitation types on *per-* and polyfluoroalkyl substance concentrations in rain. *Sci. Total Environ.* 890, 164051. doi:10.1016/j.scitotenv.2023.164051

Orellana, R., Macaya, C., Bravo, G., Dorochesi, F., Cumsille, A., Valencia, R., et al. (2018). Living at the frontiers of life: extremophiles in Chile and their potential for bioremediation. *Front. Microbiol.* 9, 2309. doi:10.3389/fmicb.2018.02309

Papale, M., Giannarelli, S., Francesconi, S., Di Marco, G., Mikkonen, A., Conte, A., et al. (2017). Enrichment, isolation and biodegradation potential of psychrotolerant polychlorinated-biphenyl degrading bacteria from the Kongsfjorden (Svalbard Islands, High Arctic Norway). *Mar. Pollut. Bull.* 114, 849–859. doi:10.1016/j.marpolbul.2016.11.011

Papale, M., Lo Giudice, A., Rappazzo, A. C., Azzaro, M., and Rizzo, C. (2022). A first glimpse on cold-adapted PCB-oxidizing bacteria in edmonson point lakes (northern victoria land, Antarctica). *Water* 14, 109. doi:10.3390/w14010109

Pearce, D. A. (2012). "Extremophiles in Antarctica: life at low temperatures," in *Adaption of microbial life to environmental extremes: novel research results and application*. Editors H. Stan-Lotter and S. Fendrihan (Vienna: Springer), 87–118.

Persaud, D., Criscitiello, A. S., Spencer, C., Lehnherr, I., Muir, D. C. G., Silva, A. O. D., et al. (2024). A 50 year record for perfluoroalkyl acids in the high arctic: implications for global and local transport. *Environ. Sci. Process. Impacts* 26, 1543–1555. doi:10.1039/D4EM00219A

Pickard, H. M., Criscitiello, A. S., Spencer, C., Sharp, M. J., Muir, D. C. G., De Silva, A. O., et al. (2018). Continuous non-marine inputs of per- and polyfluoroalkyl substances to the High Arctic: a multi-decadal temporal record. *Atmos. Chem. Phys.* 18, 5045–5058. doi:10.5194/acp-18-5045-2018

REACH (2024). REACH regulation - European commission. Available online at: https://environment.ec.europa.eu/topics/chemicals/reach-regulation_en (Accessed November 18, 2024).

Ren, J., Point, A. D., Baygi, S. F., Fernando, S., Hopke, P. K., Holsen, T. M., et al. (2022). Bioaccumulation of polyfluoroalkyl substances in the Lake Huron aquatic food web. *Sci. Total Environ.* 819, 152974. doi:10.1016/j.scitotenv.2022.152974

Renfrew, D., and Pearson, T. W. (2021). The social life of the "forever chemical.". *Environ. Soc. (N.Y.).* 12, 146–163. doi:10.3167/ares.2021.120109

Reth, M., Berger, U., Broman, D., Cousins, I. T., Nilsson, E. D., and McLachlan, M. S. (2011). Water-to-air transfer of perfluorinated carboxylates and sulfonates in a sea spray simulator. *Environ. Chem.* 8, 381–388. doi:10.1071/EN11007

Rigét, F., Bossi, R., Sonne, C., Vorkamp, K., and Dietz, R. (2013). Trends of perfluorochemicals in Greenland ringed seals and polar bears: indications of shifts to decreasing trends. *Chemosphere* 93, 1607–1614. doi:10.1016/j.chemosphere.2013.08.015

Roberts, K. E., Lamoureux, S. F., Kyser, T. K., Muir, D. C. G., Lafrenière, M. J., Iqaluk, D., et al. (2017). Climate and permafrost effects on the chemistry and ecosystems of High Arctic Lakes. *Sci. Rep.* 7, 13292. doi:10.1038/s41598-017-13658-9

Ross, I., McDonough, J., Miles, J., Storch, P., Thelakkat Kochunarayanan, P., Kalve, E., et al. (2018). A review of emerging technologies for remediation of PFASs. *Remediat. J.* 28, 101–126. doi:10.1002/rem.21553

Routti, H., Aars, J., Fuglei, E., Hanssen, L., Lone, K., Polder, A., et al. (2017). Emission changes dwarf the influence of feeding habits on temporal trends of per- and polyfluoroalkyl substances in two arctic top predators. *Environ. Sci. Technol.* 51, 11996–12006. doi:10.1021/acs.est.7b03585

Saritha, V. K., Krishnan, K. P., and Mohan, M. (2023). Perfluorooctanoic acid in the sediment matrices of Arctic fjords, Svalbard. *Mar. Pollut. Bull.* 192, 115061. doi:10.1016/j.marpolbul.2023.115061

Schrenk, D., Bignami, M., Bodin, L., Chipman, J. K., del Mazo, J., Grasl-Kraupp, B., et al. (2020). Risk to human health related to the presence of perfluoroalkyl substances in food. *EFSA J.* 18, e06223. doi:10.2903/j.efsa.2020.6223

Schuur, E. A. G., McGuire, A. D., Schädel, C., Grosse, G., Harden, J. W., Hayes, D. J., et al. (2015). Climate change and the permafrost carbon feedback. *Nature* 520, 171–179. doi:10.1038/nature14338

Schwanz, T. G., Llorca, M., Farré, M., and Barceló, D. (2016). Perfluoroalkyl substances assessment in drinking waters from Brazil, France and Spain. *Sci. Total Environ.* 539, 143–152. doi:10.1016/j.scitotenv.2015.08.034

Senevirathna, S. T. M. L. D., Krishna, K. C. B., Mahinroosta, R., and Sathasivan, A. (2022). Comparative characterization of microbial communities that inhabit PFAS-rich contaminated sites: a case-control study. *J. Hazard. Mater.* 423, 126941. doi:10.1016/j.jhazmat.2021.126941

Sha, B., Johansson, J. H., Tunved, P., Bohlin-Nizzetto, P., Cousins, I. T., and Salter, M. E. (2022). Sea spray aerosol (SSA) as a source of perfluoroalkyl acids (PFAAs) to the atmosphere: field evidence from long-term air monitoring. *Environ. Sci. Technol.* 56, 228–238. doi:10.1021/acs.est.1c04277

Shan, G., Xiang, Q., Feng, X., Wu, W., Yang, L., and Zhu, L. (2021). Occurrence and sources of per- and polyfluoroalkyl substances in the ice-melting lakes of Larsemann Hills, East Antarctica. *Sci. Total Environ.* 781, 146747. doi:10.1016/j.scitotenv.2021.146747

Sherman-Bertinetti, S. L., Gruber, K. J., and Remucal, C. K. (2024). Preferential partitioning of per- and polyfluoroalkyl substances in freshwater ice. *Environ. Sci. Technol.* 58, 15214–15223. doi:10.1021/acs.est.4c04636

Shi, Y.-L., Pan, Y.-Y., Liang, L.-N., and Cai, Y.-Q. (2015). An on-line solid phase extraction–liquid chromatography tandem mass spectrometry method for the determination of perfluoroalkyl substances in the Antarctic ice core samples. *Chin. Chem. Lett.* 26, 1073–1078. doi:10.1016/j.cclet.2015.05.038

Singh, K., Kumar, N., Kumar Yadav, A., Singh, R., and Kumar, K. (2023). Per-and polyfluoroalkyl substances (PFAS) as a health hazard: current state of knowledge and strategies in environmental settings across Asia and future perspectives. *Chem. Eng. J.* 475, 145064. doi:10.1016/j.cej.2023.145064

Skaar, J. S., Ræder, E. M., Lyche, J. L., Ahrens, L., and Kallenborn, R. (2019). Elucidation of contamination sources for poly- and perfluoroalkyl substances (PFASs) on Svalbard (Norwegian Arctic). *Environ. Sci. Pollut. Res.* 26, 7356–7363. doi:10.1007/s11356-018-2162-4

Smorada, C. M., Sima, M. W., and Jaffé, P. R. (2024). Bacterial degradation of perfluoroalkyl acids. *Curr. Opin. Biotechnol.* 88, 103170. doi:10.1016/j.copbio.2024.103170

Sonne, C., Jenssen, B. M., Rinklebe, J., Lam, S. S., Hansen, M., Bossi, R., et al. (2023). EU need to protect its environment from toxic per- and polyfluoroalkyl substances. *Sci. Total Environ.* 876, 162770. doi:10.1016/j.scitotenv.2023.162770

Stemmler, I., and Lammel, G. (2010). Pathways of PFOA to the Arctic: variabilities and contributions of oceanic currents and atmospheric transport and chemistry sources. *Atmos. Chem. Phys.* 10, 9965–9980. doi:10.5194/acp-10-9965-2010

Sulbaek Andersen, M. P., Nielsen, O. J., Hurley, M. D., Ball, J. C., Wallington, T. J., Ellis, D. A., et al. (2005). Atmospheric chemistry of 4:2 fluorotelomer alcohol (n-$C_4F_9CH_2CH_2OH$): products and mechanism of Cl atom initiated oxidation in the presence of NO_x. *J. Phys. Chem. A* 109, 1849–1856. doi:10.1021/jp045672g

Sun, M., Arevalo, E., Strynar, M., Lindstrom, A., Richardson, M., Kearns, B., et al. (2016). Legacy and emerging perfluoroalkyl substances are important drinking water contaminants in the cape fear river watershed of North Carolina. *Environ. Sci. Technol. Lett.* 3, 415–419. doi:10.1021/acs.estlett.6b00398

Tartu, S., Bourgeon, S., Aars, J., Andersen, M., Lone, K., Jenssen, B. M., et al. (2017). Diet and metabolic state are the main factors determining concentrations of perfluoroalkyl substances in female polar bears from Svalbard. *Environ. Pollut.* 229, 146–158. doi:10.1016/j.envpol.2017.04.100

Teymourian, T., Teymoorian, T., Kowsari, E., and Ramakrishna, S. (2021). A review of emerging PFAS contaminants: sources, fate, health risks, and a comprehensive assortment of recent sorbents for PFAS treatment by evaluating their mechanism. *Res. Chem. Intermed.* 47, 4879–4914. doi:10.1007/s11164-021-04603-7

Thomas, D. N., and Dieckmann, G. S. (2002). Antarctic Sea ice--a habitat for extremophiles. *Science* 295, 641–644. doi:10.1126/science.1063391

Tomy, G. T., Budakowski, W., Halldorson, T., Helm, P. A., Stern, G. A., Friesen, K., et al. (2004). Fluorinated organic compounds in an eastern arctic marine food web. *Environ. Sci. Technol.* 38, 6475–6481. doi:10.1021/es049620g

UNEP (2022). National environmental action Plan 2022-2030. Available online at: https://leap.unep.org/en/countries/lk/national-legislation/national-environmental-action-plan-2022-2030 (Accessed July 28, 2024).

U.S. EPA (2022). Drinking water health advisory: hexafluoropropylene oxide (HFPO) dimer acid (CASRN 13252-13-6) and HFPO dimer acid ammonium salt (CASRN 62037-80-3), also known as "GenX chemicals." EPA/822/R-22/005.

US EPA (2024). PFAS national primary drinking water regulation. Federal Register, 89(82), 31592–31681. Available online at: https://www.federalregister.gov/documents/2024/04/26/2024-07773/pfas-national-primary-drinking-water-regulation (Accessed February 20, 2025).

US EPAO (2019). Addition of certain PFAS to the TRI by the national Defense authorization act. Available online at: https://www.epa.gov/toxics-release-inventory-tri-program/addition-certain-pfas-tri-national-defense-authorization-act (Accessed February 24, 2025).

US EPAO (2021). Per- and polyfluoroalkyl substances (PFAS). Available online at: https://www.epa.gov/sdwa/and-polyfluoroalkyl-substances-pfas (Accessed February 20, 2025).

US EPAO (2025). EPA adds nine additional PFAS to the toxics release inventory. Available online at: https://www.epa.gov/newsreleases/epa-adds-nine-additional-pfas-toxics-release-inventory (Accessed February 24, 2025).

Valdersnes, S., Nilsen, B. M., Breivik, J. F., Borge, A., and Maage, A. (2017). Geographical trends of PFAS in cod livers along the Norwegian coast. *PLoS ONE* 12, e0177947. doi:10.1371/journal.pone.0177947

Van de Vijver, K. I., Hoff, P. T., Das, K., Van Dongen, W., Esmans, E. L., Jauniaux, T., et al. (2003). Perfluorinated chemicals infiltrate ocean waters: link between exposure levels and stable isotope ratios in marine mammals. *Environ. Sci. Technol.* 37, 5545–5550. doi:10.1021/es0345975

Villanger, G. D., Kovacs, K. M., Lydersen, C., Haug, L. S., Sabaredzovic, A., Jenssen, B. M., et al. (2020). Perfluoroalkyl substances (PFASs) in white whales (*Delphinapterus leucas*) from Svalbard – a comparison of concentrations in plasma sampled 15 years apart. *Environ. Pollut.* 263, 114497. doi:10.1016/j.envpol.2020.114497

von Appen, W.-J. (2018). *The expedition PS114 of the research vessel POLARSTERN to the Fram Strait in 2018*. Bremerhaven, Germany: Berichte zur Polar- und Meeresforschung.

Vonk, J. E., Tank, S. E., Bowden, W. B., Laurion, I., Vincent, W. F., Alekseychik, P., et al. (2015). Reviews and syntheses: effects of permafrost thaw on Arctic aquatic ecosystems. *Biogeosciences* 12, 7129–7167. doi:10.5194/bg-12-7129-2015

Wackett, L. P., and Robinson, S. L. (2020). The ever-expanding limits of enzyme catalysis and biodegradation: polyaromatic, polychlorinated, polyfluorinated, and polymeric compounds. *Biochem. J.* 477, 2875–2891. doi:10.1042/BCJ20190720

Wang, X., Chen, M., Gong, P., and Wang, C. (2019). Perfluorinated alkyl substances in snow as an atmospheric tracer for tracking the interactions between westerly winds and the Indian Monsoon over western China. *Environ. Int.* 124, 294–301. doi:10.1016/j.envint.2018.12.057

Wang, X., Halsall, C., Codling, G., Xie, Z., Xu, B., Zhao, Z., et al. (2014). Accumulation of perfluoroalkyl compounds in Tibetan mountain snow: temporal patterns from 1980 to 2010. *Environ. Sci. Technol.* 48, 173–181. doi:10.1021/es4044775

Wang, Y., Li, X., Zheng, Z., Shi, Y., and Cai, Y. (2021a). Chlorinated polyfluoroalkyl ether sulfonic acids in fish, dust, drinking water and human serum: from external exposure to internal doses. *Environ. Int.* 157, 106820. doi:10.1016/j.envint.2021.106820

Wang, Z., Buser, A. M., Cousins, I. T., Demattio, S., Drost, W., Johansson, O., et al. (2021b). A new OECD definition for per- and polyfluoroalkyl substances. *Environ. Sci. Technol.* 55, 15575–15578. doi:10.1021/acs.est.1c06896

Wang, Z., Cousins, I. T., Scheringer, M., and Hungerbuehler, K. (2015a). Hazard assessment of fluorinated alternatives to long-chain perfluoroalkyl acids (PFAAs) and their precursors: *status quo*, ongoing challenges and possible solutions. *Environ. Int.* 75, 172–179. doi:10.1016/j.envint.2014.11.013

Wang, Z., Xie, Z., Mi, W., Möller, A., Wolschke, H., and Ebinghaus, R. (2015b). Neutral poly/per-fluoroalkyl substances in air from the atlantic to the Southern Ocean and in antarctic snow. *Environ. Sci. Technol.* 49, 7770–7775. doi:10.1021/acs.est.5b00920

Wania, F. (2007). A global mass balance analysis of the source of perfluorocarboxylic acids in the Arctic Ocean. *Environ. Sci. Technol.* 41, 4529–4535. doi:10.1021/es070124c

Wee, S. Y., and Aris, A. Z. (2023). Revisiting the "forever chemicals". *PFOA PFOS Expo. Drink. water. npj Clean Water* 6, 1–16. doi:10.1038/s41545-023-00274-6

Wild, S., McLagan, D., Schlabach, M., Bossi, R., Hawker, D., Cropp, R., et al. (2015). An antarctic research station as a source of brominated and perfluorinated persistent organic pollutants to the local environment. *Environ. Sci. Technol.* 49, 103–112. doi:10.1021/es5048232

Xie, Z., and Kallenborn, R. (2023). Legacy and emerging per- and poly-fluoroalkyl substances in polar regions. *Curr. Opin. Green Sustain. Chem.* 42, 100840. doi:10.1016/j.cogsc.2023.100840

Xie, Z., Wang, Z., Mi, W., Möller, A., Wolschke, H., and Ebinghaus, R. (2015). Neutral poly-/perfluoroalkyl substances in air and snow from the arctic. *Sci. Rep.* 5, 8912. doi:10.1038/srep08912

Xin, X., Kim, J., Ashley, D. C., and Huang, C.-H. (2023). Degradation and defluorination of per- and polyfluoroalkyl substances by direct photolysis at 222 nm. *ACS Est. Water* 3, 2776–2785. doi:10.1021/acsestwater.3c00274

Yamashita, N., Taniyasu, S., Petrick, G., Wei, S., Gamo, T., Lam, P. K. S., et al. (2008). Perfluorinated acids as novel chemical tracers of global circulation of ocean waters. *Chemosphere* 70, 1247–1255. doi:10.1016/j.chemosphere.2007.07.079

Yeung, L. W. Y., Dassuncao, C., Mabury, S., Sunderland, E. M., Zhang, X., and Lohmann, R. (2017). Vertical profiles, sources, and transport of PFASs in the Arctic Ocean. *Environ. Sci. Technol.* 51, 6735–6744. doi:10.1021/acs.est.7b00788

Yi, L., Peng, Q., Liu, D., Zhou, L., Tang, C., Zhou, Y., et al. (2019). Enhanced degradation of perfluorooctanoic acid by a genome shuffling-modified Pseudomonas parafulva YAB-1. *Environ. Technol.* 40, 3153–3161. doi:10.1080/09593330.2018.1466918

Yin, S., and Villagrán, D. (2022). Design of nanomaterials for the removal of per- and poly-fluoroalkyl substances (PFAS) in water: strategies, mechanisms, challenges, and opportunities. *Sci. Total Environ.* 831, 154939. doi:10.1016/j.scitotenv.2022.154939

Young, C. J., Furdui, V. I., Franklin, J., Koerner, R. M., Muir, D. C. G., and Mabury, S. A. (2007). Perfluorinated acids in arctic snow: new evidence for atmospheric formation. *Environ. Sci. Technol.* 41, 3455–3461. doi:10.1021/es0626234

Yu, Y., Zhang, K., Li, Z., Ren, C., Chen, J., Lin, Y.-H., et al. (2020). Microbial cleavage of C–F bonds in two C6 per- and polyfluorinated compounds via reductive defluorination. *Environ. Sci. Technol.* 54, 14393–14402. doi:10.1021/acs.est.0c04483

Zalasiewicz, J., Waters, C. N., Williams, M., and Summerhayes, C. P. (2019). *The Anthropocene as a geological time unit: a guide to the scientific evidence and current debate* (Cambridge: Cambridge University Press).

Zhang, D., Li, J., Li, X., Wang, M., Zhong, Y., Chen, G., et al. (2023). Phytoremediation of fluoroalkylethers (ether-PFASs): a review on bioaccumulation and ecotoxilogical effects. *Sci. Total Environ.* 865, 161260. doi:10.1016/j.scitotenv.2022.161260

Zhang, X., Lohmann, R., and Sunderland, E. M. (2019). Poly- and perfluoroalkyl substances in seawater and plankton from the northwestern atlantic margin. *Environ. Sci. Technol.* 53, 12348–12356. doi:10.1021/acs.est.9b03230

Zhang, X., Zhang, Y., Dassuncao, C., Lohmann, R., and Sunderland, E. M. (2017). North Atlantic Deep Water formation inhibits high Arctic contamination by continental perfluorooctane sulfonate discharges. *Glob. Biogeochem. Cycles* 31, 1332–1343. doi:10.1002/2017GB005624

Zhang, Y., Qv, Z., Wang, J., Yang, Y., Chen, X., Wang, J., et al. (2022a). Natural biofilm as a potential integrative sample for evaluating the contamination and impacts of PFAS on aquatic ecosystems. *Water Res.* 215, 118233. doi:10.1016/j.watres.2022.118233

Zhang, Z., Sarkar, D., Biswas, J. K., and Datta, R. (2022b). Biodegradation of per- and polyfluoroalkyl substances (PFAS): a review. *Bioresour. Technol.* 344, 126223. doi:10.1016/j.biortech.2021.126223

Zhao, Z., Xie, Z., Möller, A., Sturm, R., Tang, J., Zhang, G., et al. (2012). Distribution and long-range transport of polyfluoroalkyl substances in the Arctic, Atlantic Ocean and Antarctic coast. *Environ. Pollut.* 170, 71–77. doi:10.1016/j.envpol.2012.06.004

Zhou, Y., Wang, X., Chen, M., Fu, J., Zhu, T., Wang, C., et al. (2024a). Proglacial river sediments are a substantial sink of perfluoroalkyl substances released by glacial meltwater. *Commun. Earth Environ.* 5, 68–11. doi:10.1038/s43247-024-01223-y

Zhou, Y., Wang, X., Wang, C., Ji, Z., Niu, X., and Dong, H. (2024b). Fate of 'forever chemicals' in the global cryosphere. *Earth-Science Rev.* 259, 104973. doi:10.1016/j.earscirev.2024.104973

Article II

Arctic and sub-Arctic marine diatom responses to PFAS exposure: Understanding physiological changes and resilience.

Graphical Abstract

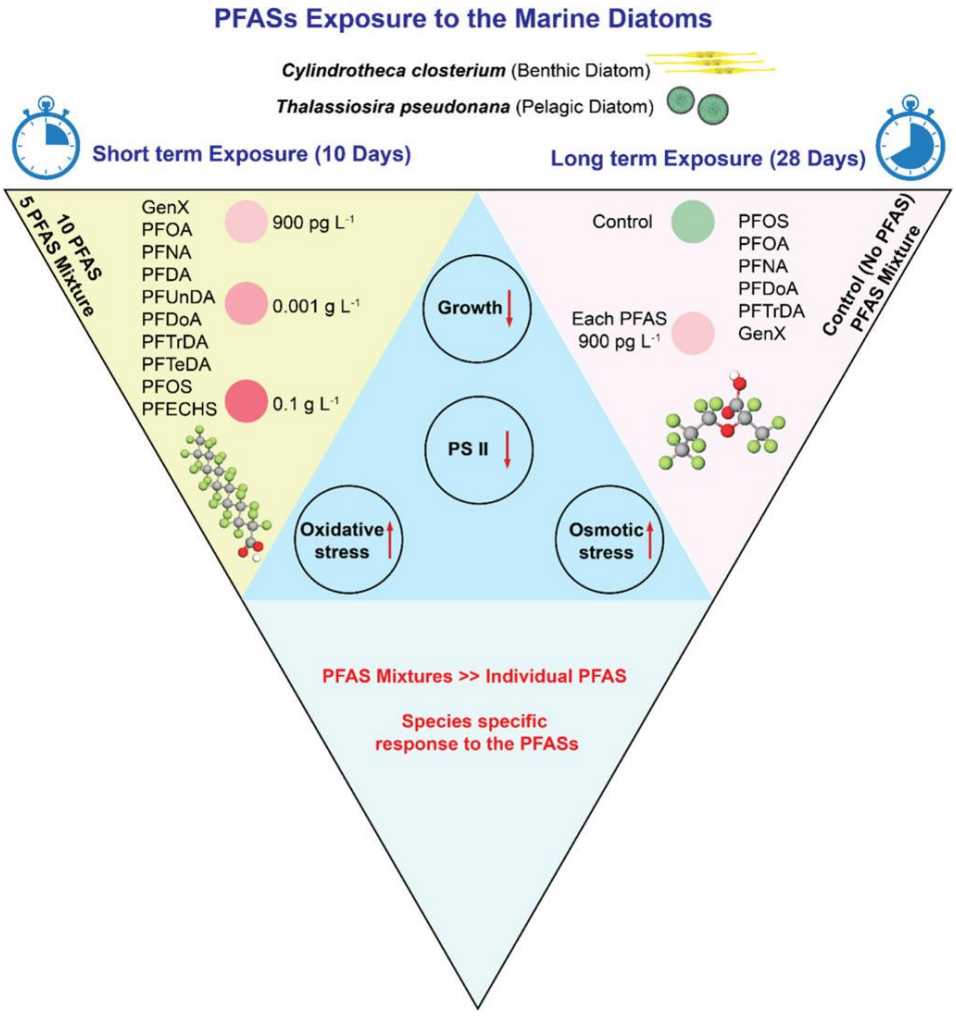

Aquatic Toxicology 289 (2025) 107562

Contents lists available at ScienceDirect

Aquatic Toxicology

journal homepage: www.elsevier.com/locate/aqtox

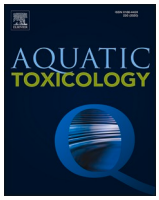

Arctic and sub-Arctic marine diatom responses to PFAS exposure: Understanding physiological changes and resilience

Ashani Arulananthan [a,b,**], Bettina Scholz [b], Ulf Karsten [c,d], Hans-Peter Grossart [e,f,*], Auður Sigurbjörnsdóttir [a], Óttar Rolfsson [g], Hanna Joerss [h], Bernardo Duarte [i,j], Oddur Þór Vilhelmsson [a,k]

[a] Faculty of Natural Resource Sciences, University of Akureyri, Iceland
[b] BioPol ehf. Marine Biotechnology, Skagaströnd, Iceland
[c] Department of Applied Ecology and Phycology, Institute of Biological Sciences, University of Rostock, Germany
[d] Department of Maritime Systems, Interdisciplinary Faculty, University of Rostock, Germany
[e] Department of Plankton and Microbial Ecology, Leibniz-Institute of Freshwater Ecology and Inland Fisheries, Stechlin, Germany
[f] Institute of Biochemistry and Biology, Potsdam University, Potsdam, Germany
[g] Department of Biochemistry and Molecular Biology, Faculty of Medicine, University of Iceland, Reykjavik, Iceland
[h] Institute of Coastal Environmental Chemistry, Helmholtz-Zentrum Hereon, Geesthacht, Germany
[i] MARE—Marine and Environmental Sciences Centre & ARNET—Aquatic Research Network Associated Laboratory, Faculdade de Ciências da Universidade de Lisboa, Campo Grande, 1749-016 Lisbon, Portugal
[j] Departamento de Biologia Vegetal, Faculdade de Ciências da Universidade de Lisboa, Campo Grande,1749-016 Lisbon, Portugal
[k] The Biomedical Center of the University of Iceland, Reykjavík, Iceland

A R T I C L E I N F O

Keywords:
PFAS
Arctic and sub-Arctic marine diatoms
Stress response
PFAS toxicity
Growth inhibition

A B S T R A C T

Per- and polyfluoroalkyl substances (PFAS) are persistent organic pollutants widely detected across diverse ecosystems. Despite regulatory bans on several PFAS compounds, PFAS remain prevalent in remote areas like the Arctic, raising significant ecological health concerns. This study addresses a critical knowledge gap regarding the effects of PFAS on unicellular primary producers, with a focus on diatom physiology and fitness. Two ecologically important Arctic and sub-Arctic diatom species, *Cylindrotheca closterium* and *Thalassiosira pseudonana,* as well as legacy long-chain PFAS, and two emerging PFAS replacements were investigated. Exposures were conducted for 10 days at three concentrations (100 mg/L, 1 mg/L, and 0.9 ng/L). Following the 10 d (short-term) toxicity assessment, one PFAS mixture was exposed for 28 days (long-term) at an environmentally relevant concentration of 0.9 ng/L. Physiological and biochemical responses, including growth, photosynthetic capacity, stress biomarkers, and metabolic changes, were assessed. Results revealed distinct impacts of PFAS on individual PFAS and their mixtures. Perfluorooctane sulfonic acid (PFOS), perfluorooctanoic acid (PFOA), perfluorononanoic acid (PFNA), perfluorododecanoic acid (PFDoA), perfluorotridecanoic acid (PFTrDA), and perfluorotetradecanoic acid (PFTeDA) often exhibited the most detrimental effects on both species relative to controls. PFAS mixtures exhibited synergistic impacts, with increasing effects as the number of PFAS compounds increased. Both diatoms exhibited significant reductions in growth and photochemical efficiency of photosystem II, along with elevated proline and total antioxidant activity, during short-term exposure to PFAS. During the long-term experiment, after the exponential growth phase (after 14 d), growth rates were not significantly different from those of the controls, suggesting potential compensatory responses over time. Despite the mild growth inhibition, enhanced biochemical activity relative to controls indicates sustained metabolic adjustment under prolonged PFAS exposure. These findings emphasize the potential impacts of PFAS, specially in mixtures, on disrupting primary producers in cold marine ecosystems, highlighting the need to assess the cumulative effects of pollutants on foundational Arctic biota.

* Corresponding author at: Leibniz-Institute of Freshwater Ecology and Inland Fisheries, Neuglobsow, Germany.
** Corresponding author at: Faculty of Natural Resource Science, University of Akureyri, Iceland.
E-mail addresses: ashani@unak.is (A. Arulananthan), hanspeter.grossart@igb-berlin.de (H.-P. Grossart).

https://doi.org/10.1016/j.aquatox.2025.107562
Received 20 May 2025; Received in revised form 2 September 2025; Accepted 3 September 2025
Available online 10 September 2025

1. Introduction

The Anthropocene epoch is stressing fragile ecosystems with climate change and temperature increases, along with pollutants such as microplastics (MPs) and persistent organic pollutants (POPs), which threaten sensitive habitats, including Arctic (de Wit et al., 2019; Jouanneau et al., 2023; Zhao et al., 2012). Of note, per- and polyfluoroalkyl substances (PFAS) are frequently referred to as "emerging contaminants" (Manojkumar et al., 2023), and environmental levels of these substances have been systematically assessed since the last two decades (Dai et al., 2025; ITRC, 2023; Trilla-Prieto et al., 2025; US EPA, 2021). However, the identification of intricate mixtures of contaminants is now raising pertinent questions about their potential impacts on human health and the environment (Antonopoulou et al., 2024; Bernardini et al., 2021; Davis et al., 2024; Lukić Bilela et al., 2023).

PFAS are synthetic chemicals characterized by a robust fluorocarbon backbone (C-F bond energy ~530kJ/mol), and a functional group, which may include carboxylate (-COO^-), sulfonate (-$SO3^-$), hydroxyl (-OH^-), or amide (-$CONH_2$) structures (Wang et al., 2018). This unique configuration renders PFAS remarkably durable and resistant to breakdown. Due to their high surface activity, these substances are used in various industrial applications, including everyday items such as cosmetics, non-stick cookware, and waterproof fabrics (Gaines, 2023). Over 4700 distinct PFAS compounds have been identified, garnering significant attention due to their persistent nature (ECHA, 2024; ITRC, 2023; US EPA, 2021). Nevertheless, PFAS eventually spread into the environment at the end of their lifecycle and became widely distributed across all environmental compartments, including remote areas such as the Arctic and Antarctic (Casal et al., 2017b; Casas et al., 2023; Trilla-Prieto et al., 2025; Zhao et al., 2012; Zhou et al., 2024).

Despite its remote location, Arctic communities were burdened by visible ice cover loss and the silent infiltration of pollutants, such as PFAS (Ahrens et al., 2023; Armitage, 2009). Recent studies have revealed the widespread occurrence of perfluorobutanoic acid (PFBA) and trifluoroacetic acid (TFA) in atmospheric deposition, as documented in snow and ice cores from Lake Haze and Svalbard (Hartz et al., 2023; MacInnis et al., 2019). In ice cores from the High Arctic, background levels of perfluorooctanoic acid (PFOA) ranged from 60 to 166 pg/L, while hexafluoropropylene oxide dimer acid (HFPO-DA, known as GenX), a replacement for PFOA, was detected in Arctic seawater, underscoring their ongoing long-range transport (Joerss et al., 2019).

Thereby, detecting these pollutants in Arctic waters, fresh snow, and ice sheets has raised concerns regarding their effects on marine life at various trophic levels (Ali et al., 2021; Dai et al., 2025; Hartz et al., 2024). In Arctic biota, PFOS (perfluorooctanesulfonic acid) and long-chain PFCAs (perfluorocarboxylic acids) (C9-C11) have been reported at concentrations of 1–40 ng/g wet weight in liver and plasma of apex predators such as polar bears and ringed seals (Gebbink et al., 2016; Routti et al., 2016). Despite well-documented bioaccumulation in apex predators, such as polar bears, whales, seals, and seabirds, there has been limited focus on the foundational components of the base of food web, particularly Arctic marine diatoms (Casal et al., 2017a; Chen et al., 2023; Routti et al., 2019).

Diatoms are a dominant group of phytoplankton, a type of microscopic algae, serving as primary producers in freshwater and marine ecosystems (Benoiston et al., 2017). They play a critical role in global carbon cycling and oxygen production, accounting for 25 % of global primary production (Falkowski, 2012), and are key to the biological carbon pump, facilitating the export of organic carbon to deep oceans, aiding long-term CO_2 sequestration (Hopkinson et al., 2011; Mahmoudnia, 2023). Although studies on phytoplankton and microalgae communities have shown that PFAS can disrupt photosynthesis, growth, and molecular and cellular integrity, the ecotoxicological consequences on cold-adapted diatom communities in polar environments remain scarce (Beena Ramachandran Nair, 2025; Latała et al., 2009; Li et al., 2024; Liao et al., 2025; Shi et al., 2024; Zhao et al., 2023). In addition, any adverse effect on diatoms could propagate through the food web, affecting zooplankton, fish, and other higher trophic levels (Bernardo-Cravo et al., 2020; Braune et al., 2005; Brun et al., 2019; Hallanger et al., 2011). Recent findings of PFAS in Arctic phytoplankton and zooplankton indicate contamination at the base of the marine ecosystem, yet the physiological impacts on Arctic diatoms remain unclear (Ma et al., 2022). Additionally, the combined effects of multiple PFAS exposures, so-called 'cocktail effect,' immediate and long-term effects, as well as the cellular defence mechanisms against these chemicals, by diatoms under such stressors, are also poorly understood (Dale et al., 2022; Liu et al., 2022; Pietropoli et al., 2025). Additionally, existing ecotoxicological studies on marine algae and diatoms typically focus on legacy PFAS such as PFOS and PFOA, which are long-chain PFAS, under regulation (Liao et al., 2024; Rodea-Palomares et al., 2012; Shi et al., 2024; Zhang et al., 2024). Studies indicate that ether-based and shorter-chain alternative PFAS, such as GenX, have similar toxicological profiles (Guo et al., 2024; Y. Li et al., 2021). This highlights the need for further detailed research and assessments of various legacy compounds to understand their ecological impacts.

In this context, this study aims to provide a comprehensive assessment of the effects of long-chain and replacement PFAS on two ecologically distinct marine diatoms: *Cylindrotheca closterium* is a benthic representative living on top of coastal soft bottoms, and *Thalassiosira pseudonana* is a member of the phytoplankton living in the water column, also occurring in polar waters off Iceland. Both species were exposed to defined concentrations of PFAS under controlled laboratory conditions, and a suite of physiological and biochemical responses was measured. Based on this experimental framework, we hypothesize that exposure of marine diatoms to PFAS is reflected by alterations in their physiology, ultimately compromising their fitness.

2. Materials and methods

2.1. Diatom culture conditions

The benthic *Cylindrotheca closterium* and the pelagic *Thalassiosira pseudonana* were used to investigate the effects of PFAS across different environmental compartments, due to their distinct ecological niches and relevance to Arctic marine habitats. These contrasting habitats, benthos and pelagial, are known to influence PFAS distribution and bioavailability, potentially shaping species-specific exposure and response patterns (Dai et al., 2018; Pascariello et al., 2019; Wu et al., 2021).

The unicellular xenic Arctic and sub-Arctic diatoms *C. closterium* isolated from Svalbard samples) and *T. pseudonana* (strain DCG 0682 from BCCM/DCG at the Ghent University, Belgium) were acquired from the BioPol Marine Biotechnology Centre and cultured in 2 L Erlenmeyer flasks containing artificial seawater salt (distilled water + 35 g/L sea salt, Tropic Marin Bio-Actif), made up of f/2 medium, 30 S_A (absolute salinity unit), and pH 8.00 prepared according to Guillard (1975). All cultures and all experimental units were carried out with a photoperiod set at 12 h light: 12 h dark by positioning two vertical white, 100 μmol photons $m^{-2}s^{-1}$ (fluorescent lights -TREVOS a.s. TYP: PRIMA 158, Model: PCc, S, ta, 230 V, 50 Hz, 1 × 58 W IP 66, positioned parallel to the flasks from two sides), with an average temperature of 16 ± 0.5 °C. This temperature is near the growth optimum of many benthic diatom species from the Arctic (Karsten et al., 2012). Additionally, the cultures were gently shaken three times daily, and the arrangement (position around the light) of the culture flasks was randomly altered every day throughout the experiment. This was performed to ensure uniform light and temperature conditions for all treatments and controls, thereby preventing positional bias effects.

2.2. Experimental design and PFAS assays

Short-term (up to exponential growth phase: 10 d old) and long-term (28 d) experiments were conducted to capture a comprehensive picture

of PFAS toxicity on the tested marine diatoms. The short-term PFAS exposure allowed us to evaluate immediate physiological and biochemical stress responses in the exponential growth phase. In contrast, the long-term experiment was designed to assess sustained effects and potential resilience or adaptation over time under environmentally relevant PFAS concentrations. This dual approach enabled us to distinguish between acute vs. chronic impacts, which is essential for understanding ecological risks and diatom population stability in PFAS-contaminated environments.

For the short-term PFAS toxicity assessment, 10 types of individual PFAS assays and five PFAS mixtures were tested at three different concentrations (Table 1). The tested PFAS included seven long-chain PFCAs (C8 to C14), two PFSAs (perfluoroalkyl sulfonic acids) (C8, linear and cyclic) and one perfluoroalkyl ether carboxylic acid (HFPO-DA, marketed as its ammonium salt under the trade name of GenX).

The concentrations tested—100 mg/L (high), 1 mg/L (mid), and 0.9 ng/L (low)—were chosen as they were recorded in different environmental matrices and biota. The high and mid concentrations reported for PFAS in landfill leachate (Sabba et al., 2025; Tolaymat et al., 2023). In addition, 100 mg/L was chosen because it has been used in PFAS toxicity tests on diatoms without causing lethal effects; for example, perfluorooctanoic acid (molecular weight 414.07 g/mol) inhibited the growth of *Skeletonema marinoi* at 368.52 mg/L, with an EC50 (Latała et al., 2009). Arctic environments and biota samples showed concentrations ranging from ng to pg per liter (Sabba et al., 2025; Tolaymat et al., 2023). In surface waters of the northwest Atlantic, PFAS levels are typically in the pg range, ranging from 60 to 900 pg/L (Zhang et al., 2019) and in Antarctica (Trilla-Prieto et al., 2025). Conversely, the 0.9 ng/L level was used to assess whether environmental PFAS levels already affect diatom physiology. Mixture concentrations were set at half the maximum effective concentration of individual PFAS tested, which is the concentration inducing a response midway between baseline and maximum.

Each assay was spiked in 100 mL Erlenmeyer flasks containing 25 mL freshly prepared f/2 medium and 25 mL diatom culture. The experiments were performed in four batches: the first and fourth batches contained *C. closterium,* whereas the middle batches, containing *T. pseudonana* and their controls, were also maintained and analyzed. The initial cell density was maintained roughly the same across each run of the assays and controls; hence, growth was measured from their respective starting point densities.

Later, a long-term experiment was conducted in a 5 L flask containing 2 L of f/2 medium and 3 L of diatom culture, utilizing the lowest environmentally relevant concentration of 0.9 ng/L of PFOS, PFOA, PFNA (perfluorononanoic acid), PFDoA (perfluorododecanoic acid), PFTrDA (perfluorotridecanoic acid), and HFPO-DA. This concentration was selected because many of the PFAS tested in this study reported values within the ranges observed in the polar regions (Xie and Kallenborn, 2023). This composition was selected after the short-term experiments for molecular analysis, due to its weak physiological responses.

All experiments were performed in glass flasks which were thoroughly washed three to four times with distilled water prior to use. To reduce the risk of background contamination from PFAS, researchers wore pure cotton lab coats and nitrile gloves. All sampling and processing were performed under the fume hood and laminar flow bench, which were thoroughly cleaned with 90 % isopropanol. All culture and experimental flasks were sealed with sterile cotton wool.

2.3. Sample analysis

Sampling for biochemical screening, OD, cell count, photosystem II (PS II) efficiency, chlorophyll *a*, proline, lipid, protein, and total antioxidant capacity (TAC) was conducted at the end of the short-term experiments. For the long-term experiments, sampling was performed at $t = 0$ h, 48 h, 96 h, 168 h, 336 h, and at the experiment's conclusion (672 h). Diatom pellets were collected by centrifugation for 5 min at 2500 x *g* and 4 °C (Sorvall Legend Mach 1.6 R). Subsequently, the pellets were frozen in liquid nitrogen, freeze-dried, and stored at −80 °C until analysis of chlorophyll a, protein, and lipid. Centrifuged pellets for proline analysis were frozen in liquid nitrogen and stored at −80 °C.

2.4. Diatom growth and inhibition analysis

Diatom cell growth was assessed by counting fixed cells (2 % Lugol's solution) using a Neubauer counting chamber with 0.1 mm depth (LO Laboroptik GmbH, Germany) under a light microscope (OMAX 40X-100X compound microscope equipped with a 5MP camera and a mechanical stage) at 40x magnification (5 squares were counted). To compare the relative effects of individual PFAS and their mixture, growth inhibition rates (%) were calculated for each treatment across three concentrations in both diatom species.

The growth inhibition rate (%) was used to identify the PFAS with the most substantial impact and to gain insights into possible synergistic or antagonistic effects of the mixture. If a PFAS mixture has a greater impact than its individual PFAS components, it suggests synergistic or additive effects, and if the mixture shows less impact than its individual components, it suggests antagonistic effects. For the short-term experiment, growth was measured as the number of live cells counted under the microscope as per the following equation,

Table 1
Details of individual PFAS and mixtures (M1-M5) used for short-term (10 d) experiments. Mixture 5 (PFOS, PFOA, PFNA, HFPO-DA, PFDoA, PFTrDA each at 0.9 ng/L) was used in long-term experiments.

PFAS compounds and formula	CAS number	MW (g • mol^{-1})	High concentration (mg • L^{-1})	Mid concentration (mg • L^{-1})	Low concentration (ng • L^{-1})
PFOA	335–67–1	414.1	100	1	0.9
PFNA	375–95–1	464.1	100	1	0.9
PFDA	335–76–2	514.1	100	1	0.9
PFUnDA	2058–94–8	564.1	100	1	0.9
PFDoA	307–55–1	614.1	100	1	0.9
PFTrDA	72,629–94–8	664.1	100	1	0.9
PFTeDA	376–06–7	714.1	100	1	0.9
PFOS	1763–23–1	538.2	100	1	0.9
PFECHS	335–24–0	462.1	100	1	0.9
HFPO-DA	13,252–13–6	330.5	100	1	0.9
PFAS mixtures					
M1: PFOA, PFNA			Each 50	Each 0.5	Each 0.9
M2: PFOA, PFNA, HFPO-DA			Each 50	Each 0.5	Each 0.9
M3: PFOA, PFNA, HFPO-DA, PFDoA			Each 50	Each 0.5	Each 0.9
M4: PFOA, PFNA, PFUnDA, HFPO-DA			Each 50	Each 0.5	Each 0.9
M5: PFOS, PFOA, PFNA, HFPO-DA, PFDoA, PFTrDA			Each 50	Each 0.5	Each 0.9

$$Growth\ Inhibition\ _t(\%) = \left(1 - \frac{cell\ count_{pfas}}{cell\ count_{Control}}\right) \times 100\%$$

$Cell\ count_{pfas}$ is the growth of the PFAS-treated group, and $Cell\ count_{control}$ is the growth of the control group at the end of the 10-day experiment.

Furthermore, for the long-term experiment, a logistic growth model was developed, and based on it, the carrying capacity (K), growth rate (r), and inhibition ratio (IR) were calculated as follows:

K= parameter fitted by the logistic model to the cell count data over time

r= growth rate fitted by the logistic model to the cell count data

$$IR = \frac{(K_{control}) - (K_{treatment})}{K_{control}} \times 100\%$$

$K_{control}$: carrying capacity for the control group

$K_{treatment}$: carrying capacity for the PFAS treatment group

$$\mu_t = \frac{\ln(N_t) - \ln(N_0)}{t - t_0}$$

N_t is the final cell count at the end of the experiment, and N_0 is the initial cell count. To identify the logarithmic growth phase, a growth curve was plotted based on cell density.

2.5. Photosystem II efficiency

PSII efficiency was measured by pulse-amplitude modulation (PAM) fluorometry (PAM2500; Heinz Walz, GmbH), using the Pam_Win-4 Software for operation and data analysis. Diatom cells were dark-acclimated for 20 min to allow complete oxidation of the PSII reaction centers. Next, 400 μL of diatom cells was loaded into a suspension cuvette (KS-2500) and a magnetic stirrer with a fiber optics holder. A saturation pulse (by a red-LED with a peak illumination at 640 nm set for 200 ms at 4000 μmol photons $m^{-2}s^{-1)}$ was provided to measure the maximum photochemical efficiency of PSII (*Fv/Fm*) and was measured automatically by the PamWin-4 V4.02v software (van Kooten and Snel, 1990). Two fluorescence ratio parameters were calculated to estimate the efficiency of photosystem II using the excitation energy for photochemistry. *Fo* is the minimum chlorophyll fluorescence yield when all photosystem II reaction centres are opened, recorded with low measuring light intensities, and *Fm* is the maximum chlorophyll fluorescence yield when all photosystem II reaction centers are closed by a saturation pulse.

2.6. Chlorophyll a concentration

Chlorophyll concentration was measured using 3 mg of freeze-dried diatom pellets, treated with 1.5 mL of 90 % cold acetone and sonicated for 5 min under dim light. The resulting mixture was centrifuged at 1600 × *g* for 5 min, and the absorbance of the supernatant was measured at 647 nm and 664 nm using a spectrophotometer. The concentration (mg/g dry weight) of chlorophyll *a* was calculated based on the following equation (Wellburn, 1994): $Chl\ a = (12.25 \times A_{664} - 2.79 \times A_{647})/W) \times V/1000$, where A stands for the absorbance at different wavelengths, W is the dry weight (mg per gram) of diatom cells used for extraction, and V is the volume of acetone used for extraction in mL.

2.7. Protein assay

Protein from freeze-dried samples (3 mg) was extracted by adding 1.5 mL of 0.1 M NaOH followed by sonication for 1 min and kept at 4 °C for 30 min. Later, the samples were centrifuged at 2500 × *g* for 5 min, and the supernatant was used to measure protein content based on Bradford's assay method, at 595 nm in a microplate reader using a spectrophotometer (Bradford, 1976). Bovine serum albumin standards (0,10, 20, 30, 40, 50 μg/mL) were used to establish the calibration curve and used to calculate the protein content as $Y = 0.0147x + 0.0046$, R^2= 0.9923.

2.8. Lipid analysis

Total lipids were extracted from the diatom using a single-step procedure, as described by Axelsson and Gentili (2014). The pellets were harvested using a 2:1 chloroform:methanol (v/v) dispersion in a solvent system, followed by the addition of 2 mL of 0.73 % NaCl water to produce a 2:1:0.8 system of chloroform: methanol: water (v/v/v). The diatom paste was resuspended in a 2:1 chloroform:methanol (v/v) solution by vigorously shaking the tube for a few seconds, until the biomass was dispersed in the solvent system. Phase separation was facilitated by 2 min of centrifugation at 840 × *g*, and the lower nonpolar phase was recovered for analysis using a Pasteur pipette, evaporated, and weighed to obtain the crude lipid extract (CLE) value. The total lipid rate (TLR) was calculated gravimetrically and expressed as a percentage of dry cell weight.

2.9. Total antioxidant activity

According to Prieto et al. (1999), the total antioxidant reagent (TAC) was prepared with 0.6 M sulfuric acid, 28 mM sodium phosphate, and 4 mM ammonium molybdate, each at 100 mL, and thoroughly mixed. The reaction mixture (300 μL) was added to 3 mL TAC reagent and incubated at 95 °C for 90 min. Absorbance was measured at 695 nm, and the total antioxidant activity was expressed as the number of equivalents of the Trolox standards. Trolox standards (2.5, 5, 7.5, and 10 μg/mL) were used for calibration ($y = 0.0092x - 0.0004$, $R^2 = 0.9969$). Based on the standard curve, TAC was measured, and the TAC per cell was calculated in μg/mL.

2.10. Proline analysis

Proline concentrations were measured spectrophotometrically using ninhydrin according to the method developed by Bates et al., (1973), as modified by Nothnagel, (1995). Diatom pellets were suspended in 400 μL distilled water, and 2 mL of ninhydrin reagent (1.25 g ninhydrin in 50 mL of 6 M phosphoric acid and acetic acid (3:2 v/v), and 2 mL of acetic acid (75 %) were added. The mixture was vortexed for 15 s and then heated for 1 h at 100 °C. Afterwards, the reaction mixture was cooled in an ice bath, and 3 mL of toluene was added. The mixture was then thoroughly mixed and cooled again in an ice bath. The mixture was centrifuged for 5 min at 1631 × *g*, the top red phase was removed with a Pasteur pipette, and the proline concentration (absorbance) was measured at 520 nm using toluene as a blank. The proline concentrations were calculated per cell from the standard calibration curve prepared from the proline standards (100 nm to 600 nm), $y = 0.00005x + 0.0035$, R^2= 0.9925.

All readings were performed in triplicate. All spectrophotometric readings were taken using a microplate reader (Grenier BIO—ONE, 96 well, PS, F-Bottom, clear) from CLARIOstar® *Plus,* except for the proline absorbance, which was measured using a UV/Visible Scanning Spectrophotometer (Shimadzu UV-1800). While measuring the absorbance for each analysis, to eliminate the influence of the solvent on the assays, a blank control of the respective extraction or indicator solutions was used and quantified under the same conditions.

2.11. Data analysis and statistics

All statistical analyses and visualizations were performed using R version 4.2.1 (R Core Team, 2024) and the "ggplot2" package (Wickham, 2016). In the short-term experiment, since the data did not meet the normality assumption, the Kruskal-Wallis test was used to evaluate the significance of differences between treatments and species. A post-hoc test then identified specific differences ($p < 0.05$) between

the control group and the PFAS treatments. All tests were conducted at a significance level of $\alpha = 0.05$. Additionally, multivariate principal component analysis (PCA) was employed to explore the variations among the tested parameters, treatments, concentrations, and species.

Permutational multivariate analysis of variance (PERMANOVA) was conducted to assess the effects of species, sublethal concentration, and PFAS exposure, as well as their interactions, on the composite biochemical response (TAC, protein, lipid, and chlorophyll a). The analysis was based on Bray-Curtis dissimilarity matrix with 999 permutations. Analysis of variance (ANOVA) was performed to check the statistical significance and species-specific sensitivity to PFAS and mixtures.

Additionally, pairwise PERMANOVA tests were conducted to compare each treatment to the control within each species and concentration level, identifying differential effects of individual versus mixture PFAS exposures across concentrations. Non-metric multidimensional scaling (nMDS) was applied to examine differences in multivariate biochemical profiles between treatments with individual PFAS compounds and mixtures across both diatom species. This ordination was based on Bray-Curtis dissimilarities computed from normalized biochemical parameters, providing a two-dimensional visualization of the multivariate space.

3. Results

3.1. Growth inhibition in diatoms exposed to PFAS

Diatoms subjected to high and mid concentrations exhibited a significant reduction ($p < 0.05$) in growth compared to the control groups in both species, *C. closterium* and *T. pseudonana* (Fig. 1). For both diatom species, the percentage inhibition generally increased as PFAS concentration increased from low to high (Fig. 1). Mixtures (M1-M5) often showed higher inhibition than the individual PFAS assays tested, especially at mid- and high concentrations for both species. Additionally, the mixtures exhibited additive effects for both species at all three concentrations.

At low concentration, *T. pseudonana* exhibited less growth inhibition (~ 2–11 %) for all tested PFAS and mixtures (Fig. 1). Among the individual assays, PFOS. PFTrDA and PFDoA showed >10 % of inhibition. At mid concentration, GenX still showed the lowest inhibition (~ 27 %), PFDoA, PFUnDA, M4, and M5 caused high inhibition (> 75 %). Growth inhibition was very high (75–96 %) at higher concentrations for all tested PFAS assays, except GenX, which caused a notable inhibition (~ 42 %).

C. closterium also showed high inhibition at high concentrations across all compounds (~52–92 %), but GenX showed a comparatively lower inhibition (~ 38 %) among the individual PFAS and mixtures. Additionally, substantial growth reductions (~30–88 %) were recorded at mid-concentration for all compounds. GenX and PFECHS showed modest inhibition (~15 %), PFTrDA, PFTeDA and mixtures showed an

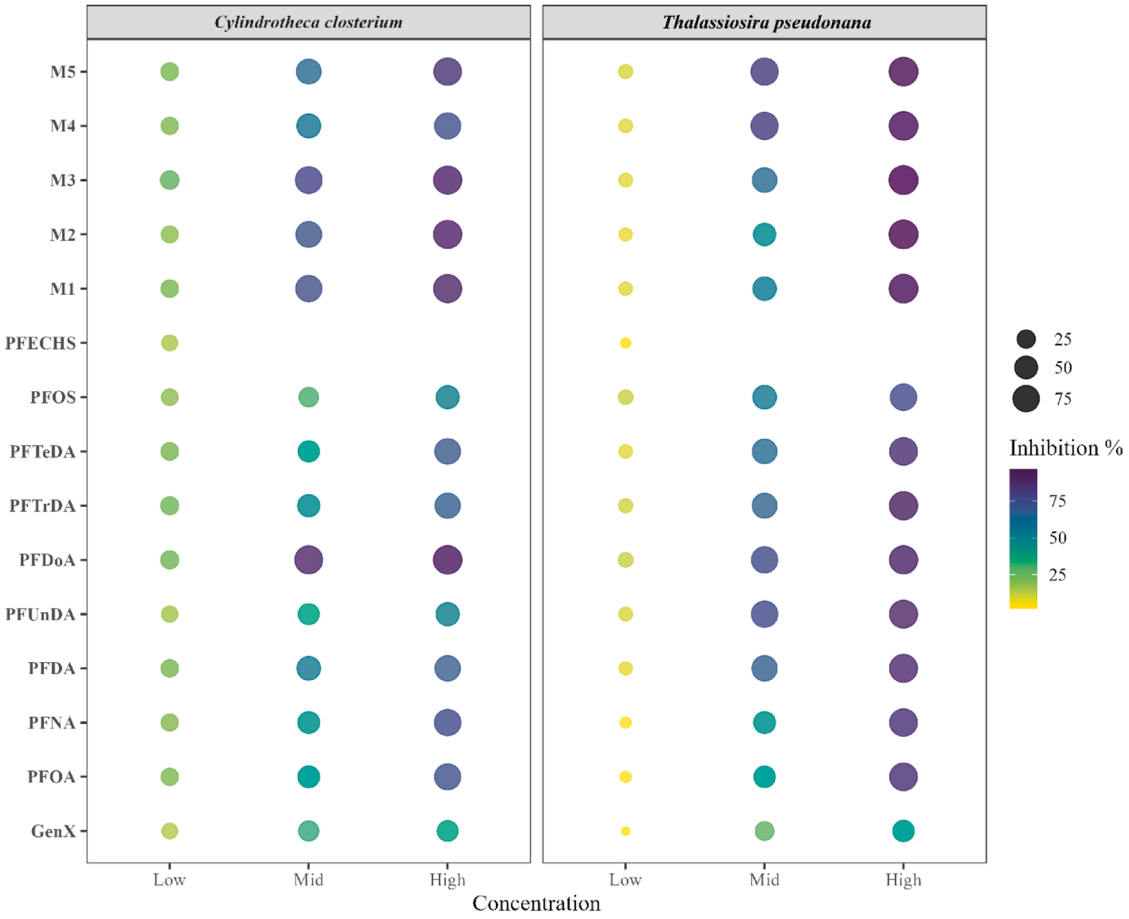

Fig. 1. Growth inhibition of *Cylindrotheca closterium* (left) and *Thalassiosira pseudonana* (right) in response to 10 individual PFAS and their mixtures during the short-term exposure. Each row represents a different PFAS and mixture, and the columns denote three concentration levels: Low (0.9 ng/L), Mid (1 mg/L), and High (100 mg/L). The degree of inhibition (%) in terms of cell count for each species is illustrated by the size and color intensity of the circles, with darker and larger circles indicating greater inhibition. Color gradients range from yellow (low inhibition, <10 %) to light green (<25 %) and dark purple (high inhibition,>60 %).

inhibition > 22 % when *C. closterium* was exposed to low concentration (Fig. 1).

In the long-term experiment, there was a moderate reduction in cell densities after 96 h for both species (Fig. 2). The specific growth rate over the first 14 d was calculated for each treatment. *T. pseudonana* exhibited a growth rate of 3360 cells/mL/hin the control group, which decreased to 3211 cells/mL/hrunder PFAS exposure, corresponding to a 2.88 % inhibition. In contrast, *C. closterium* showed no significant inhibition (0.16 %), with growth rates of 1363 cells/mL/h and 1338 cells/mL/hin control and PFAS-treated groups, respectively after 14 d These results suggest that PFAS exposure exerted only a subtle inhibitory effect on the growth of both diatom species under the tested conditions, with *T. pseudonana* showing slightly greater sensitivity compared to *C. closterium* during the exponential growth phase, as indicated by natural log-based growth rates.

3.2. Impaired photosynthetic efficiency (PSII) and chlorophyll a

In the short-term experiment, there was a significant decrease in chlorophyll *a* at high and mid concentrations for both species (Fig. 3), except for a deviation observed in M1 for *T. pseudonana* at mid concentration. Notably, the decline of chlorophyll *a* in *C. closterium* was substantially higher than for *T. pseudonana* in the treatments PFCAs ≤10 and mixtures M1-M3. PSII activity was not detected in any of the high-concentration mixtures, in either species. Furthermore, PSII activity was detected at a very low level among the PFCAs > C10 in *T. pseudonana* for both high and mid concentrations.

In the low concentration tests, chlorophyll *a* generally increased in most assays, with notable rises observed for PFDoA, M2, and M3 for *T. pseudonana.* However, PSII activity of *T. pseudonana* was slightly increased only in PFOS and PFUnDA, while it was lower than the control in treatments with PFTeDA, PFECHS, and mixtures. On the other hand, PSII activity of *C. closterium* remained relatively low across all tested assays, specifically for C8-C12 PFCAs and mixtures M1-M3. At the same time, they were closer to the control in C13-C14, PFOS, PFECHS, M4, and M5, although some instances of increased chlorophyll *a* were noted with PFCAs greater than C10 (Fig. 3).

During the long-term exposure period, PSII activity in *T. pseudonana* was marginally higher than that of the control group up to 96 h, after which it experienced a slight decline for the remainder of the study, despite an observable increasing trend in chlorophyll *a* following the exponential phase (after 336 h) as illustrated in Fig. 4. Conversely, *C. closterium* exhibited a decreasing pattern of PSII activity throughout the evaluated time points, although the chlorophyll *a* concentration remained comparable to that of the control, except at 168 h, where a notable increase was observed.

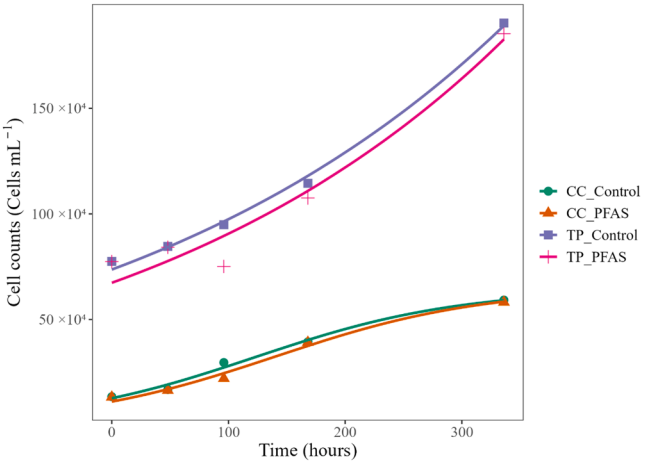

Fig. 2. The logistic growth model showed changes in diatom cell density up to the exponential phase when exposed to a PFAS mixture (GenX, PFOS, PFOA, PFNA, PFDoA, PFTrDA; each PFAS at 0.9 ng/L) for 336 h (14 d). CC_Control: *Cylindrotheca closterium* control., CC_PFAS: *Cylindrotheca closterium* exposed to PFAS., TP_Control: *Thalassiosira pseudonana* control, TP_PFAS: *Thalassiosira pseudonana* PFAS treated.

3.3. Metabolic shifts: protein and lipid content

Protein levels decreased significantly at high and medium concentrations, while a moderate reduction was noted at low concentrations in both species. An exception was observed in PFUnDA for *C. closterium* (Fig. 3). Additionally, a decline in lipid content was observed in low-concentration PFAS, such as C8-C12 PFCAs, GenX, and all PFAS mixtures, for *T. pseudonana*. Conversely, increased lipid content was observed in low-concentration PFAS assays, including PFUnDA, PFTeDA, PFOS, PFECHS, M4, and M5, in *T. pseudonana*. In *C. closterium*, an upsurge in crude lipid content occurred when exposed to low concentrations of PFOA, PFUnDA, PFTeDA, PFECHS, along with mid concentrations of PFDA, PFTeDA, and M1 during short-term PFAS exposure (Fig. 3).

Furthermore, long-term exposure to PFAS mixtures resulted in a reduction in protein content across all tested time points for both species. In *C. closterium*, lipid content dropped after 168 h, although a slight increase was observed after 49 h. Meanwhile, in *T. pseudonana*, lipid content rose compared to the control up to 96 h, but then significantly decreased after 168 h (Fig. 4).

3.4. PFAS induced proline accumulation and antioxidant activity

The indicators of osmotic stress, measured by proline accumulation, and oxidative stress, indicated by total antioxidant activity (TAC), were significantly elevated in both species at high and medium concentrations across all treatments (Fig. 3). Proline accumulation in *T. pseudonana* was markedly greater in high concentration C8-C12 PFAS, and in the mid and high concentrations of PFOS. Conversely, *C. closterium* exhibited significantly greater proline accumulation in all tested individual assays and mixtures at mid- and high concentrations compared to the control. Notably, in low concentrations, proline accumulation increased as the PFAS chain length surpassed C10 (Fig. 3). In particular, *C. closterium* showed lower values for specific low-concentration assays, such as GenX, PFOA, and PFTrDA, compared to *T. pseudonana*.

Total antioxidant activity surged exponentially in both species upon exposure to high and medium concentrations of PFAS and mixtures, excluding GenX (Fig. 3). Specifically, when the diatoms were exposed to PFAS mixtures (M1-M5) at high concentrations, TAC in *T. pseudonana* was eight times higher than in controls. At the same time, in *C. closterium*, the values were ten times greater for PFDoA, PFTrDA, and PFTeDA in M4 and M5, as well as for assays M3-M5 in *T. pseudonana*. However, no significant increase was observed in lower concentration assays for either species.

During long-term exposure to the PFAS mixture (M5), proline and TAC levels showed moderate increases in *T. pseudonana* throughout the experiment. At 96 h, *C. closterium* exhibited higher TAC and proline accumulation compared to its respective control (Fig. 4).

3.5. Statistical interpretation of sublethal changes

The impact of PFAS on the two tested diatoms was evaluated based on different sublethal endpoints, including proline, TAC, protein, and chlorophyll a concentration, comparing cells exposed to PFAS with control samples (Fig. 5). Statistically significant differences were found between PFAS assays with measured biochemical parameters and their controls at high and mid concentrations (Fig. 5) (Supplementary Table S1-S2), indicating severe physiological disruption. Long-chain PFCAs (>C11) and PFOS significantly affected *T. pseudonana*, inducing

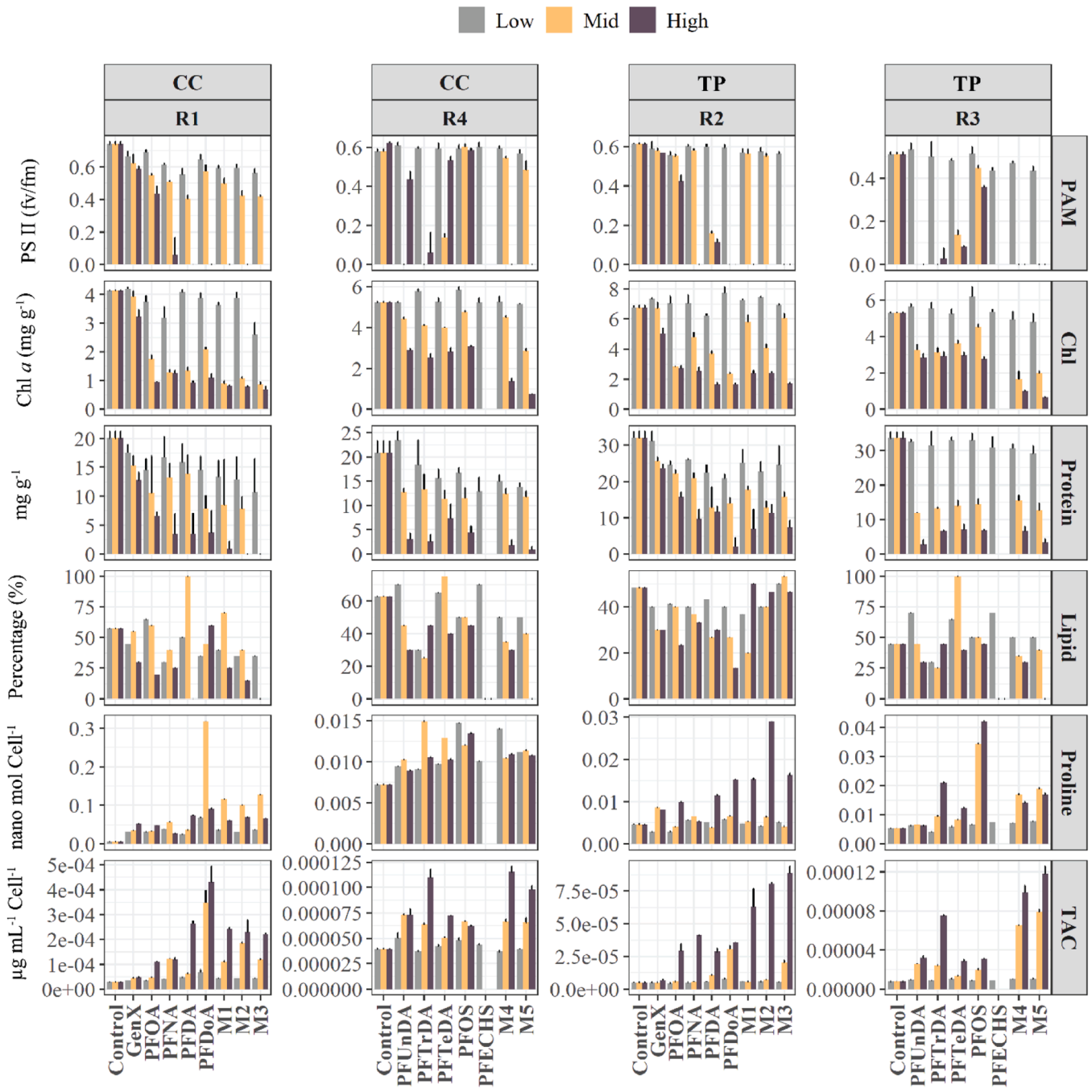

Fig. 3. Sub-lethal changes in diatoms exposed for 10 days to PFAS and their mixtures were demonstrated, along with the responses of their respective control groups in each run (R1-R4). From top to bottom, the following biochemical responses showed: PAM- Photosynthetic efficiency (PSII) measurements (Fv/Fm), chlorophyll a concentration, protein concentration, lipid (crude lipid percentage), total antioxidant capacity (TAC), and proline concentration. Data are shown for CC: *Cylindrotheca closterium* (R1 and R4), and TP: *Thalassiosira pseudonana* (R2 and R3). In both species, PFECHS was not tested at high and mid-concentration.

strong stress responses, including reduced protein and chlorophyll a content, and increased proline levels, as well as changes in antioxidant levels. *T. pseudonana* was more tolerant to individual PFAS at lower dose but responded strongly at high and mid concentrations during the short-term exposure (Fig. 5).

Severe impacts of PFAS were correlated with a significant decline in protein and lipid content, as well as a decline in photosynthesis performance ($p < 0.05$), and significantly higher TAC and proline levels, indicating oxidative stress ($p < 0.05$) (Fig. 5). These sublethal effects did not immediately kill cells but compromised their functions sufficiently to reduce growth rates in the long run.

In most cases, individual PFAS and mixtures exhibited synergistic effects on diatom growth, photosynthesis efficiency, and other stress responses. Notably, *C. closterium* revealed antagonistic effects for M4 and M5 in proline and protein production; M4 demonstrated antagonistic effects on chlorophyll *a* content and TAC activity, while M1 and M3 also showed antagonistic effects on chlorophyll *a* content *in T. pseudonana.*

The PERMANOVA results for short-term PFAS exposure showed that the species × concentration ($R^2 = 5.9$ %), species × PFAS ($R^2 = 8.8$ %), and concentrations × PFAS ($R^2 = 15.3$ %) interactions demonstrated that responses varied both by species and across the exposure gradient. The significant three-way interactions ($R^2 = 8.5$ %) further suggest that biochemical responses to PFAS are regulated in a species- and

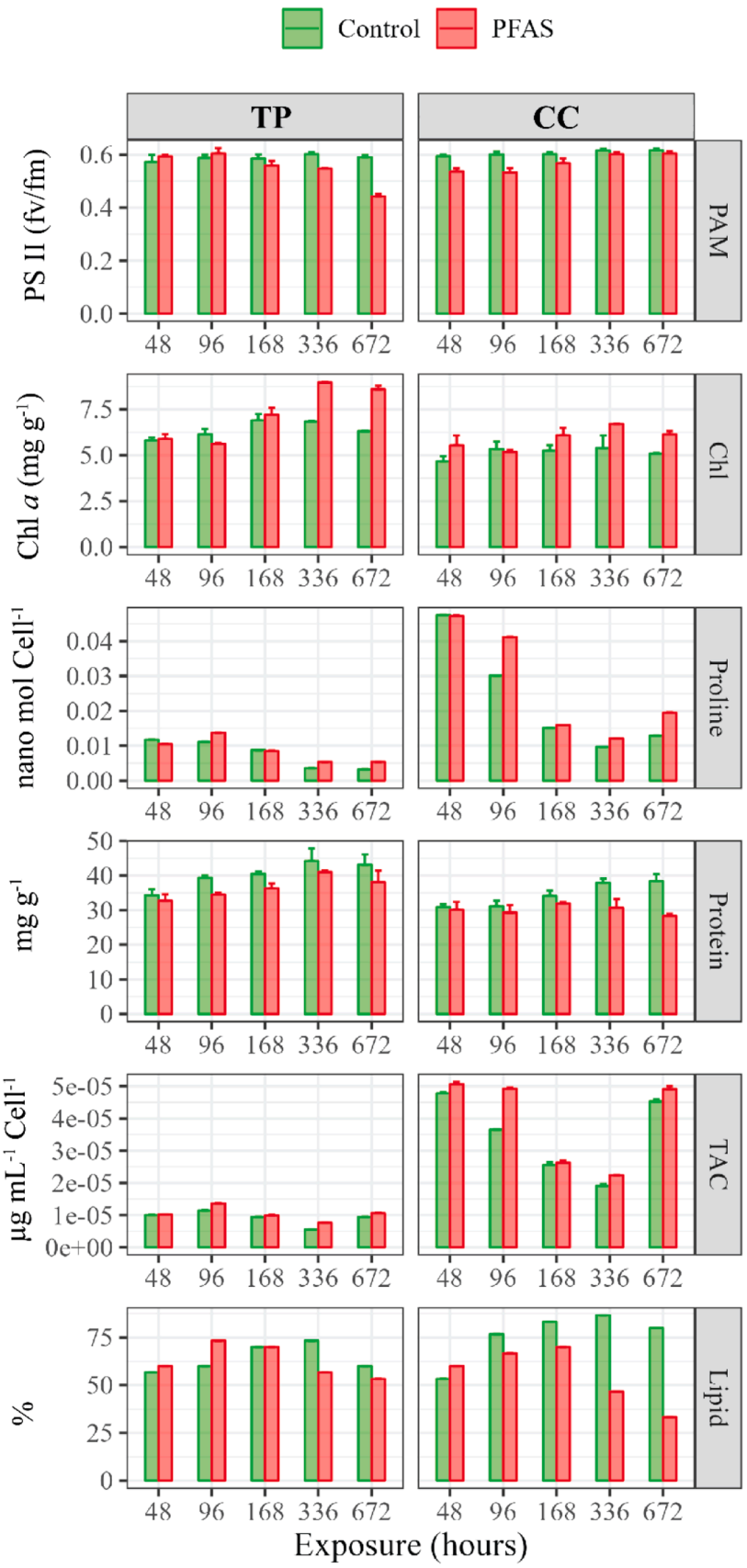

Fig. 4. Biochemical changes during the long-term PFAS exposure at 0.9 ng/L concentration (each PFOA, PFNA, PFDoA, PFTrDA, PFOS, and GenX) showed (red color bars are for PFAS-treated samples and green color is control): PAM- photosynthetic efficiency PSII (Fv/Fm), Chl *a*: Chlorophyll *a* concentrations in dry weight, osmoregulatory proline changes, protein, TAC- total antioxidant activity changes, and crude lipid in the examined species *Thalassiosira pseudonana* and *Cylindrotheca closterium*.

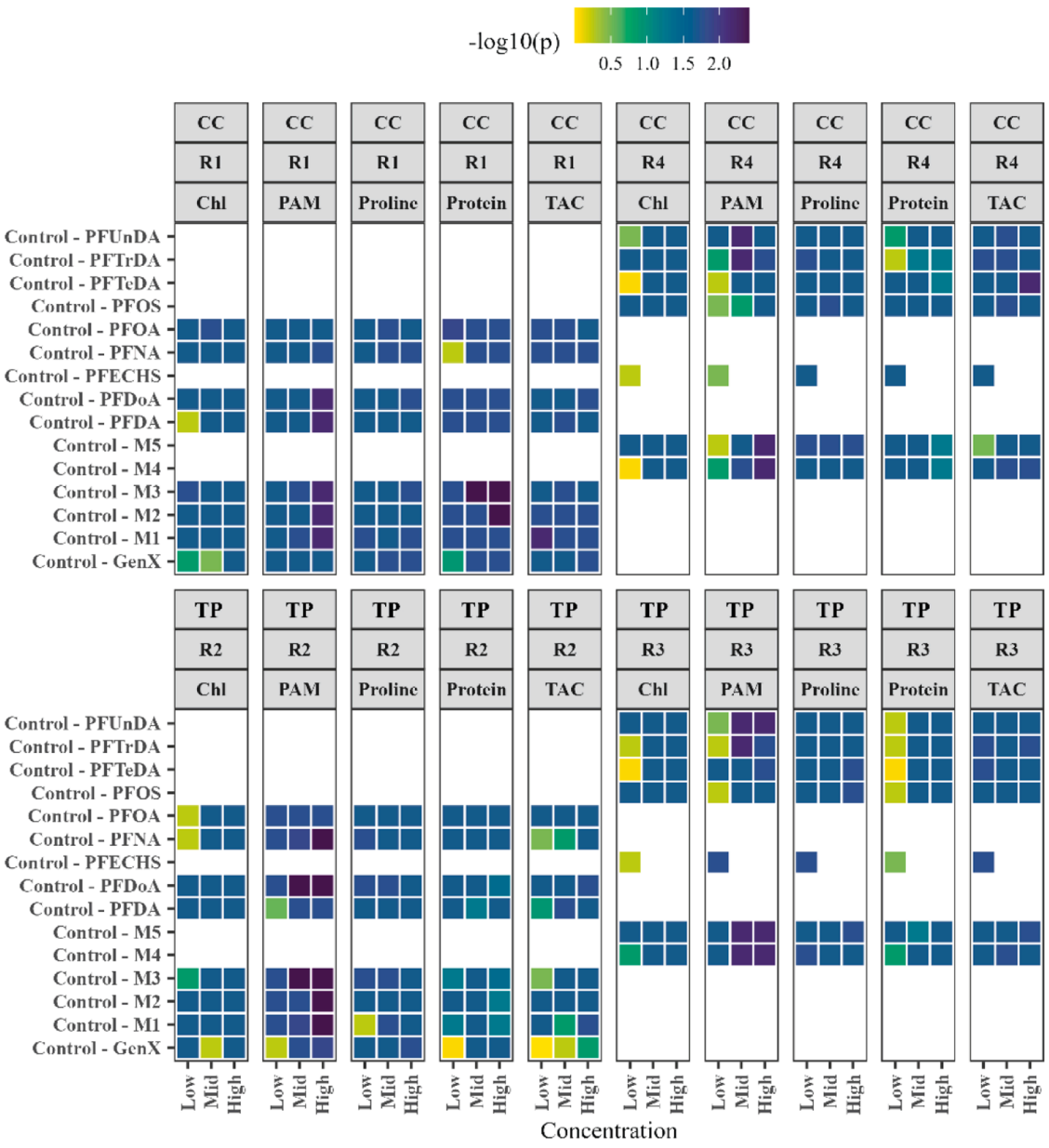

Fig. 5. Statistical significance of physiological and biochemical responses of *Thalassiosira pseudonana* (tp) and *Cylindrotheca closterium* (CC), to the tested 10 individual PFAS and their mixtures. Heatmap color display statistical significance levels based on *p*-values: dark blue ($p < 0.001$), navy blue ($p < 0.01$), green ($p < 0.05$), and yellow or light green ($p > 0.05$, no significance).

concentration-specific manner. Overall, the PERMANOVA model explained 83.8 % of the total multivariate variation in biochemical response, leaving only 16.2 % as unexplained residual variation, underscoring the robustness of the experimental factors in shaping biochemical outcomes (Supplementary Table S2).

However, in the long-term experiment, the species × exposure time interaction alone was not significant ($p = 0.401$), indicating that time-related biochemical dynamics were consistent within species in the absence of PFAS. Overall, the model explained 91.4 % of the total variance in biochemical profiles, indicating a strong species and time-dependent effect of PFAS exposure. Yet, species × PFAS interaction was significant ($p = 0.001$), indicating that the benthic and the pelagic diatom species studied in this study differed in their biochemical responses to PFAS (Supplementary Table S3).

3.6. nMDS ordination of biochemical responses by PFAS type and species

In the short-term, PFAS exposure, showed clear segregation of samples based on both PFAS type and species, with minimal overlap in the 95 % confidence ellipses surrounding group centroids. Diatoms exposed to PFAS mixtures (in blue circle and triangle in Fig. 6) showed broader dispersion, particularly in *C. closterium*, suggesting more pronounced biochemical responses compared to individual PFAS exposure (red). The clustering of individual PFAS-exposed *T. pseudonana* was more compact, implying more homogeneous response patterns within this group. Importantly, *C. closterium* displayed a greater spread along nMDS1, indicating more pronounced shifts in biochemical profiles relative to *T. pseudonana* (Fig. 6). These patterns suggest that both PFAS mixture complexity and species-specific physiology play a significant role in shaping biochemical responses under PFAS-induced stress.

Fig. 7 shows the nMDS for the long-term PFAS exposure, where distinct clustering is observed between the control (green) and PFAS-

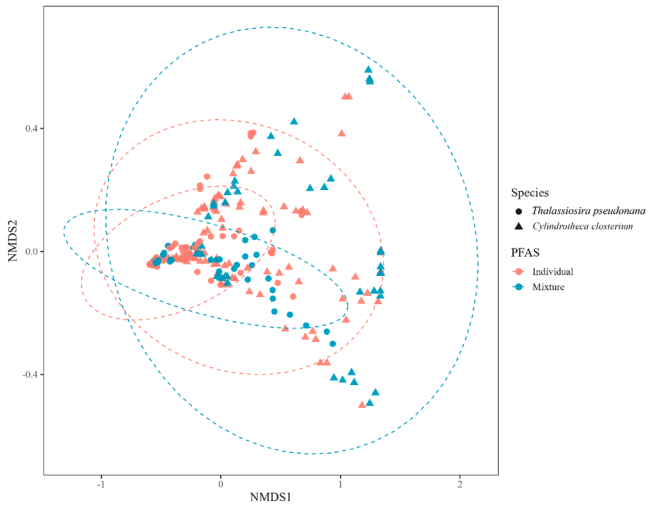

Fig. 6. Non-metric multidimensional scaling (nMDS) ordination based on Bray-Curtis dissimilarities of biochemical responses resulted from short-term PFAS exposure in *Cylindrotheca closterium* (▲) and *Thalassiosira pseudonana* (●). Individual PFAS compounds exposure results showed in red, and PFAS mixture responses showed in blue. Dashed ellipses represent 95 % confidence intervals around group centroids. Both diatoms exposed to PFAS mixtures tended to occupy broader ranges along both NMDS1 and NMDS2 axes, indicating stronger metabolic modulations compared to individual PFAS exposures.

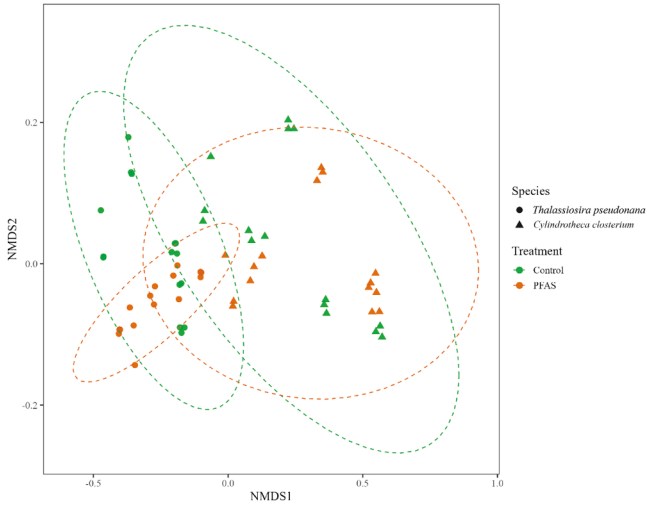

Fig. 7. Non-metric multidimensional scaling (nMDS) ordination based on Bray-Curtis dissimilarities of biochemical responses resulted from long-term PFAS exposure in *Cylindrotheca closterium* (▲) and *Thalassiosira pseudonana* (●). PFAS-exposed groups are shown in orange, and control group responses are shown in green. Dashed ellipses represent 95 % confidence intervals around group centroids.

exposed (orange) groups for both *T. pseudonana* and *C. closterium*, with minimal overlap in the 95 % confidence ellipses. This indicates a consistent and reproducible alteration in overall biochemical changes following PFAS exposure. The separation between PFAS treatments was more pronounced in *C. closterium*, as evidenced by wider spatial spread between PFAS and control centroids along the nMDS. In *T. pseudonana,* although treatment groups were also separable, they displayed slightly greater overlap, suggesting relatively subtler biochemical shifts in *T. pseudonana.* These ordination patterns support the PERMANOVA results, confirming both PFAS exposure and species type significantly influence the biochemical responses, with *C. closterium*, exhibiting higher sensitivity to PFAS stress.

4. Discussion

4.1. Species-specific sensitivity and diatom physiology

Species-specific sensitivity is related to structural and ecological traits (Latata et al., 2009). The studied diatoms, *C. closterium* and *T. pseudonana,* showed differing sensitivities based on PFAS chain length. The benthic diatom *C. closterium* was mainly affected by PFCAs (C8-C12) and GenX, whereas the pelagic diatom *T. pseudonana* was significantly impacted as the chain length increased. Notably, *C. closterium* was particularly susceptible to acids, PFCAs with chain lengths of ≤C12 and their mixtures. In contrast, *T. pseudonana* displayed heightened sensitivity to longer-chain PFCAs (≥C11), which resulted in significant detriments to its photosynthetic and metabolic functions. Acute effects by long-chain PFAS are likely due to the chain length, and membrane disruption impairs photosynthesis and cell viability (Chlorophyll *a*↓, PSII↓, TAC↑, proline ↑).

The observed differences in PFAS sensitivity align known aspects of diatom physiology. For instance, green algae *Chlorella vulgaris* tend to be more tolerant of PFAS exposure compared to the diatom *Skeletonema marinoi*, largely due to differences in cell wall composition (Latała et al., 2009). Green algae possess robust, cellulose-based cell walls, whereas diatoms are encased in silica-based frustules, which appear more susceptible to PFCA-induced disruption (Liu et al., 2022; Xue et al., 2022). Diatom silica frustules are porous and chemically active, so they do not block PFAS uptake. Their negative surface charge under experimental conditions could initially repel anionic PFAS; however, cations like Mg2+ and Ca2+ in seawater might bridge to extracellular polymeric substances (EPS), thereby increasing local accumulation (Arslan and Gamal El-Din, 2021; Li et al., 2022). *C. closterium* cells mainly grow on or near surfaces and have unique polysaccharides or mucilage secretions to attach to substrates (Staats et al., 2000; F. Zhang et al., 2019). These EPS may concentrate or adsorb organic compounds and pollutants in micro-layers (biofilms), which enhance PFAS exposure (Xiao and Zheng, 2016).

Comparatively higher inhibition of *C. closterium* observed in short-term exposure experiments suggests that benthic diatoms are more vulnerable, possibly due to the way PFAS bind in organic matter. This binding may lead to an early decline in diatom populations; however, over time, the amount of bioavailable PFAS may decrease, allowing these species to recover and resume growth. Furthermore, long-term exposure to PFAS at harmful concentrations may lead to population declines, particularly for non-motile diatom species, such as *T. pseudonana*, that cannot relocate. In contrast, due to its motility *C. closterium* might escape higher PFAS concentrations on sediment surfaces if chemical gradients exist, however, if the environment is contaminated uniformly, both species could suffer. In the laboratory trials where PFAS were spiked without physical barriers, these highly fluorinated chemicals likely adsorbed directly into cell membranes and impacted the diatom physiology (Davis et al., 2024). Additionally, variations in cell size, shape, and motility can influence overall exposure and the potential for detoxification or avoidance when cells are exposed to PFAS (Falasco et al., 2009).

In addition, adherence to glass materials, extracellular secretions, and differences in lipid composition could also affect the species interactions (Hu et al., 2025; Yu et al., 2025; Zenobio et al., 2022; Zhang et al., 2022) may reduce the amount of certain long-chain PFAS entering or interacting with diatom cells. Although the concentration of PFAS used for long-term study (0.9 ng/L) is far below the critical micelle concentration, the amphiphilic nature of these compounds, combined with high ionic strength and alkaline pH in f/2 media, may facilitate the formation of surface-active monolayers or loose surface accumulation. Such behavior could influence interactions with diatom cell surfaces and the dynamics of nutrient uptake.

4.2. PFAS chemistry and mechanisms of PFAS toxicity

PFAS impacts can vary depending on structure, functional group, chain length, and environmental behavior (Arulananthan et al., 2025; OECD, 2022; US EPA, 2021; Zhi et al., 2024). Among the longer-chain perfluoroalkyl carboxylic acids (PFCAs) (C11-C14), PFUnDA, PFDoA, PFTrDA, and PFTeDA are notably lacking in toxicity data, which complicates comparative analyses. However, it is presumed that their longer chain length would influence their physicochemical behavior similarly to other long-chain PFAS. Furthermore, the linear relationship between PFCA lipophilicity (chain length) and toxicity serves as a predictive tool for understanding how other PFAS might affect diatoms (Brendel et al., 2018; Guelfo et al., 2021; Niu et al., 2019; Yu et al., 2025).

Cyclic and linear PFAS forms can differ in their uptake and impacts. For example, the linear PFOS exhibited notable cellular stress, despite its low concentration, which was comparable in both studied diatoms. In contrast, cyclic C8 PFSA (PFECHS) caused higher stress in *C. closterium* than in *T. pseudonana*, indicating species-specific uptake pathways and physiological resilience as explained in other studies (Liu et al., 2022; Mahoney et al., 2023; Niu et al., 2019). Further, PFOS exposure (at low concentration) resulted in significant reduction in growth (OD↓, protein↓, lipid↓), although TAC response was moderate, indicating a routed antioxidant defense (Pietropoli et al., 2025; Xue et al., 2022).

Mechanistically, PFAS impacts stems from multiple pathways. Sublethal effects observed in our study include membrane disruption, oxidative stress, interference with nutrient transport, and protein depletion, all of which contribute to reduced growth rates over time (Liu et al., 2022; Shi et al., 2024; Xue et al., 2022). Longer-chain PFCAs such as PFDoA appear more disruptive in most cases due to their hydrophobic tails inserting into lipid bilayers, while the anionic head interacts with proteins or cations, ultimately compromising membrane integrity and cell function (Ahrens and Bundschuh, 2014; Antonopoulou et al., 2024).

Mixture effects were also evident in the studied combinations for both species. The additive and synergistic effects of combined PFAS exposures highlight the importance of studying PFAS as mixtures rather than isolated compounds. These mixtures likely trigger multiple stress pathways simultaneously, reinforcing the cumulative nature of impacts (Y. Li et al., 2021; Liu et al., 2022; Niu et al., 2019).

PFAS exist in ionized forms under typical marine conditions (pH 8–8.5), with carboxylic and sulfonic acids showing low pKa values and remaining fully anionic forms (Hu et al., 2025; ITRC, 2023). These ionic forms interact with cations such as Na^{+}, Ca^{2+}, Mg^{2+}, which are abundant in seawater, and also aggregate with certain biomolecules or metabolites (Table 2) (ITRC, 2023). This may potentially influence bioavailability and partitioning into lipid membranes, which favours less polar molecules (Li et al., 2021; Rodea-Palomares et al., 2012). Sulfonic acids like PFOS ($pKa \leq 3$) are not only fully ionized but also display higher water solubility and stronger protein-binding affinity compared to carboxylates of the same chain length (Liao et al., 2025, 2024; Rodea-Palomares et al., 2012). These properties significantly affect their uptake and toxicity.

The physicochemical traits of PFAS impact their environmental mobility and interactions with diatom cells. Longer-chain PFAS ($C > 10$) tend to be less water soluble but more likely to bind to organic matter or cell surfaces. Although this can reduce free dissolved concentrations, it may also lead to PFAS accumulation in microenvironments, i.e., biofilms or interfaces, where diatoms reside, potentially enhancing localized exposure (Arslan and Gamal El-Din, 2021; Dai et al., 2018; Zenobio et al., 2022). Such behavior complicates direct assumptions about toxicity based solely on solubility.

Bioavailability further influences impacts beyond just concentration. In our tests, the lower apparent impacts of C13-C14 PFCAs may stem

Table 2
PFAS (used in this study) characteristics, behaviour, uses and fate in the marine environment (ECHA, 2024; Medina et al., 2021; U.S. EPA, 2022; US EPA, 2021).

PFAS Compound	Formula	Water (marine) Solubility (25 °C)	Partitioning Behavior	pKa	Applications	Toxicity data on Aquatic organisms
PFOA (Perfluorooctanoic Acid)	C7F15COOH	Slightly lower to freshwater but moderately high, 3300 mg/L	Moderate sorption; Remains in the water column	1.3	firefighting foam, cosmetics, greases, lubricants, paints, and adhesives	oxidative stress, endocrine disruption, alterations in hormone levels and affecting reproduction in fish
PFNA (Perfluorononanoic Acid)	C8F17COOH	Slightly lower than freshwater, 9.5 g/L	high sorption to sediments; Partition to sediments	−0.21	lubricating oil additive, surfactant, cleaning, textile finishing agent, liquid crystal display panels	Endocrine disruption, reproductive toxicity
PFDA (Perfluorodecanoic Acid)	C9F19COOH	Lower solubility than shorter chains; 5.14 g/L	Strongly binds to sediments	2.58	Firefighting foam, personal care products and cosmetics, food packaging materials	Liver toxicity, oxidative stress, and inflammation
PFUnDA (Perfluoroundecanoic acid)	C10F21COOH	Low, 1.20E-04 g/L	Strongly binds to sediments	0.52 ± 0.10	Firefighter, textiles, food packaging materials, flour polish and cosmetics	Limited data; presumed similar to other long-chain PFCAs
PFDoA (Perfluorododecanoic Acid)	C11F23COOH	Low;further reduced by salinity; 4.81E-06 g/L	Strongly binds to sediments	0.52 ± 0.10	personal care products, coating, paints and varnishes, floor covering	Limited data; presumed similar to PFDA
PFTrDA (Perfluorotridecanoic Acid)	C12F25COOH	Very low;7.3E-6 g/L	Strongly binds to sediments	0.52 ± 0.10	apparel, coating, personal care products and cosmetics, paper and packaging	Limited data; presumed similar to other long-chain PFCAs
PFTeDA (Perfluorotetradecanoic Acid)	C13F27COOH	Very low; 1.90E-06 g/L	Strongly binds to sediments	0.52 ± 0.10	personal care products and cosmetics and floor covering, apparel	Limited data; presumed similar to other long-chain PFCAs
PFOS (Perfluorooctane Sulfonic Acid)	C8F17SO3H	bit lower than freshwater; 680mg/L	Binds to sediments and organic matter	<1.0	fire-fighting foams, alkaline cleaners, floor polishes, metal plating baths, and etching acids for circuit boards;	endocrine disruption, reproductive toxicity
PFECHS (Perfluoroethylcyclohexane Sulfonate)	C8F16SO3 (cyclohexane ring)	limited data; 1.35e-3 mol/L	Binds to sediments and organic matter	−1.12	erosion inhibitor in air hydraulic fluid, introduced to marine water through airport-related activities	Limited data; presumed similar to PFOS
HFPO-DA (Hexafluoropropylene Oxide Dimer Acid,"GenX")	C6HF11O3	High, slightly reduced in saline solutions; >751 g/L	Remains in water column	2.84	cabling materials, semiconductor manufacturing, pharmaceutical and biotech manufacturing	Liver toxicity, hematological effects

from their reduced solubility and stronger adsorption to organic matter, which limits their interaction with diatom cells (Catherine et al., 2019; Dai et al., 2025; Du et al., 2023; Zheng et al., 2017). However, this does not preclude cellular effects, as PFAS may still accumulate on surfaces or within EPS layers where diatoms interact (ITRC, 2023; Wu et al., 2019; Zenobio et al., 2022). Besides, variability in toxicity data across marine sepceis highlights a gap in understanding PFAS impacts on diatoms. While studies on both freshwater algae *Pseudokirchneriella subcapitata* and marine diatoms like *Skeletonema costatum,* and *T. pseudonana* have been studied in different concentrations (1–10 mg/L), and showed growth reductions (Liao et al., 2025, 2024; Shi et al., 2024; Wu et al., 2019), there is lack of comparable data for Arctic diatoms. Thus, while extrapolation is necessary, direct comparisons remain imperfect due to differences in species-specific physiology, PFAS behavior, and environmental conditions.

4.3. Relevance to Arctic ecosystems and ecological implications

These findings are particularly significant for coastal regions, where PFAS contamination is on the rise due to long-range atmospheric and oceanic transport in the Arctic (Zhou et al., 2024). In benthic zones, greater PFAS accumulation in sediments may increase vulnerability in taxa such as *C. closterium*, thereby affecting benthic-pelagic coupling. In pelagic zones, species such as *T. pseudonana* may also be affected if PFAS spread evenly through melting sea ice or persistently mix water layers (Ahrens et al., 2023; Hartz et al., 2023; MacInnis et al., 2019). Moreover, the persistence and bioaccumulative potential of longer-chain PFAS raise significant concerns regarding chronic exposure, particularly in polar and benthic environments, where these compounds may persist and concentrate over time (Dai et al., 2025; Hartz et al., 2024).

Given PFAS's stability in cold, nutrient-poor environments, chronic exposure scenarios like those modelled here are ecologically plausible. Our results support emerging evidence that Arctic planktonic and benthic microbes are susceptible to even low pg/L PFAS levels (Davis et al., 2024; Yu et al., 2025). Therefore, understanding these species-specific responses under realistic conditions is vital for ecological risk assessments.

Since the diatoms are the most important primary producers in the marine realm, any disruptions raise substantial concerns regarding broader ecological impacts. The long-chain PFCAs and legacy compounds, such as PFOS, exert significant physiological and population-level stress on diatom species, with implications for the health of broader ecosystems. GenX, a short-chain PFCA, has milder effects on both diatom species in this study, supporting the idea that replacement PFAS are less bioactive. However, further validation is necessary, as documented instances indicate higher toxicity levels in other aquatic organisms and algae (Table 2) (Hu et al., 2025; Joerss et al., 2020; Y. Li et al., 2021; Niu et al., 2019). Notably, a reduction in growth rate was observed across all tested treatments, even at the lowest concentration, which suggests that physiological disruptions may result in decreased population growth (Guo et al., 2024; Liu et al., 2021; Niu et al., 2019). This highlights the necessity for scrutinizing replacement PFAS with similar rigor.

Sublethal biochemical responses indicate that PFAS contamination may silently compromise diatom function prior to observable declines in population. The mixture of PFAS compounds consistently induced stronger toxic responses compared to individual compounds, indicating potential synergistic effects that traditional assessments of single substances may overlook. Additionally, other identified PFAS impacts, such as growth inhibition and impaired photosynthetic activity, point to diminished energy flow and primary productivity within marine systems (Liao et al., 2025). Given the key role diatoms play in carbon fixation, oxygen generation, and nutrient cycling, any long-term decrease in their functionality or population could lead to extensive repercussions for ecosystem stability, subsequently impacting other communities and climate regulation (Guo et al., 2024).

4.4. Limitations

This study represents an initial screening of the effects of PFAS on Arctic and sub-Arctic marine diatoms, acknowledging its exploratory nature and the broader goal of contributing to the knowledge gap regarding PFAS impacts on polar microalgae. Our experimental design was adapted from the experimental setup of the OECD Test Guideline 201 (OECD, 2006) (Supplementary Table S4), which is tailored for freshwater diatoms under temperate conditions. Given the inherently slower growth rates of Arctic diatoms, we extended the exposure durations beyond the OECD-recommended 72-h window, conducting 10-d and 28-d tests, to more accurately capture both acute and chronic responses, with exponential growth typically occurring 8–10 d Additionally, due to challenges in achieving sufficient biomass resulting from slow growth, the number of replicates was limited, with subsamples serving as substitutes.

Consequently, these results are intended to support hypothesis formation rather than conclusively identifying species responses to treatments, and the effects of PFAS should be considered preliminary. To ensure consistency in initial dense cell density and reduce dilution stress, we employed a 1:1 inoculum-to-medium ratio; however, this approach likely elevated dissolved organic carbon (DOC) levels compared to those in natural seawater. Elevated DOC and EPS may have reduced the freely dissolved PFAS concentrations through sorption, thereby potentially underestimating the impacts.

Therefore, our findings can be considered conservative, and future studies should incorporate DOC measurements to quantify PFAS bioavailability better and refine toxicity assessments. We also acknowledge that PFAS concentrations in exposure were not analytically verified, and interpretations are based on nominal concentrations. Sorption to DOC or other particulates may have reduced free PFAS concentrations, again reinforcing the conservative nature of the observed toxic effects.

5. Conclusion

This study highlighted the complex effects of various PFAS and their mixtures on Arctic and sub-Arctic marine diatoms. *C. closterium* showed higher sensitivity in short-term exposure but demonstrated greater resilience than *T. pseudonana* under prolonged PFAS exposure. Both legacy long-chain PFCAs and ether-based substitutes, like GenX, disrupted cellular functions as evidenced by impaired PSII activity and metabolite alterations in *C. closterium* and *T. pseudonana.* Both species studied showed biochemical responses to low PFAS concentrations, with mixtures being more toxic. This highlights the importance of considering both additive and synergistic effects in ecological risk assessments. The strong correlation between biochemical biomarkers, such as protein, proline, and TAC, and growth inhibition confirms the reliability of these indicators in detecting early and integrated responses to PFAS stress.

These findings highlight the need for targeted risk assessments of both legacy PFAS and replacement compounds in Arctic and sub-Arctic marine ecosystems. Such assessments should extend beyond freshwater model organisms to better understand the unique vulnerabilities of marine primary producers in cold, saline environments already impacted by rising sea surface temperatures and increased pollution loading.

Funding

The Icelandic Research Fund has supported the work in the frame of the project "Per- and poly-fluoroalkyl substances (PFAS) meet Arctic and sub-Arctic marine diatoms and their associated symbionts" (RANNIS ID: 239548–051).

CRediT authorship contribution statement

Ashani Arulananthan: Writing – original draft, Visualization, Methodology, Investigation, Formal analysis, Conceptualization. **Bettina Scholz:** Writing – review & editing, Validation, Supervision, Resources, Project administration, Methodology, Investigation, Funding acquisition, Formal analysis, Data curation, Conceptualization. **Ulf Karsten:** Writing – review & editing, Supervision, Methodology, Data curation, Conceptualization. **Hans-Peter Grossart:** Writing – review & editing, Visualization, Supervision, Resources, Methodology, Data curation, Conceptualization. **Auður Sigurbjörnsdóttir:** Writing – review & editing, Supervision, Software, Resources, Methodology. **Óttar Rolfsson:** Writing – review & editing, Supervision, Resources, Methodology, Conceptualization. **Hanna Joerss:** Writing – review & editing, Visualization, Validation, Methodology, Data curation, Conceptualization. **Bernardo Duarte:** Writing – review & editing, Validation, Conceptualization. **Oddur Þór Vilhelmsson:** Writing – review & editing, Supervision, Software, Resources, Project administration, Methodology, Funding acquisition, Conceptualization.

Declaration of competing interest

The author is an Editorial Board Member/Editor-in-Chief/Associate Editor/Guest Editor for this journal and was not involved in the editorial review or the decision to publish this article.

Acknowledgements

We wish to thank the diatom taxonomists Dr. Konrad Schultz, Applied Ecology & Phycology, University of Rostock, and Dr. Jonas Zimmermann, Diatom Research Group, Botanical Garden and Botanical Museum, Berlin, for their support in verifying diatom species. We also thank the lab manager, Andrés Tryggvi Jakobsson, Dr. Sean Scully, and Eva María Ingvadóttir, from the Faculty of Natural Resource Sciences at the University of Akureyri, for their support in lab work and handling equipment. We also appreciate the assistance and support provided by Arctic Therapeutics.

Supplementary materials

Supplementary material associated with this article can be found, in the online version, at doi:10.1016/j.aquatox.2025.107562.

Data availability

Data will be made available on request.

References

Ahrens, L., Bundschuh, M., 2014. Fate and effects of poly- and perfluoroalkyl substances in the aquatic environment: a review. Environ. Toxicol. Chem. 33, 1921–1929. https://doi.org/10.1002/etc.2663.

Ahrens, L., Rakovic, J., Ekdahl, S., Kallenborn, R., 2023. Environmental distribution of per- and polyfluoroalkyl substances (PFAS) on Svalbard: local sources and long-range transport to the Arctic. Chemosphere 345, 140463. https://doi.org/10.1016/j.chemosphere.2023.140463.

Ali, A.M., Langberg, H.A., Hale, S.E., Kallenborn, R., Hartz, W.F., Mortensen, Å.-K., Ciesielski, T.M., McDonough, C.A., Jenssen, B.M., Breedveld, G.D., 2021. The fate of poly- and perfluoroalkyl substances in a marine food web influenced by land-based sources in the Norwegian Arctic. Environ. Sci.: Process. Impacts 23, 588–604. https://doi.org/10.1039/D0EM00510J.

Antonopoulou, M., Spyrou, A., Tzamaria, A., Efthimiou, I., Triantafyllidis, V., 2024. Current state of knowledge of environmental occurrence, toxic effects, and advanced treatment of PFOS and PFOA. Sci. Total Environ. 913, 169332. https://doi.org/10.1016/j.scitotenv.2023.169332.

Armitage, J.M., 2009. Modeling the global fate and transport of perfluoroalkylated substances (PFAS).

Arslan, M., Gamal El-Din, M., 2021. Removal of per- and poly-fluoroalkyl substances (PFASs) by wetlands: prospects on plants, microbes and the interplay. Sci. Total Environ. 800, 149570. https://doi.org/10.1016/j.scitotenv.2021.149570.

Arulananthan, A., Vilhelmsson, O., Karsten, U., Grossart, H.-P., Sigurbjornsdottir, A., Rolfsson, Ó., Joerss, H., Scholz, B., 2025. Per-and polyfluoroalkyl substances (PFAS) in the Cryosphere -Occurrence, organismic accumulation, ecotoxicological impacts, transformation, and management strategies. Front. Environ. Sci. 13. https://doi.org/10.3389/fenvs.2025.1559941.

Axelsson, M., Gentili, F., 2014. A Single-Step Method for Rapid Extraction of Total Lipids from Green Microalgae. PLoS One 9, e89643. https://doi.org/10.1371/journal.pone.0089643.

Bates, L.S., Waldren, R.P., Teare, I.D., 1973. Rapid determination of free proline for water-stress studies. Plant Soil 39, 205–207. doi:10.1007/BF00018060.

Beena Ramachandran Nair, G., 2025. Plankton community composition: disentangling the roles of environmental parameters and PFAS.

Benoiston, A.-S., Ibarbalz, F.M., Bittner, L., Guidi, L., Jahn, O., Dutkiewicz, S., Bowler, C., 2017. The evolution of diatoms and their biogeochemical functions. Philos. Trans. R Soc. L. B Biol. Sci. 372, 20160397. https://doi.org/10.1098/rstb.2016.0397.

Bernardini, I., Matozzo, V., Valsecchi, S., Peruzza, L., Rovere, G.D., Polesello, S., Iori, S., Marin, M.G., Fabrello, J., Ciscato, M., Masiero, L., Bonato, M., Santovito, G., Boffo, L., Bargelloni, L., Milan, M., Patarnello, T., 2021. The new PFAS C6O4 and its effects on marine invertebrates: first evidence of transcriptional and microbiota changes in the Manila clam Ruditapes philippinarum. Environ. Int. 152, 106484. https://doi.org/10.1016/j.envint.2021.106484.

Bernardo-Cravo, A.P., Schmeller, D.S., Chatzinotas, A., Vredenburg, V.T., Loyau, A., 2020. Environmental factors and host microbiomes shape host-pathogen dynamics. Trends Parasitol. 36, 616–633. https://doi.org/10.1016/j.pt.2020.04.010.

Bradford, M.M., 1976. A rapid and sensitive method for the quantitation of microgram quantities of protein utilizing the principle of protein-dye binding. Anal. Biochem. 72, 248–254. https://doi.org/10.1016/0003-2697(76)90527-3.

Braune, B.M., Outridge, P.M., Fisk, A.T., Muir, D.C.G., Helm, P.A., Hobbs, K., Hoekstra, P.F., Kuzyk, Z.A., Kwan, M., Letcher, R.J., Lockhart, W.L., Norstrom, R.J., Stern, G.A., Stirling, I., 2005. Persistent organic pollutants and mercury in marine biota of the Canadian Arctic: an overview of spatial and temporal trends. Sci. Total Environ. 351-352, 4–56. https://doi.org/10.1016/j.scitotenv.2004.10.034.

Brendel, S., Fetter, É., Staude, C., Vierke, L., Biegel-Engler, A., 2018. Short-chain perfluoroalkyl acids: environmental concerns and a regulatory strategy under REACH. Environ. Sci. Eur. 30, 9. https://doi.org/10.1186/s12302-018-0134-4.

Brun, P., Stamieszkin, K., Visser, A.W., Licandro, P., Payne, M.R., Kiørboe, T., 2019. Climate change has altered zooplankton-fuelled carbon export in the North Atlantic. Nat. Ecol. Evol. 3, 416–423. https://doi.org/10.1038/s41559-018-0780-3.

Casal, P., González-Gaya, B., Zhang, Y., Reardon, A.J.F., Martin, J.W., Jiménez, B., Dachs, J., 2017a. Accumulation of Perfluoroalkylated Substances in Oceanic Plankton. Environ. Sci. Technol. 51, 2766–2775. https://doi.org/10.1021/acs.est.6b05821.

Casal, P., Zhang, Y., Martin, J.W., Pizarro, M., Jiménez, B., Dachs, J., 2017b. Role of Snow Deposition of Perfluoroalkylated Substances at Coastal Livingston Island (Maritime Antarctica). Environ. Sci. Technol. 51, 8460–8470. https://doi.org/10.1021/acs.est.7b02521.

Casas, G., Iriarte, J., D'Agostino, L.A., Roscales, J.L., Martinez-Varela, A., Vila-Costa, M., Martin, J.W., Jiménez, B., Dachs, J., 2023. Inputs, amplification and sinks of perfluoroalkyl substances at coastal Antarctica. Environ. Pollut. 338, 122608. https://doi.org/10.1016/j.envpol.2023.122608.

Catherine, M., Nadège, B., Charles, P., Yann, A., 2019. Perfluoroalkyl substances (PFASs) in the marine environment: spatial distribution and temporal profile shifts in shellfish from French coasts. Chemosphere 228, 640–648. https://doi.org/10.1016/j.chemosphere.2019.04.205.

Chen, Z., zhan, X., Zhang, J., Diao, J., Su, C., Sun, Q., Zhou, Y., Zhang, L., Bi, R., Ye, M., Wang, T., 2023. Bioaccumulation and risk mitigation of legacy and novel perfluoroalkyl substances in seafood: insights from trophic transfer and cooking method. Environ. Int. 177, 108023. https://doi.org/10.1016/j.envint.2023.108023.

Dai, Z., Zhang, H., Zhou, Q., Tian, Y., Chen, T., Tu, C., Fu, C., Luo, Y., 2018. Occurrence of microplastics in the water column and sediment in an inland sea affected by intensive anthropogenic activities. Environ. Pollut. 242, 1557–1565. https://doi.org/10.1016/j.envpol.2018.07.131.

Dai, S., Zhang, G., Dong, C., Yang, R., Pei, Z., Li, Y., Li, A., Zhang, Q., Jiang, G., 2025. Occurrence, bioaccumulation and trophodynamics of per- and polyfluoroalkyl substances (PFAS) in terrestrial and marine ecosystems of Svalbard. Arct. Water Res. 271, 122979. https://doi.org/10.1016/j.watres.2024.122979.

Dale, K., Yadetie, F., Horvli, T., Zhang, X., Frøysa, H.G., Karlsen, O.A., Goksøyr, A., 2022. Single PFAS and PFAS mixtures affect nuclear receptor- and oxidative stress-related pathways in precision-cut liver slices of Atlantic cod (*Gadus morhua*). Sci. Total Environ. 814, 152732. https://doi.org/10.1016/j.scitotenv.2021.152732.

Davis, S.N., Klumker, S.M., Mitchell, A.A., Coppage, M.A., Labonté, J.M., Quigg, A., 2024. Life in the PFAS lane: the impact of perfluoroalkyl substances on photosynthesis, cellular exudates, nutrient cycling, and composition of a marine microbial community. Sci. Total Environ. 927, 171977. https://doi.org/10.1016/j.scitotenv.2024.171977.

de Wit, C.A., Balmer, J., Muir, D.C.G., Vorkamp, K., Wilson, S., 2019. Chemicals of emerging Arctic concern: preface. Emerg. Contam. 5, 1–3. https://doi.org/10.1016/j.emcon.2018.12.001.

Du, M., Pu, Q., Li, X., Yang, H., Hao, N., Li, Q., Zhao, Y., Li, Y., 2023. Perfluoroalkyl and polyfluoroalkyl substances (PFAS) adsorbed on microplastics in drinking water: implications for female exposure, reproductive health risk and its mitigation strategies through in silico methods. J. Clean. Prod. 391, 136191. https://doi.org/10.1016/j.jclepro.2023.136191.

ECHA, 2024. Per- and polyfluoroalkyl substances (PFAS) - ECHA [WWW Document]. https://echa.europa.eu/hot-topics/perfluoroalkyl-chemicals-pfas (accessed 11.18.24).

Falasco, E., Bona, F., Badino, G., Hoffmann, L., Ector, L., 2009. Diatom teratological forms and environmental alterations: a review. Hydrobiologia 623, 1–35. https://doi.org/10.1007/s10750-008-9687-3.

Falkowski, P., 2012. Do tiny floating microorganisms in the ocean's surface waters play a massive role in controlling the global climate?

Gaines, L.G.T., 2023. Historical and current usage of per- and polyfluoroalkyl substances (PFAS): a literature review. Am. J. Ind. Med. 66, 353–378. https://doi.org/10.1002/ajim.23362.

Gebbink, W.A., Bossi, R., Rigét, F.F., Rosing-Asvid, A., Sonne, C., Dietz, R., 2016. Observation of emerging per- and polyfluoroalkyl substances (PFASs) in Greenland marine mammals. Chemosphere 144, 2384–2391. https://doi.org/10.1016/j.chemosphere.2015.10.116.

Guelfo, J.L., Korzeniowski, S., Mills, M.A., Anderson, J., Anderson, R.H., Arblaster, J.A., Conder, J.M., Cousins, I.T., Dasu, K., Henry, B.J., Lee, L.S., Liu, J., McKenzie, E.R., Willey, J., 2021. Environmental sources, chemistry, fate, and transport of per- and polyfluoroalkyl substances: state of the science, key knowledge gaps, and recommendations presented at the august 2019 SETAC focus topic meeting. Environ. Toxicol. Chem. 40, 3234–3260. https://doi.org/10.1002/etc.5182.

Guillard, R.R.L., 1975. Culture of Phytoplankton for Feeding Marine Invertebrates, in: Smith, W.L., Chanley, M.H. (Eds.), Culture of Marine Invertebrate Animals: Proceedings — 1st Conference on Culture of Marine Invertebrate Animals Greenport. Springer US, Boston, MA, pp. 29–60. doi:10.1007/978-1-4615-8714-9_3.

Guo, W., Hao, W., Xiao, W., 2024. Emerging Perfluorinated Chemical GenX: environmental and Biological Fates and Risks. Environ. Health. https://doi.org/10.1021/envhealth.4c00164.

Hallanger, I.G., Warner, N.A., Ruus, A., Evenset, A., Christensen, G., Herzke, D., Gabrielsen, G.W., Borgå, K., 2011. Seasonality in contaminant accumulation in Arctic marine pelagic food webs using trophic magnification factor as a measure of bioaccumulation. Environ. Toxicol. Chem. 30, 1026–1035. https://doi.org/10.1002/etc.488.

Hartz, W.F., Björnsdotter, M.K., Yeung, L.W.Y., Hodson, A., Thomas, E.R., Humby, J.D., Day, C., Jogsten, I.E., Kärrman, A., Kallenborn, R., 2023. Levels and distribution profiles of Per- and Polyfluoroalkyl Substances (PFAS) in a high Arctic Svalbard ice core. Sci. Total Environ. 871, 161830. https://doi.org/10.1016/j.scitotenv.2023.161830.

Hartz, W.F., Björnsdotter, M.K., Yeung, L.W.Y., Humby, J.D., Eckhardt, S., Evangeliou, N., Ericson Jogsten, I., Kärrman, A., Kallenborn, R., 2024. Sources and Seasonal Variations of Per- and Polyfluoroalkyl Substances (PFAS) in surface snow in the Arctic. Environ. Sci. Technol. 58, 21817–21828. https://doi.org/10.1021/acs.est.4c08854.

Hopkinson, B.M., Dupont, C.L., Allen, A.E., Morel, F.M.M., 2011. Efficiency of the CO2-concentrating mechanism of diatoms. Proc. Natl. Acad. Sci. 108, 3830–3837. https://doi.org/10.1073/pnas.1018062108.

Hu, J.-J., Yu, S.-K., Yin, C., Peng, F.-J., Liu, S.-S., Pan, C.-G., Yu, K., 2025. Sorption and mechanisms of legacy and emerging per- and polyfluoroalkyl substances (PFASs) on different particle size fractions of marine sediments. Environ. Res. 278, 121643. https://doi.org/10.1016/j.envres.2025.121643.

ITRC, 2023, 2023. Per- and Polyfluoroalkyl Substances (PFAS) [WWW Document]. ITRC. https://itrcweb.org/pfas-guidance/ (accessed 2.24.25).

Joerss, H., Apel, C., Ebinghaus, R., 2019. Emerging per- and polyfluoroalkyl substances (PFASs) in surface water and sediment of the North and Baltic Seas. Science of The Total Environment 686, 360–369. doi:10.1016/j.scitotenv.2019.05.363.

Joerss, H., Xie, Z., Wagner, C.C., Von Appen, W.-J., Sunderland, E.M., Ebinghaus, R., 2020. Transport of Legacy Perfluoroalkyl Substances and the Replacement Compound HFPO-DA through the Atlantic Gateway to the Arctic Ocean—Is the Arctic a Sink or a Source? Environ. Sci. Technol. 54, 9958–9967. https://doi.org/10.1021/acs.est.0c00228.

Jouanneau, W., Léandri-Breton, D.-J., Herzke, D., Moe, B., Nikiforov, V.A., Pallud, M., Parenteau, C., Gabrielsen, G.W., Chastel, O., 2023. Does contaminant exposure disrupt maternal hormones deposition? A study on per- and polyfluoroalkyl substances in an Arctic seabird. Sci. Total Environ. 868, 161413. https://doi.org/10.1016/j.scitotenv.2023.161413.

Karsten, U., Schlie, C., Woelfel, J., Becker, B., 2012. Benthic Diatoms in Arctic Seas – Ecological Functions and Adaptations. Polarforschung 81, 77–84.

Latała, A., Nędzi, M., Stepnowski, P., 2009. Acute toxicity assessment of perfluorinated carboxylic acids towards the Baltic microalgae. Environ. Toxicol. Pharmacol. 28, 167–171. https://doi.org/10.1016/j.etap.2009.03.010.

Li, J., Zheng, T., Liu, C., 2021a. Soil acidification enhancing the growth and metabolism inhibition of PFOS and Cr(VI) to bacteria involving oxidative stress and cell permeability. Environ. Pollut. 275, 116650. https://doi.org/10.1016/j.envpol.2021.116650.

Li, Y., Liu, X., Zheng, X., Yang, M., Gao, X., Huang, J., Zhang, L., Fan, Z., 2021b. Toxic effects and mechanisms of PFOA and its substitute GenX on the photosynthesis of *Chlorella pyrenoidosa*. Sci. Total Environ. 765, 144431. https://doi.org/10.1016/j.scitotenv.2020.144431.

Li, J., Li, X., Da, Y., Yu, J., Long, B., Zhang, P., Bakker, C., McCarl, B.A., Yuan, J.S., Dai, S. Y., 2022. Sustainable environmental remediation via biomimetic multifunctional lignocellulosic nano-framework. Nat. Commun. 13, 4368. https://doi.org/10.1038/s41467-022-31881-5.

Li, X., Ma, Y., Zhang, Y., Zhang, X., Li, H., Sun, Y., Niu, Z., 2024. Porphyrin metabolism and carbon fixation response of Skeletonema costatum at different growth phases to mixed emerging PFASs at environmental concentrations. Environ. Sci.: Process. Impacts 26, 1465–1475. https://doi.org/10.1039/D4EM00137K.

Liao, J., Sun, B., Wang, C., Cao, Z., Wu, Z., An, X., Liang, Z., Huang, X., Lu, Y., 2024. Uptake and cellular responses of *Microcystis aeruginosa* to PFOS in various environmental conditions. Ecotoxicol. Environ. Saf. 272, 116041. https://doi.org/10.1016/j.ecoenv.2024.116041.

Liao, J., Lu, Y., Liu, Y., Sun, B., Zhang, K., Wang, C., Lei, H., Cao, Z., 2025. How heatwaves impact microalgae in the presence of environmentally relevant PFAS concentration: metabolic shifts and challenges posed. J. Hazard. Mater. 484, 136640. https://doi.org/10.1016/j.jhazmat.2024.136640.

Liu, X., Li, Y., Zheng, X., Zhang, L., Lyu, H., Huang, H., Fan, Z., 2021. Antioxidant mechanisms of *Chlorella pyrenoidosa* under acute GenX exposure. Sci. Total Environ. 797, 149005. https://doi.org/10.1016/j.scitotenv.2021.149005.

Liu, X., Zheng, X., Zhang, L., Li, J., Li, Y., Huang, H., Fan, Z., 2022. Joint toxicity mechanisms of binary emerging PFAS mixture on algae (*Chlorella pyrenoidosa*) at environmental concentration. J. Hazard. Mater. 437, 129355. https://doi.org/10.1016/j.jhazmat.2022.129355.

Lukić Bilela, L., Matijošytė, I., Krutkevičius, J., Alexandrino, D.A.M., Safarik, I., Burlakovs, J., Gaudêncio, S.P., Carvalho, M.F., 2023. Impact of per- and polyfluorinated alkyl substances (PFAS) on the marine environment: raising awareness, challenges, legislation, and mitigation approaches under the One Health concept. Mar. Pollut. Bull 194, 115309. https://doi.org/10.1016/j.marpolbul.2023.115309.

Ma, T., Ye, C., Wang, T., Li, X., Luo, Y., 2022. Toxicity of Per- and Polyfluoroalkyl Substances to Aquatic Invertebrates, Planktons, and Microorganisms. Int J Environ. Res. Public Health 19, 16729. https://doi.org/10.3390/ijerph192416729.

MacInnis, J.J., Lehnherr, I., Muir, D.C.G., St. Pierre, K.A., St. Louis, V.L., Spencer, C., De Silva, A.O., 2019. Fate and Transport of Perfluoroalkyl Substances from Snowpacks into a Lake in the High Arctic of Canada. Environ. Sci. Technol. 53, 10753–10762. https://doi.org/10.1021/acs.est.9b03372.

Mahmoudnia, A., 2023. The role of PFAS in unsettling ocean carbon sequestration. Environ. Monit. Assess. 195, 310. https://doi.org/10.1007/s10661-023-10912-8.

Mahoney, H., Cantin, J., Xie, Y., Brinkmann, M., Giesy, J.P., 2023. Perfluoroethylcyclohexane sulphonate, an emerging perfluoroalkyl substance, disrupts mitochondrial membranes and the expression of key molecular targets *in vitro*. Aquat. Toxicol. 257, 106453. https://doi.org/10.1016/j.aquatox.2023.106453.

Manojkumar, Y., Pilli, S., Rao, P.V., Tyagi, R.D., 2023. Sources, occurrence and toxic effects of emerging per- and polyfluoroalkyl substances (PFAS). Neurotoxicol. Teratol. 97, 107174. https://doi.org/10.1016/j.ntt.2023.107174.

Niu, Z., Na, J., Xu, W., Wu, N., Zhang, Y., 2019. The effect of environmentally relevant emerging per- and polyfluoroalkyl substances on the growth and antioxidant response in marine *Chlorella* sp. Environ. Pollut. 252, 103–109. https://doi.org/10.1016/j.envpol.2019.05.103.

Nothnagel, J., R Core Team, 1995. Effects of salinity and light intensity on the osmolyte concentrations, cell volumes and growth rates of the Antarctic sea-ice diatoms Chaetoceros sp. and Navicula sp. with emphasis on the amino acid proline). Berichte zur Polarforschung = Reports on Polar Research. Bremerhaven, Germany. doi:10.2312/BzP_0161_1995.

OECD, 2006. Test No. 201: Alga, Growth Inhibition Test, OECD Guidelines for the Testing of Chemicals, Section 2: Effects on Biotic Systems. OECD Publishing. https://doi.org/10.1787/9789264069923-en.

OECD, 2022. Synthesis Report on Understanding Side-Chain Fluorinated Polymers and Their Life Cycle, OECD Series on Risk Management of Chemicals. OECD. https://doi.org/10.1787/e13559f7-en.

Pascariello, S., Mazzoni, M., Bettinetti, R., Manca, M., Patelli, M., Piscia, R., Valsecchi, S., Polesello, S., 2019. Organic Contaminants in Zooplankton of Italian Subalpine Lakes: patterns of Distribution and Seasonal Variations. Water (Basel) 11, 1901. https://doi.org/10.3390/w11091901.

Pietropoli, E., Schumann, S., Moressa, A., Gallocchio, F., Zonta, G., Santovito, G., Irato, P., 2025. Naturally occurring environmental PFAS mixtures induce significant oxidative damage and nuclei fragmentation in *Dendrobaena veneta*. Chemosphere 378, 144413. https://doi.org/10.1016/j.chemosphere.2025.144413.

Prieto, P., Pineda, M., Aguilar, M., 1999. Spectrophotometric quantitation of antioxidant capacity through the formation of a phosphomolybdenum complex: specific application to the determination of vitamin E. Anal. Biochem. 269, 337–341. https://doi.org/10.1006/abio.1999.4019.

R Core Team, 2024. R: The R Project for Statistical Computing [WWW Document]. URL https://www.r-project.org/ (accessed 9.16.25).

Rodea-Palomares, I., Leganés, F., Rosal, R., Fernández-Piñas, F., 2012. Toxicological interactions of perfluorooctane sulfonic acid (PFOS) and perfluorooctanoic acid (PFOA) with selected pollutants. J. Hazard. Mater 201-202, 209–218. https://doi.org/10.1016/j.jhazmat.2011.11.061.

Routti, H., Gabrielsen, G.W., Herzke, D., Kovacs, K.M., Lydersen, C., 2016. Spatial and temporal trends in perfluoroalkyl substances (PFASs) in ringed seals (Pusa hispida) from Svalbard. Environ. Pollut. 214, 230–238. https://doi.org/10.1016/j.envpol.2016.04.016.

Routti, H., Atwood, T.C., Bechshoft, T., Boltunov, A., Ciesielski, T.M., Desforges, J.-P., Dietz, R., Gabrielsen, G.W., Jenssen, B.M., Letcher, R.J., McKinney, M.A., Morris, A. D., Rigét, F.F., Sonne, C., Styrishave, B., Tartu, S., 2019. State of knowledge on current exposure, fate and potential health effects of contaminants in polar bears from the circumpolar Arctic. Sci. Total Environ. 664, 1063–1083. https://doi.org/10.1016/j.scitotenv.2019.02.030.

Sabba, F., Kassar, C., Zeng, T., Mallick, S.P., Downing, L., McNamara, P., 2025. PFAS in landfill leachate: practical considerations for treatment and characterization. J. Hazard. Mater 481, 136685. https://doi.org/10.1016/j.jhazmat.2024.136685.

Shi, J., Hu, M., Xia, Z., Zhang, J., Wang, Z., Li, L., Zhao, Y., 2024. Influence of perfluoroalkyl substances, with focus on perfluorobutanoic acid on the responding characteristics and molecular mechanisms of *Thalassiosira pseudonana*. Ecotoxicol. Environ. Saf. 285, 117048. https://doi.org/10.1016/j.ecoenv.2024.117048.

Staats, N., Stal, L.J., Mur, L.R., 2000. Exopolysaccharide production by the epipelic diatom *Cylindrotheca closterium*: effects of nutrient conditions. J. Exp. Mar. Biol. Ecol. 249, 13–27. https://doi.org/10.1016/S0022-0981(00)00166-0.

Tolaymat, T., Robey, N., Krause, M., Larson, J., Weitz, K., Parvathikar, S., Phelps, L., Linak, W., Burden, S., Speth, T., Krug, J., 2023. A critical review of perfluoroalkyl and polyfluoroalkyl substances (PFAS) landfill disposal in the United States. Sci. Total Environ. 905, 167185. https://doi.org/10.1016/j.scitotenv.2023.167185.

Trilla-Prieto, N., Dachs, J., Iriarte, J., Berrojalbiz, N., Colomer-Vidal, P., Casas, G., Garcia-Garin, O., Vila-Costa, M., Jiménez, B., 2025. Accumulation of perfluoroalkyl acids as forever chemicals in Antarctic waters. Commun. Earth Environ. 6, 545. https://doi.org/10.1038/s43247-025-02535-3.

US EPA, O., 2021. Per- and Polyfluoroalkyl Substances (PFAS) [WWW Document]. https://www.epa.gov/sdwa/and-polyfluoroalkyl-substances-pfas (accessed 2.20.25).

van Kooten, O., Snel, J.F.H., 1990. The use of chlorophyll fluorescence nomenclature in plant stress physiology. Photosynth. Res. 25, 147–150. https://doi.org/10.1007/BF00033156.

Wang, H., Zhang, X., Liu, Y., Liu, J., 2018. Stabilization of Liposomes by Perfluorinated Compounds. ACS Omega 3, 15353–15360. https://doi.org/10.1021/acsomega.8b02448.

Wellburn, A.R., 1994. The Spectral Determination of Chlorophylls *a* and *b*, as well as total carotenoids, using various solvents with spectrophotometers of different resolution. J. Plant Physiol. 144, 307–313. https://doi.org/10.1016/S0176-1617(11)81192-2.

Wickham, H., 2016. Create Elegant Data Visualisations Using the Grammar of Graphics ggplot2 [WWW Document]. URL https://ggplot2.tidyverse.org/ (accessed 9.16.25).

Wu, J., Jiang, R., Lin, W., Ouyang, G., 2019. Effect of salinity and humic acid on the aggregation and toxicity of polystyrene nanoplastics with different functional groups and charges. Environ. Pollut. 245, 836–843. https://doi.org/10.1016/j.envpol.2018.11.055.

Wu, J., Gu, L., Hua, Z., Liang, Z., Chu, K., He, X., 2021. Per-, poly-fluoroalkyl substances (PFASs) pollution in benthic riverine ecosystem: integrating microbial community coalescence and biogeochemistry with sediment distribution. Chemosphere 281, 130977. https://doi.org/10.1016/j.chemosphere.2021.130977.

Xiao, R., Zheng, Y., 2016. Overview of microalgal extracellular polymeric substances (EPS) and their applications. Biotechnol. Adv. 34, 1225–1244. https://doi.org/10.1016/j.biotechadv.2016.08.004.

Xie, Z., Kallenborn, R., 2023. Legacy and emerging per- and poly-fluoroalkyl substances in polar regions. Curr. Opin. Green Sustain. Chem. 42, 100840. https://doi.org/10.1016/j.cogsc.2023.100840.

Xue, X., Gao, N., Xu, F., 2022. Toxicity of perfluooctane sulfonate (PFOS) and perfluorobutane sulfonate (PFBS) to *Scenedesmus obliquus*: photosynthetic characteristics, oxidative damage and transcriptome analysis. Environ. Pollut. 315, 120397. https://doi.org/10.1016/j.envpol.2022.120397.

Yu, L., Liu, X., Hua, Z., Xing, X., Xue, H., 2025. Fate variations of Per- and polyfluoroalkyl substances in diverse aquatic environments: an overlooked influence of hydrodynamics. Water Res. 282, 123628. https://doi.org/10.1016/j.watres.2025.123628.

Zenobio, J.E., Salawu, O.A., Han, Z., Adeleye, A.S., 2022. Adsorption of per- and polyfluoroalkyl substances (PFAS) to containers. J. Hazard. Mater. Adv. 7, 100130. https://doi.org/10.1016/j.hazadv.2022.100130.

Zhang, F., Ding, Z., Gong, H., Chi, J., 2019a. Effects of microphytobenthos Cylindrotheca closterium on the fate of di-n-butyl phthalate in an aquatic microcosm. Mar. Pollut. Bull. 140, 101–106. https://doi.org/10.1016/j.marpolbul.2019.01.033.

Zhang, X., Lohmann, R., Sunderland, E.M., 2019b. Poly- and Perfluoroalkyl Substances in Seawater and Plankton from the Northwestern Atlantic Margin. Environ. Sci. Technol. 53, 12348–12356. https://doi.org/10.1021/acs.est.9b03230.

Zhang, Ying, Qv, Z., Wang, Jingwen, Yang, Y., Chen, X., Wang, Jingzhen, Zhang, Yanfeng, Zhu, L., 2022. Natural biofilm as a potential integrative sample for evaluating the contamination and impacts of PFAS on aquatic ecosystems. Water Res. 215, 118233. https://doi.org/10.1016/j.watres.2022.118233.

Zhang, B., Wang, Z., Li, D., Li, L., Zhao, Yirong, Tang, X., Zhao, Yan, 2024. Reactive oxygen species mediated extracellular polymeric substances production assisting the recovery of Thalassiosira pseudonana from polystyrene micro and nanoplastics exposure. Environ. Pollut. 348, 123850. https://doi.org/10.1016/j.envpol.2024.123850.

Zhao, Z., Xie, Z., Möller, A., Sturm, R., Tang, J., Zhang, G., Ebinghaus, R., 2012. Distribution and long-range transport of polyfluoroalkyl substances in the Arctic, Atlantic Ocean and Antarctic coast. Environ. Pollut. 170, 71–77. https://doi.org/10.1016/j.envpol.2012.06.004.

Zhao, Z., Zheng, X., Han, Z., Yang, S., Zhang, H., Lin, T., Zhou, C., 2023. Response mechanisms of *Chlorella sorokiniana* to microplastics and PFOA stress: photosynthesis, oxidative stress, extracellular polymeric substances and antioxidant system. Chemosphere 323, 138256. https://doi.org/10.1016/j.chemosphere.2023.138256.

Zheng, H., Wang, F., Zhao, Z., Ma, Y., Yang, H., Lu, Z., Cai, Minggang, Cai, Minghong, 2017. Distribution profiles of per- and poly fluoroalkyl substances (PFASs) and their re-regulation by ocean currents in the East and South China Sea. Mar. Pollut. Bull. 125, 481–486. https://doi.org/10.1016/j.marpolbul.2017.08.009.

Zhi, Y., Lu, X., Munoz, G., Yeung, L.W.Y., De Silva, A.O., Hao, S., He, H., Jia, Y., Higgins, C.P., Zhang, C., 2024. Environmental occurrence and biotic concentrations of ultrashort-chain perfluoroalkyl acids: overlooked global organofluorine contaminants. Environ. Sci. Technol. 58, 21393–21410. https://doi.org/10.1021/acs.est.4c04453.

Zhou, Y., Wang, X., Wang, C., Ji, Z., Niu, X., Dong, H., 2024. Fate of 'forever chemicals' in the global cryosphere. Earth-Sci. Rev. 259, 104973. https://doi.org/10.1016/j.earscirev.2024.104973.

Article III

PFAS at environmental concentration alters metabolic and gene expression patterns in two model marine diatoms: Decoding survival and acclimation mechanisms.

Graphical Abstract

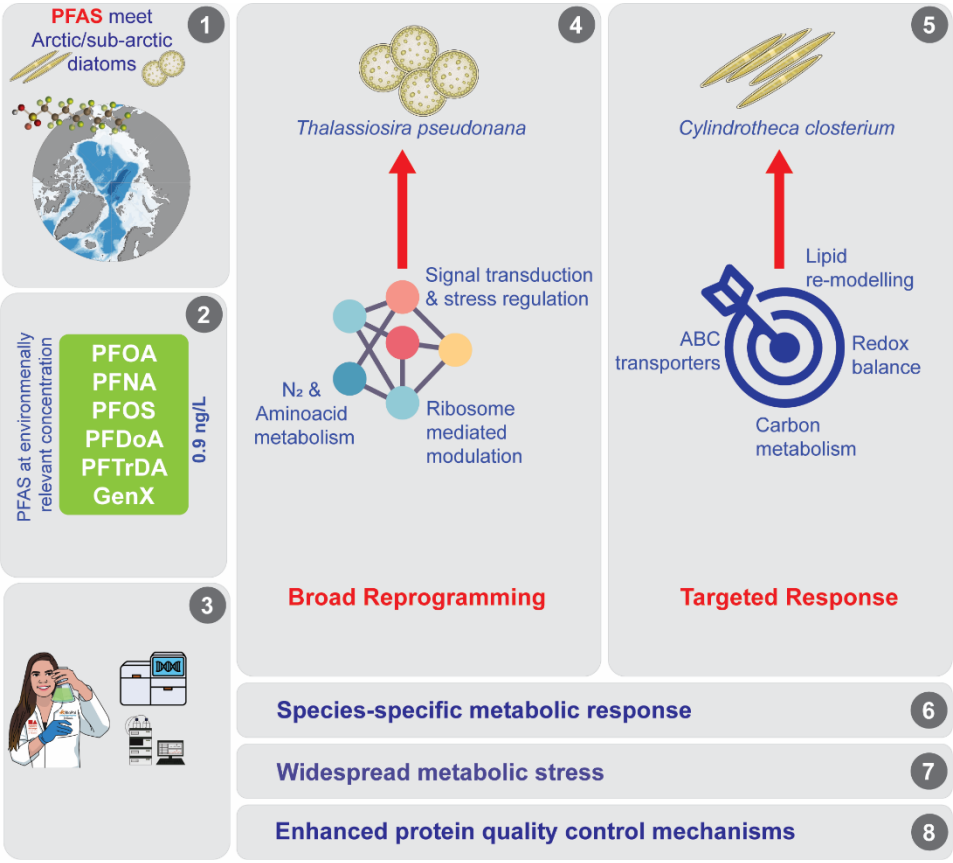

PFAS at environmental concentration alters metabolic and gene expression patterns in two model marine diatoms: Decoding survival and acclimation mechanisms

Ashani Arulananthan[1,2], Oddur Þór Vilhelmsson[1,3], Óttar Rolfsson[4], Hans-Peter Grossart[5,6], Auður Sigurbjörnsdóttir[1], Ulf Karsten[7,8], Marie Wünsch[9], Ralf Ebinghaus[10], Hanna Joerss[11], Bernardo Duarte[12, 13,] Zophonías O. Jónsson[14], Bettina Scholz[1,2]*

[1]*Faculty of Natural Resource Science, University of Akureyri. Iceland.*

[2]*BioPol ehf. Marine Biotechnology, Skagaströnd, Iceland.*

[3]*The Biomedical Center of the University of Iceland, Reykjavík, Iceland.*

[4]*Department of Biochemistry and Molecular Biology, Faculty of Medicine, University of Iceland, Reykjavik, Iceland.*

[5]*Department of Plankton and Microbial Ecology, Leibniz-Institute of Freshwater Ecology and Inland Fisheries, Stechlin, Germany.*

[6]*Institute of Biochemistry and Biology, Potsdam University, Potsdam, Germany.*

[7]*Department of Applied Ecology and Phycology, Institute of Biological Sciences, University of Rostock, Germany.*

[8]*Department of Maritime Systems, Interdisciplinary Faculty, University of Rostock, Germany.*

[9]*Department of Molecular Stress Physiology, Institute of Biosciences, University of Rostock, Germany.*

[10] *Helmholtz-Zentrum Hereon Institute of Coastal Environmental Chemistry, Geesthacht, Germany*

[11]*Institute of Coastal Environmental Chemistry, Helmholtz-Zentrum Hereon, Geesthacht, Germany.*

[12]*MARE—Marine and Environmental Sciences Centre & ARNET—Aquatic Research Network Associated Laboratory, Faculdade de Ciências da Universidade de Lisboa, Campo Grande, 1749-016 Lisbon, Portugal.*

[13]*Departamento de Biologia Vegetal, Faculdade de Ciências da Universidade de Lisboa, Portugal.*[14] *Faculty of Life and Environmental Sciences, University of Iceland, Reykjavik, Iceland.*

[*]*Corresponding author*: ashani@unak.is

Abstract

Arctic marine diatoms are key primary producers vital for polar food webs and global carbon cycling. These ecosystems face increasing exposure to pollutants like per- and polyfluoroalkyl substances (PFAS). The effects of long-term exposure to a PFAS mixture, PFOA, PFNA, PFOS, PFDoA, PFTrDA, and GenX, each at environmentally relevant concentrations of 0.9 ng/L, on the benthic *Cylindrotheca closterium* and the pelagic *Thalassiosira pseudonana* were investigated by high-throughput PacBio ISO RNA-seq and UPLC-MS/MS metabolomic profiles. *T. pseudonana* mounts a deep, multi-pathway reconfiguration of core housekeeping metabolism, whereas *C. closterium* showed a narrower response dominated by ABC-mediated efflux and central carbon metabolism. PFAS exposure resulted in the metabolic depletion of amino acids, sugars, and osmolytes, while transcriptionally activating carbon-repartitioning, nitrogen, and proline metabolism, transport, and redox systems in *C. closterium*. *T. pseudonana* undergoes a metabolic shift from growth and high nitrogen demand toward a stress-acclimated state that prioritizes a redox homeostasis, membrane repair, and protective secondary metabolite-rich survival state rather than growth. These findings show that environmentally relevant PFAS concentrations are already sufficient to impact key metabolic and regulatory processes in species-specific manner in marine diatoms. The study highlights the delicate balance between acclimation and vulnerability of Arctic diatoms to PFAS pollution.

1.0 Introduction

Among emerging pollutants, PFAS have received increasing attention because of their exceptional resistance to thermal, chemical, and biological degradation (Wang Z *et al.* 2017, US EPA 2021, Wang X *et al.* 2023, Arulananthan, Vilhelmsson *et al.* 2025). These properties have led to a wide range of industrial and consumer applications, including firefighting foams, non-stick cookware, waterproof fabrics and paper coatings, electroplating, fluoropolymer production, and waterproof cosmetics (Glüge *et al.* 2020, Meegoda *et al.* 2020, Whitehead *et al.* 2021, Lukić Bilela *et al.* 2023). However, the stable chemical nature that makes PFAS technically useful also enables their environmental persistence. They tend to bind to proteins and plasma membranes, resulting in accumulation in biota, including humans (Fischer *et al.* 2024, Birchfield *et al.* 2025). Accordingly, many long-chain PFAS show toxic effects on aquatic organisms, disrupting metabolism, oxidative balance, and reproduction (Xue, Gao, and Xu 2022, Dai *et al.* 2025).

After the use of several long-chain PFAS substances was banned, their short-chain replacements, such as HFPO-DA (hexafluoropropylene oxide dimer acid; FRD-903; marketed as its ammonium salt GenX), and 6:2 FTS (fluorotelomer sulfonic acid), are now increasingly detected, raising similar concerns about their persistence and toxicity (Guo et al., 2024; Li et al., 2021; Wang et al., 2023). The widespread occurrence of PFAS, even in remote polar regions like Arctic and

Antarctica, highlights their mobility due to atmospheric and oceanic circulation, and raises concerns about their potential impact on sensitive marine ecosystems (Antonopoulou et al., 2024; Joerss et al., 2020; Trilla-Prieto et al., 2025; Wang et al., 2023; Zhang et al., 2024). In polar regions, despite the region's remoteness from emission sources, limited degradation and continuous deposition promote their persistence in seawater, sea ice, and sediments, leading to continuous exposure of local microbial communities (Garnett *et al.* 2019, 2021, 2022, Hartz *et al.* 2024, Arulananthan, Vilhelmsson *et al.* 2025, Dai *et al.* 2025). PFAS are globally detected in surface waters including the Arctic and drinking waters, with concentrations ranging from pg L^{-1} to ng L^{-1} which even reached concentrations in the mg L^{-1} range near waste water discharge points and firefighting training centres (Hartz *et al.* 2023, Saritha, Krishnan, and Mohan 2023, Davis *et al.* 2024, Grung *et al.* 2024, Lohmann *et al.* 2024, Dai *et al.* 2025). The mean PFAS concentration across selected regions in the Arctic was 740pg L^{-1} and reaching up to 1,544 pg L^{-1} in an ice core from Svalbard (Hartz *et al.* 2023, 2024). Oceanographic studies show that Atlantic inflow and other current systems efficiently carry PFAS into Arctic surface waters (Joerss *et al.* 2020), where they become available to plankton communities. Experimental and field studies demonstrate that phytoplankton and zooplankton communities readily accumulate PFAS from seawater (Casal *et al.* 2017, Rigét *et al.* 2019), forming bioavailable concentrations at the base of the food web that subsequently bio-magnify into fish, seabirds, and marine mammals. Recent research on PFAS meta-analysis also points out the potential of bio-magnification, whereby PFAS concentrations typically increase by roughly a factor of two per trophic level. This underscores the particular vulnerability of apex predators and humans dependent on marine resources, especially in polar regions (Ricolfi *et al.* 2025).

As key primary producers, marine diatoms represent an early biological interface for PFAS uptake and stress response. Diatoms sustain entire marine food webs including Arctic coastal and pelagic ecosystems. Through their high primary production and role in the biological carbon pump, they are major contributors to global carbon cycling and climate regulation (Hopkinson *et al.* 2011, Karsten *et al.* 2012, Debenest, Silvestre, and Pinelli 2013, Falciatore and Mock 2022). However, their ecological functions and cellular balance are increasingly threatened by anthropogenic contaminants such as PFAS. Disruption of the metabolic and transcriptional functions of phytoplankton can alter key processes, such as carbon fixation and nutrient flux.

Together, transcriptomics and metabolomics provide a complementary, biological network view of how PFAS disturb cellular functions. Thus, both approaches are well-suited to unravel subtle stress responses at environmentally realistic exposure levels (Mao X *et al.* 2021, Mao W *et al.* 2023, Flynn *et al.* 2025). Although traditional endpoints, such as growth inhibition, photosynthesis, and oxidative stress, demonstrate that PFAS can impair algal physiology, they provide

limited insight into the underlying mechanisms (Li Y *et al.* 2021, Davis *et al.* 2024, Liao *et al.* 2024a, 2025a). Recent high-throughput transcriptomics studies in algae and other aquatic species have shown that structurally diverse PFAS elicit distinct expression signatures, enabling the identification of sensitive pathways that can inform hazard assessments beyond a small subset of well-studied compounds (Boltes, Rosal, and García-Calvo 2012, Liao *et al.* 2024b, 2025b, Shi *et al.* 2024, Flynn *et al.* 2025).

In parallel, metabolomics has emerged as a powerful tool for capturing the downstream biochemical consequences of PFAS exposure, including the disruption of central carbon metabolism, energy production, lipid homeostasis, and nucleotide and amino acid metabolism (Liao *et al.* 2025a). Thus, integrating transcriptomic and metabolomic information offers a more comprehensive understanding of PFAS toxicity, linking altered gene regulation with measurable metabolic phenotypes that are directly relevant to cellular fitness and ecosystem functioning.

Existing omics studies on microalgae and other organisms have mainly focused on single legacy PFAS, short-term exposure, and certain common metabolic pathways, such as antioxidant defence, fatty acid metabolism, and photosynthesis. Only a few studies have examined the effects of combined next-generation PFAS, such as GenX, in mixtures at environmentally relevant concentrations (Li Y *et al.* 2021, Zhang QY *et al.* 2024). Transcriptomic data studied in *Thalassiosira* sp. linked PFAS exposure to the modulation of core metabolic pathways, including carbon fixation, glycolysis, the pentose phosphate pathway, and the tricarboxylic acid cycle (TCA), along with the activation of DNA repair mechanisms (Shi *et al.* 2024, Liao *et al.* 2025a). Likewise, metabolic studies have revealed that PFAS can differentially regulate fatty acid synthesis, TCA intermediates and the TCA cycle itself, purine and pyrimidine metabolism, and redox homeostasis, with contrasting outcomes depending on the compound identity and exposure time (Shi *et al.* 2024, Zhang QY *et al.* 2024, Liao *et al.* 2025a). However, long-term low-dose mixture exposures that reflect real field conditions remain underrepresented, and integrated transcriptome metabolome analyses that simultaneously cover long-chain and emerging PFAS, such as GenX, in marine microalgae are particularly scarce (Guo, Hao, and Xiao 2024, Karamat *et al.* 2024, Liao *et al.* 2024a).

By jointly characterizing gene expression and metabolite profiles in cells exposed to a defined mixture of PFAS at environmental concentrations, the present study addresses these gaps and aims to elucidate the coordinated molecular responses that underlie PFAS-induced stress and potential acclimation in two ecologically distinct, fully sequenced model marine diatoms, *Thalassiosira pseudonana* (pelagic, centric) and *Cylindrotheca closterium* (benthic, pennate). These species are broadly accepted biological models for ecotoxicological research, because, together, they represent different ecological niches and

complementary biological traits, allowing pollution effects to be assessed from the cellular to molecular levels across both pelagic and benthic environments. A mixture of PFAS compounds at 0.9 ng L-1 was added to each diatom culture. At different time points, physiological parameters were evaluated to assess the diatom's fitness changes upon PFAS exposure. Based on preliminary biochemical analysis, different metabolic pathway disruptions were identified (Arulananthan, Scholz *et al.* 2025). These include, for example, protein reduction across all time points in both species, and photosynthetic machinery dysfunction evidenced by declining PSII activity and variable chlorophyll content. In addition, stress response mechanisms like proline accumulation indicating osmoregulatory stress responses, antioxidant system activation through spiked TAC changes and species-specific biochemical response patterns - with *C. closterium* showing greater sensitivity to PFAS, also reflected in both transcriptomic and metabolic analyses.

PFAS exposure alters diatom metabolic and transcriptional processes in marine diatoms, affecting pathways associated with cellular homeostasis, carbon metabolism, and nutrient utilization. Although the present study focused on marine diatoms under laboratory conditions, these findings provide mechanistic insights into how persistent pollutants may influence physiological stress responses and acclimatory processes of ecologically important Arctic phytoplankton.

2.0 Materials and Methods:

2.1 Experimental design

The long-term exposure design was specifically intended to investigate chronic PFAS exposure responses and potential physiological acclimation processes occurring over multiple generations of diatom growth, rather than acute short-term toxicity responses. An extended exposure period was selected to better evaluate long-term metabolic and transcriptional adjustments under environmentally relevant chronic PFAS stress conditions.

Semicontinuous cultures of the Arctic benthic diatom *C. closterium* (isolated from Svalbard samples) and the sub-Arctic pelagic species *T. pseudonana* (strain DCG 0682, BCCM/DCG, Ghent University, Belgium, isolated from Schelde River, Belgium) were maintained in artificial seawater prepared from distilled water supplemented with 35 g L^{-1} sea salt (Tropic Marin Bio-Actif). Cultures were grown in f/2 medium according to Guillard (1975) at a salinity of 30 S_A and pH 8.0. All cultures were maintained at 16 ± 0.5 ºC under 12 h light: 12 h dark period with an irradiance of 100 µmol photons m^{-2} s^{-1} using fluorescent lamps positioned on two sides of the flasks. All cultures were gently shaken three times daily to avoid sedimentation of the cells. Diatoms exposed to PFAS, and their molecular responses were assessed and compared to those of non-exposed controls. The diatoms were exposed for 28 days to a mixture of long-chain PFAS compounds,

perfluorooctanoic acid (PFOA), perfluorononanoic acid (PFNA), perfluorododecanoic acid (PFDoA), perfluorooctane sulfonic acid (PFOS), perfluorotridecanoic acid (PFTrDA), and GenX, each at 0.9 ng L^{-1}. Stock solutions (1000 µg mL^{-1}) of each PFAS were prepared in artificial seawater dissolved in distilled water (Supplementary Table M1). Prior to the experiments, working solutions of PFAS were prepared by serial dilution of the same stock solution. Following the exposure period, diatom biomass from both PFAS-treated and control groups of both species was harvested by centrifugation at 2,500 × g at 4°C (Sorvall Legend Mach 1.6 R) for 5 minutes and immediately stored at -80 °C for subsequent metabolomic and transcriptomic analyses. Details on diatom cultivation and the experimental design are provided by (Arulananthan, Scholz *et al.* 2025) and in the Supplementary Figure M1 and Table M1.

2.2 Metabolome analysis

Metabolites were extracted from 100 mg of wet-weight diatom pellets in three phases. First, the pellets were suspended in 750 µL of cold 70% methanol and sonicated for 10 s (BRANSON 1510 sonicator). The samples were vortexed and centrifuged (Centrifuge Eppendorf 5424 R, Eppendorf, Hamburg) at 13000 rpm for 10 min. The extraction step was repeated with an additional 750 µL of 70% methanol, and the resulting supernatants were pooled. Prior to drying, pooled extracts were spiked with internal standards (15 µL of a cocktail solution) (In Supplementary Table S1, Supplementary Table 1). The final concentration of each internal standard in the reconstituted extract is provided in Supplementary Table S1. Finally, extracts were vacuum-dried using a SpeedVap (Eppendorf Concentrator 530, Hamburg, Germany) and stored at -80 °C until further analysis.

2.2.1 UPLC -qTOF -MS analysis

Metabolomic profiling was conducted using an Acquity ultra-high-performance liquid chromatography (UPLC) system coupled to a Synapt XS quadrupole time-of-flight mass spectrometer (Waters, Manchester, UK) equipped with an electrospray ionization interface (ESI) source (Paglia *et al.* 2012, 2014).

Dried metabolite extracts were reconstituted in 1 ml acetonitrile (ACN): water (H_2O) (50:50, v/v), diluted to the same proportion of ACN: H_2O and analyzed. Chromatographic separation was achieved under acidic hydrophilic interaction liquid chromatography (HILIC) using an Acquity amide column (1.7 µm, 2.1 × 150 mm; Waters). Mobile phase A consisted of 100% ACN and mobile phase B consisted of 100% H_2O, both containing 0.1% formic acid. The elution gradient was as follows: 0 min, 99% A; 7 min, 30% A; 7.1 min, 99% A; and 10 min, 99% A. The flow rate was 0.4 mL/min, the column temperature 45 °C, and the injection volume 7.5 µL. A column equilibration period of an additional 4 min at initial gradient conditions (99% A) was applied between injections. The HILIC column was equilibrated according to the manufacturer's instructions injecting at least 30

pool samples to minimize retention time drift prior to sample analysis. In addition, the pooled quality control (QC) samples, prepared by combining aliquots from all biological extracts and procedural blanks processed identically to study sample, were injected periodically throughout the analytical sequence to monitor instrument stability, signal drift, and retention time reproducibility.

All samples were analyzed separately in positive and negative ionization modes. The mass spectrometer was operated at a capillary voltage of 1.5 kV, with the sampling and extraction cones set to 30 and 5 V, respectively. The cone and dissolvent gas flows were 50 and 800 L h^{-1}, respectively, while the source and dissolvent gas temperatures were 120 and 500 °C, respectively. MS spectra were acquired in centroid mode from m/z 50 to 1000 with a scan time of 0.3 s. Leucine enkephalin (2 ng μL^{-1}) was used as lock mass for mass correction (*m/z* 556.2771 and 554.2615 in the positive and negative modes, respectively).

2.2.2 Data processing and metabolite annotation

Raw MassLynx data files acquired in positive and negative ionization modes. Endometabolites were identified by targeted feature extraction based on their m/z and retention times matched to an inhouse reference standard library. Chromatographic peak integration of the metabolites was performed using Targetlynx V4.2 (Waters, Manchester, UK). The integrated peaks were normalized to their closest eluting internal standard. Retention time matching tolerance was set at ± 0.06 min and accurate mass tolerance at 3 ppm for metabolite annotations. Signal-to-noise thresholds used for feature acceptance were set at 5. Features with CV>25 % across pool samples were removed. Metabolite annotations were considered putative unless confirmed using an inhouse database and MS/MS fragmentation spectra (Paglia *et al.* 2014). Features identified solely by accurate mass were considered putatively annotated. Annotation confidence levels followed previously established metabolomics reporting guidelines (Schymanski *et al.* 2014). For a comparative analysis, the MetaboAnalyst 6.0 web application was used to identify the differentially expressed metabolites (DEMs) based on their fold change (≥2 or ≤ 0.5) in comparison to their respective controls and t-test (adjusted p-value > 0.05) (Pang *et al.* 2024).

2.3 Transcriptomic analysis

2.3.1 Iso-Seq library construction and sequencing

After 28 days of exposure, diatom pellets were harvested and sent to BGI Tech Solutions (Hong Kong, China) Genomics for library construction, PacBio ISO sequencing, *de novo*, and initial bioinformatic analysis. Total RNA was extracted using TRIzol reagent, and mRNA was enriched using oligo (dT) -attached magnetic beads. The fragmentation buffer in the ALFA-SEQ RNA library Prep Kit (mCHIP, Guangzhou, China) was added to the mRNA solution to obtain short fragments. Total RNA was reverse transcribed into first-strand cDNA using a

UMI-based PCR cDNA Synthesis kit. After PCR optimization, large-scale PCR was performed to synthesize the second-strand cDNA. After another large-scale PCR, the DNA was ready for SMRTbell (single-molecule, real-time) template preparation and sequencing on the PacBio Sequel II platform of Gene Denovo Biotechnology. Before sequencing, the cDNA libraries were partially size-selected (>4 kb using BluePippin^{TM}) and pooled with non-size-selected libraries. This ensured that both long and short transcripts were captured in the final sequencing run.

2.3.2 PacBio sequencing data processing and analysis

The quality of the PacBio reads was checked using FastQC (Andrews 2010). The qualified sequencing data produced by Pacific Biosciences (PacBio) Sequel were processed using SMRT Link (v10.1) analysis through reads of insert, classification, and clustering to obtain consensus full-length isoforms.

The circular consensus sequence (CCS) was produced via self-correction, followed by designation into full-length transcript structures of 5' primer, 3'primer, and polyA tail structures (Supplementary Table 1-4). After obtaining the CCS sequences, the primer sequences were mapped to the CCS sequences, and an in-house written script was used to detect primer sequences at both ends of the CCS sequences and their orientations. UMI sequences were extracted according to the positions of the polyA tails and 3' primer sequences. Reads of inserts generated from SMRT cell cDNA molecules, by removing cDNA primers and polyA sequences from reads, and then reads of inserts classified into full-length, chimeric, and non-chimeric reads. Finally, only full-length non-chimeric reads were used in subsequent analysis (Supplementary Table 5-6).

This module predicts *de novo* consensus isoforms from classified reads of the insert using the ICE (interactive clustering and error correction) algorithm, then polishes the predicted consensus isoforms using Quiver, and classifies the polished isoforms into high QV or low QV isoforms based on user-specified criteria. The default minimum Quiver accuracy needed to classify an isoform as high quality is 0.99 for libraries below 3 K. For libraries between 3-6 K, the minimum Quiver accuracy was set to 0.98. For libraries between 5 and 10 K, the minimum Quiver accuracy was set to 0.95.

2.3.3 Isoform duplication and quantification of expression

High-quality isoforms were obtained for each sample after SMRT analysis. The samples were merged for further clustering and redundancy analysis to obtain the final unique isoform sequence. Isoform expression levels were estimated based on the number of full-length non-chimeric (FLNC) reads (circular consensus sequences, CCS) supporting each isoform. Expression counts were normalized according to total sample counts, and FPKM (fragments per kilobase of transcript per million mapped reads) values were calculated by the BGI PacBio

Iso-Seq pipeline. After clustering and redundancy removal using CD-HIT, the number of CCS reads associated with each non-redundant isoform was counted and used as a measure of expression abundance.

Differential expression analysis between control and PFAS-treated samples was performed using a Poisson distribution-based method (PoissonDis), which models read counts as discrete random variables (Audic and Claverie 1997). For each isoform, the number of reads observed in the two samples was compared under the assumption that read counts follow a Poisson distribution with equal expectation under the null hypothesis of no differential expression. The probability of observing the difference in read counts between samples was calculated based on the total number of mapped reads in each sample. P-values were adjusted using the false discovery rate (FDR) method. Isoforms with a fold change ≥ 2 and an FDR ≤ 0.001 were considered as differentially expressed genes (DEGs). Finally, the differentially expressed genes (DEGs)`across samples were detected using PossionDis algorithm for DEG detection (Audic and Claverie 1997), applying of logFC ≥ 2, and p- value ≤ 0.001, and in-depth clustering and functional enrichment analyses were performed. BUSCO (benchmarking universal single-copy orthologs) genes based on conservative and universal single-copy orthologs were selected from OrthoDB to assess transcriptome integrity.

Because biological replicates were not included in the Iso-Seq, the Poisson-based method does not account for biological variability. Therefore, the identified DEGs should be interpreted as candidate differentially expressed isoforms rather than statistically definitive results. Consequently, qRT-PCR was performed on randomly selected isoforms to validate the gene expression pattern derived from RNA sequencing (Supplementary Table 9). First-strand cDNA was synthesized using the SuperScript™ IV VILO™ master mix (Invitrogen) according to the manufacturer's protocol. PowerUp™ SYBR™ Green master mix (applied biosystems). The qRT-PCR was carried out on CFX Connect™ Real-Time PCR system (Bio Rad, Hercules, CA, USA) and obtained Ct (cycle threshold) values were analysed using the $2^{-\Delta\Delta CT}$ method (Schmittgen and Livak 2008). qRT-PCR results were consistent with the expression patterns resulting from RNA-seq data, confirming these genes expression patterns in PFAS-treated samples vs. their controls. Thereby, the accuracy and robustness of our transcriptome sequence analysis were confirmed.

2.3.4 Transcripts function annotation

Transcripts were annotated with the Pfam (v14.6) (Finn *et al.* 2016) using hmmscan. Blastn (v2.2.23) (Altschul *et al.* 1990) was used to search against the NCBI nucleotide NT database, and Diamond (v0.8.31) to annotate transcripts with the NCBI non-redundant protein (NR), KOG (Koonin *et al.* 2004), KEGG (Kanehisa and Goto 2000), and SwissProt (Boeckmann *et al.* 2003) databases

(Supplementary doc 2 and 3). We used GO annotation based on Blast2GO (v2.5.0) (Conesa *et al.* 2005) and NR annotation results. More information about all workflows is provided in Supporting Information I, and all other sequence analyses and quality checks were performed according to previous literature (Shi *et al.* 2024, Zhuo-Xing Shi *et al.* 2024). The GO and KEGG enrichment analysis were performed in R using hypergeometric testing implemented through the clusterProfiler package (version 3.18.1), referencing the studied functional annotations file (Supplementary doc 2).

3.0 Results

3.1 Overview of omics responses in both species

In both diatom species studied, PFAS exposure caused consistent yet contrasting changes in their metabolomic and transcriptomic profiles (Figure 1 - 3). In *C. closterium*, targeted metabolomics revealed pervasive depletion of central metabolite pools, including amino acids, TCA intermediates, soluble sugars, and nucleotides, while the transcriptomic response was comparatively modest and primarily related to ABC transporters and the pentose phosphate pathway (Supplementary doc 2 and 3).

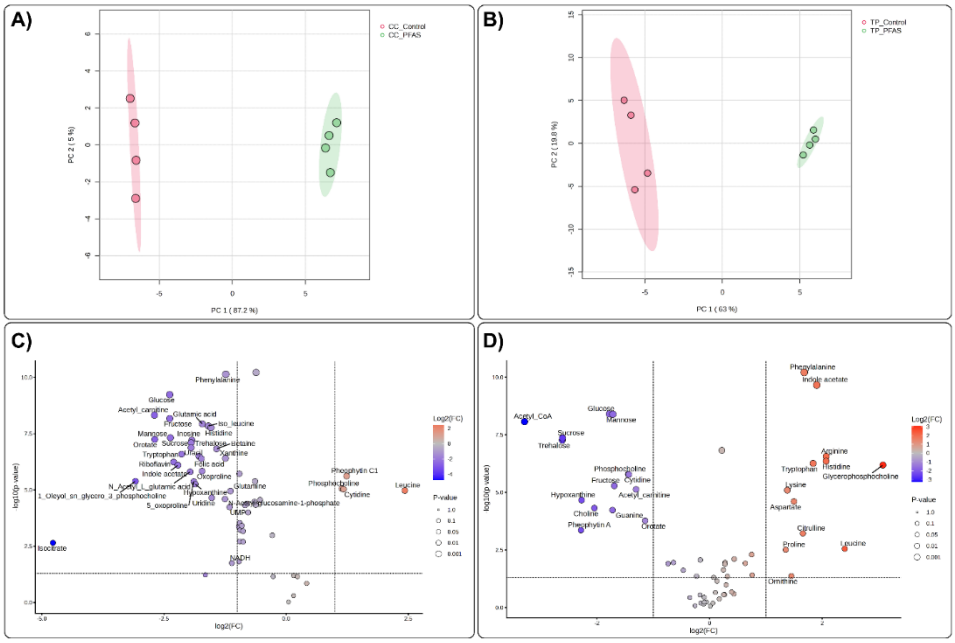

Figure 1: PCA score plots illustrating clear separation between control and PFAS-treated samples for A) *C. closterium,* B) *T. pseudonana*), with ellipses representing group confidence intervals and percentages indicating the variance explained by each principal component. Endometabolite changes in response to PFAS exposure shown in volcano plots: C) *C. closterium* and D) *T. pseudonana*),

revealing differentially accumulated endometabolites in red circles and repressed ones in purple circles, with log2 fold change plotted against log10 (p value); color indicates direction and magnitude change, and point size reflects statistical significance.

In *T. pseudonana*, metabolite pools were more selectively reconfigured, aromatic and compatible amino acids, glycerophosphocholine, and carnitine accumulated, while acetyl-CoA and several nucleotide bases declined, accompanied by broad transcriptional activation of central carbon metabolism, peroxisomal β-oxidation, secondary metabolism, and photosynthesis, together with strong repression of nitrogen acquisition and ribosomal genes.

3.2 Endometabolome changes in response to PFAS exposure

Targeted metabolite profiling identified 59 endometabolites categorized into amino acids and derivatives, carbohydrates, nucleotides, organic acids, and other categories. Metabolites are reported as normalized peak areas relative to internal standards and are interpreted as relative concentration changes rather than absolute cellular quotas. PFAS exposure led to significant changes in both species compared to their controls, as shown by clear separation in the PCA plots after 28 days (Figure 2A-D). PC1 explained 87.2% and 63% of the total variance in *C. closterium* and *T. pseudonana*, respectively, and primarily drove treatment separation, while PC2 accounted for 5% and 19.8% of the variance. Volcano plots ($log_2FC \geq 1$ or ≤ 0.5, adjusted $p < 0.05$) showed that 58% of metabolites were significantly dysregulated in *C. closterium* (4 up, 30 down) and 44% in *T. pseudonana* (12 up, 14 down) (Figure 2C, D).

3.2.1 *Cylindrotheca closterium*

In *C. closterium,* more proteinogenic amino acids (phenylalanine, histidine, tryptophan, glutamic acid, valine, and threonine) were significantly lower in PFAS-treated cells ($log_2FC \sim -1$ to -2.5). Soluble sugars, including glucose, fructose, and mannose ($log_2FC \sim -2.3$), as well as sucrose and trehalose ($log_2FC \sim -2$), were depleted. Nucleotide pool members (UMP, AMP, hypoxanthine, inosine, uridine, adenine, adenosine, guanine, cytidine, uracil, and orotate) tended to be lower in PFAS-exposed cells. Despite these decreases in end-point sugars, several intermediate glycolytic metabolites slightly increased but not FDR-significant, suggesting that reduced sugar pools are not driven by a simple block in mid-glycolysis (Figure 2).

Several measured osmolytes, including betaine, carnitine, and acetyl-carnitine, as well as folic acid and riboflavin, also decreased in *C. closterium*, indicating perturbations of energy homeostasis and one-carbon/redox metabolism. Depletion of folate is therefore consistent with reduced biomass production, while decreased riboflavin is indicative of chloroplast stress, because riboflavin biosynthesis in

plants and algae occurs in the plastids. We note that our targeted panel covers a defined set of central osmolytes, including betaine, carnitine, acetyl-carnitine, and compatible amino acids such as proline, but does not comprehensively cover all known algal osmolytes (e.g., DMSP, homarine, and polyols). Therefore, decreases in measured osmolytes could be partially offset by unmeasured compatible solutes, and this possibility should be considered when interpreting osmolyte-related responses. Consistent with the broad metabolite depletion, *C. closterium* accumulated phosphocholine, a product of membrane breakdown and choline recycling, suggesting that PFAS exposure simultaneously impairs both biosynthetic capacity and membrane integrity.

3.2.2 Thalassiosira pseudonana

In contrast, *T. pseudonana* accumulated aromatic and essential amino acids and showed a strong increase in glycerophosphocholine under PFAS exposure (Figure 2). Ornithine, arginine, and citrulline were upregulated, indicating redistribution of nitrogen and assimilation capacity. Elevated proline and tryptophan levels, alongside decreased phenylalanine and tyrosine (precursors for carotenoid pigments) (Figure 2). Whereas *C. closterium* accumulates phosphocholine, *T. pseudonana* accumulates glycerophosphocholine and carnitine, a pattern consistent with a shift towards membrane remodeling via increased fatty acid beta-oxidation rather than membrane breakdown; glycerophosphocholine can serve as a precursor for rebuilding phosphocholine.

Sugars and nucleotide bases (hypoxanthine, guanine, cytidine, and orotate) were significantly downregulated ($\log_2$FC ~ -1.5 to -2) in *T. pseudonana*, indicating stress on nucleotide metabolism. *T. pseudonana* maintained TCA intermediates somewhat better than *C. closterium,* but showed depletion of acetyl-CoA. As with *C. closterium*, interpretations of osmolyte changes in *T. pseudonana* are constrained by the coverage of our targeted panel; further untargeted metabolomics would be needed to fully characterize the osmolyte landscape**.**

3.3 Transcriptional reprogramming reveals disruption of energy and metabolic homeostasis

3.*3.1 Transcriptome-wide overview and pathway enrichment*

Full-length transcriptome sequencing of *T. pseudonana* resulted in 125,793 transcripts isoforms. Differential expression analysis identified 3,096 significantly differentially expressed transcripts (hereafter referred to as DEGs) ($|\log_2\text{FoldChange}| \geq 1$ and FDR ≤ 0.001) in the PFAS-treated cultures relative to the *T. pseudonana* control. Among the differentially DEGs, 1,823 were upregulated and 1,273 were downregulated (Figure 3A).

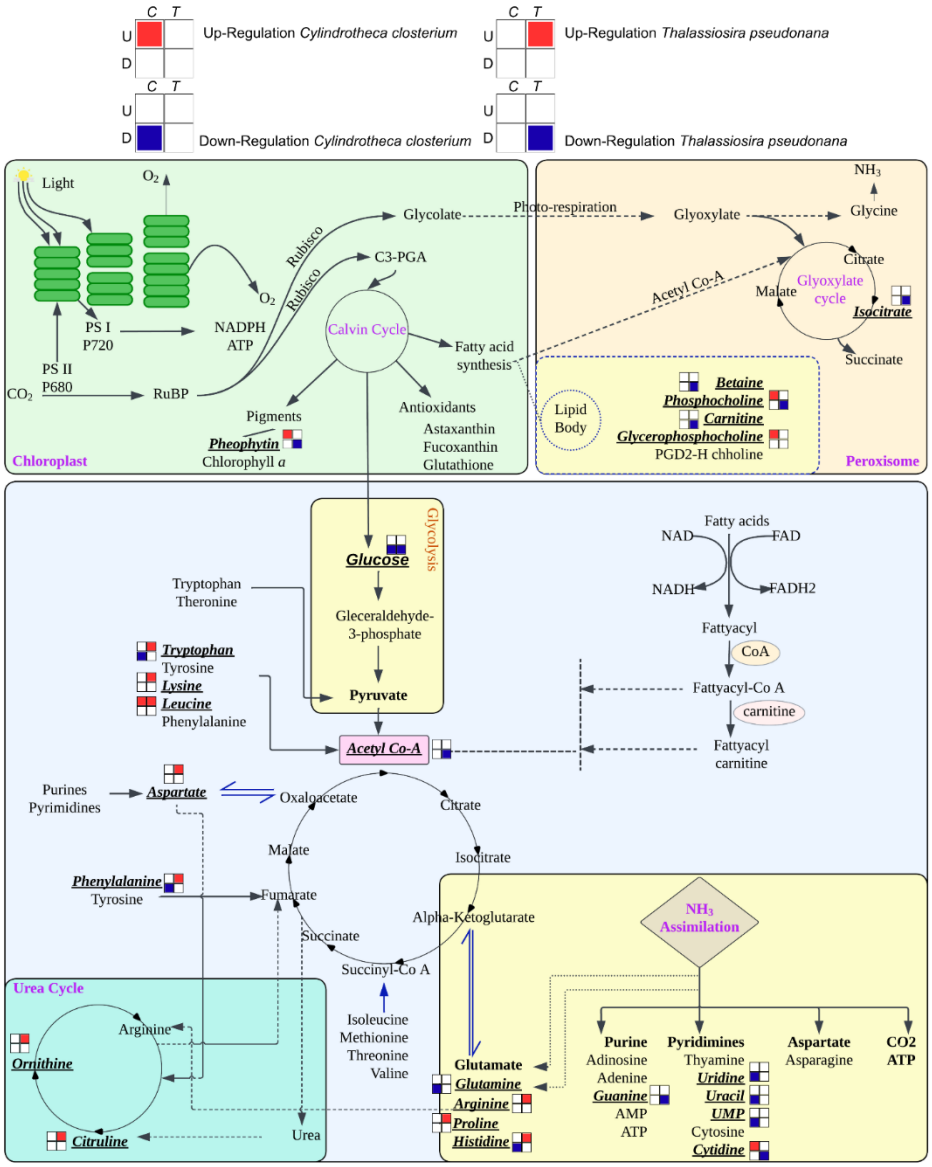

Figure 2: Integrated metabolic map showing species-specific metabolite regulation in *Thalassiosira pseudonana* and *Cylindrotheca closterium.* The diagram summarizes the key metabolic pathways of carbon, lipid, and nitrogen across the chloroplast, peroxisome, mitochondria, cytosol, and urea cycle. Colored squares indicate species, with the left boxes for *C. closterium* and the right-side boxes for *T. pseudonana,* with red denoting upregulation and purple denoting downregulation under PFAS exposure. Also, the respective metabolites marked in the panel were underlined and bolded in font.

KEGG annotation hits resulted 40,047 isoforms in *T. pseudonana* (Supplementary doc 2) and among 923 significant DEGs enriched into 92 pathways. However, according to the adjusted p-values (q-values) < 0.05, only 17 pathways were enriched with a higher number of DEGs. Another 10 pathways with borderline trends (q-value < 0.0506) were also studied because they were biologically important (Figure 3B).

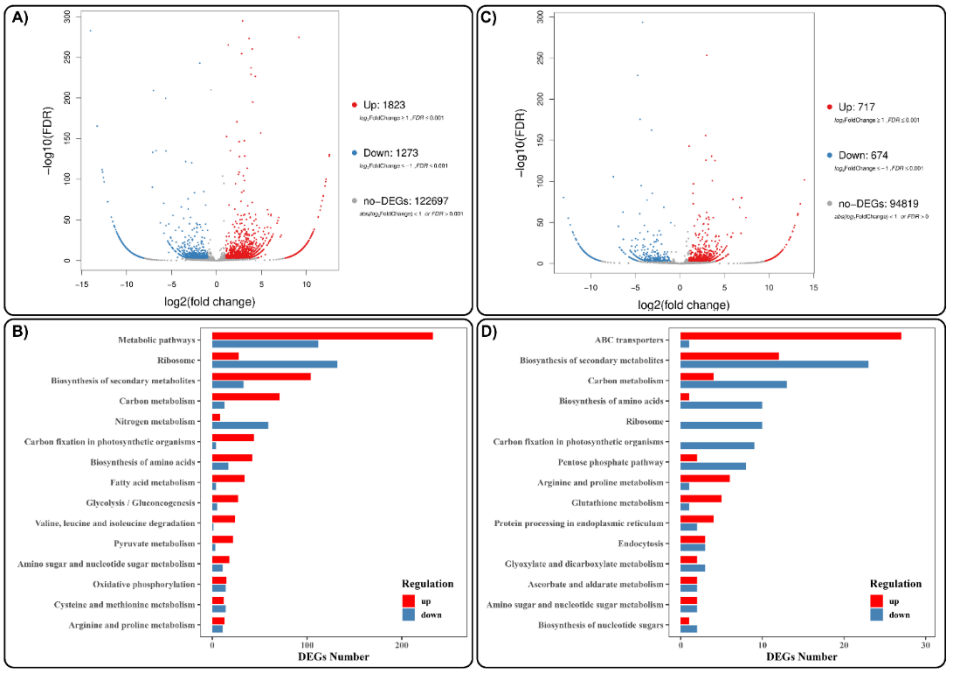

Figure 3: Differential gene expression (DEGs) and functional enrichment analysis of the studied diatom species. In the volcano plots A) & C), each dot represents a gene, plotted as $\log_2$(fold change) on the x-axis and $-\log_{10}$(FDR) on the y-axis. Red dots indicate significantly upregulated genes ($\log_2FC \geq 1$, FDR $\leq$ 0.001; n = 717), blue dots indicate significantly downregulated genes ($\log_2FC \leq -1$, FDR $\leq$ 0.001; n = 674), and gray dots represent non-differentially expressed genes (n = 94,819). B) & D) Directionality of differential expression across the enriched KEGG pathways. Bar plots summarize the number of upregulated (red) and downregulated (blue) DEGs within each significantly enriched KEGG pathway. A) and B): DEGs between classification between TP_C (*Thalassiosira pseudonana*_ control) and TP_P (*Thalassiosira pseudonana*_ PFAS treated sample), and C) and D): CC_C (*Cylindrotheca closterium*_ control) and CC_P (*Cylindrotheca closterium*_ PFAS treated sample).

In *C. closterium,* 9, 6210 isoforms were annotated, with 717 upregulated and 674 downregulated (Figure 3C). In contrast to *T. pseudonana*, *C. closterium* showed fewer significantly enriched pathways, with 193 significant DEGs - all associated to 55 annotated KEGG pathways (Supplementary doc 3). Among these, two KEGG pathways showed statistically significant DEGs enrichment following FDR correction (adjusted p-value < 0.05) (Figure 3D). Notably, isoforms associated with ABC transporters were predominantly upregulated (27 up, 1 down), whereas several pentose phosphate pathway-associated isoforms were downregulated (2 up, 8 down) (Supplementary doc 3). In addition, enriched pathways included carbon fixation in photosynthetic organisms, carbon metabolism, arginine and proline metabolism, and ubiquinone and other terpenoid-quinone biosynthesis pathways.

The KEGG bar plot for *T. pseudonana* shows that PFAS exposure primarily affects broad metabolic pathways, central carbon activation of energy (71 up, 6 down), secondary metabolites (104 up, 33 down), membrane remodelling (34 up, 4 down), peroxisome (16 up, 3 down), photosynthesis (20 up), signalling and stress (86 up, 77 down), and xenobiotic genes (25 up, 11 down), while translation (28 up, 132 down), nitrogen metabolism (8 up, 59 down), and ER-degradation routes were considerably repressed (Figure 3B, and Figure 4A). The GO bar plots further summarized the same DEGs at a higher level of functional annotation (Supplementary Fig. 3).

GO enrichment analysis of candidate DEGs revealed a strong enrichment of biological processes associated with nitrate metabolism, nitrate assimilation, and reactive nitrogen species metabolism, suggesting substantial transcriptional adjustments in nitrogen utilization and redox-related metabolic functions under long-term PFAS exposure. Enriched molecular functions included oxidoreductase activities linked to NAD/NADP-dependent reactions, transporter-associated functions, and structural constituents of ribosomes, including potential alterations in oxidative stress regulation, membrane-associated transport, and translational processes (Figure 4 A-B). Stress management is supported by ATP-dependent activities, transporter functions, antioxidant activity, and protein-folding chaperones, which together maintain energy balance, redox homeostasis, and proteome integrity in cells.

3.4 *Key metabolic pathway regulations in T. pseudonana*

3.4.1 *Coordinated photosystem repair sustain energy production under PFAS stress*

Glycolysis (27 up, 5 down), carbon metabolism (71 up, 13 down), pyruvate metabolism (22 up, 3 down), TCA (11 up, 2 down), and propanoate metabolism (18 up, 1 down) (xy) were biased toward upregulation (Figures 3B). PFAS exposure led to the upregulation of the D1 protein in photosystem II, PsbA, and MSP proteins (PsbO, Psb27, and Psb28), and the light-harvesting chlorophyll

(Lhc) protein complex genes encoding Lhca1, Lhca4, Lhca5, Lhcb2, and Lhcb4 (Figure 5A).

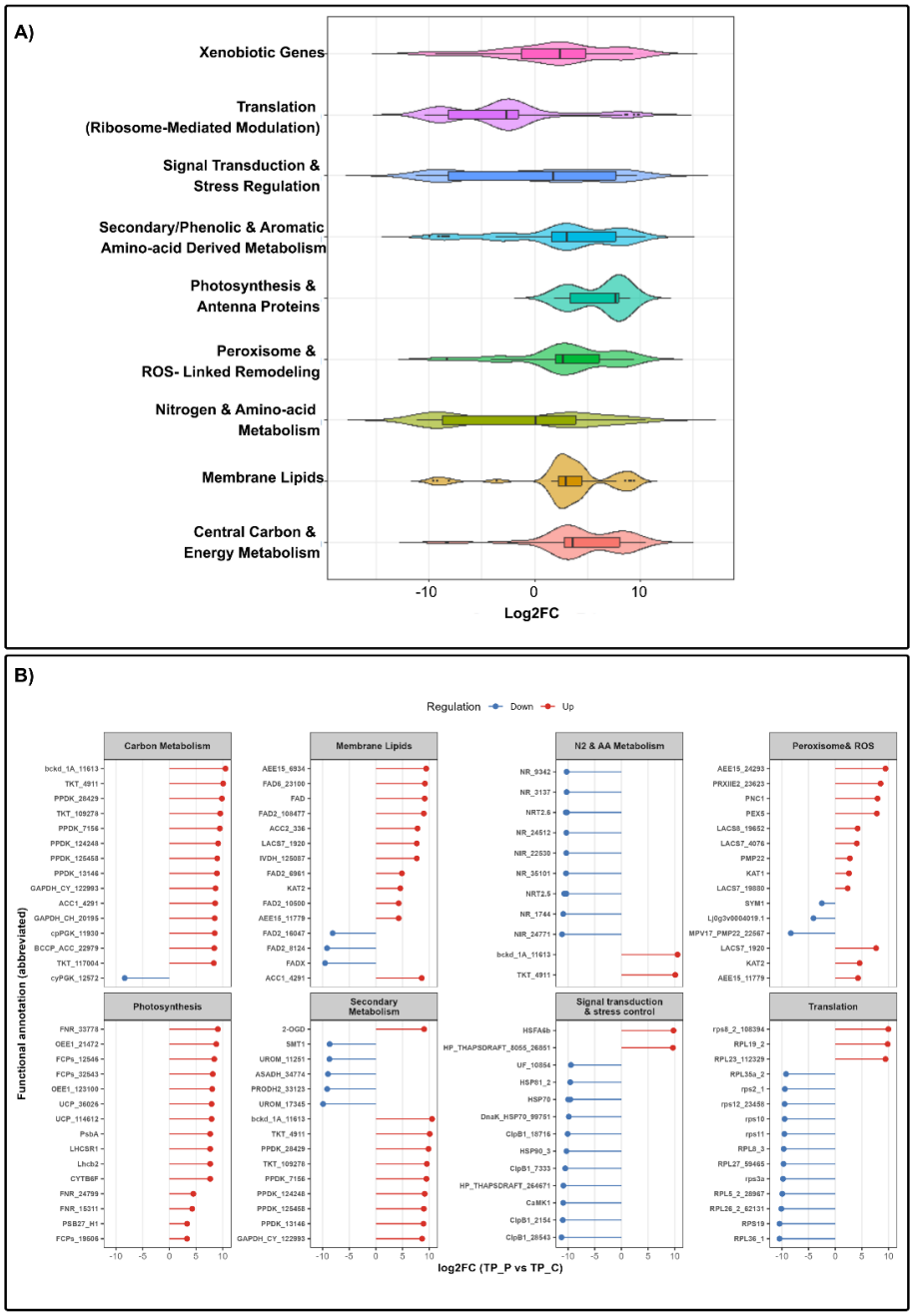

Figure 4: Summary of the distribution of DEGs in *T. pseudonana* among the key functional categories in terms of their log2 fold changes. A) The categories in the

violin plots show the predominant metabolic groups and their reprogramming, as indicated by log2FC. Translation and nitrogen metabolism-related genes were slightly centred on the negative side, suggesting a tendency toward repression relative to other stress-responsive groups. B) Differential regulation of selected key genes across major metabolic and stress response pathways. The plot shows log2 fold changes for individual genes grouped by functional annotation, including carbon, lipid, and nitrogen metabolism, photosynthesis, ROS handling, signal transduction, stress management, and translation (ribosome modulation). Abbreviations and details of panel B are provided in the supplementary doc 4.

This pattern indicates compensatory synthesis and repair of PSII and associated antenna complexes to prevent extensive chloroplast damage under PFAS-induced photo-inhibitory stress. Consistent with this, increased levels of chlorophyll *a* and pheophytin *a* were detected in both metabolomic analysis, and phytochemical screening revealed slightly decreased PSII activity (Arulananthan et al., 2025b, Supplementary Figure 5).

The upregulation of key Calvin cycle and glycolytic interface enzymes, including transketolase (TKT) and glyceraldehyde-3-phosphate dehydrogenase (GAPDH), coupled with downregulation of pyruvate dehydrogenase (PDH) components, points to a bottleneck in pyruvate-to-acetyl-CoA conversion, consistent with metabolomic evidence of acetyl-CoA depletion. Pyruvate phosphate dikinase (PPDK), GAPDH, PGK, isocitrate lyase, and propanoate-cycle enzymes were activated (log_2FC ~2 to 8); the very high average induction of TKT and PPDK (log_2FC ~8 to 9.5) indicates strong rerouting of carbon through the pentose phosphate pathway and flexible PEP/pyruvate cycling (Figure 5C). Upregulated GAPDH, PGK, and TCA/glyoxylate components sustained glycolytic/TCA flux to provide energy and carbon skeletons, enabling diatoms to maintain basal metabolism and feed secondary and repair pathways (Figure 5B and C).

3.4.2 *Membrane remodeling and peroxisomal β-oxidation as a PFAS hallmark*

Fatty acid metabolism and biosynthesis of unsaturated fatty acids were dominated by upregulation (34 up, 4 down, and 17 up, 4 down, respectively), and the peroxisome pathway included mostly upregulated genes (16 up, 3 down) (Figure 3-4). Many genes annotated under fatty acid biosynthesis are significantly upregulated, namely FabF (3-oxoacyl-[acyl-carrier-protein] synthase), FabG3-oxoacyl-[acyl-carrier-protein] reductase, MECR (mitochondrial enoyl-3-oxoacyl-[acyl-carrier-protein] reductase, acetyl-CoA carboxylase1), long-chain acyl-CoA synthetases (ACS), and elongation of very long-chain fatty acids (ELOV) (Figure 5B, D).

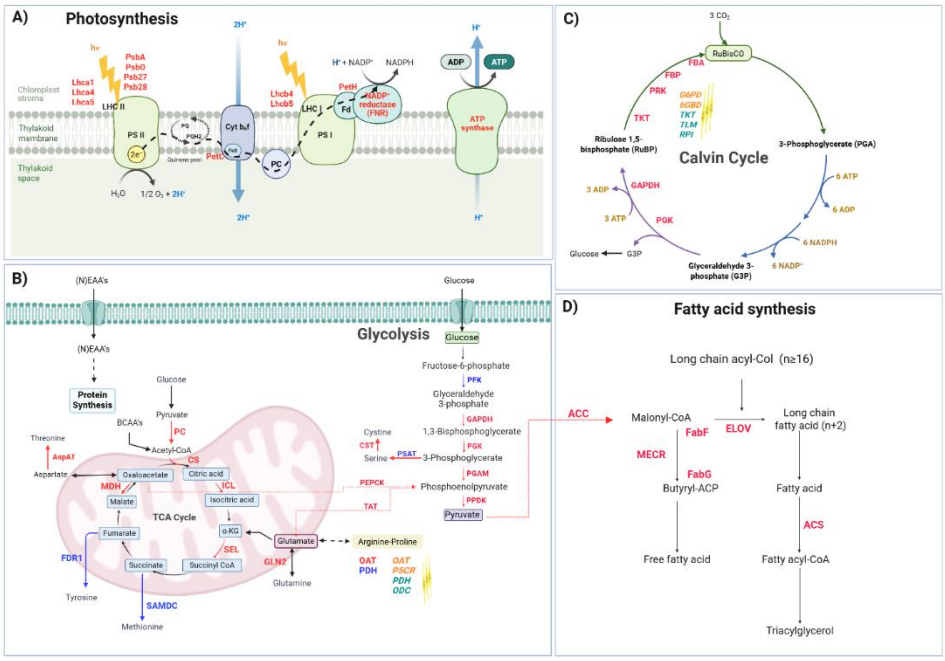

Figure 5: Schematic diagram of KEGG-based pathway analysis showing the key responses and mechanisms of *T. pseudonana* under PFAS exposure. This overview highlights the coordinated pathway-level responses underlying gene expression reprogramming in diatoms exposed to PFAS: A)-Photosynthesis-related gene expression changes, B) key gene changes in the glycolytic pathway, C) Calvin cycle related gene expression changes, and D) Fatty acid synthesis related gene expression changes. The differential expression is indicated with red font (upregulation) and blue font (downregulation) for *T. pseudonana*. There are a few places in the diagram that show the DEGs of *C. closterium* marked along with its pennate shape in yellow mark, and the fonts are in orange (upregulation) and green (downregulation).

Lhca1, Lhca4, Lhca5- light harvesting chlorophyll *a/c* binding protein complex(Lhc); PsbA- Photosystem II protein D1; PsbO- Oxygen-evolving enhancer protein 1; Psb 27-Psb28-Photosystem II repair protein; PetC- cytochrome b6-f complex iron-sulfur subunit; FNR- ferredoxin-NADP+ reductase; PrtH -Ferredoxin NADP+ reductase. **B).** AspAT-aspartate aminotransferase; MDH- malate dehydrogenase; PC-pyruvate carboxylase; CS-citrate synthase; ICL-isocitrate lyase; SEL-succinyl-CoA ligase; GLN2/GS- Glutamine synthetase(down in TP); OAT-ornithine aminotransferase; PDH-Proline dehydrogenase (down in TP and CC); ODC- Ornithine decarboxylase (down in TP, CC), OCDA- ornithine cyclodeaminase, OTA-ornithine transaminase (up in CC); TAT-Tyrosine aminotransferase; PEPCK- phosphoenolpyruvate carboxykinase; PC-pyruvate carboxylase; TKT-transketolose, CST-cysteine synthase; PSAT-Phosphoserine aminotransferase 1 (down in TP); PFK- phosphofructokinase; GAPDH- glyceraldehyde-

3-phosphate dehydrogenase; PGK- phosphoglycerate kinase; PGAM -phosphoglycerate mutase; PPDK - Pyruvate phosphate dikinase **C).** FBA -fructose-bisphosphate aldolase; FBP - fructose-1–6-bisphosphatase; PRK- Phosphoribulokinase; TKT – transketolose. G6PD -glucose-6-phosphate dehydrogenase; 6GBD -6-phosphogluconate dehydrogenase; TKT – transketolase; TLM – transketolose like enzyme; RPI- ribose-5-phosphate isomerase; GAPDH ; glyceraldehyde 3-phosphate dehydrogenase; PGK - phosphoglycerate kinase. **D).** ACC -Acetyl-CoA carboxylases; MECR -mitochondrial enoyl-3-oxoacyl-[acyl-carrier-protein; FabF -3-oxoacyl-[acyl-carrier-protein] synthase; FabG - 3-oxoacyl-[acyl-carrier-protein] reductase; ELOV -elongation of long-chain fatty acids; ACS- long-chain acyl-CoA synthetases.

Multiple FAD2-type Δ12 fatty acid desaturases upregulated ($log_2FC \sim 2.6$ to 9.2), alongside acyl-CoA C20 Δ5 desaturases (ACCs), ADS3-type plastid desaturases ($log_2FC \sim 3$), peroxisomal 3-ketoacyl-CoA thiolases (KAT1/2) ($log_2FC \sim 2$ to 4.6), and peroxisomal acyl-CoA oxidase 4 (ACX4, $log_2FC \sim 2$) (Figure 6A). Fatty acid desaturation and peroxisomal β-oxidation components (PEX5, PEX7, PTS1/2, ACX4, ACAA1), and peroxidoxin-2E-2 were upregulated, while cytosolic APX1 and 2-Cys peroxiredoxin strongly downregulated ($log_2FC \sim -9.5$ to -3.6).

Furthermore, under the peroxisome and ROS metabolism-related annotation, the upregulation of glutamate-cysteine ligase and cysteine synthase indicates a reinforcement of glutathione biosynthesis. Strongly upregulated genes encoding chitin synthases and chitinases ($log_2FC\sim 2$ to 9), UDP-glucuronate 4-epimerases (GAE family, $log_2FC \sim 1.3$ to 8.7), and several predicted peroxisomal proteins and glucosamine-fructose-6-phosphate amidotransferase (glmS) showed both up- and downregulation (Supplementary doc 2).

3.4.3 *Nitrogen assimilation and amino acid metabolism*

PFAS exposure in *T. pseudonana* induces coordinated reprogramming of nitrogen metabolism toward nitrogen conservation and internal recycling. Of the 67 DEGs, 59 genes were downregulated, and eight were upregulated. All detected nitrate transporter (Nrt) genes were strongly downregulated (log2FC -8.3 to -10.7), nitrate reductase (NR), was predominantly repressed (17 of 18 isoforms, log_2FC -3.6 to -10.9), and downstream NIT-6-amino acid-associated and nitrite reductase NirA were strongly downregulated (log_2FC -8 to -11) (Figure 6B). In contrast, enzymes associated with intracellular ammonium re-assimilation are also activated. Several isoforms encoding glutamate dehydrogenase (GDH) were strongly upregulated (log_2FC +4.2 to +9.6), and glutamate synthase (GOGAT) displayed isoform-specific regulation, with one isoform strongly induced and another repressed, consistent with selective remodelling rather than complete shutdown of the GS-GOGAT cycle (Figure 6B).

Biosynthesis of amino acid-related genes was largely upregulated (42 up, 17 down). Arginine and proline metabolism both contain a mixture of highly induced and strongly repressed genes, particularly at the polyamine/proline interface of the metabolic pathway. The combination of strong downregulation of nitrate reduction, glutamate synthase (GLN2), GOGAT, phosphoserine aminotransferase (PSAT) (log2FC~ -3 to -9), POX2 (log2FC~ -9), ODC (log2FC~ -3 to -8), and SAMDC (log_2FC~ -8 to -10), occurred alongside upregulation of OAT (log_2FC~ 2 to 5), cysteine synthase (log2FC~ 4 to 8), aspartate aminotransferase, and tyrosine aminotransferase (TAT) (log_2FC~ 2 to 5) (Figure 5B & C).

Furthermore, ER-associated degradation and ubiquitin system-related genes (CDC48, cullins, ubiquitin, and vacuolar sorting receptors) were upregulated, indicating enhanced protein turnover and quality control. Multiple HSP70 and HSP90 (BiP, HSP81/90) and chloroplast HSP90-5 were strongly downregulated, while a subset of small ER-localized HSPs was upregulated, indicating a qualitative modification of chaperone networks.

3.4.4 *Secondary metabolites, aromatic amino acids derived and redox metabolism*

DEGs associated with the biosynthesis of secondary metabolites were dominated by strong upregulation (104 up, 33 down) with a smaller set of downregulated polyamine and nucleotide metabolism genes. Multiple transketolase (TKT) and PPDK genes showed consistently high, positive log2FC (~8 to 10). PFAS exposure activated Ca^{2+}-and lipid-derived signaling networks, with upregulation of CIPK, CPK, PLC, PKC-like kinases, and the full MAPK cascade (MAPKKK, MAPKK, and MAPK) (Figure 6C). 2OG-Fe(II) oxygenase and zeta-carotene desaturase/amine oxidoreductase showed log2FC ~9, while cysteine synthase and sulfate adenyltransferases reached log2FC ~7.5 to 8.0. Phenylalanine-tyrosine-linked TKT genes, TATs, and METK were considerably upregulated (log2FC ~2.5). Downregulation of uroporphyrinogen-III C-methyltransferase (cobA) (log2FC ~ -9 to -10), and cycloartenol and 24-methylenesterol methyltransferases (SMT1/3) (log2FC -3.5 to -9) were recorded.

3.4.5 *Translation is suppressed while protein quality control is enhanced*

In *T. pseudonana*, KEGG and GO analyses revealed that translational reprogramming is a major component of the PFAS stress response in this species. The ribosome pathway contained 160 significantly changed DEGs: 132 ribosomal proteins were predominantly downregulated (many log_2FC < -3) and 28 were upregulated, including ubiquitin-fusion ribosomal subunits, the largest count of any KEGG category in *T. pseudonana* (Figures 5 and 7D). Cytosolic 80S ribosomes showed broad transcriptional activation, with many 40S (S13a, S8, S9, S12, S13, -15a, S27a) and 60S (L4, L5, L10, L18, L19, L21, L23, L27, L28, L34, L36, L37a, PO, L40) proteins highly induced. Ubiquitin-ribosome fusion proteins

Ub-S27 and Ub-L40 were strongly induced, consistent with ubiquitin-dependent quality control of nascent chains. In contrast, plastid and mitochondrial ribosomal proteins (L2, L5, L10, L16, S12, L14, L26, L27, S19, S21) were among the most strongly repressed transcripts, indicating a coordinated downshift of organellar translational machinery (Figure 6D).

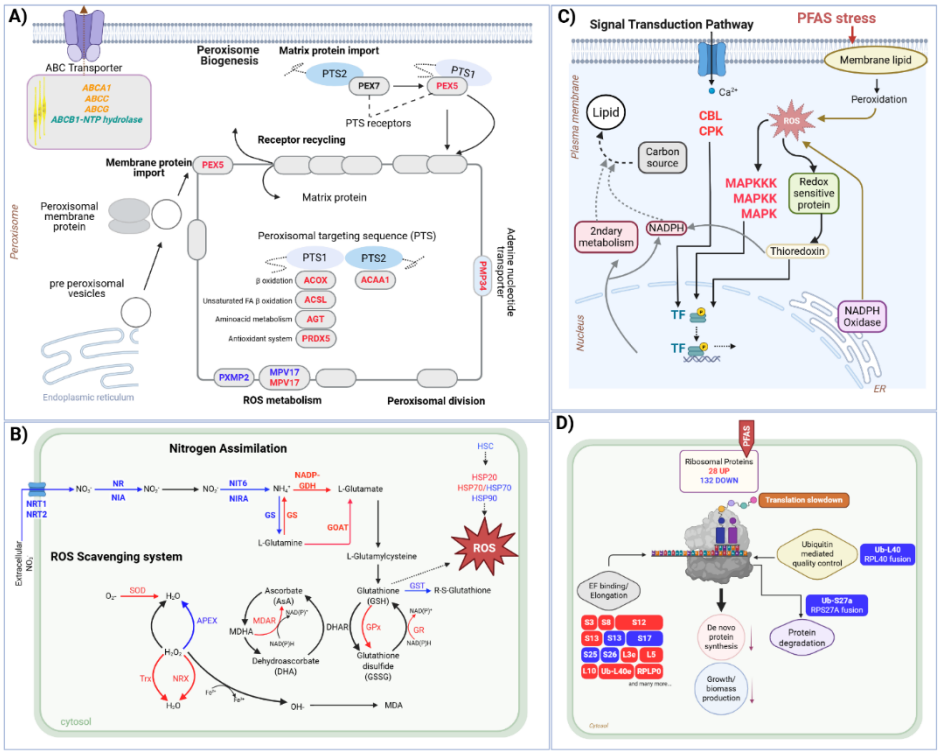

Figure 6: Schematic diagrams of KEGG-based pathway analysis showing the key responses and mechanisms of *T. pseudonana* under PFAS exposure. A). ATP caste, peroxisome-mediated stress response, and protein regulation, B). Nitrogen assimilation and ROS scavenging system, C). Secondary metabolite synthesis and signal transduction. D). Ribosomal translation. Differential expression is indicated by red font (upregulation) and blue font (downregulation) for *T. pseudonana*. A few places in the diagram show the DEGs of *C. closterium* marked with a needle-like species mark. The fonts are colored orange (upregulation) and green (downregulation). ABCA1, ABCC, ABCG, ABCB1-NTP hydrolase: ATP binding cassette units; PEX5 -peroxisomal β-oxidation components; ACOX -precursor of hydrogenase glutaryl-coa dehydrogenase (GCD1; ACSL -Long-chain acyl-CoA synthetases (AMP-forming); AGT -alanine-glyoxylate transaminase / serine-glyoxylate transaminase / serine-pyruvate transaminase; PRDX5 -Alkyl hydroperoxide reductase/peroxiredoxin ; PXMP2 – peroxisomal membrane protein ; MPV17 – Peroxisomal membrane protein MPV17 and related proteins; ACAA1 -3-ketoacyl-coa thiolase, mitochondrial. B). NRT1, NRT2- nitrate transporter; NR- nitrate reductase; NIA-

nitrate reductase; NIRA - nitrite reductase-ferredoxin dependent; GS -glutamate synthase; GDH- glutamate dehydrogenase; GOAT- glutamate synthase; SOD- superoxide dismutase; Trx- thioredoxin M-type; NRX -thioredoxin -like; MDA -malondialdehyde; MDAR – monodehydroascorbate reductase; GSH -glutathione; GST -glutathione S-transferase; AsA -reduced ascorbic acid; GPx – glutathione peroxidase; GR- glutathione reductase; ROS -reactive oxygen species; HSC- heat shock protein chaperones; HSP20,70,90 – heat shock proteins. C). MAPKKK - mitogen-activated protein kinase kinase kinase; MAPKK 0mitogen-activated protein kinase kinase; MAPK – mitogen-activated protein kinase; CBL -interacting protein kinase; CPK – Calcium dependent protein kinase. D). S3,8,12,13,17,25,26,26- ribosomal small subunit proteins; L3e, L5,10, - ribosomal large subunit prteins; Ubiquitin ribosome fusion proteins- Ub-L40e; RPLP0; Ub-L40; Ub-S27a; RPS27A; RPL40.

3.5 Key transcriptional responses in *C. closterium*

In contrast to *T. pseudonana,* the DEG set in *C. closterium* was considerably more limited and did not show prominent enrichment of DEGs across metabolic pathways, including ribosome biogenesis and nitrogen metabolism, which showed the largest responses in *T. pseudonana*. The most notable transcriptome reprogramming in *C. closterium* was the broad induction of ATP-binding cassette (ABC cassette), which is consistent with the activation of a multixenobiotic resistance reported under stress (Lauritano *et al.* 2015, Zheng JW *et al.* 2016). The upregulated genes encoded the ABCA1 subfamily, FAD binding domain (log2FC ~ 11), ABCA1-like putative ABC transporter (log2FC ~ 10), ABCA1-like lipid transporter (log2FC ~ 10), ABCC-type multidrug resistance-associated transporters (log2FC~2 to 10), and ABCB/MDR-type exporters (P-glycoprotein-like) (log2FC ~ 9). In contrast, ABCB1-like P-loop NTP-hydrolase was strongly downregulated (log2FC ~ -10.6) (Figure 6A). Arginine-proline metabolism is reprogrammed towards proline accumulation via strong upregulation of ornithine aminotransferase (OAT) (log_2FC ~ 11) genes, which channel arginine/ornithine towards proline and glutamate, and proline-5-carboxylate reductase (P5CR log_2FC ~ 3.6). In parallel, ornithine decarboxylase (OD log_2FC ~ -9.4) was repressed, suggesting reduced flux to polyamines in favor of proline synthesis. Additionally, a set of ubiquinone O-methyltransferases (COQ3-like (log_2FC ~ - 9) indicates suppression of the terminal ubiquinone biosynthesis step (Figure 4, Supplementary doc 3).

Central carbon metabolism was slightly reprogrammed, with repression of the Calvin cycle and pentose shunt rearrangements (Triosephosphate isomerase (TIM) log_2FC ~ -3.2; RPI log_2FC -10.6 to -3.9; Transketolase (TKT) log_2FC ~-3.6) alongside induction of oxidative PPP dehydrogenases glucose-6-phosphate dehydrogenase (G6PD) and 6-phosphogluconate dehydrogenase (6PGD) (both log_2FC ~3). The cell thus redirects carbon through the NADPH-generating oxidative PPP rather than toward glycolytic endpoints, despite the metabolomic depletion of external soluble sugars. Drained TCA intermediate pools and reduced NADH indicate impaired mitochondrial carbon oxidation, while transcriptomic

upregulation of mitochondrial carriers and redox enzymes supports remodelling of respiratory flux. Metabolite depletion of membrane lipids and osmolytes, combined with transcriptomic upregulation of lipid-remodeling enzymes, sterol transporters, and SREBP, suggests active membrane re-engineering, while increased pheophytin C1 and decreased light-harvesting complex transcripts indicate photosynthetic antenna remodeling and partial breakdown. Strongly upregulated redox- and ROS-related enzymes, monodehydroascorbate reductases, FAD-dependent oxidoreductases, Lon protease, and glutathione-related oxidoreductases, indicate that antioxidant systems help maintain redox homeostasis despite declining metabolic pool levels.

4. 0 Discussion

4.1 *Thalassiosira pseudonana*: an active, membrane-centered acclimation strategy

4.1.1 Photosynthesis and central carbon flow

In *T. pseudonana*, PFAS exposure triggered coordinated transcriptional reprogramming of photosynthesis and central carbon metabolism that is robustly supported by the metabolite profiles. The upregulation of PsbA, MSP proteins, fucoxanthin-chlorophyll *a/c* antenna complexes, and LHCSR1-like photoprotective proteins indicates active photosystem repair and antenna reorganization to sustain ATP/NADPH supply while managing PFAS-induced photo-inhibitory stress (Liu *et al.* 2025). This contrasts sharply with PFOS-stressed chlorophytes, where PSI, PSII, LHCs, the cytochrome b6/f complex, and RuBisCO are broadly downregulated (Xue et al., 2022), and with another study testing 100 ng L^{-1} PFOS and GenX that found downregulation of Cytb6/f and PetH alongside upregulation of PsbA, resulting in overall disruption of the photosynthetic unit (Li Y *et al.* 2021). The distinct response observed here may be attributable to the concentration and type of PFAS studied, particularly their differential effects on transmembrane processes and water movement (Wu *et al.* 2025).

Metabolically, maintained TCA intermediates but depleted acetyl-CoA, together with upregulated glycolytic and Calvin cycle genes and downregulated PDH, indicate a bottleneck in pyruvate-to-acetyl-CoA conversion. Strong induction of PPDK and TKT (log_2FC ~8 to 9.5) supports rerouting of carbon through the pentose phosphate pathway to boost NADPH and ATP-efficient anaplerosis for antioxidant regeneration. This elevated carbon flux co-occurs with growth inhibition and oxidative stress, indicating that fixed carbon is preferentially channelled into repair and defence rather than biomass accumulation (Shi *et al.* 2024). Upregulation of TKT and GAPDH also contrasts with PFOS-induced repression of PGK and PRK in chlorophytes, indicating that diatoms maintain RuBP regeneration and triose-phosphate export, analogous to responses observed under silicon starvation (Smith *et al.* 2016).

4.1.2 Nitrogen assimilation, amino acids, and osmolytes

The combined metabolomic and transcriptomic data indicate that PFAS exposure induces a quasi-nitrogen-stress state in *T. pseudonana*, managed through suppression of energetically expensive nitrate assimilation and enhanced internal nitrogen recycling. Near-complete downregulation of all Nrt genes, most NR isoforms, and NirA, alongside upregulation of GDH isoforms and selective GOGAT induction, indicates a switch from external nitrate assimilation to internal ammonium recycling. This mirrors N-saving strategies described under N-starvation in *Phaeodactylum. tricornutum* (Remmers *et al.* 2018) and suggests that PFAS-induced energy stress indirectly activates an N-saving strategy.

Metabolite data reinforce this interpretation, accumulation of ornithine, arginine, citrulline, proline, and tryptophan, alongside decreases in phenylalanine and tyrosine, is consistent with redistribution of nitrogen into compatible solutes and aromatic precursors with antioxidant and photoprotective functions (Li P *et al.* 2020, Li J, Sun, and Li 2022, Yang *et al.* 2024). Repression of ODC and SAMDC alongside upregulation of OAT, cysteine synthase, and TATs points to a deliberate shift away from polyamine-driven proliferation towards stress-tolerant, low-growth reallocation (Ginguay *et al.* 2017).

Repressed proline dehydrogenase favours proline accumulation as a compatible solute and ROS scavenger, while enhanced cysteine synthesis supports glutathione- and thiol-based defences. We note that dissolved inorganic nitrogen concentrations were not measured directly during the exposure period; consequently, we infer nitrogen stress and redistribution from molecular signatures rather than from direct nutrient drawdown measurements. Furthermore, because our targeted metabolomics panel covers only a defined subset of central osmolytes, compensatory contributions from unmeasured osmolytes cannot be entirely ruled out. All cultures were maintained under controlled and identical media and aeration regimes, but systematic treatment-by-treatment measurements of salinity, pH, and temperature were not collected; therefore, subtle abiotic contributions to osmolyte shifts cannot be entirely excluded and should be addressed in future studies.

4.1.3 Membrane remodelling, beta-oxidation, and ROS management

Transcriptional enrichment of fatty acid biosynthesis, desaturation, and peroxisomal pathways, together with metabolomic accumulation of glycerophosphocholine and carnitine, converge on a membrane-centred PFAS stress response in *T. pseudonana*. Strong induction of FabF, FabG, MECR, acetyl-CoA carboxylase, ACS, and ELOV enzymes supports enhanced fatty acid turnover and membrane lipid remodelling (Xie *et al.* 2013). FAD2-type desaturases, peroxisomal ACX4, and KAT1/2 thiolases indicate active peroxisomal beta-oxidation and a shift in ROS detoxification towards

peroxisome-localized H_2O_2 processing (Smith *et al.* 2016). These changes likely reflect both adaptive adjustment of bilayer packing and replacement of peroxidised PUFAs to restore photosynthetic and transport functions under PFAS-induced oxidative stress (Vasilev *et al.* 2022). PFAS as surfactant-like compounds disrupt membrane structure and fluidity (Fitzgerald *et al.* 2018), activating lipid-derived signalling cascades that trigger extensive lipid remodelling and beta-oxidation (Li-Beisson *et al.* 2019, Wang H *et al.* 2020, Liu *et al.* 2025).

Multiple studies have reported elevated ROS, lipid peroxides, and antioxidant enzyme activities in microalgae in the presence of PFAS and other contaminants (Boltes et al., 2012; Li-Beisson et al., 2019; Wang et al., 2023; Yang et al., 2021). *T. pseudonana's* strong induction of peroxiredoxin, thioredoxin, and glutaredoxin systems, ACOX4, and peroxisomal transporters indicates that ROS signalling and detoxification are central to its PFAS response, tightly coupled to lipid turnover (Koletti *et al.* 2025). Upregulation of glutamate-cysteine ligase and cysteine synthase reinforces glutathione biosynthesis, consistent with GPX, GR, and GSH pathways buffering PFAS-induced lipid peroxidation (Chakravarty and Poluri 2025). Coordinated upregulation of chitin synthases, chitinases, and UDP-glucuronate 4-epimerases further implies restructuring of the extracellular matrix as an additional buffer against PFAS-induced oxidative stress (Gu and Bar-Peled 2004, Dong *et al.* 2016).

4.1.4 Secondary metabolite activation and ROS scavenging

Activation of Ca^{2+-} and lipid-derived signalling networks (CIPK, CPK, PLC, PKC, MAPK cascade) suggests that PFAS trigger a membrane- and Ca^{2+}dependent signalling response supporting induction of aromatic and carotenoid biosynthetic genes (Zhang Y *et al.* 2026). Strong induction of 2OG-Fe(II) oxygenase, carotenoid desaturase, and selected isoprenoid enzymes indicates activation of redox-intensive secondary metabolism channelling flux into carotenoids and phenolic derivatives that serve as photo-protectants and ROS scavengers (Wang Y *et al.* 2021, Yang *et al.* 2021). This response is consistent with photoinhibition where ROS-induced damage to photosystems is counterbalanced by carotenoid-mediated quenching and de novo synthesis of photosystem components to maintain photosynthetic capacity (Kim *et al.* 2023).

The coordinated upregulation of aromatic amino acids (TKT-driven supply and TATs) and S-adenosylmethionine-dependent methylation (METK) enables synthesis and modification of aromatic compounds to quench ROS and stabilise membranes (Wang H *et al.* 2020). Repression of tetrapyrrole and sterol branch points (cobA, SMT1/3) potentially indicate reallocation away from growth-oriented pigments towards targeted protective secondary metabolites.

4.1.5 Translation control and protein quality management

In *T. pseudonana*, the coordinated ribosomal response, with 132 mostly organellar ribosomal proteins downregulated and specific cytosolic components and ubiquitin-fusion proteins upregulated, suggests a strategic reallocation of translational resources from plastids and mitochondria to the cytosol, a pattern observed in diatom stress responses more broadly (Remmers *et al.* 2018, Thangaraj *et al.* 2021). Similar transcriptional responses involving oxidative stress management and metabolic acclimation have been reported in many algae-related molecular stress responses (Xue, Gao, and Xu 2022, Shi *et al.* 2024, Flynn *et al.* 2025). This is consistent with PFOA- and polystyrene microplastic-induced translation slowdown aimed at limiting the synthesis of damage-prone proteins while selectively degrading oxidised and misfolded ones (Zhao *et al.* 2024, Chakravarty and Poluri 2025).

ER-associated degradation and ubiquitin-proteasome components were upregulated, while HSP70 and HSP90 were broadly downregulated and a subset of small ER-localised HSPs was induced, indicating qualitative modification of chaperone networks rather than global induction. This coordinated proteostasis response extends the antioxidant narrative from damage repair to damage avoidance and may be particularly important for diatom cells experiencing chronic environmental PFAS exposure.

4.2 *Cylindrotheca closterium:* metabolic depletion and transporter-based defence

4.2.1 Metabolic depletion and central carbon status

In *C. closterium*, PFAS exposure manifests primarily as pervasive depletion of central metabolites rather than broad transcriptional reprogramming, indicating a species less able to buffer PFAS-induced perturbations through metabolic rewiring. Strong decreases in proteinogenic amino acids, soluble sugars, TCA intermediates, nucleotides, and measured osmolytes (betaine, carnitine, acetyl-carnitine, folate, riboflavin) collectively indicate impaired biosynthetic capacity, energy homeostasis, and membrane integrity. These metabolites are important for maintaining mitochondrial beta-oxidation and the acetyl-CoA balance (carnitine system) (Houten and Wanders 2010), for one-carbon metabolism (riboflavin) (Jordan *et al.* 1999). Amino acid depletion is expected to impair protein synthesis and energy transfer (Wang J *et al.* 2024, Zheng X, Qiu, and Li 2026), with valine depletion being particularly relevant given its role in protein folding and structural stability (AL Mughram *et al.* 2023).

Despite the broad metabolite depletion, the cell redirects carbon through NADPH-generating oxidative PPP (G6PD and 6PGD induction) rather than glycolytic endpoints, while transcriptomic upregulation of lipid-remodelling enzymes, sterol transporters, and SREBP indicates that *C. closterium* attempts active membrane re-engineering even as its metabolic reserves are depleted.

Increased pheophytin C1 and decreased light-harvesting complex transcripts indicate photosynthetic antenna remodelling and partial breakdown, and strongly upregulated redox/ROS enzymes suggest that antioxidant systems help maintain redox homeostasis despite declining metabolic pool levels. Together, these patterns imply that *C. closterium* relies on limited NADPH-generating routes and targeted lipid remodelling, with a net drain of central metabolic reserves.

4.2.2 ABC transporter-based xenobiotic defence

The most prominent transcriptional signature in *C. closterium*, is the massive induction of ABC transporter genes across the ABCA, ABCB, ABCC, and ABCG subfamilies, consistent with activation of a multi-xenobiotic resistance (MXR) programme (Lauritano *et al.* 2015, Zheng JW *et al.* 2016). ABCA, ABCC, and ABCG transporters support membrane lipid homeostasis, efflux of oxidative damage products, and chemical defence, and their upregulation reflects an attempt to restore membrane lipid asymmetry and composition under PFAS stress. The selective downregulation of ABCB1-like P-loop NTP-hydrolase (log_2FC ~-10.6) indicates selective remodelling within the ABCB subfamily rather than a uniform response.

4.2.3 Arginine-proline and nitrogen metabolism

In *C. closterium*, arginine-proline metabolism was reprogrammed towards proline accumulation through OAT and P5CR induction with ODC repression, mirroring the proline-based osmolyte strategy in *T. pseudonana* but achieved with far fewer total DEGs and without the broader nitrogen-assimilation reprogramming. COQ3-like suppression further reflects concurrent remodelling of mitochondrial quinone biosynthesis (Beale *et al.* 2022, Shi *et al.* 2024). Whether *C. closterium*'s limited transcriptomic response reflects a genuinely distinct acclimation strategy or a less sensitive response due to fewer annotated genes and lower annotation coverage requires further investigation with fully annotated genome resources.

4.3 Species-specific PFAS strategies: a comparative perspective

The contrasting responses of *T. pseudonana* and *C. closterium,* highlight how different cellular architectures and ecological strategies shape diatom responses to PFAS. *T. pseudonana* (centric, pelagic) deployed active, multi-layered acclimation involving compensatory photosystem repair, carbon flux rerouting, nitrogen recycling, membrane lipid remodelling, and translation slowdown, while sustaining redox homeostasis through peroxisomal beta-oxidation, carotenoid biosynthesis, and glutathione reinforcement. *C. closterium* (pennate, epipelic) relied primarily on transporter-mediated chemical defence (MXR) and targeted proline biosynthesis with limited broader metabolic rewiring and experienced a net drain of central metabolic reserves. This pattern suggests that *T. pseudonana*

may be more physiologically plastic in response to PFAS, while *C. closterium*, may be more vulnerable to metabolic depletion under prolonged exposure. At environmentally relevant concentrations, these species-specific strategies will most probably influence diatom community composition in PFAS-contaminated marine environments.

The integration of metabolomics and transcriptomics provided convergent evidence for key responses, including the acetyl-CoA bottleneck, the quasi-N-stress state, membrane remodelling, and proline-based osmolyte responses, that would not have been apparent from either dataset alone. This multi-omic approach revealed the broad scope of *T. pseudonana*'s cellular reprogramming and the metabolically draining nature of *C. closterium*'s constrained response, illustrating the value of combined omics analyses for characterising PFAS toxicity in marine microalgae and potentially in other microorganisms.

Conclusion

At environmentally relevant low concentrations of PFAS, the studied marine model diatoms exhibited species-specific molecular and biochemical adjustments. In *T. pseudonana*, the response was dominated by broad transcriptomic reprogramming, together with the selective accumulation of membrane-related and compatible-solute metabolites, reflecting an adaptive response that maintains redox and membrane homeostasis under stress. In *C. closterium*, by contrast, PFAS exposure was characterized by broad depletion of key metabolites, including those associated with membranes and compatible solute-associated metabolites, together with a narrower transcriptomic response, indicating a more depletion-dominant stress phenotype. PFAS as membrane-active surfactant-like contaminants, interact with species-specific differences in cell-surface organization, membrane-remodeling capacity, osmotic buffering, and carbon-allocation strategy, consequently, pelagic and benthic diatoms do not buffer membrane-active PFAS stress in the same way.

These species-specific differences highlight that PFAS hazard assessment cannot be derived from a single model diatom or a single omics layer, as species differences influence both the mode of cellular disruption and the most sensitive endpoints for evaluation. At the same time, mechanistic inference remains limited by methodological constraints, as concurrent water chemistry, dissolved nutrient measurements, and extracellular polymeric substance analyses were not conducted; the nitrogen- and osmolyte-related patterns observed here were interpreted as cellular response signatures rather than direct evidence of medium nutrient depletion or osmotic balance. PFAS mixture precludes attribution of the observed molecular responses to individual compounds. While this approach reflects environmentally relevant exposure scenarios, future studies employing single-compound exposures at different concentrations and systematically

structured sub-mixtures would help clarify compound-specific effects and better connect specific PFAS to unique molecular and physical outcomes.

Data availability

All sequencing data generated in this study are available at NCBI SRA platform under the accession ID PRJNA1445241 (https://www.ncbi.nlm.nih.gov/sra/PRJNA1445241). All other data are available from the corresponding author upon request.

Conflict of Interest

The authors declare that they have no commercial or financial relationships that could be construed as a potential conflict of interest.

Funding

The Icelandic Research Fund has supported the work in the frame of the project "Per- and poly-fluoroalkyl substances (PFAS) meet Arctic and sub-Arctic marine diatoms and their associated symbionts" (RANNIS ID: 239548-051).

Acknowledgements

Our sincere thanks to doctoral students Li Anderson, and Arnar Ingi Vilhjálmsson at the Department of Biochemistry and Molecular Biology, Faculty of Medicine, University of Iceland, Reykjavik, Iceland for their assistance in the UPLC-MS/MS analyses. Also, extend thanks to the lab manager, Andrés Tryggvi Jakobsson and Dr. Scully from the Faculty of Natural Resource Sciences at the University of Akureyri, for their support in lab work and handling equipment. Also, extend our hanks to Dr. Jason Woodhouse, Dr. Sven Patrik Tobias-Hunedeldt, and Dr. Alice Retter for their guidance in transcriptomics data analysis from the Department of Plankton and Microbial Ecology, Leibniz-Institute of Freshwater Ecology and Inland Fisheries, Stechlin, Germany. We also appreciate the assistance and support provided by Prof. Bernard Lepetit in RT-PCR analysis at the University of Rostock, Germany. The authors would like to thank Fundação para a Ciência e a Tecnologia (FCT) for funding MARE (Marine and Environmental Sciences Centre, http://doi.org/10.54499/UIDB/04292/2020 and http://doi.org/10.54499/UIDP/04292/2020) and ARNET (Aquatic Research Network Associated Laboratory, http://doi.org/10.54499/LA/P/0069/2020).

References

AL Mughram MH, Catalano C, Herrington NB *et al.* 3D interaction homology: The hydrophobic residues alanine, isoleucine, leucine, proline and valine play different structural roles in soluble and membrane proteins. *Front Mol Biosci* 2023;**10**:1116868. https://doi.org/10.3389/fmolb.2023.1116868.

Altschul SF, Gish W, Miller W *et al.* Basic local alignment search tool. *Journal of Molecular Biology* 1990;**215**(3):403–10. https://doi.org/10.1016/S0022-2836(05)80360-2.
Andrews S. FastQC: A Quality Control tool for High Throughput Sequence Data (Version 0.12.1). Babraham Bioinformatics, Babraham Institute, Cambridge, United Kingdom., 2010. https://www.bioinformatics.babraham.ac.uk/projects/fastqc/ (31 May 2026, date last accessed).
Antonopoulou M, Spyrou A, Tzamaria A *et al.* Current state of knowledge of environmental occurrence, toxic effects, and advanced treatment of PFOS and PFOA. *Science of The Total Environment* 2024;**913**:169332. https://doi.org/10.1016/j.scitotenv.2023.169332.
Arulananthan A, Vilhelmsson O, Karsten U *et al.* Per-and polyfluoroalkyl substances (PFAS) in the Cryosphere -Occurrence, organismic accumulation, ecotoxicological impacts, transformation, and management strategies. *Front Environ Sci* 2025;**13**. https://doi.org/10.3389/fenvs.2025.1559941.
Arulananthan A, Scholz B, Karsten U *et al.* Arctic and sub-Arctic marine diatom responses to PFAS exposure: Understanding physiological changes and resilience. *Aquatic Toxicology* 2025;**289**:107562. https://doi.org/10.1016/j.aquatox.2025.107562.
Audic S, Claverie JM. The significance of digital gene expression profiles. *Genome Res* 1997;**7**(10):986–95. https://doi.org/10.1101/gr.7.10.986.
Beale DJ, Sinclair GM, Shah R *et al.* A review of omics-based PFAS exposure studies reveals common biochemical response pathways. *Science of The Total Environment* 2022;**845**:157255. https://doi.org/10.1016/j.scitotenv.2022.157255.
Birchfield AS, Musayev FN, Castillo AJ *et al.* Broad PFAS Binding with Fatty Acid Binding Protein 4 Is Enabled by Variable Binding Modes. *JACS Au* 2025;**5**(6):2469–74. https://doi.org/10.1021/jacsau.5c00504.
Boeckmann B, Bairoch A, Apweiler R *et al.* The SWISS-PROT protein knowledgebase and its supplement TrEMBL in 2003. *Nucleic Acids Res* 2003;**31**(1):365–70. https://doi.org/10.1093/nar/gkg095.
Boltes K, Rosal R, García-Calvo E. Toxicity of mixtures of perfluorooctane sulphonic acid with chlorinated chemicals and lipid regulators. *Chemosphere* 2012;**86**(1):24–9. https://doi.org/10.1016/j.chemosphere.2011.08.041.
Casal P, González-Gaya B, Zhang Y *et al.* Accumulation of Perfluoroalkylated Substances in Oceanic Plankton. *Environ Sci Technol* 2017;**51**(5):2766–75. https://doi.org/10.1021/acs.est.6b05821.
Chakravarty S, Poluri KM. Microalgae-based treatment of per- and polyfluoroalkyl substances-interaction, bioremediation, challenges, and opportunities. *Journal of Water Process Engineering* 2025;**78**:108825. https://doi.org/10.1016/j.jwpe.2025.108825.
Conesa A, Götz S, García-Gómez JM *et al.* Blast2GO: a universal tool for annotation, visualization and analysis in functional genomics research.

Bioinformatics (Oxford, England) 2005;**21**(18):3674–6. https://doi.org/10.1093/bioinformatics/bti610.
Dai S, Zhang G, Dong C *et al.* Occurrence, bioaccumulation and trophodynamics of per- and polyfluoroalkyl substances (PFAS) in terrestrial and marine ecosystems of Svalbard, Arctic. *Water Res* 2025;**271**:122979. https://doi.org/10.1016/j.watres.2024.122979.
Davis SN, Klumker SM, Mitchell AA *et al.* Life in the PFAS lane: The impact of perfluoroalkyl substances on photosynthesis, cellular exudates, nutrient cycling, and composition of a marine microbial community. *Science of The Total Environment* 2024;**927**:171977. https://doi.org/10.1016/j.scitotenv.2024.171977.
Debenest T, Silvestre J, Pinelli E. Diatoms in Ecotoxicology. In: Férard JF, Blaise C (eds.), *Encyclopedia of Aquatic Ecotoxicology*. Dordrecht: Springer Netherlands, 2013, 295–304. https://doi.org/10.1007/978-94-007-5704-2_29.
Dong HP, Dong YL, Cui L *et al.* High light stress triggers distinct proteomic responses in the marine diatom Thalassiosira pseudonana. *BMC Genomics* 2016;**17**(1):994. https://doi.org/10.1186/s12864-016-3335-5.
Falciatore A, Mock T (eds.). *The Molecular Life of Diatoms*. Cham: Springer International Publishing, 2022. https://doi.org/10.1007/978-3-030-92499-7.
Finn RD, Coggill P, Eberhardt RY *et al.* The Pfam protein families database: towards a more sustainable future. *Nucleic Acids Res* 2016;**44**(D1):D279–85. https://doi.org/10.1093/nar/gkv1344.
Fischer FC, Ludtke S, Thackray C *et al.* Binding of Per- and Polyfluoroalkyl Substances (PFAS) to Serum Proteins: Implications for Toxicokinetics in Humans. *Environ Sci Technol* 2024;**58**(2):1055–63. https://doi.org/10.1021/acs.est.3c07415.
Fitzgerald NJM, Wargenau A, Sorenson C *et al.* Partitioning and Accumulation of Perfluoroalkyl Substances in Model Lipid Bilayers and Bacteria. *Environ Sci Technol* 2018;**52**(18):10433–40. https://doi.org/10.1021/acs.est.8b02912.
Flynn KM, Bush K, Cavallin J *et al.* Transcriptomic response of an algal species (Raphidocelis subcapitata) exposed to 22 per- and polyfluoroalkyl substances. *Environmental Toxicology and Chemistry* 2025;**44**(4):995–1006. https://doi.org/10.1093/etojnl/vgaf022.
Garnett J, Halsall C, Thomas M *et al.* Mechanistic Insight into the Uptake and Fate of Persistent Organic Pollutants in Sea Ice. *Environ Sci Technol* 2019;**53**(12):6757–64. https://doi.org/10.1021/acs.est.9b00967.
Garnett J, Halsall C, Thomas M *et al.* Investigating the Uptake and Fate of Poly- and Perfluoroalkylated Substances (PFAS) in Sea Ice Using an Experimental Sea Ice Chamber. *Environ Sci Technol* 2021;**55**(14):9601–8. https://doi.org/10.1021/acs.est.1c01645.
Garnett J, Halsall C, Winton H *et al.* Increasing Accumulation of Perfluorocarboxylate Contaminants Revealed in an Antarctic Firn Core (1958–2017). *Environ Sci Technol* 2022;**56**(16):11246–55. https://doi.org/10.1021/acs.est.2c02592.

Ginguay A, Cynober L, Curis E *et al.* Ornithine Aminotransferase, an Important Glutamate-Metabolizing Enzyme at the Crossroads of Multiple Metabolic Pathways. *Biology (Basel)* 2017;**6**(1):18. https://doi.org/10.3390/biology6010018.

Glüge J, Scheringer M, Cousins IT *et al.* An overview of the uses of per- and polyfluoroalkyl substances (PFAS). *Environ Sci: Processes Impacts* 2020;**22**(12):2345–73. https://doi.org/10.1039/D0EM00291G.

Grung M, Hjermann DØ, Rundberget T *et al.* Low levels of per- and polyfluoroalkyl substances (PFAS) detected in drinking water in Norway, but elevated concentrations found near known sources. *Science of The Total Environment* 2024;**947**:174550. https://doi.org/10.1016/j.scitotenv.2024.174550.

Gu X, Bar-Peled M. The Biosynthesis of UDP-Galacturonic Acid in Plants. Functional Cloning and Characterization of Arabidopsis UDP-d-Glucuronic Acid 4-Epimerase. *Plant Physiol* 2004;**136**(4):4256–64. https://doi.org/10.1104/pp.104.052365.

Guo W, Hao W, Xiao W. Emerging Perfluorinated Chemical GenX: Environmental and Biological Fates and Risks. *Environ Health* published online 17 Dec. 2024. https://doi.org/10.1021/envhealth.4c00164.

Hartz WF, Björnsdotter MK, Yeung LWY *et al.* Levels and distribution profiles of Per- and Polyfluoroalkyl Substances (PFAS) in a high Arctic Svalbard ice core. *Science of The Total Environment* 2023;**871**:161830. https://doi.org/10.1016/j.scitotenv.2023.161830.

Hartz WF, Björnsdotter MK, Yeung LWY *et al.* Sources and Seasonal Variations of Per- and Polyfluoroalkyl Substances (PFAS) in Surface Snow in the Arctic. *Environ Sci Technol* 2024;**58**(49):21817–28. https://doi.org/10.1021/acs.est.4c08854.

Hopkinson BM, Dupont CL, Allen AE *et al.* Efficiency of the CO2-concentrating mechanism of diatoms. *Proceedings of the National Academy of Sciences* 2011;**108**(10):3830–7. https://doi.org/10.1073/pnas.1018062108.

Houten SM, Wanders RJA. A general introduction to the biochemistry of mitochondrial fatty acid β-oxidation. *Journal of Inherited Metabolic Disease* 2010;**33**(5):469–77. https://doi.org/10.1007/s10545-010-9061-2.

Joerss H, Xie Z, Wagner CC *et al.* Transport of Legacy Perfluoroalkyl Substances and the Replacement Compound HFPO-DA through the Atlantic Gateway to the Arctic Ocean—Is the Arctic a Sink or a Source? *Environ Sci Technol* 2020;**54**(16):9958–67. https://doi.org/10.1021/acs.est.0c00228.

Jordan DB, Bacot KO, Carlson TJ *et al.* Plant Riboflavin Biosynthesis: CLONING, CHLOROPLAST LOCALIZATION, EXPRESSION, PURIFICATION, AND PARTIAL CHARACTERIZATION OF SPINACH LUMAZINE SYNTHASE*. *Journal of Biological Chemistry* 1999;**274**(31):22114–21. https://doi.org/10.1074/jbc.274.31.22114.

Kanehisa M, Goto S. KEGG: Kyoto Encyclopedia of Genes and Genomes. *Nucleic Acids Res* 2000;**28**(1):27–30. https://doi.org/10.1093/nar/28.1.27.

Karamat A, Tehrani ,Rouzbeh, Foster ,Gregory D. *et al.* Plant responses to per- and polyfluoroalkyl substances (PFAS): a molecular perspective. *International Journal of Phytoremediation* 2024;**26**(2):219–27. https://doi.org/10.1080/15226514.2023.2232874.

Karsten U, Schlie C, Woelfel J *et al.* Benthic Diatoms in Arctic Seas – Ecological Functions and Adaptations. *Polarforschung 81, 77-84* 2012:77–84.

Kim JH, Ahn JW, Park EJ *et al. Overexpression of S-Adenosylmethionine Synthetase in Recombinant Chlamydomonas for Enhanced Lipid Production*. 2023;**33**(3):310–8. https://doi.org/10.4014/jmb.2212.12009.

Koletti A, Skliros D, Dervisi I *et al.* Oxidative Stress Responses in Microalgae: Modern Insights into an Old Topic. *Applied Microbiology* 2025;**5**(2):37. https://doi.org/10.3390/applmicrobiol5020037.

Koonin EV, Fedorova ND, Jackson JD *et al.* A comprehensive evolutionary classification of proteins encoded in complete eukaryotic genomes. *Genome Biol* 2004;**5**(2):R7. https://doi.org/10.1186/gb-2004-5-2-r7.

Lauritano C, Orefice I, Procaccini G *et al.* Key genes as stress indicators in the ubiquitous diatom Skeletonema marinoi. *BMC Genomics* 2015;**16**(1):411. https://doi.org/10.1186/s12864-015-1574-5.

Li J, Sun J, Li P. Exposure routes, bioaccumulation and toxic effects of per- and polyfluoroalkyl substances (PFASs) on plants: A critical review. *Environment International* 2022;**158**:106891. https://doi.org/10.1016/j.envint.2021.106891.

Li P, Oyang X, Xie X *et al.* Phytotoxicity induced by perfluorooctanoic acid and perfluorooctane sulfonate via metabolomics. *Journal of Hazardous Materials* 2020;**389**:121852. https://doi.org/10.1016/j.jhazmat.2019.121852.

Li Y, Liu X, Zheng X *et al.* Toxic effects and mechanisms of PFOA and its substitute GenX on the photosynthesis of *Chlorella pyrenoidosa*. *Science of The Total Environment* 2021;**765**:144431. https://doi.org/10.1016/j.scitotenv.2020.144431.

Liao J, Huang L, Liu Y *et al.* Metabolomic analysis reveals contrasting effects of PFOS and PFAS on cyanobacterial bloom and metabolic pathways in eutrophic water. *Environmental Pollution* 2025;**375**:126340. https://doi.org/10.1016/j.envpol.2025.126340.

Liao J, Huang L, Liu Y *et al.* Metabolomic analysis reveals contrasting effects of PFOS and PFAS on cyanobacterial bloom and metabolic pathways in eutrophic water. *Environmental Pollution* 2025;**375**:126340. https://doi.org/10.1016/j.envpol.2025.126340.

Liao J, Sun B, Wang C *et al.* Uptake and cellular responses of *Microcystis aeruginosa* to PFOS in various environmental conditions. *Ecotoxicology and Environmental Safety* 2024;**272**:116041. https://doi.org/10.1016/j.ecoenv.2024.116041.

Liao J, Sun B, Wang C *et al.* Uptake and cellular responses of *Microcystis aeruginosa* to PFOS in various environmental conditions. *Ecotoxicology and Environmental Safety* 2024;**272**:116041. https://doi.org/10.1016/j.ecoenv.2024.116041.

Li-Beisson Y, Thelen JJ, Fedosejevs E *et al.* The lipid biochemistry of eukaryotic algae. *Progress in Lipid Research* 2019;**74**:31–68. https://doi.org/10.1016/j.plipres.2019.01.003.

Liu Z, Cao X, Wu M *et al.* Mechanisms of PFBA toxicity in *Chlorella vulgaris*: Photosynthesis, oxidative stress, and antioxidant impairment. *Environmental Research* 2025;**273**:121228. https://doi.org/10.1016/j.envres.2025.121228.

Lohmann R, Abass K, Bonefeld-Jørgensen EC *et al.* Cross-cutting studies of per- and polyfluorinated alkyl substances (PFAS) in Arctic wildlife and humans. *Science of The Total Environment* 2024;**954**:176274. https://doi.org/10.1016/j.scitotenv.2024.176274.

Lukić Bilela L, Matijošytė I, Krutkevičius J *et al.* Impact of per- and polyfluorinated alkyl substances (PFAS) on the marine environment: Raising awareness, challenges, legislation, and mitigation approaches under the One Health concept. *Marine Pollution Bulletin* 2023;**194**:115309. https://doi.org/10.1016/j.marpolbul.2023.115309.

Mao W, Li M, Xue X *et al.* Bioaccumulation and toxicity of perfluorooctanoic acid and perfluorooctane sulfonate in marine algae *Chlorella sp. Science of The Total Environment* 2023;**870**:161882. https://doi.org/10.1016/j.scitotenv.2023.161882.

Mao X, Ge M, Wang X *et al.* Transcriptomics and Metabolomics Analyses Provide Novel Insights into Glucose-Induced Trophic Transition of the Marine Diatom Nitzschia laevis. *Marine Drugs* 2021;**19**(8):art. 8. https://doi.org/10.3390/md19080426.

Meegoda JN, Kewalramani JA, Li B *et al.* A Review of the Applications, Environmental Release, and Remediation Technologies of Per- and Polyfluoroalkyl Substances. *International Journal of Environmental Research and Public Health* 2020;**17**(21):art. 21. https://doi.org/10.3390/ijerph17218117.

Paglia G, Magnúsdóttir M, Thorlacius S *et al.* Intracellular metabolite profiling of platelets: Evaluation of extraction processes and chromatographic strategies. *Journal of Chromatography B* 2012;**898**:111–20. https://doi.org/10.1016/j.jchromb.2012.04.026.

Paglia G, Williams JP, Menikarachchi L *et al.* Ion Mobility Derived Collision Cross Sections to Support Metabolomics Applications. *Anal Chem* 2014;**86**(8):3985–93. https://doi.org/10.1021/ac500405x.

Pang Z, Lu Y, Zhou G *et al.* MetaboAnalyst 6.0: towards a unified platform for metabolomics data processing, analysis and interpretation. *Nucleic Acids Res* 2024;**52**(W1):W398–406. https://doi.org/10.1093/nar/gkae253.

Remmers IM, D'Adamo S, Martens DE *et al.* Orchestration of transcriptome, proteome and metabolome in the diatom *Phaeodactylum tricornutum* during nitrogen limitation. *Algal Research* 2018;**35**:33–49. https://doi.org/10.1016/j.algal.2018.08.012.

Ricolfi L, Yang Y, Pottier P *et al.* Unravelling the magnitude and drivers of PFAS trophic magnification: a meta-analysis. *Nat Commun* 2025;**16**(1):10720. https://doi.org/10.1038/s41467-025-65746-4.

Rigét F, Bignert A, Braune B *et al.* Temporal trends of persistent organic pollutants in Arctic marine and freshwater biota. *Science of The Total Environment* 2019;**649**:99–110. https://doi.org/10.1016/j.scitotenv.2018.08.268.

Saritha VK, Krishnan KP, Mohan M. Perfluorooctanoic acid in the sediment matrices of Arctic fjords, Svalbard. *Marine Pollution Bulletin* 2023;**192**:115061. https://doi.org/10.1016/j.marpolbul.2023.115061.

Schmittgen TD, Livak KJ. Analyzing real-time PCR data by the comparative CT method. *Nat Protoc* 2008;**3**(6):1101–8. https://doi.org/10.1038/nprot.2008.73.

Schymanski EL, Jeon J, Gulde R *et al.* Identifying Small Molecules via High Resolution Mass Spectrometry: Communicating Confidence. *Environ Sci Technol* 2014;**48**(4):2097–8. https://doi.org/10.1021/es5002105.

Shi J, Hu M, Xia Z *et al.* Influence of perfluoroalkyl substances, with focus on perfluorobutanoic acid on the responding characteristics and molecular mechanisms of *Thalassiosira pseudonana*. *Ecotoxicology and Environmental Safety* 2024;**285**:117048. https://doi.org/10.1016/j.ecoenv.2024.117048.

Smith SR, Glé C, Abbriano RM *et al.* Transcript level coordination of carbon pathways during silicon starvation-induced lipid accumulation in the diatom Thalassiosira pseudonana. *New Phytologist* 2016;**210**(3):890–904. https://doi.org/10.1111/nph.13843.

Thangaraj S, Palanisamy SK, Zhang G *et al.* Quantitative Proteomic Profiling of Marine Diatom Skeletonema dohrnii in Response to Temperature and Silicate Induced Environmental Stress. *Front Microbiol* 2021;**11**. https://doi.org/10.3389/fmicb.2020.554832.

Trilla-Prieto N, Dachs J, Iriarte J *et al.* Accumulation of perfluoroalkyl acids as forever chemicals in Antarctic waters. *Commun Earth Environ* 2025;**6**(1):545. https://doi.org/10.1038/s43247-025-02535-3.

US EPA O. Per- and Polyfluoroalkyl Substances (PFAS), Reports and Assessments. 16 Nov. 2021. https://www.epa.gov/sdwa/and-polyfluoroalkyl-substances-pfas (20 Feb. 2025, date last accessed).

Vasilev J, Mix AK, Heimerl T *et al.* Inferred Subcellular Localization of Peroxisomal Matrix Proteins of Guillardia theta Suggests an Important Role of Peroxisomes in Cryptophytes. *Front Plant Sci* 2022;**13**. https://doi.org/10.3389/fpls.2022.889662.

Wang H, Fan H, Liu H *et al.* Oxidative stress response mechanism of *Scenedesmus obliquus* to ionic liquids with different number of methyl-substituents. *Journal of Hazardous Materials* 2020;**399**:122847. https://doi.org/10.1016/j.jhazmat.2020.122847.

Wang J, Tian Q, Zhou H *et al.* Physiological regulation of microalgae under cadmium stress and response mechanisms of time-series analysis using metabolomics. *Science of The Total Environment* 2024;**916**:170278. https://doi.org/10.1016/j.scitotenv.2024.170278.

Wang L, Yang T, Pan Y *et al.* The Metabolism of Reactive Oxygen Species and Their Effects on Lipid Biosynthesis of Microalgae. *Int J Mol Sci* 2023;**24**(13):11041. https://doi.org/10.3390/ijms241311041.

Wang X, Liu Y, Zhang X *et al.* Bioaccumulation, tissue distribution, and maternal transfer of novel PFOS alternatives (6:2 Cl-PFESA and OBS) in wild freshwater fish from Poyang Lake, China. *Chemosphere* 2023;**336**:139253. https://doi.org/10.1016/j.chemosphere.2023.139253.

Wang Y, Shi Y, Li K *et al.* Roles of the 2-Oxoglutarate-Dependent Dioxygenase Superfamily in the Flavonoid Pathway: A Review of the Functional Diversity of F3H, FNS I, FLS, and LDOX/ANS. *Molecules* 2021;**26**(21):6745. https://doi.org/10.3390/molecules26216745.

Wang Z, DeWitt JC, Higgins CP *et al.* A Never-Ending Story of Per- and Polyfluoroalkyl Substances (PFASs)? *Environ Sci Technol* 2017;**51**(5):2508–18. https://doi.org/10.1021/acs.est.6b04806.

Whitehead HD, Venier M, Wu Y *et al.* Fluorinated Compounds in North American Cosmetics. *Environ Sci Technol Lett* 2021;**8**(7):538–44. https://doi.org/10.1021/acs.estlett.1c00240.

Wu H, Huang X, Duan X *et al.* Meta-analysis evaluates toxicity of PFAS to microalgae: Mechanisms and ecological risks. *Journal of Hazardous Materials* 2025;**496**:139328. https://doi.org/10.1016/j.jhazmat.2025.139328.

Xie WH, Pang F, Niu YF *et al.* Functional characterization of an ACCase subunit from the diatom Phaeodactylum tricornutum expressed in Escherichia coli. *Biotechnology and Applied Biochemistry* 2013;**60**(3):330–5. https://doi.org/10.1002/bab.1091.

Xue X, Gao N, Xu F. Toxicity of perfluooctane sulfonate (PFOS) and perfluorobutane sulfonate (PFBS) to *Scenedesmus obliquus*: Photosynthetic characteristics, oxidative damage and transcriptome analysis. *Environmental Pollution* 2022;**315**:120397. https://doi.org/10.1016/j.envpol.2022.120397.

Yang W, Gao P, Ye Z *et al.* Micro/nano-plastics and microalgae in aquatic environment: Influence factor, interaction, and molecular mechanisms. *Science of The Total Environment* 2024;**934**:173218. https://doi.org/10.1016/j.scitotenv.2024.173218.

Yang W, Gao X, Wu Y *et al.* Chemical- and species-specific toxicity of nonylphenol and octylphenol to microalgae *Chlorella pyrenoidosa* and *Scenedesmus obliquus*. *Environmental Toxicology and Pharmacology* 2021;**81**:103517. https://doi.org/10.1016/j.etap.2020.103517.

Zhang QY, Xu LL, Zhong MT *et al.* Gestational GenX and PFOA exposures induce hepatotoxicity, metabolic pathway, and microbiome shifts in weanling mice. *Science of The Total Environment* 2024;**907**:168059. https://doi.org/10.1016/j.scitotenv.2023.168059.

Zhang Y, Duan J, Zheng Y *et al.* Transcriptomic Responses of the Marine Diatom Phaeodactylum tricornutum to High Carbon and Low Nitrogen Stress. *Ecology and Evolution* 2026;**16**(1):e72754. https://doi.org/10.1002/ece3.72754.

Zhao Z, Zheng X, Han Z *et al.* Polystyrene microplastics enhanced the effect of PFOA on *Chlorella sorokiniana*: Perspective from the cellular and molecular levels. *Journal of Hazardous Materials* 2024;**465**:133455. https://doi.org/10.1016/j.jhazmat.2024.133455.

Zheng JW, Li DW, Lu Y *et al.* Molecular exploration of algal interaction between the diatom *Phaeodactylum tricornutum* and the dinoflagellate *Alexandrium tamarense*. *Algal Research* 2016;**17**:132–41. https://doi.org/10.1016/j.algal.2016.04.019.

Zheng X, Qiu J, Li A. Effects of perfluorooctanesulfonic acid on *Thalassiosira minima*: Insights from growth, photosynthesis, oxidative stress, and toxin biosynthesis. *Journal of Hazardous Materials* 2026;**508**:141960. https://doi.org/10.1016/j.jhazmat.2026.141960.

Zhuo-Xing Shi, Xiang L, Zhao HM *et al.* High-throughput single-molecule long-read RNA sequencing analysis of tissue-specific genes and isoforms in lettuce (Lactuca sativa L.). *Commun Biol* 2024;**7**(1):920. https://doi.org/10.1038/s42003-024-06598-4.

Supplementary details

PFAS at environmental concentration alters metabolic and gene expression patterns in two model marine diatoms: Decoding survival and adaptation mechanisms

Ashani Arulananthan[1,2], Oddur Þór Vilhelmsson[1,3], Óttar Rolfsson[4], Hans-Peter Grossart[5,6], Auður Sigurbjörnsdóttir[1], Ulf Karsten[7,8], Marie Wünsch[9], Ralf Ebinghaus[10], Hanna Joerss[11], Bernardo Duarte[12, 13,] Zophonías O. Jónsson[14], Bettina Scholz[1,2]*

[1]*Faculty of Natural Resource Science, University of Akureyri. Iceland.*
[2]*BioPol ehf. Marine Biotechnology, Skagaströnd, Iceland.*
[3]*The Biomedical Center of the University of Iceland, Reykjavík, Iceland.*
[4]*Department of Biochemistry and Molecular Biology, Faculty of Medicine, University of Iceland, Reykjavik, Iceland.*
[5]*Department of Plankton and Microbial Ecology, Leibniz-Institute of Freshwater Ecology and Inland Fisheries, Stechlin, Germany.*
[6]*Institute of Biochemistry and Biology, Potsdam University, Potsdam, Germany.*
[7]*Department of Applied Ecology and Phycology, Institute of Biological Sciences, University of Rostock, Germany.*
[8]*Department of Maritime Systems, Interdisciplinary Faculty, University of Rostock, Germany.*
[9]*Department of Molecular Stress Physiology, Institute of Biosciences, University of Rostock, Germany.*
[10] *Helmholtz-Zentrum Hereon Institute of Coastal Environmental Chemistry, Geesthacht, Germany*
[11]*Institute of Coastal Environmental Chemistry, Helmholtz-Zentrum Hereon, Geesthacht, Germany.*
[12]*MARE—Marine and Environmental Sciences Centre & ARNET- Aquatic Research Network Associated Laboratory, Faculdade de Ciências da Universidade de Lisboa, Campo Grande, 1749-016 Lisbon, Portugal.*
[13]*Departamento de Biologia Vegetal, Faculdade de Ciências da Universidade de Lisboa, Portugal.*[14] *Faculty of Life and Environmental Sciences, University of Iceland, Reykjavik, Iceland.*

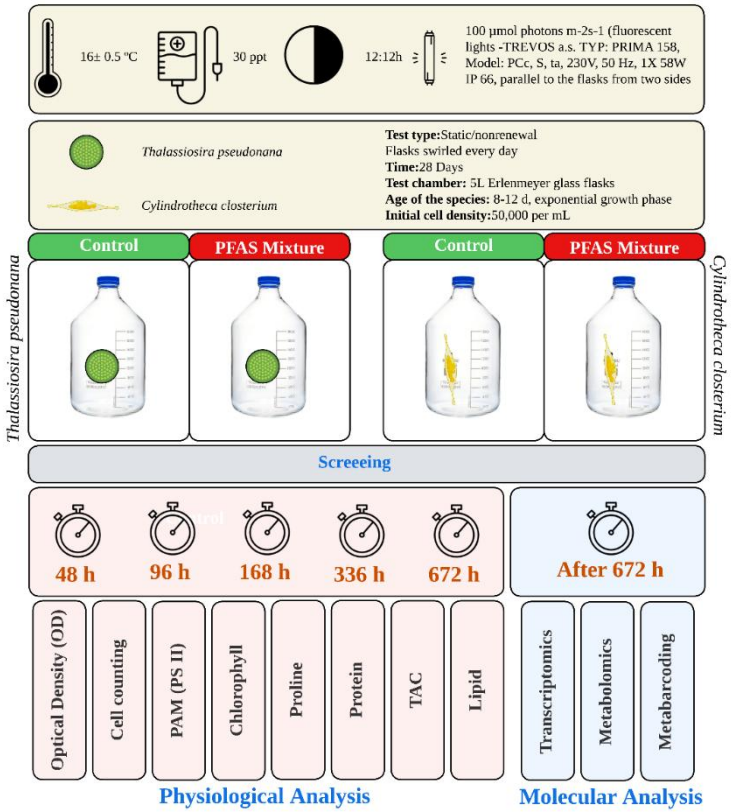

Supplementary Figure M1: Experimental design of PFAS exposure along with the laboratory conditions of cultures, control and sampling points for measuring biochemical and molecular analyses parameters were shown.

Table M1: Details of individual PFAS mixtures added for the 28 days exposure experiment: PFOS, PFOA, PFNA, HFPO-DA, PFDoA, PFTrDA each at 0.9 ng/L.

PFAS compounds and formula	CAS number	MW ($g \cdot mol^{-1}$)	Low concentration ($ng \cdot L^{-1}$)
PFOA (Perfluorooctanoic Acid)	335-67-1	414.1	0.9
PFNA (Perfluorononanoic Acid)	375-95-1	464.1	0.9
PFDoA (Perfluorododecanoic Acid)	307-55-1	614.1	0.9
PFTrDA (Perfluorotridecanoic Acid)	72629-94-8	664.1	0.9
PFOS (Perfluorooctane Sulfonic Acid)	1763-23-1	538.2	0.9
HFPO-DA (Hexafluoropropylene Oxide Dimer Acid,"GenX")	13252-13-6	330.5	0.9

Abbreviations:

Figure 5: A). Lhca1, Lhca4, Lhca5- light harvesting chlorophyll *a/c* binding protein complex (Lhc)
PsbA- Photosystem II protein D1; PsbO- Oxygen-evolving enhancer protein 1; Psb 27- Psb28-Photosystem II repair protein; PetC- cytochrome b6-f complex iron-sulfur subunit; FNR- ferredoxin-NADP+ reductase; PrtH -Ferredoxin NADP+ reductase. **B).** AspAT-aspartate aminotransferase; MDH- malate dehydrogenase; PC-pyruvate carboxylase; CS- citrate synthase; ICL-isocitrate lyase; SEL-succinyl-CoA ligase; GLN2/GS- Glutamine synthetase(down in TP); OAT-ornithine aminotransferase; PDH-Proline dehydrogenase (down in TP and CC); ODC- Ornithine decarboxylase (down in TP, CC), OCDA- ornithine cyclodeaminase, OTA- ornithine transaminase (up in CC); TAT-Tyrosine aminotransferase; PEPCK- phosphoenolpyruvate carboxykinase; PC-pyruvate carboxylase; TKT-transketolose, CST-cysteine synthase; PSAT-Phosphoserine aminotransferase 1 (down in TP); PFK- phosphofructokinase; GAPDH- glyceraldehyde-3-phosphate dehydrogenase; PGK- phosphoglycerate kinase; PGAM - phosphoglycerate mutase; PPDK - Pyruvate phosphate dikinase **C).** FBA -fructose-bisphosphate aldolase; FBP - fructose-1–6-bisphosphatase; PRK- Phosphoribulokinase; TKT- transketolose. G6PD -glucose-6-phosphate dehydrogenase; 6GBD -6-phosphogluconate dehydrogenase; TKT - transketolase; TLM - transketolose like enzyme; RPI- ribose-5-phosphate isomerase; GAPDH; glyceraldehyde 3-phosphate dehydrogenase; PGK -phosphoglycerate kinase. **D).** ACC -Acetyl-CoA carboxylases; MECR -mitochondrial enoyl-3-oxoacyl-[acyl-carrier-protein; FabF -3-oxoacyl-[acyl-carrier-protein] synthase; FabG - 3-oxoacyl-[acyl-carrier-protein] reductase; ELOV -elongation of long-chain fatty acids; ACS- long-chain acyl-CoA synthetases.

Figure 6. A). ABCA1, ABCC, ABCG, ABCB1-NTP hydrolase: ATP binding cassette units; PEX5 -peroxisomal β-oxidation components; ACOX -precursor of hydrogenase glutaryl-coa dehydrogenase (GCD1; ACSL -Long-chain acyl-CoA synthetases (AMP-forming); AGT -alanine-glyoxylate transaminase / serine-glyoxylate transaminase / serine-pyruvate transaminase; PRDX5 -Alkyl hydroperoxide reductase/peroxiredoxin ; PXMP2- peroxisomal membrane protein ; MPV17 – Peroxisomal membrane protein MPV17 and related proteins; ACAA1 -3-ketoacyl-coa thiolase, mitochondrial. **B).** NRT1, NRT2- nitrate transporter; NR- nitrate reductase; NIA- nitrate reductase; NIRA - nitrite reductase-ferredoxin dependent; GS -glutamate synthase; GDH- glutamate dehydrogenase; GOAT- glutamate synthase; SOD- superoxide dismutase; Trx- thioredoxin M-type; NRX -thioredoxin -like; MDA -malondialdehyde; MDAR- monodehydroascorbate reductase; GSH -glutathione; GST -glutathione S-transferase; AsA -reduced ascorbic acid; GPx – glutathione peroxidase; GR- glutathione reductase; ROS -reactive oxygen species; HSC- heat shock protein chaperones; HSP20,70,90- heat shock proteins. **C)**. MAPKKK - mitogen-activated protein kinase kinase kinase; MAPKK

0mitogen-activated protein kinase kinase; MAPK – mitogen-activated protein kinase; CBL -interacting protein kinase; CPK – Calcium dependent protein kinase. **D).** S3,8,12,13,17,25,26,26- ribosomal small subunit proteins; L3e, L5,10, - ribosomal large subunit proteins; Ubiquitin ribosome fusion proteins- Ub-L40e; RPLP0; Ub-L40; Ub-S27a; RPS27A; RPL40

Supplementary Table 1: Internal standard compounds added for the end metabolite analysis.

Internal standard added [µL] **Water (H2O):acetonitile (ACN) = 1:1 added [µL]**	**Solvent for Stock-Solution**
19:0 Lyso PC	ACN:H2O=1:1
Adenine-15N2	ACN:H2O=1:1
Alanine d4	ACN:H2O=1:1
AMP 13C10 15N5	ACN:H2O=1:1
Arginine (13C,15N4)	ACN:H2O=1:1
Carnitine d9	ACN:H2O=1:1
Citric acid (13C6)	ACN:H2O=1:1
Cysteine 13C3, 15N	ACN:H2O=1:1
Glucose 13C6	ACN:H2O=1:1
Glutamic Acid d5	ACN:H2O=1:1
Glutamine (15N2)	ACN:H2O=1:1
Lysine d4	ACN:H2O=1:1

Malonic acid d4	ACN:H2O=1:1
Phenylalanine d2	ACN:H2O=1:1
Phtalic Acid d4	ACN:H2O=1:1
Succinic acid d4	ACN:H2O=1:1
1.2 Choline	ACN:H2O=1:1

Summary of sequencing data and data quality control (Tables and figures).
Diatoms samples sequenced on PacBio Sequel platform, build 4 PacBio IsoSeq libraries. Throughout this document, ***Thalassiosira pseudonana*** **samples are indicated as CG_P: PFAS-treated sample, and CG_C: Control sample**, While *Cylindrotheca closterium* samples are indicated as CC_P: PFAS-treated sample, and CC_C: Control sample.

Supplementary Table 2: Polymerase reads summary.

Sample	Library	Cell Number	Total Reads	Total Base (GB)	MaxLength (bp)	MeanLength (bp)	N50 Length (bp)
CG_P	WHPBCYLjfwvT0-10R20241010-004	1	207315	24.16	395225	116544.7	209240
CG_C	WHPBCYLjfwvT0-10R20241010-002	1	312202	36.55	446440	117064.5	211098
CC_P	WHPBCYLjfwvT0-10R20241010-003	1	295114	33.51	413563	113560.6	202122
CC_C	WHPBCYLjfwvT0-10R20241010-001	1	489977	54.31	434259	110850.7	195608

Supplementary Table 3: Subreads summary. *Thalassiosira pseudonana* samples are indicated as CG_P: PFAS-treated sample, and CG_C: Control sample, While *Cylindrotheca closterium* samples are indicated as CC_P: PFAS-treated sample, and CC_C: Control sample.

Sample	Library	Cell Number	Total Reads	Total Base (GB)	MaxLength (bp)	MeanLength (bp)	N50 Length (bp)
CG_P	WHPBCYLjfwvT0-10R20241010-004	1	6419566	23.7	245672	3692.32	4400
CG_C	WHPBCYLjfwvT0-10R20241010-002	1	7676362	36	407354	4689.55	5495
CC_P	WHPBCYLjfwvT0-10R20241010-003	1	9577384	32.82	351978	3427.3	4008
CC_C	WHPBCYLjfwvT0-10R20241010-001	1	24935116	52.6	432806	2109.62	2691

Polymerase Reads length distribution

A.

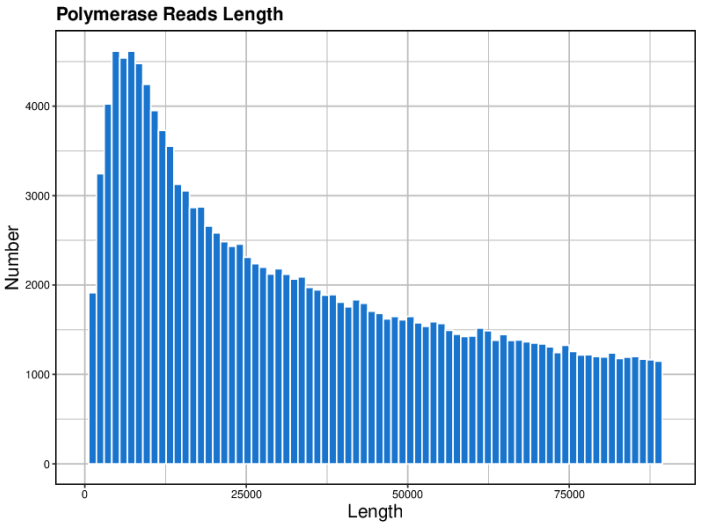

B.

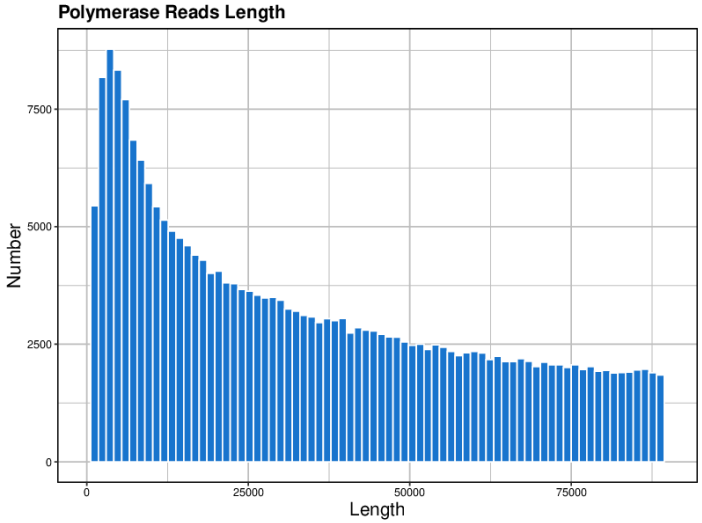

Supplementary Fig 1: Polymerase Reads length distribution. The x-axis represents the read length, and the left y-axis represents the number of reads. A-*Thalassiosira pseudonana*, B- *Cylindrotheca closterium*

2. Reads of Insert and full-length transcript detection

Reads of insert

Supplementary Table 4: CCS summary. *T. pseudonana* sequence 9,779 bp (427,155 reads) CCS (Reads of insert) in 2 SMRT cell sequencing result. In *C. closterium,* obtained sequence 6,649 bp (666,518 reads) CCS (Reads Of insert) in 2 SMRT cell sequencing.

Sample	Library	Cell Number	Reads of Insert	Mean Read Length of Insert (bp)	Mean Read Quality of Insert	Mean Number of Passes
CG_P	WHPBCYLjfwvT0-10R20241010-004	1	172737	4353	0.99	28
CG_C	WHPBCYLjfwvT0-10R20241010-002	1	254418	5426	0.99	24
CC_P	WHPBCYLjfwvT0-10R20241010-003	1	248228	3970	0.99	29
CC_C	WHPBCYLjfwvT0-10R20241010-001	1	418290	2679	0.99	34

Full-length transcript detection

Depending on whether the CCS sequences include the full 5' end primer, polyA tail, and 3' end primer, we split CCS reads into full-length non- chimeric (FLNC) and non-full-length. Finally, only full-length non-chimeric reads are used in subsequent analysis. The results of FLNC reads are summarized in Table 4.

Supplementary Table 5: Summary of FLNC reads.

Sample	Library	Cell Number	Classifyed ROI	Full-length non-chimeric reads	Mean FL per ROI	Mean Read Quality	Mean Number of Passes	Mean full-length non-chimeric read length(bp)
CG_P	WHPBCYLjfwvT0-10R20241010-004	1	166804	665481	4	0.99	25	915.4
CG_C	WHPBCYLjfwvT0-10R20241010-002	1	250025	1274093	5.1	0.99	22	963.5
CC_P	WHPBCYLjfwvT0-10R20241010-003	1	243731	1139029	4.7	0.99	26	720.9
CC_C	WHPBCYLjfwvT0-10R20241010-001	1	391141	1216741	3.1	0.99	31	636.7

3. Full-length non-chimeric (FLNC) read clustering

We used the official isoseq3 toolkits' program cluster to integrate the full-length non- chimeric (FLNC) reads into consistent sequences(consensus). For a summary of the Reads clustering of each library, see Table 5.

Supplementary Table 6: Information summary table for Read clustering of each library

Sample	Library	Cell Number	Total isoforms	Mean Quality	Mean isoforms length (bp)	Mean Full length coverage
CG_P	WHPBCYLjfwvT0-10R20241010-004	1	66293	1	904	8
CG_C	WHPBCYLjfwvT0-10R20241010-002	1	118266	1	912	9
CC_P	WHPBCYLjfwvT0-10R20241010-003	1	68787	1	617	14
CC_C	WHPBCYLjfwvT0-10R20241010-001	1	55881	1	451	19

4 Merge libraries and remove redundancy

The high-quality sequences obtained after clustering of each library are finally merged together to remove redundancy. The final transcript sequence obtained after deduplication is summarized in Table6. The situation of each sample after deduplication is summarized in Table 7.

Supplementary Table 7: Number of transcripts.

Library	sLibrary_genes	[AllSamples]_genes
CG_P:WHPBCYLjfwvT0-10R20241010-004	66293	59931
CG_C:WHPBCYLjfwvT0-10R20241010-002	118266	105491
TOTAL	184559	125793
CC_P:WHPBCYLjfwvT0-10R20241010-003	68,787	60,507
CC_C:WHPBCYLjfwvT0-10R20241010-001	55,881	50,822
TOTAL	124,668	96,210

Supplementary Table 8: Summary of the final transcript sequence obtained after deduplication.

Species	Total_number	Total_length	N50	N90	Max_length	Min_length	Sequence_GC(%)
T. pseudonana	125793	121864270	1318	465	16139	59	46.28%
C. closterium	96210	54707596	735	263	15479	49	43.75%

A.

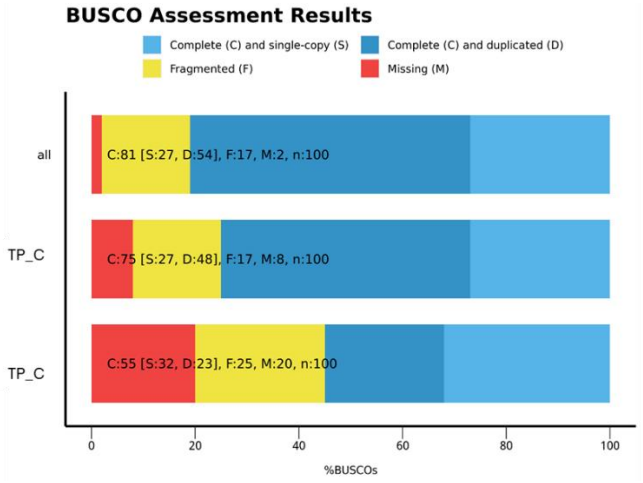

B.

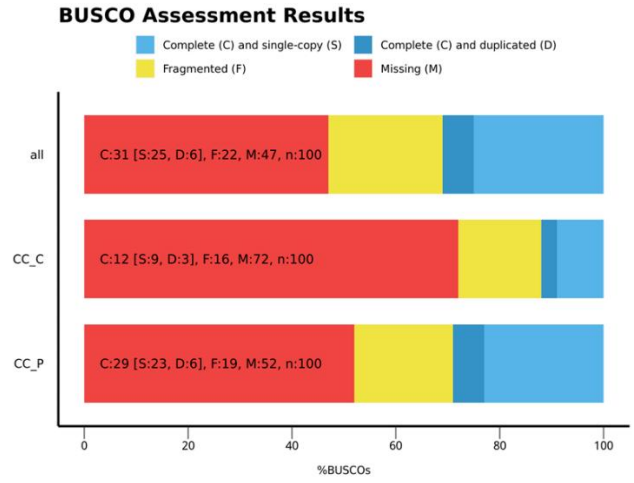

Supplementary Figure 2: BUSCO assembly evaluation results, A-*Thalassiosira pseudonana*, B- *Cylindrotheca closterium*. We used the single-copy ortholog database BUSCO to evaluate the quality of assembled transcripts. By comparing with conserved genes, the integrity of transcriptome assembly is explained to a certain extent. C (complete): Match the sequence on the BUSCO database; F (fragmented): Only partial sequences can be compared on the BUSCO database; D (duplicate): Multiple genes aligned to the same BUSCO; M (missing) Filtered sequence.

A. B.

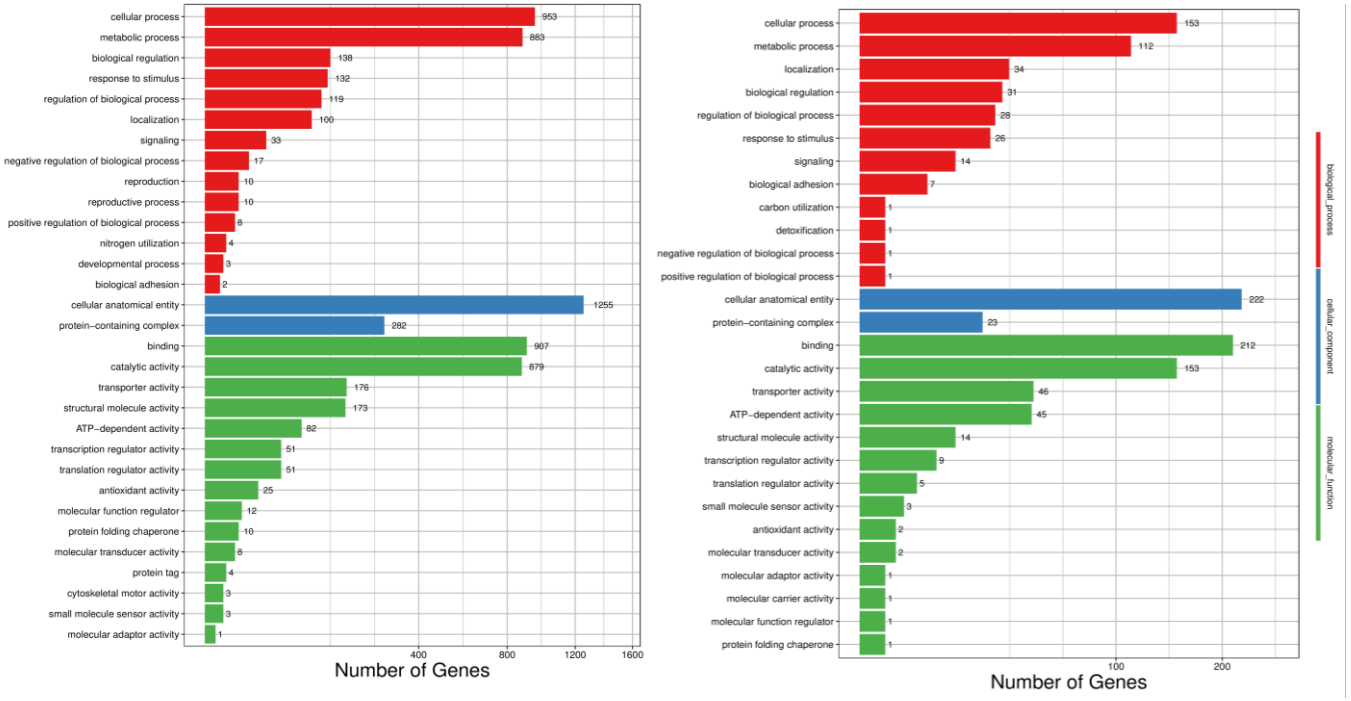

Supplementary Figure 3:DEGs annotated gene ontology (GO) functional classification for the studied species; A) TP_C (*Thalassiosira pseudonana*) and B) *Cylindotheca closterium.* Genes were categorized into three main GO domains: biological process (red), cellular component (blue), and molecular function (green). The distribution highlights the predominance of genes involved in core cellular activities and biochemical functions.

Supplementary Table 9: RT-PCR candidate isoforms tested from *Thalassiosira pseudonana* and their primer details along with the expression pattern resulted in the RNA-sequencing and qRT-PCR.

Isoforms denoting genes- isoform_19178 (FTR1): ferrous iron transmembrane transporter, isoform_18384: GTPase activity, translation elongation factor activity (GTP_EFTU_D3_Up), isoform_34234: sodium:phosphate symporter activity (NaPh Sym), isoform_9423: Tubulin C terminal domain, translation elongation factor, isoform_33123 (GTP_EFTU_D3): Proline dehydrogenase 1 (PDH2), isoform_30363: actin filament bundle assembly(reference gene).

Isoforms tested and their primer details				**RNA-sequencing expression**		**qRT-PCR expression**	
Isoform	Forward primer (5'→3')	Reverse primer (5'→3')	Product length (bp)	log2FoldΔ(TP_P/TP_C)	Regulation (TP_P/TP_C)	log2FoldΔ(TP_P/TP_C)	Regulation (TP_P/TP_C)
isoform_19178	GAATCGCTGTTGGCTTCGC	AGACTTCTTCGAACTCGTGAC	153	10.009689	Up	5.42	Up
isoform_18384	GAGTTCGAGCCAAGTCAGCC	CAGACAATACCCGCAGCAAGAT	164	9.1658392	Up	2.45	Up
isoform_34234	ACGGACATCAAGCATGC	GCTCAGACAATCGAGCC		8.7296207	Up	14.24	Up
isoform_9423	ATGTTGCCGTCCTCGTCATCG	CGGAGTAGTCACAAGAGTCCA	119	-10.67534	Down	−2.90	Down
isoform_33123	GAGAGCATCGAAAAGGCTGT	CGCTTCTTCAGCTCTCGACC		-9.138272	Down	−3.47	Down
isoform_30363	GCAACGCCATAGAGTACGCCA	AGGTCTCGTGCCAGCTCTTC	136	-0.007349	*		

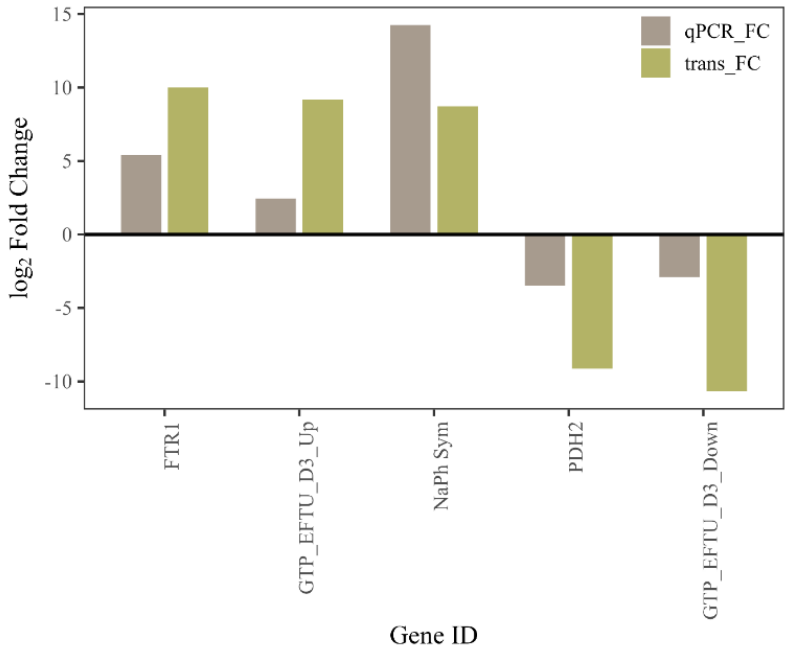

Supplementary Figure 4: RT-PCR (qPCR) candidate isoforms from *Thalassiosira pseudonana* tested and their primer details along with the expression pattern resulted in the RNA-sequencing and qRT-PCR. Isoforms denoting genes- isoform_19178 (FTR1): ferrous iron transmembrane transporter, isoform_18384: GTPase activity, translation elongation factor activity (GTP_EFTU_D3_Up), isoform_34234: sodium:phosphate symporter activity (NaPh Sym), isoform_9423: Tubulin C terminal domain, translation elongation factor, isoform_33123 (GTP_EFTU_D3): Proline dehydrogenase 1 (PDH2). qPCR-FC: log_2 fold change of isoforms tested, and trans_FC is the expression levels resulted from the RNA-Sequencing of *Thalassiosira pseudonana.*

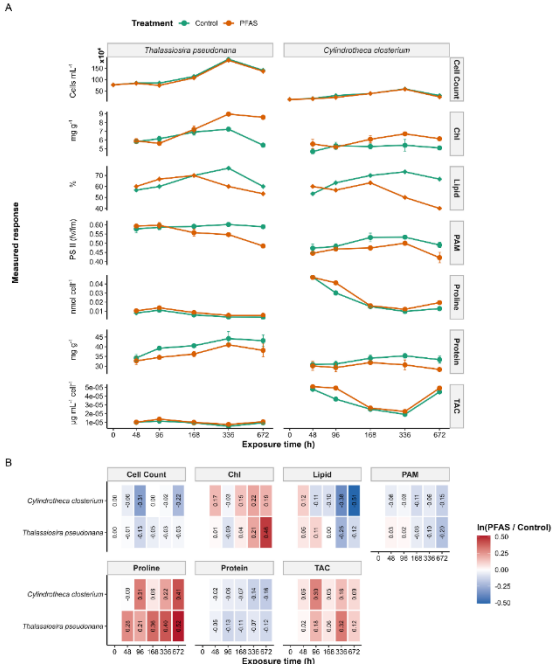

Supplementary Figure 5: Summary of physiological measurements collected during the long-term exposure time points. Pane A line graphs (from top to bottom) show the cell count, chlorophyll *a* concentration, lipid, PAM measurements for PSII activity, proline concentration, protein content, and total antioxidant activity. Panel B heat map shows the overview of how PFAS impacted the diatom physiology when compared to their controls. The parameters were shown in natural log values (ln), shown in the following order from left to right: cell count, chlorophyll *a* concentration, lipid content, PAM (PSII activity), proline, protein, and total antioxidant activity.

Article IV

Environmentally relevant PFAS exposure drives taxon-specific restructuring of marine diatom phycosphere microbiomes

Graphical Abstract

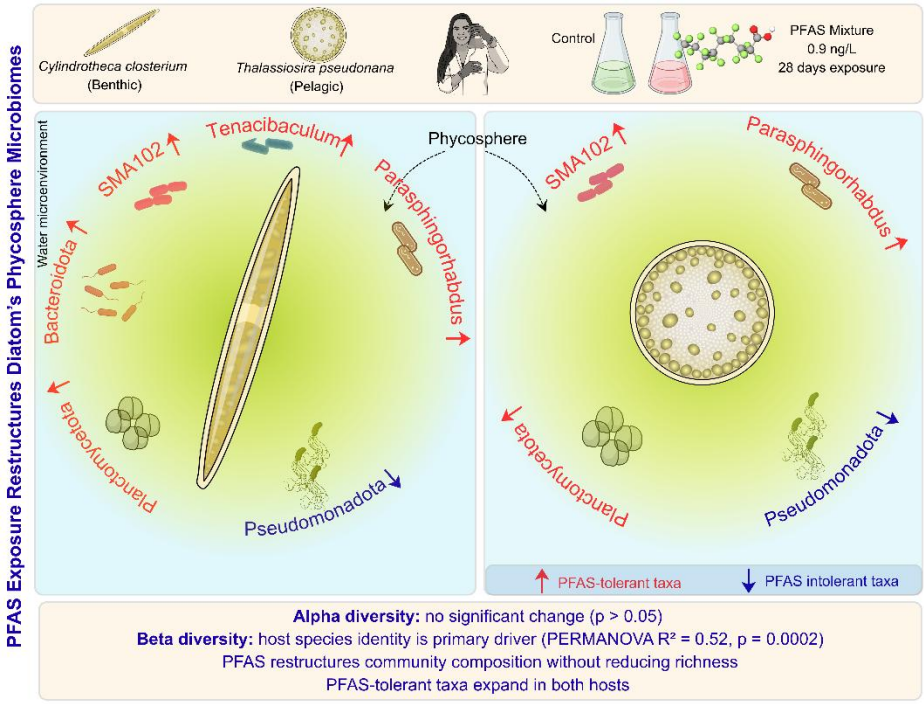

Environmentally relevant PFAS exposure drives taxon-specific restructuring of marine diatom phycosphere microbiomes

Ashani Arulananthan[1,2], Oddur Þór Vilhelmsson[1,3], Auður Sigurbjörnsdóttir[1], Hans-Peter Grossart[4,5], Ulf Karsten6,[6,7], Bettina Scholz[1, 2]*

[1]Faculty of Natural Resource Science, University of Akureyri. Iceland.
[2]BioPol ehf. Marine Biotechnology, Skagaströnd, Iceland.
[3]The Biomedical Center of the University of Iceland, Reykjavík, Iceland.
[4]Department of Plankton and Microbial Ecology, Leibniz-Institute of Freshwater Ecology and Inland Fisheries, Stechlin, Germany.
[5]Institute of Biochemistry and Biology, Potsdam University, Potsdam, Germany.
[6]Department of Applied Ecology and Phycology, Institute of Biological Sciences, University of Rostock, Germany.
[7]Department of Maritime Systems, Interdisciplinary Faculty, University of Rostock, Germany.

**Corresponding author: ashani@unak.is*

Abstract

Per- and polyfluoroalkyl substances (PFAS) are globally detected persistent contaminants increasingly detected in coastal marine environments, yet their effects on phytoplankton-associated microbiomes remain poorly understood. This study characterized phycosphere bacterial communities associated with the marine diatom species *Cylindrotheca closterium* (CC) and *Thalassiosira pseudonana* (TP) under PFAS-exposed and control conditions using 16S rRNA V4-region amplicon sequence variant (ASV) analysis. PFAS exposure restructured the bacterial communities in a host-dependent manner. At the family level, both PFAS-treated communities showed convergent enrichment of Phycisphaeracae (CC:14.6% →18.4%; TP: 37.5% →45.3%) and Sphingomonadaceae (CC:1.4% →3.9%; TP: 8.5% →12.9%), alongside depletion of Alteromonadaceae (CC:10.8% →8.2%; TP: 8.8% →0.9%), Cyclobacteriaceae (CC:17.1% →14.6%; TP: near elimination), and Marinobacteraceae (TP: 9.6% →2.8%). Nannocystaceae (Myxococcota) exapanded exclusively in the *C. Closterium* (7.0% →10.6%), and Rhizobiaceae increased selectively *T. pseudonana* (9.6 % →2.8%). At the genus level, SM1A02 (Phycisphaerae) and *Parasphingorhabdus* were enriched in both phycospheres, identifying them as candidate PFAS-exposure indicators. Alpha diversity indices were not significantly altered by PFAS exposure in neither species, with Shannon diversity remaining stable in *C. closterium* (4.43 VS 4.38), and declining moderately in *T. pseudonana* (3.19 vs. 2.87). Further, alpha diversity metrics masked pronounced compositional restructuring at the phylum and genus levels, with PFAS acting as a selective force that shifted community composition without reducing overall diversity, a pattern consistent with community reorganization rather than collapse. These findings demonstrate that PFAS exposure restructures the marine diatom phycosphere microbiome through a combination of convergent and host-species-specific mechanisms, shifting communities from copiotrophic, high-turnover assemblages toward oligotrophic-dominated states under controlled laboratory conditions. Further studies are needed to elucidate the underlying survival mechanisms and their functional roles with the implications for biogeochemical cycling in PFAS-contaminated marine systems.

1.0 Introduction

Marine diatoms account for approximately 20% of global carbon fixation, making them central to the biogeochemical cycling of carbon and nitrogen and to the attenuation of atmospheric carbon dioxide (CO_2) (Falkowski, 2012a; Geider et al., 2001). Their ecological significance extends beyond primary production: diatoms sustain productive coastal and polar food webs and underpin much of the biological productivity on which coastal and open ocean economies depend (Falkowski, 2012b; Friedland et al., 2021).

A key dimension of the ecological significance of diatoms is the intimate metabolic relationship these microalgae maintain with associated bacterial communities (Seymour et al., 2017). This relationship is neither simply mutualistic nor simply antagonistic, but dynamic, chemically mediated, and fundamental to nutrient cycling (Grossart et al., 2005; Simon et al., 2002). Bacteria compete with diatoms for dissolved inorganic nutrients while simultaneously recycling organic matter from dying diatom cells and reintroducing it into the food web via protozoa, heterotrophic microalgae, and zooplankton in what Azam et al., (1983) first described as the microbial loop. Microbial interactions are concentrated within the phycosphere, the diffusion-dominated microenvironment surrounding the diatom cell, analogous to the terrestrial rhizosphere, where diatoms release extracellular polymeric substances rich in fucose, galactose, mannose, and chitin, and bacteria reciprocally supply essential growth factors, including vitamin B12, iron, and amino acids such as phenylalanine (Amin et al., 2015; Cruz-López and Maske, 2016; Daly et al., 2023; Tran et al., 2023; Zhu et al., 2024; Zoccarato et al., 2022). Chemotactic bacteria detect these dissolved metabolites, position themselves relative to the host cell, and assemble accordingly. Thereby, they produce a highly dynamic microbial community whose composition is conspicuously variable between and within diatom species across pelagic, epipelagic, and benthic habitats (Di Costanzo et al., 2021; Grossart, 1999; Grossart et al., 2005). The resulting interactions range from mutualistic to antagonistic, shaped by a chemical ecology that is largely understood only when organic pollutants are inferred.

In the Anthropocene, this classic structure is increasingly threatened by several chemical contaminants, including per- and polyfluoroalkyl substances (PFAS), which have the potential to disrupt this finely tuned mutualism (Schaider et al., 2017; US EPA, 2021). The exceptional strength of the carbon-fluorine (C-F) bond confers resistance to biodegradation, rendering PFAS environmentally persistent. Considering their widespread use in consumer goods such as non-stick cookware, water -repellent textiles, food packaging, paints, and cosmetics over the past several decades, their persistence makes them ubiquitous in marine and seashore environments (Glüge et al., 2020). Once in the water column, their hydrophobic and lipophilic character drives bioaccumulation across all trophic levels (Cara et al., 2022; Dai et al., 2025). Regulatory scrutiny of long-chain PFAS has

accelerated, prompting a transition to short-chain and branched variants whose ecological implications remain poorly constrained (Hamid et al., 2024). Although complete biological mineralization of PFAS is rarely achieved in controlled laboratory trials, certain bacteria can transform specific functional groups, and limited evidence suggests that a few microbial species initiate cleavage of C-F bonds under particular conditions. Nonetheless, the C-F backbone of long-chain PFAS remains highly resistant to microbial breakdown (Bentel et al., 2019; Huang and Jaffé, 2019a). How PFAS alters the bacterial community structure within the diatom phycosphere, particularly at environmentally relevant concentrations in marine ecosystems, including polar ones, remains largely unknown.

Studies examining microbial communities in PFAS-contaminated environments consistently demonstrate differential taxon-level responses, indicating that PFAS contamination act as a selective force restructuring community composition rather than suppressing it uniformly. Specific bacteria that have the potential to break down and biotransform PFAS thrive in PFAS-contaminated environments (Bentel et al., 2019; Choi and Kan, 2024; Skinner et al., 2025; Xin et al., 2023). In soil and aquatic systems, PFAS exposure frequently restructures microbial communities by enriching stress-tolerant taxa, particularly within the Proteobacteria, while reducing the abundance of more sensitive groups such as Actinobacteria and Chloroflexi. Although several bacterial taxa have been associated with PFAS biotransformation, their capacity is generally limited and often restricted to partial transformation rather than complete mineralization (Shittu et al., 2023a). Field surveys of fire-training area soils with PFAS concentration reaching 531 μg kg^{-1} (dry weigh)t dominated by PFOS, showed enrichment of stress-tolerant taxa including Proteobacteria, Acidobacteria, and Bacteroidetes alongside a significant reduction in bacterial diversity at highly contaminated plots (Zhang et al., 2022a). Where biotransformation occurs, a meta-analysis of 97 microbial PFAS biotransformation studies confirms that it remains partial and is strongly dependent on chain length, branching geometry, and headgroup chemistry; functional groups such as sulfonates and carboxylates can be modified, but cleavage of the C-F backbone is rarely achieved, and anaerobic biotransformation pathways remain critically underexplored (Skinner et al., 2025). Wackett (2022) further argues that microbial degradation of heavily fluorinated compounds is rare and that progress in bioremediation demands elucidating the physiological mechanisms underlying C-F bond cleavage. Critically, these findings derive almost exclusively from soil, freshwater, and wastewater matrices. Yet, their relevance to marine phycosphere communities, where bacterial composition is tightly coupled to host diatom metabolite chemistry, remains entirely unexplored. Whether diatom species that occupy fundamentally different habitats, e.g. benthic vs. pelagic, harbour bacterial assemblages with different intrinsic vulnerabilities to PFAS is unknown.

Our previous studies Arulananthan et al. (2025a) demonstrated that environmentally relevant PFAS mixtures can affect marine diatoms even at concentrations representative of those measured in Arctic and other marine surface waters (Hartz et al., 2024; Lin et al., 2020). Exposure to a PFAS mixture at 0.9 ng L^{-1} induced measurable changes in photosynthetic performance, chlorophyll content, protein and lipid dynamics, antioxidant responses, and osmoregulatory stress markers despite only limited effects on long-term population growth (Arulananthan et al. 2025a). Subsequent transcriptomic and metabolomic analyses revealed extensive molecular reprogramming under the same exposure conditions. Together, these findings demonstrated that PFAS can modify diatom physiology and metabolism at concentrations several orders of magnitude below those typically used in laboratory toxicity studies, suggesting that ecologically relevant PFAS levels may influence not only the algal host itself but also the surrounding phycosphere environment. Because diatom-associated bacterial communities are strongly regulated by host-derived metabolites, nutrient fluxes, and cell-surface properties, we hypothesized that these subtle but persistent host responses would propagate to the microbiome level and result in measurable restructuring of phycosphere bacterial communities.

2.0 Materials and methods

2.1 Experimental design

Semi-cultures of the arctic benthic diatom *Cylindrotheca closterium* and the sub-Arctic pelagic species *Thalassiosira pseudonana* were exposed to PFAS, and changes in associated bacterial community composition were assessed and compared to those without (controls). A mixture of PFAS compounds (PFOA, PFNA, PFOS, PFDoA, PFTrDA, and GenX, each at 0.9 ng/L) was added to 5000 mL of each diatom culture (2000 mL f/2 medium and 3000 mL of diatom culture in f/2 medium) and exposed for 28 days. After 28 days of exposure, 500 mL of both diatom cultures from both PFAS-treated and control groups were harvested by centrifugation and immediately stored at -80 °C for subsequent DNA extraction. Details on diatom origin, cultivation and experimental design, including the PFAS spiking conditions, are provided by Arulananthan et al. (2025a).

2.2 Amplicon sequencing and analysis

Bacterial community composition was assessed by targeting the V4 region of the 16S rRNA gene via sequencing and ASV determination. DNA extraction was performed using the DNeasy PowerSoil Kit (Qiagen) according to the manufacturer´s instructions from the diatom pellets, and the DNA samples were sent to NOVOGENE for sequencing. PCR amplifications targeted the V4 regions with the primer pair 515F (5´GTGCCAGCMGCCGCGGTAA-3′) and 806R (5′-

GGACTACHVGGGTTCTAAT-3′) (Caporaso et al., 2011). All samples were sequenced on a NovaSeq6000 platform (NOVOGENE, UK).

The resulting sequences were quality filtered using Cutadapt plugin by removing adaptor and primer sequences (3.3), and high-quality reads were then merged using FLASH (v1.2.11) (Magoč and Salzberg, 2011). Then the qualified sequences were de-noised using DADA2 (Callahan et al., 2016) plugin in the Qiime2 (Bolyen et al., 2019) pipeline with default parameters, to achieve single-nucleotide resolution based on error profiles within the samples. The denoised sequences, referred to as ASVs, were annotated for species classification using the sklearn-based Naïve Bayes classifier (scikit) implemented in Qiime2 and the SILVA 16S rRNA database (v138). All raw data have been submitted to the NCBI Sequence Read Archive (SRA) under the accession ID BioProject PRJNA1445241.

Based on the ASV data, rarefaction curves and alpha diversity indices were calculated using Mothur (v1.30.1). The absolute ASV abundance was normalized using a sequence number standard corresponding to the sample with the lowest sequence number. Subsequently, alpha diversity indices (richness, Shannon diversity, Pielou´s Evenness, and Chao1) and beta diversity were calculated. The similarity between bacterial communities across different samples was assessed by calculating the Bray-Curtis dissimilarity matrix and then using principal coordinate analysis in the R Vegan (v2.4-3) package (Hill et al., 2003) for visualization. To assess the statistical significance and the percentage of variation in the treatment, the permutational multivariate analysis of variance (PERMANOVA, n = 9999) test was conducted using the R Vegan (v2.4-3) package. Changes in bacterial community composition between PFAS-exposed samples and their respective controls for each species were visualized using relative abundances at the phylum, order, family, and genus levels.

To contextualize bacterial community shifts within an ecological framework, genera resolved at the ASV level were assigned to six functional guilds based on their eco-physiological traits documented in peer-reviewed literature (Supplementary table 1). Each genus was assigned to the guild most consistent with its dominant metabolic and ecological role in marine environments. Genera with well-documented but ambiguous and dual roles were assigned to the guild representing their primary function in a phycosphere context.

3.0 Results

3.1 Bacterial community composition: Phylum, order and family level

The bacterial communities associated with the phycosphere of *C. closterium* (CC) and *T. pseudonana* (TP) were dominated by four phyla across all treatment groups (with PFAS and controls): Pseudomonadota, Planctomycetota, Bacteroidota, and Myxococcota (CC only), collectively accounting for > 96% of total reads in each group. Despite this shared high-level framework, both host

species harboured compositionally distinct phycosphere communities, with Planctomycetota constituting 40% of TP control reads compared to only 16% in CC controls, and Myxococcota contributing 7% in CC controls while being essentially absent from TP (< 0.01%). Pseudomonadota was the dominant phylum in CC controls (50%) but was proportionally lower in TP controls (43%), reflecting the greater Planctomycetota representation in the pelagic diatom phycosphere (Figure 1a).

Under PFAS exposure, the relative abundance of Pseudomonadota were lower in both species (CC: 50% to 42%; TP: 43% to 36%). The absolute difference was equivalent at the phylum level, but as described below, the underlying class-level mechanisms differed fundamentally between species. Planctomycetota were increased in both species under PFFAS exposure (CC: 16% to 19%; TP: 40% to 47%), with the largest absolute enrichment in TP consistent with its higher baseline representation. Bacteroidota was slightly enriched in CC (23% to 26%) but was quite stable in TP (17% to 16%). Myxococcota were higher in CC under PFAS exposure (7% to 11%) and was not recorded from TP in both control and PFAS-treated groups (Figure 1a).

The most pronounced order level changes (Figure 1b) under PFAS exposure in CC was Flavobacteriales (Family Flavobacteriaceae) (6% vs. 11%), Nannocystales (Myxococcota) were increased (7% vs. 11%), while Rhodobacterales were reduced (15% vs. 9%). Sphingomonadales were higher (1% vs. 4%) in CC, and (9% vs. 13%) in TP, confirming cross-species but enrichment at order level noticed mainly in TP. Moreover, in TP, Enterobacterales and Pseudomonadales were lower under PFAS exposure (9% vs. 1%) and (10% vs. 3%), respectively. This collectively accounted for the majority of the lower fraction of Gammaproteobacteria.

At the family level, order-level signals were confirmed with greater resolution. Phycispharaceae showed the same dynamics, increased in both species under PFAS exposure, as Phycisphaerales at all levels. Cyclobacteriaceae (including *Marivirga*) were markedly lower in CC (17% to 15%) and nearly absent in TP. Alteromonadaceae were significantly lower in TP (9% vs. 1%) and less in CC (11% vs. 8%). Sphingomonadaceae were higher in both species following PFAS exposure. Paracoccaceae (Rhodobacterales) were lower in CC (15% vs. 9%) and remained low in TP (1%). Marinobacteraceae were lower in TP (10% vs. 3%) and didn't change much in CC (5% vs. 4%) (Figure 1c).

3.2 Genus-level composition: key taxa

Between-species baseline differences at the genus level were substantial (Figure 1d). SM1A02 (Phycisphaeraceae) was the most abundant taxon in TP controls (38%) and the second most abundant in CC controls (15%) and was higher under PFAS exposure in both diatom species (CC, i.e. 15% vs. 18%; TP,

i.e. 38% vs. 45%), representing the only genus consistently higher in the phycosphere of both diatoms (Figure 1 d).

Muricauda constituted 14% of all TP control reads but was essentially absent from CC. *Marivirga* constituted 16% of all CC control reads but was absent from TP. *Alteromonaas* was present in both species at baseline (CC: 11%; TP: 9%). *Marinobacter* had a higher proportion in TP (10%) than in CC controls (5%).

In *C. Closterium,* under PFAS exposure, *Tenacibaculum* showed the highest difference at genus-level in CC (2% vs. 6%), but also unclassified Nannocystaceaea, *Parasphingorhabdus,* and *Idiomarina* were higher (7% vs. 11%), (1% vs. 4%), and (3,5% vs. 4%), respectively. In contrast, *Marivirga, Alteromonas*, and *Antarctobacter* were lower (16% vs. 13%), (11% vs. 8%), and (9% vs. 5%), respectively. Both *Cyanobium* PCC-6307 and w *Paracoccaceae* were much lower (2% vs. <0.1%) and (15% vs. 9%), respectively.

The dominant PFAS exposure response in TP was the almost complete absence of *Alteromonas* and Marinobacter, i.e. (9% vs. 1%) and (10% vs. 3%), respectively. *Parasphingorhabdus* and *Marinicauda* were higher, i.e. (8% vs. 12%) and (2% vs. 4%), respectively, whereas *Muricauda* remained the same (~14%). *Tenacibaculum*, present at 0.2% in TP controls, almost disappeared under PFAS exposure. This absence is stark contrast to CC, where it was higher (i.e. 2% vs. 6%) and the stability of *Muricauda* in TP represented the two most compelling between-species divergence at genus level under PFAS exposure.

3.3 Alpha diversity of phycosphere bacterial communities

Analysis of alpha diversity indices across the four experimental groups reveals a biologically meaningful and host-species-specific pattern that extends well beyond a simple PFAS-induced diversity reduction (Figure 2). The phycosphere of *C. closterium* supported a markedly higher bacterial richness and diversity than that of *T. pseudonana*, as reflected by Chao1 estimates of 259.4 vs. 143.1 and Shannon indices (H') of 4.428 vs. 3.186 for both species controls, respectively (Figure 3). These differences indicate that the benthic diatom phycosphere is inherently richer and more diverse in bacterial taxa than the pelagic phycosphere in the absence of PFAS.

On the other hand, PFAS exposure did not significantly alter alpha diversity in *C. closterium* ($p > 0.05$ for all indices). Chao 1 was moderately lower (259.4 vs. 193.7), Shannon H' remained almost the same (4.428 vs. 4.378), and Pielou's evenness (J') was marginally higher (0.553 vs. 0.579). The slightly lower estimated richness and a higher evenness indicate minor attrition of rare taxa without a profound change in the dominant community structure, demonstrating genuine resilience of the overall diversity architecture in the *C. closterium* phycosphere.

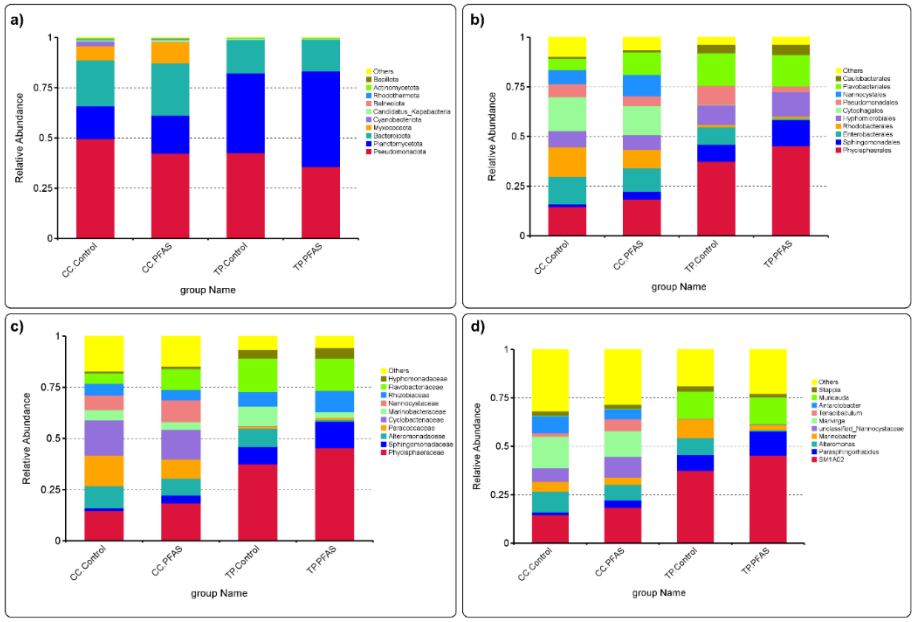

Figure 1: Relative abundance (mean of four replicates) of bacterial taxonomic classification of the 10 most abundant bacterial taxa of both *Cylindrotheca closterium* and *Thalassiosira pseudonana* cultures. Panels are sectioned into different taxonomic levels as following: a) phylum , b) order, c) family, and d): genus level phycosphere composition.

In the phycosphere of *T. pseudonana*, PFAS exposure produced a divergent and internally paradoxical response. Chao1 was substantially higher, i.e., 143.1 vs. 246.0 (↑71.9%), whereas Shannon H' index was 3.186 vs. 2.868 (↓10.0%), and Pielou's J' evenness index was lower, 0.446 to 0.362 (↓18.8%) (Figure 2). However, all trends were statistically in-significant, yet directionally consistent. This combination of elevated ASV detection with reduced effective diversity reflects a possible collapse of previously dominant copiotrophs: *Alteromonas* and *Marinobacter* were much lower (90% and 74% lower read numbers), releasing competitive pressure that permitted detection of formerly rare taxa. Thereby, the proportional abundance concentrated toward a few lineages with higher relative abundance following PFAS exposure, e.g. SM1A02 and *Parasphingorhabdus*.

At the phylum level, changes in Pseudomonadota were much more pronunced in *T. pseudonana* (40.8% lower) vs. in *C. closterium* (only 1.1% lower) following PFAS exposure. As a result, this phylum level attrition was identified as the primary driver of effective PFAS-driven diversity loss in the pelagic phycosphere of *T. pseudonana*. The host-specificity of individual taxa responses is further illustrated by the opposing fate of *Tenacibaculum* (fold change 2.92 in CC vs 0.01

in TP), a divergence undetectable at the alpha diversity level. Alpha diversity indices therefore mask substantial compositional restructuring, whereas beta diversity and genus level composition analyses provide the diagnostic resolution necessary to characterize these community-level responses of phycosphere bacteria.

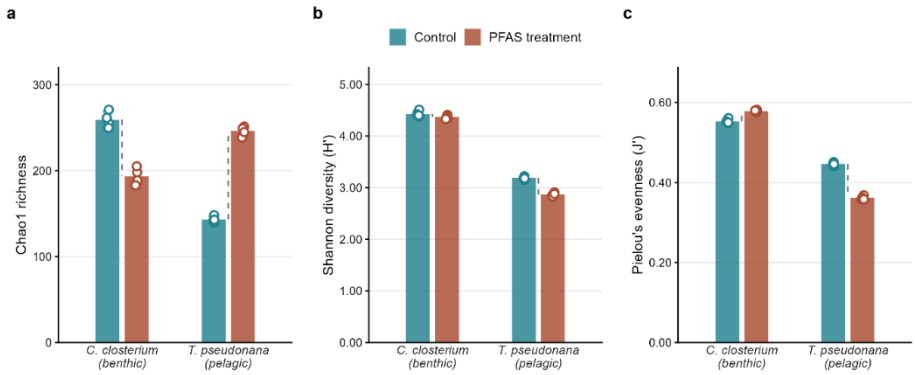

Figure 2: Alpha diversity indices of *Cylindrotheca closterium* (CC) and *Thalassiosira pseudonana* (TP) without and with PFAS exposure. Panel a) Chao1 shows host-specific reorganization, i.e. CC loses richness under PFAS exposure, while TP gains richness. b) Shannon index shows contrasting effective diversity, i.e. CC is similar while TP is lower under PFAS exposure, indicating that TP undergoes bacterial community skewing despite a richness increase. c) Pielou's J' completes the picture, i.e. the bacterial community of TP becomes less even under PFAS while that of CC becomes marginally more even.

3.4 Beta diversity of phycosphere bacterial communities

Beta diversity analysis consistently demonstrated that host diatom species identity was the primary determinant of phycosphere bacterial community structure, with all ordination methods separating *C. closterium* and *T. pseudonana* samples into distinct compositional clusters. Within *C. closterium*, UPGMA clustering of weighted UniFrac distances revealed tight grouping of all eight samples (four replicates per treatment group; scale bar: 0 - 0.125 weighted UniFrac units in 0.025 increments), with control and PFAS-treated replicates intermixing throughout the clade, confirming that PFAS exposure did not substantially alter the abundance-weighted community structure of the *C. closterium* phycosphere (Figure 3).

In contrast to the cohesive clustering observed in *C. closterium, T. pseudonana* exhibited markedly higher within-group dispersion, with control and PFAS-treated replicates partially intermixing across the UPGMA clade and no consistent treatment-driven clustering detectable. Notably, one control replicate (TP.C3) and one PFAS-treated replicate (TP.P3) showed compositionally divergent profiles,

branching on long terminal stems in both weighted and unweighted UniFrac UPGMA dendrograms, suggesting that these individuals harboured atypical phycosphere assemblages relative to their within-treatment peers. These divergent replicates likely contributed disproportionately to the elevated within-group dispersion observed in this species. A sensitivity analysis confirmed that the direction of PFAS-associated compositional trends, specifically the enrichment of Phycisphaeraceae and near-elimination of Alteromonadaceae and Cyclobacteriaceae, was consistent regardless of whether these replicates were included, and they were therefore retained in all subsequent analyses to preserve the integrity of the biological replicate set.

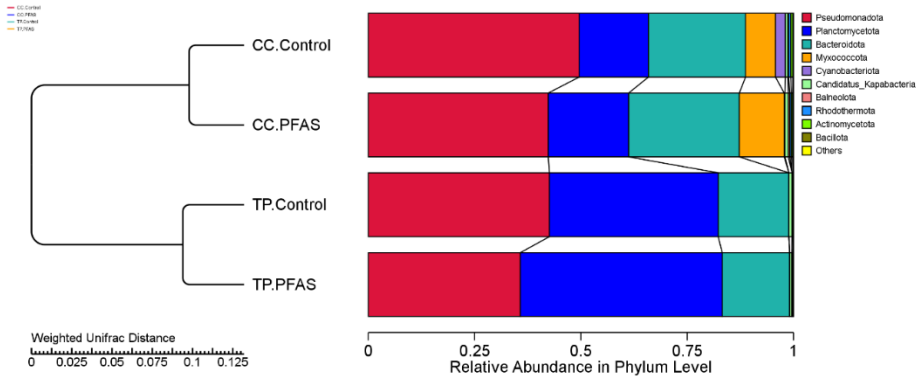

Figure 3: UPGMA clustering based on weighted UniFrac distances and corresponding bacterial community composition at the phylum level for diatom phycosphere communities exposed to PFAS and control conditions (both species). The dendrogram (left) shows the similarity in community structure among PFAS-treated groups and their respective controls, with branch length proportional to weighted UniFrac distance. The primary bifurcation separates *C. closterium* (CC) and *T. pseudonana* (TP) samples into distinct clades, indicating that host species identity is the dominant driver of phycosphere community composition. Within each species, PFAS-treated and control groups cluster closely, with a slightly larger internal branch length observed in the TP clade reflecting PFAS-associated enrichment of Planctomycetota. Stacked bar plots (right) display the relative abundance of major bacterial phyla across all four experimental groups.

PERMANOVA (9,999 permutations) of weighted UniFrac distances confirmed that host diatom species identity was the primary and most significant determinant of phycosphere bacterial community composition ($F = 15.30$, $R2 = 0.52$, $p = 0.0002$), with all pairwise comparisons between *C. closterium* and *T. pseudonana* groups reaching significance ($p = 0.0305$). In contrast, PFAS treatment did not significantly explain community variance whether species were analysed

independently (*C. closterium*: F= 0.22, R^2 =0.04, p = 0.969; *T. pseudonana*: F= 0.74, R^2 =0.11, p = 0.680; weighted UniFrac), nor when PFAS exposure treatment effects were tested across the full dataset (F= 0.31, R^2 =0.02, p = 0.874). Although whole-community PERMANOVA did not detect a statistically significant treatment effect, our results demonstrate that PFAS exposure drives consistent, taxon-specific restructuring of the phycosphere microbiome at the family level, detectable via differential abundance analysis rather than ordination-based beta-diversity metrics.

3.5 Functional significance of the phycosphere

Functional guild composition differed markedly between the studied diatom species and shifted in a guild-specific manner under PFAS exposure (Figure 4). In *C. closterium,* the six guilds were distributed relatively evenly in controls (each contributing 6-26%), indicating a functionally diverse bacterial phycosphere community. Under PFAS, the relative abundance of Planctomycetota (surface-associated oligotroph guild) increased from 18% (control) to 22% (PFAS treatment), and the polymer or EPS -degrader or particle -associated Bacteriodota guild increased from 26% to 28%, while the hydrocarbon or xenobiotic degrader guild decreased from 20% to 16%. The hydrophobic-organic/xenobiotic-associated heterotroph guild, however, increased from 6% to 10%, suggesting selective enrichment of guilds with affinity for contaminant substrates under PFAS exposure.

In *T. pseudonana*, the Planctomycetota/surface-associated oligotroph guild was already dominant in controls (41%) and further increased under PFAS (49%), indicating strong reinforcement of oligotrophic dominance under chemical stress. The most pronounced PFAS-induced change in TP was the near-elimination of the hydrocarbon/xenobiotic degrader guild, which declined from 19% in controls to 4% under PFAS exposure. The polymer/EPS-degrader guild was almost stable (19% vs. 21%), and the other/polled low-abundance taxa guild increased from 10% to 14%, reflecting community evenness loss and concentration of reads into fewer dominant guilds.

4.0 Discussion

4.1 Functional convergence and taxonomic divergence

The higher baseline dominance of Planctomycetota in the TP phycosphere compared to CC likely reflects intrinsic species-specific differences in cell surface biochemistry and EPS composition between these two phylogenetically distant diatoms, the pennate *C. closterium* and the centric *T. pseudonana,* rather than their natural ecological niches, since both species were maintained under identical laboratory culture conditions. The transcriptional upregulation of chitin synthase isoforms and glycosyltransferase family 2 members observed in T. *pseudonana* under both control and PFAS conditions is consistent with a constitutively chitin-

rich EPS substrate that selectively recruits SM1A02 as a specialist polysaccharide degrader, independent of environmental nutrient regime.

Enrichment of *Fluviicola, Balneola*, and *Parasphingorhabdus* (upper-right quadrant; higher in both CC and TP under PFAS) alongside depletion of *Alteromonas*, *Marinobacter,* and *Marivirga* (lower-left quadrant; lower in both species) revealed convergent functional restructuring across hosts (Figure 5). The majority of genera nonetheless showed asymmetric, species-specific responses, with notably stronger depletion of hydrocarbon- and xenobiotic-degrading taxa and particle-associated heterotrophs in TP, while strong depletion of polymer- and EPS-degrading *Spongiibacterium* and *Roseivirga* occurred specifically in CC. The co-existence of depleted taxa such as *Sulfitobacter* and *Marivirga* alongside enriched genera including *Algimonas* and *Tenacibaculum* within the same PFAS-treated phycospheres demonstrates that genus-level resolution is necessary for capturing differential responses within taxonomic classes that share broad physiological characterization but diverge in specific metabolic traits. This guild-shift pattern is broadly consistent with findings that PFOS and PFOA (at >10 ng/L) favour stress-tolerant taxa (Okpanachi et al., 2025; Schaefer et al., 2023), and with evidence that active sulfate-reducing Desulfobacterota can remove PFOS under anaerobic conditions during diatom blooms (Siebers et al., 2024). Martinez-Varela et al. (2020) confirmed that Gammaproteobacteria including *Pseudomonas,* in the sea-surface microlayer (SML) at the coast of the Antarctica Livingston Island co-occur with PFAS accumulating in the SML via atmospheric deposition. Their biotransformation capacity under marine salinity conditions still remains untested.

4.2 Differential survival of bacterial taxa under PFAS exposure: Gammaproteobacteria decline and Alphaproteobacteria show resilience

The much lower relative abundance of Gammaproteobacteria in the TP phycosphere (18.4 % vs. 3.6% of all reads) under PFAS exposure represents the most significant community shift observed in this study, in contrast to moderately lower relative abundance in CC (21.6% vs. 18.3%). This pattern is consistent with the known sensitivity of copiotrophic Gammaproteobacteria to organic contaminants (Cerro-Gálvez et al., 2020; P. Lin et al., 2025; Ma et al., 2026; Yang et al., 2025). At the order level, in TP, the lower relative abundance was attributable primarily to Enterobacterales and Pseudomonadales, which at the family level was confirmed by the near-elimination of Alteromonadaceae and Marinobacteraceae.

Alteromonas and *Marinobater* are recognized copiotrophs and bloom-responsive opportunists in marine phycosphere that exploit labile dissolved organic matter (DOM) released by phytoplankton(Gärdes et al., 2011; Seymour et al., 2017). Their suppression is consistent with the observation that PFAS compounds disrupt cell membrane integrity and inhibit enzymatic activity in gram-negative^{-} heterotrophs at environmentally relevant concentrations,

particularly in sulfonates such as PFOS (Xue et al., 2022). The differential sensitivity of bacteria in the TP vs. CC phycospheres may reflect host-mediated differences in EPS composition and DOM quality: *T. pseudonana* releases 2,3-dihydroxypropane-1-sulfonate (DHPS) and sulfonated metabolites that specifically attract Gammaproteobacterial copiotrophic partners (Seymour et al., 2017; Zhu et al., 2024), and PFAS-induced disruption of sulfonated exudate chemistry may result in a disproportionate disadvantage for these taxa in the TP phycosphere.

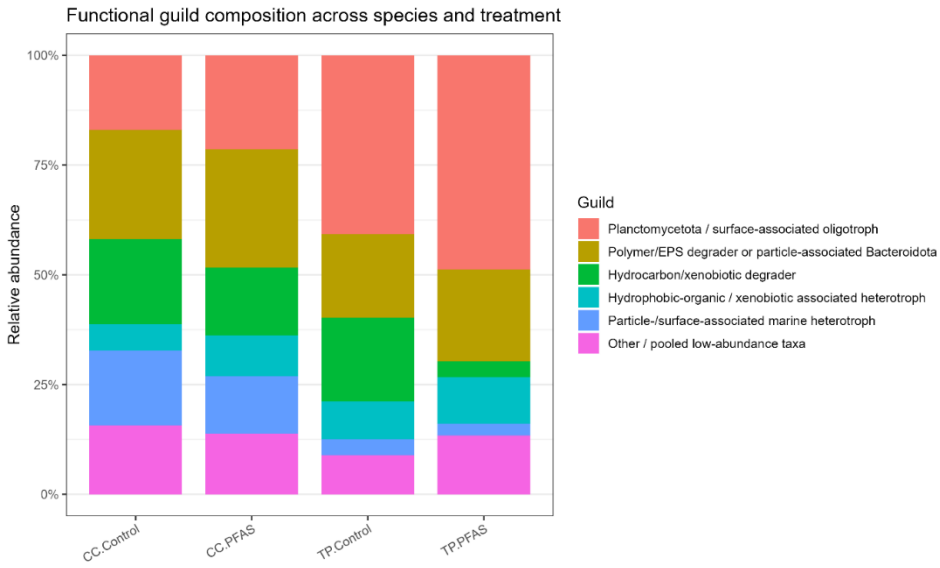

Figure 4: Functional guild composition of the bacterial community associated with benthic *Cylindrotheca closterium* and pelagic *Thalassiosira pseudonana* under control and PFAS-exposed conditions. The bars represent the relative abundance (%) of each functional guild per sample. Different colour of guild categories reflect ecologically and functionally annotated bacteria genera based on literature-curated assignments.

Simultaneously, Alphaproteobacteria had a higher relative abundance in TP under PFAS, while marginally lower in CC. This opposing within-phylum response, concealed by the aggregate Pseudomonadata phylum-level signal, indicates that Alphaproteobacterial lineages are not simply resistant to PFAS but are competitively favored when Gammaproteobacteria showed a lower relative abundance. Rhizobiaceae and *Antarctobacter* in TP contributed most to this difference. Alphaproteobacteria are broadly recognized as oligotrophic strategists with smaller cell sizes, higher surface-area-to-volume ratios, and membrane compositions less vulnerable to amphiphilic surfactants (Shittu et al.,2023a). The

phylum-level resilience of Proteobacteria as a whole, reported in contaminated sediments and wastewater systems (Ojewole et al., 2023), may therefore mask a fundamental ecophysiological shift within this phylum from fast-growing, DOM-responsive Gammaproteobacteria towards slower-growing but chemically tolerant Alphaproteobacterial lineages. A variety of functional roles have been proposed for Alphaproteobacteria in symbiotic associations, including inorganic and organic nutrient scavenging and abiotic stress relief (Sigurbjörnsdóttir et al. 2014, 2015, Cernava et al. 2017).

4.3 PFAS-tolerant taxa: SM1A02 (Planctomycetota) and Sphingomonadales

Among PFAS-favoured taxa, Sphingomonadales and its constituent genus *Parasphingorhabdus* also give attention. Sphingomonadales are gram-negative Alphaproteobacteria with sphingolipid- and glycosphingolipid-rich membranes that confer structural stability against amphiphilic compounds, including fluorinated surfactants(Ahrens et al., 2009; Huang and Jaffé, 2019b), and members of this order are among the few bacterial lineages documented to metabolise highly recalcitrant halogenated aromatic compounds (Jin et al., 2023; Vingiani et al., 2022). The cross-species higher relative abundance of Sphingomonadales in both CC and TP phycospheres following PFAS exposure suggests a general tolerance mechanism operative across diatom phycosphere microenvironments. Thereby, its higher response amplitude in the benthic *C. closterium* may additionally reflect host-specific EPS characteristics that facilitate Sphingomonadales colonization. The contemporaneous enrichment of both SM1A02 and Sphingomonadales, lineages with fundamentally different physiologies, suggests a convergent community response in which distinct PFAS-tolerant taxa fill the competitive vacuum created by copiotrophic Gammaproteobacterial collapsecompounds (Yin et al., 2019).

The anammox bacteria SM1A02 (Planctomycetota: Phycisphaerae), likely to play important roles nitrogen cycling, are the dominant phycosphere taxon in TP and the second most abundant in CC. They have been found to be enriched by PFAS presence in other systems, such as in wastewater reactors and in constructed wetlands (Feng et al. 2023, Qian et al. 2023), and were indeed found to be enriched under PFAS in both diatom species in the present study, indicating a PFAS-tolerant phenotype. Planctomycetota possess distinctive cell plan characteristics, compartmentalized cytoplasm, and intracellular membrane systems, and unusual cell wall chemistry lacking peptidoglycan that may confer physical resilience against membrane-disrupting compounds (Wu et al., 2022, 2021). Planctomycetes have been reported to persist and increase in relative abundance in PFAS-contaminated aquatic systems due to their metabolic versatility and unusual cell architecture (Wu et al., 2022). Consistently higher relative abundances of SM1A02 across both diatom host species, despite their divergent phycosphere chemistries, identify this genus as a potential bioindicator of PFAS exposure in

marine phytoplankton microbiomes (Zhu et al., 2024). Notably, higher relative abundances of both Planctomycetes and Sphingomonadales occurred contemporaneously across hosts, suggesting a convergent community response as PFAS-tolerant lineages with fundamentally different physiologies potentially benefit from the collapse of more sensitive competitors such as Gammaproteobacteria (Yin et al., 2019). *Acidimicrobium sp*. and *Pseudomonas parafulva* are among the few bacterial species demonstrated to actively transform PFAS compounds (Huang and Jaffé, 2019a; Shittu et al., 2023b), and neither was detected in the present study at any taxonomic level resolved by 16S rRNA V4 amplicon sequencing. This absence does not preclude cryptic biotransformation activity, as defluorination pathways in reductive conditions may be mediated by diverse lineages not currently characterized (Bentel et al., 2019; Ma and Olivares, 2025; Skinner et al., 2025). The patterns observed in our study, high relative abundances of known heterotrophic (potential PFAS-degrading) lineages and low relative abundances of copiotrophic Gammaproteobacteria, are more consistent with differential survival strategies and competitive restructuring under PFAS exposure rather than active PFAS degradation (Karlsson et al., 2019).

4.4 Tenacibaculum divergence and host-specific phycosphere structuring

The most striking taxon-level divergence between diatom host species in the present study dataset was the opposing response of *Tenacibaculum* (Flavobacteriaceae) in CC vs. TP cultures. *Tenacibaculum* are obligate marine Falvobacteria with gliding motility and a demonstrated capacity for EPS production for colonization of biotic surfaces, including diatom frustules (Abell and Bowman, 2005; Seymour et al., 2017). In the benthic *CC* phycosphere, *Tenacibaculum* enrichment under PFAS may reflect enhanced adhesion to the diatom surface as PFAS can alter EPS architecture, consistent with the documented ability of bacteria to exploit changes in diatom extracellular chemistry as colonization cues(Daly et al., 2023; Xiao et al., 2024; Zhang et al., 2022b). In the pelagic *TP* phycosphere, the near-complete absence of *Tenacibaculum* (10 reads under PFAS vs. 1,300 reads in the controls) indicates that the TP phycosphere loses the EPS-rich microenvironment required for Tenacibaculum attachment under PFAS stress, or that sulfonated PFAS compounds are selectively toxic to this genus in the TP context. The Flavobacteriaceae order-level pattern corroborates this: relative abundance increased in CC (5.7% → 10.9%) but remained neutral in TP, suggesting that the entire CC Flavobacteriaceae community benefited from access to PFAS-modified diatom-derived organic matter.

4.5 Environmental context, translational constraints and carbon pump implications

PFAS exposure in the present study was conducted under controlled laboratory conditions at concentrations overlapping those reported in estuarine surface waters (52 -117 ng/L) (W. Lin et al., 2025). Translating these results to natural coastal environments requires consideration of how salinity fluctuations, seasonal temperature shifts, and tidal mixing modulate PFAS bioavailability and phycosphere chemistry. In cold-water systems, Alteromonadales may face compounded stress from both PFAS-mediated membrane disruption and temperature-imposed growth constraints (Godin-Roulling et al., 2015), which could amplify the community shifts observed here. Conversely, the broader temperature tolerance of Planctomycetes and Sphingomonadales is consistent with their persistence under both cold conditions and PFAS exposure in this study. PFAS concentrations have been shown to alter microbial carbon, nitrogen, and phosphorus cycling in estuarine communities primarily through indirect shifts in community composition (W. Lin et al., 2025), a mechanism that appears to operate equivalently in the diatom phycospheres studied here.

Biofilm structure and EPS stability in the phycosphere of benthic diatoms such as *C. closterium* are also temperature-sensitive, where low light and low-temperature would impair diatom EPS production (Daly et al., 2023), which would alter substrate availability for EPS-degrading phycosphere bacteria and change the competitive landscape in which PFAS effects occur. Thereby, diatom-bacteria interactions mediated through EPS represent an additional axis of environmental modulation. *T. pseudonana* releases 2,3-dihydroxypropane-1-sulfonate (DHPS) to specifically recruit *Ruegeira pomerovi* for vitamin B12 supply, creating a highly specific chemical dialogue that is substrate-dependent and potentially PFAS sensitive (Cruz-López and Maske, 2016; Di Costanzo et al., 2023). Bacterial colonization of diatom surfaces through chemotaxis toward physico-chemical phycosphere gradients mediated by quorum-sensing molecules and pilus formation genes particularly in Rhodobacterales (Amin et al., 2015; Falciatore and Mock, 2022; Gram et al., 2002), and PFAS compounds, as amphiphilic surfactants capable of disrupting membrane receptor function, may interfere with cell-cell signalling pathways that regulate phycosphere community assembly.

Disruption of diatom-bacterial partnerships by PFAS, operating substantially through host-mediated transcriptional reprogramming rather than direct bacterial toxicity, represents a more insidious mechanism of ecological impact than previously recognized. The selective elimination of *Alteromonas,* Cyclobacteriaceae, and Cyanobacteria alongside enrichment of Planctomycetota and Myxococcota shifts the phycosphere from a copiotrophic, high-turnover carbon cycle towards a slower, oligotrophic regime dominated by recalcitrant polysaccharide degraders. This transition would reduce the efficiency of the

biological carbon pump in PFAS-contaminated coastal zones(Ahrens and Bundschuh, 2014; Evich et al., 2022).

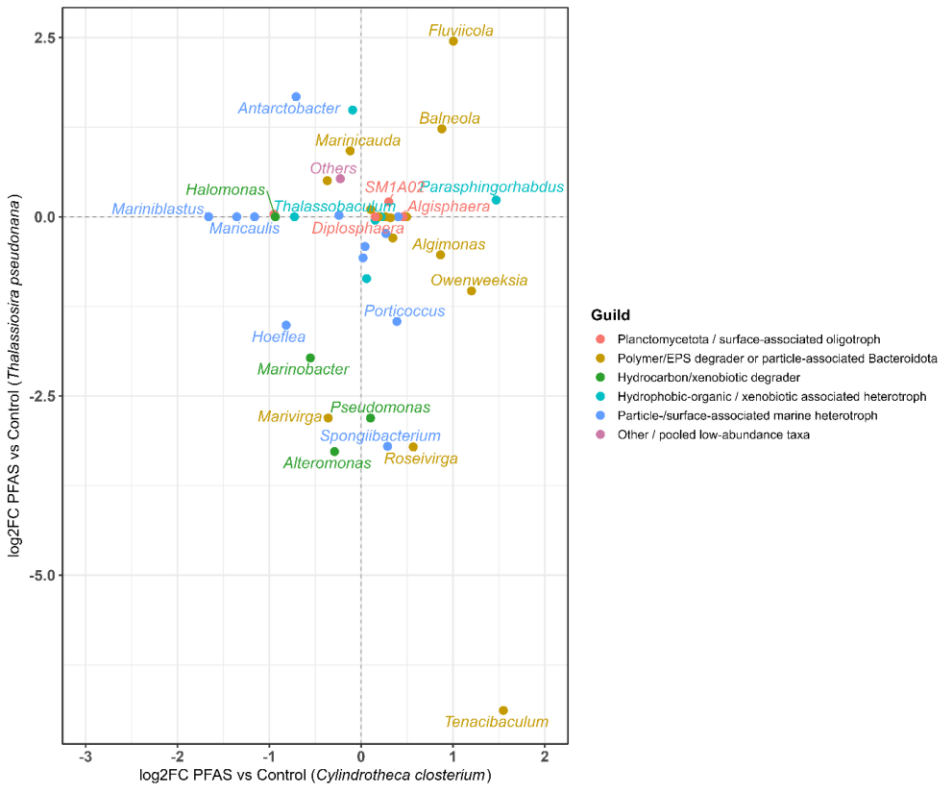

Figure 5: Genus-level $\log_2$ fold-change ($\log_2$ FC) response to PFA exposure in the bacterial communities associated with *Cylindrotheca closterium* (CC) and *Thalassiosira pseudonana* (TP). Each point represents a bacterial genus, positioned according to its relative abundance change (PFAS vs. Control) in CC (x-axis), and TP (y-axis). Positive values indicate higher relative abundance under PFAS exposure; negative values indicate lower relative abundances. Points are color-coded by functional guild based marked on the right panel. Genus labels shown for ecologically relevant top-responding taxa. A pseudo-count of 1 was added prior to $\log_2$FC calculation to avoid unidentified values for absent taxa.

Conclusion

This study demonstrates that an environmentally relevant PFAS mixture can restructure the diatom phycosphere microbiome without producing significant changes in bulk bacterial diversity metrics. Bacterial richness was not significantly altered at environmentally relevant concentrations, while community composition underwent consistent, taxon-specific restructuring detectable at

family and genus resolution. Host species identity was the primary determinant of community structure, yet PFAS imposed a convergent guild-level shift across both host species. Loss of xenobiotic-degrading copiotrophs, including *Alteromonas* and *Marinobacter*, from the *T. pseudonana* phycosphere indicates that current environmental PFAS levels may compromise microbial functions critical for carbon and nutrient cycling in pelagic food webs, even when standard diversity metrics appear unaffected. Resolving temporal dynamics, concentration gradients, and functional gene expression will be necessary to elucidate specific degradation pathways and refine risk thresholds for microbial community integrity in PFAS-impacted marine systems.

Data availability

All sequencing data generated in this study are available at NCBI SRA platform under BioProjectPRJNA1445241, (https://dataview.ncbi.nlm.nih.gov/object/PRJNA1445241?reviewer=ad9jntl1eknbn3vt0qdhq8cm5j). All other data are available from the corresponding author upon request.

Funding

The Icelandic Research Fund has supported the work in the frame of the project "Per- and polyfluoroalkyl substances (PFAS) meet Arctic and sub-Arctic marine diatoms and their associated symbionts" (RANNIS ID: 239548-051). ERASMUS Mobility Grants: Project codes 2024-1-IS01-KA131-HED-000204453, 2025-1-IS01-KA131-HED-000307569.

Acknowledgements

Our sincere thanks to the lab managers Andrés Tryggvi Jakobsson from the Faculty of Natural Resource Sciences at the University of Akureyri, for their support in lab work and handling equipment. We also thank Dr. Nafiu Abdulkadir for their guidance in sequence data analysis at the Department of Plankton and Microbial Ecology, Leibniz-Institute of Freshwater Ecology and Inland Fisheries, Stechlin, Germany.

References

Abell, G.C.J., Bowman, J.P., 2005. Colonization and community dynamics of class Flavobacteria on diatom detritus in experimental mesocosms based on Southern Ocean seawater☃. FEMS Microbiol Ecol 53, 379–391. https://doi.org/10.1016/j.femsec.2005.01.008

Ahrens, L., Bundschuh, M., 2014. Fate and effects of poly- and perfluoroalkyl substances in the aquatic environment: A review. Environmental Toxicology and Chemistry 33, 1921–1929. https://doi.org/10.1002/etc.2663

Ahrens, L., Felizeter, S., Sturm, R., Xie, Z., Ebinghaus, R., 2009. Polyfluorinated compounds in waste water treatment plant effluents and surface waters along the River Elbe, Germany. Marine Pollution Bulletin 58, 1326–1333. https://doi.org/10.1016/j.marpolbul.2009.04.028

Amin, S.A., Green, D.H., Hart, M.C., Küpper, F.C., Sunda, W.G., Carrano, C.J., 2009. Photolysis of iron–siderophore chelates promotes bacterial–algal mutualism. Proceedings of the National Academy of Sciences 106, 17071–17076. https://doi.org/10.1073/pnas.0905512106

Amin, S.A., Hmelo, L.R., van Tol, H.M., Durham, B.P., Carlson, L.T., Heal, K.R., Morales, R.L., Berthiaume, C.T., Parker, M.S., Djunaedi, B., Ingalls, A.E., Parsek, M.R., Moran, M.A., Armbrust, E.V., 2015. Interaction and signalling between a cosmopolitan phytoplankton and associated bacteria. Nature 522, 98–101. https://doi.org/10.1038/nature14488

Arulananthan, A., Scholz, B., Karsten, U., Grossart, H.-P., Sigurbjörnsdóttir, A., Rolfsson, Ó., Joerss, H., Duarte, B., Vilhelmsson, O.Þ., 2025. Arctic and sub-Arctic marine diatom responses to PFAS exposure: Understanding physiological changes and resilience. Aquatic Toxicology 289, 107562. https://doi.org/10.1016/j.aquatox.2025.107562

Azam, F., Fenchel, T., Field, J., Gray, J., Meyer-Reil, L., Thingstad, F., 1983. The Ecological Role of Water-Column Microbes in the Sea. Mar. Ecol. Prog. Ser. 10, 257–263. https://doi.org/10.3354/meps010257

Azam, F., Fenchel, T., Field, J.G., Gray, J.S., Meyer-Reil, L.A., Thingstad, F., 2022. The Ecological Role of Water-Column Microbes in the Sea, in: Foundations of Ecology II. University of Chicago Press, pp. 384–390.

Bentel, M.J., Yu, Y., Xu, L., Li, Z., Wong, B.M., Men, Y., Liu, J., 2019. Defluorination of Per- and Polyfluoroalkyl Substances (PFASs) with Hydrated Electrons: Structural Dependence and Implications to PFAS Remediation and Management. Environ. Sci. Technol. 53, 3718–3728. https://doi.org/10.1021/acs.est.8b06648

Bertrand, E.M., McCrow, J.P., Moustafa, A., Zheng, H., McQuaid, J.B., Delmont, T.O., Post, A.F., Sipler, R.E., Spackeen, J.L., Xu, K., Bronk, D.A., Hutchins, D.A., Allen, A.E., 2015. Phytoplankton-bacterial interactions mediate micronutrient colimitation at the coastal Antarctic sea ice edge. Proc Natl Acad Sci U S A 112, 9938–9943. https://doi.org/10.1073/pnas.1501615112

Bolyen, E., Rideout, J.R., Dillon, M.R., Bokulich, N.A., Abnet, C.C., Al-Ghalith, G.A., Alexander, H., Alm, E.J., Arumugam, M., Asnicar, F., Bai, Y., Bisanz, J.E., Bittinger, K., Brejnrod, A., Brislawn, C.J., Brown, C.T., Callahan, B.J., Caraballo-Rodríguez, A.M., Chase, J., Cope, E.K., Da Silva, R., Diener, C., Dorrestein, P.C., Douglas, G.M., Durall, D.M., Duvallet, C., Edwardson, C.F., Ernst, M., Estaki, M., Fouquier, J., Gauglitz, J.M., Gibbons, S.M., Gibson, D.L., Gonzalez, A., Gorlick, K., Guo, J., Hillmann, B., Holmes, S., Holste, H., Huttenhower, C., Huttley, G.A., Janssen, S., Jarmusch, A.K., Jiang, L., Kaehler, B.D., Kang, K.B., Keefe, C.R., Keim, P., Kelley, S.T., Knights, D., Koester, I., Kosciolek, T., Kreps, J., Langille, M.G.I., Lee, J., Ley, R., Liu, Y.-X., Loftfield, E.,

Lozupone, C., Maher, M., Marotz, C., Martin, B.D., McDonald, D., McIver, L.J., Melnik, A.V., Metcalf, J.L., Morgan, S.C., Morton, J.T., Naimey, A.T., Navas-Molina, J.A., Nothias, L.F., Orchanian, S.B., Pearson, T., Peoples, S.L., Petras, D., Preuss, M.L., Pruesse, E., Rasmussen, L.B., Rivers, A., Robeson, M.S., Rosenthal, P., Segata, N., Shaffer, M., Shiffer, A., Sinha, R., Song, S.J., Spear, J.R., Swafford, A.D., Thompson, L.R., Torres, P.J., Trinh, P., Tripathi, A., Turnbaugh, P.J., Ul-Hasan, S., van der Hooft, J.J.J., Vargas, F., Vázquez-Baeza, Y., Vogtmann, E., von Hippel, M., Walters, W., Wan, Y., Wang, M., Warren, J., Weber, K.C., Williamson, C.H.D., Willis, A.D., Xu, Z.Z., Zaneveld, J.R., Zhang, Y., Zhu, Q., Knight, R., Caporaso, J.G., 2019. Reproducible, interactive, scalable and extensible microbiome data science using QIIME 2. Nat Biotechnol 37, 852–857. https://doi.org/10.1038/s41587-019-0209-9

Callahan, B.J., McMurdie, P.J., Rosen, M.J., Han, A.W., Johnson, A.J.A., Holmes, S.P., 2016. DADA2: High-resolution sample inference from Illumina amplicon data. Nat Methods 13, 581–583. https://doi.org/10.1038/nmeth.3869

Caporaso, J.G., Lauber, C.L., Walters, W.A., Berg-Lyons, D., Lozupone, C.A., Turnbaugh, P.J., Fierer, N., Knight, R., 2011. Global patterns of 16S rRNA diversity at a depth of millions of sequences per sample. Proceedings of the National Academy of Sciences 108, 4516–4522. https://doi.org/10.1073/pnas.1000080107

Cara, B., Lies, T., Thimo, G., Robin, L., Lieven, B., 2022. Bioaccumulation and trophic transfer of perfluorinated alkyl substances (PFAS) in marine biota from the Belgian North Sea: Distribution and human health risk implications. Environmental Pollution 311, 119907. https://doi.org/10.1016/j.envpol.2022.119907

Cerro-Gálvez, E., Roscales, J.L., Jiménez, B., Sala, M.M., Dachs, J., Vila-Costa, M., 2020. Microbial responses to perfluoroalkyl substances and perfluorooctanesulfonate (PFOS) desulfurization in the Antarctic marine environment. Water Research 171, 115434. https://doi.org/10.1016/j.watres.2019.115434

Choi, G., Kan, E., 2024. Effects of perfluorooctanoic acid and perfluorooctane sulfonic acid on microbial community structure during anaerobic digestion. Bioresource Technology 393, 129999. https://doi.org/10.1016/j.biortech.2023.129999

Cruz-López, R., Maske, H., 2016. The Vitamin B1 and B12 Required by the Marine Dinoflagellate Lingulodinium polyedrum Can be Provided by its Associated Bacterial Community in Culture. Front Microbiol 7, 560. https://doi.org/10.3389/fmicb.2016.00560

Dai, S., Zhang, G., Dong, C., Yang, R., Pei, Z., Li, Y., Li, A., Zhang, Q., Jiang, G., 2025. Occurrence, bioaccumulation and trophodynamics of per- and polyfluoroalkyl substances (PFAS) in terrestrial and marine ecosystems of Svalbard, Arctic. Water Res 271, 122979. https://doi.org/10.1016/j.watres.2024.122979

Daly, G., Decorosi, F., Viti, C., Adessi, A., 2023. Shaping the phycosphere: Analysis of the EPS in diatom-bacterial co-cultures. Journal of Phycology 59, 791–797. https://doi.org/10.1111/jpy.13361

Di Costanzo, F., Di Dato, V., Romano, G., 2023. Diatom–Bacteria Interactions in the Marine Environment: Complexity, Heterogeneity, and Potential for Biotechnological Applications. Microorganisms 11, 2967. https://doi.org/10.3390/microorganisms11122967

Di Costanzo, F., Di Dato, V., van Zyl, L.J., Cutignano, A., Esposito, F., Trindade, M., Romano, G., 2021. Three Novel Bacteria Associated with Two Centric Diatom Species from the Mediterranean Sea, Thalassiosira rotula and Skeletonema marinoi. International Journal of Molecular Sciences 22, 13199. https://doi.org/10.3390/ijms222413199

Evich, M.G., Davis, M., Weber, E.J., Tebes-Stevens, C., Acrey, B., Henderson, W.M., Goodrow, S., Bergman, E., Washington, J.W., 2022. Environmental Fate of Cl-PFPECAs: Predicting the Formation of PFAS Transformation Products in New Jersey Soils. Environ. Sci. Technol. 56, 7779–7788. https://doi.org/10.1021/acs.est.1c06126

Falciatore, A., Mock, T. (Eds.), 2022. The Molecular Life of Diatoms. Springer International Publishing, Cham. https://doi.org/10.1007/978-3-030-92499-7

Falkowski, P., 2012a. Do tiny floating microorganisms in the ocean's surface waters play a massive role in controlling the global climate?

Falkowski, P., 2012b. Ocean Science: The power of plankton. Nature 483, S17–S20. https://doi.org/10.1038/483S17a

Friedland, K.D., Moisan, J.R., Maureaud, A.A., Brady, D.C., Davies, A.J., Bograd, S.J., Watson, R.A., Rousseau, Y., 2021. Trends in phytoplankton communities within large marine ecosystems diverge from the global ocean. Can. J. Fish. Aquat. Sci. 78, 1689–1700. https://doi.org/10.1139/cjfas-2020-0423

Geider, R.J., Delucia, E.H., Falkowski, P.G., Finzi, A.C., Grime, J.P., Grace, J., Kana, T.M., La Roche, J., Long, S.P., Osborne, B.A., Platt, T., Prentice, I.C., Raven, J.A., Schlesinger, W.H., Smetacek, V., Stuart, V., Sathyendranath, S., Thomas, R.B., Vogelmann, T.C., Williams, P., Woodward, F.I., 2001. Primary productivity of planet earth: biological determinants and physical constraints in terrestrial and aquatic habitats. Global Change Biology 7, 849–882. https://doi.org/10.1046/j.1365-2486.2001.00448.x

Glüge, J., Scheringer, M., Cousins, I.T., DeWitt, J.C., Goldenman, G., Herzke, D., Lohmann, R., Ng, C.A., Trier, X., Wang, Z., 2020. An overview of the uses of per- and polyfluoroalkyl substances (PFAS). Environ. Sci.: Processes Impacts 22, 2345–2373. https://doi.org/10.1039/D0EM00291G

Godin-Roulling, A., Schmidpeter, P.A.M., Schmid, F.X., Feller, G., 2015. Functional adaptations of the bacterial chaperone trigger factor to extreme environmental temperatures. Environmental Microbiology 17, 2407–2420. https://doi.org/10.1111/1462-2920.12707

Gram, L., Grossart, H.-P., Schlingloff, A., Kiørboe, T., 2002. Possible Quorum Sensing in Marine Snow Bacteria: Production of Acylated Homoserine Lactones by Roseobacter Strains Isolated from Marine Snow. Appl Environ Microbiol 68, 4111–4116. https://doi.org/10.1128/AEM.68.8.4111-4116.2002

Grossart, H.-P., 1999. Interactions between marine bacteria and axenic diatoms (Cylindrotheca fusiformis, Nitzschia laevis, and Thalassiosira weissflogii) incubated under various conditions in the lab. Aquatic Microbial Ecology 19, 1–11. https://doi.org/10.3354/ame019001

Grossart, H.-P., Levold, F., Allgaier, M., Simon, M., Brinkhoff, T., 2005. Marine diatom species harbour distinct bacterial communities. Environmental Microbiology 7, 860–873. https://doi.org/10.1111/j.1462-2920.2005.00759.x

Hacquard, S., Spaepen, S., Garrido-Oter, R., Schulze-Lefert, P., 2017. Interplay Between Innate Immunity and the Plant Microbiota. Annu Rev Phytopathol 55, 565–589. https://doi.org/10.1146/annurev-phyto-080516-035623

Hamid, N., Junaid, M., Sultan, M., Yoganandham, S.T., Chuan, O.M., 2024. The untold story of PFAS alternatives: Insights into the occurrence, ecotoxicological impacts, and removal strategies in the aquatic environment. Water Research 250, 121044. https://doi.org/10.1016/j.watres.2023.121044

Hartz, W.F., Björnsdotter, M.K., Yeung, L.W.Y., Humby, J.D., Eckhardt, S., Evangeliou, N., Ericson Jogsten, I., Kärrman, A., Kallenborn, R., 2024. Sources and Seasonal Variations of Per- and Polyfluoroalkyl Substances (PFAS) in Surface Snow in the Arctic. Environ. Sci. Technol. 58, 21817–21828. https://doi.org/10.1021/acs.est.4c08854

Hill, T.C.J., Walsh, K.A., Harris, J.A., Moffett, B.F., 2003. Using ecological diversity measures with bacterial communities. FEMS Microbiol Ecol 43, 1–11. https://doi.org/10.1111/j.1574-6941.2003.tb01040.x

Huang, S., Jaffé, P.R., 2019a. Defluorination of Perfluorooctanoic Acid (PFOA) and Perfluorooctane Sulfonate (PFOS) by Acidimicrobium sp. Strain A6. Environ. Sci. Technol. 53, 11410–11419. https://doi.org/10.1021/acs.est.9b04047

Huang, S., Jaffé, P.R., 2019b. Defluorination of Perfluorooctanoic Acid (PFOA) and Perfluorooctane Sulfonate (PFOS) by Acidimicrobium sp. Strain A6. Environ. Sci. Technol. 53, 11410–11419. https://doi.org/10.1021/acs.est.9b04047

Jin, B., Liu, H., Che, S., Gao, J., Yu, Y., Liu, J., Men, Y., 2023. Substantial defluorination of polychlorofluorocarboxylic acids triggered by anaerobic microbial hydrolytic dechlorination. Nat Water 1, 451–461. https://doi.org/10.1038/s44221-023-00077-6

Karlsson, C.M.G., Cerro-Gálvez, E., Lundin, D., Karlsson, C., Vila-Costa, M., Pinhassi, J., 2019. Direct effects of organic pollutants on the growth and gene expression of the Baltic Sea model bacterium Rheinheimera sp. BAL341. Microbial Biotechnology 12, 892–906. https://doi.org/10.1111/1751-7915.13441

Kazamia, E., Czesnick, H., Nguyen, T.T.V., Croft, M.T., Sherwood, E., Sasso, S., Hodson, S.J., Warren, M.J., Smith, A.G., 2012. Mutualistic interactions between vitamin B12 -dependent algae and heterotrophic bacteria exhibit regulation. Environ Microbiol 14, 1466–1476. https://doi.org/10.1111/j.1462-2920.2012.02733.x

Lin, P., Liu, X., Gao, Z., Yuan, Y., Liu, H., Huang, L., He, Z., Zeng, Q., Wang, S., 2025. Microplastics magnify inhibitive effects of perfluorooctanoic acid on the marine microbial loop. Environmental Research 273, 121223. https://doi.org/10.1016/j.envres.2025.121223

Lin, W., Zhao, J., Wu, X., Jiang, J., Zhou, C., Zheng, J., Zhang, C., Guo, Y., Wang, L., Ng, H.Y., Li, S., Wang, S., 2025. The effects of perfluoroalkyl substance pollution on microbial community and key metabolic pathways in the Pearl River Estuary. Ecotoxicology and Environmental Safety 298, 118293. https://doi.org/10.1016/j.ecoenv.2025.118293

Lin, Y., Jiang, J.-J., Rodenburg, L.A., Cai, M., Wu, Z., Ke, H., Chitsaz, M., 2020. Perfluoroalkyl substances in sediments from the Bering Sea to the western Arctic: Source and pathway analysis. Environment International 139, 105699. https://doi.org/10.1016/j.envint.2020.105699

Ma, D., Olivares, C.I., 2025. Perfluoroalkane Sulfonamides and Derivatives, a Different Class of PFAS: Sorption and Microbial Biotransformation Insights. Environ. Sci. Technol. 59, 10734–10749. https://doi.org/10.1021/acs.est.5c00906

Ma, X., Ma, J., Paerhati, Y., Chen, J., Zhang, J., Tian, Y., 2026. Diversity and distribution of bacterial community vertically across ecological and trophic gradient within sediments of lake Bosten area. Sci Rep 16, 5558. https://doi.org/10.1038/s41598-026-35454-0

Magoč, T., Salzberg, S.L., 2011. FLASH: fast length adjustment of short reads to improve genome assemblies. Bioinformatics 27, 2957–2963. https://doi.org/10.1093/bioinformatics/btr507

Martinez-Varela, A., Casas, G., Piña, B., Dachs, J., Vila-Costa, M., 2020. Large Enrichment of Anthropogenic Organic Matter Degrading Bacteria in the Sea-Surface Microlayer at Coastal Livingston Island (Antarctica). Front. Microbiol. 11. https://doi.org/10.3389/fmicb.2020.571983

Okpanachi, I.Y., Gotan, Y.S., Dauda, S., Otogo, R.A., Samuel, S.A., Iortsuum, D.N., Chia, M.A., 2025. Combined effect of PFOS and PFOA on phytoplankton interactions and overall community health. J Plankton Res 47, fbaf044. https://doi.org/10.1093/plankt/fbaf044

Schaefer, C.E., Hooper, J.L., Strom, L.E., Abusallout, I., Dickenson, E.R.V., Thompson, K.A., Mohan, G.R., Drennan, D., Wu, K., Guelfo, J.L., 2023. Occurrence of quantifiable and semi-quantifiable poly- and perfluoroalkyl substances in united states wastewater treatment plants. Water Research 233, 119724. https://doi.org/10.1016/j.watres.2023.119724

Schaider, L.A., Balan, S.A., Blum, A., Andrews, D.Q., Strynar, M.J., Dickinson, M.E., Lunderberg, D.M., Lang, J.R., Peaslee, G.F., 2017. Fluorinated Compounds in U.S. Fast Food Packaging. Environ. Sci. Technol. Lett. 4, 105–111. https://doi.org/10.1021/acs.estlett.6b00435

Seymour, J.R., Amin, S.A., Raina, J.-B., Stocker, R., 2017. Zooming in on the phycosphere: the ecological interface for phytoplankton–bacteria relationships. Nat Microbiol 2, 17065. https://doi.org/10.1038/nmicrobiol.2017.65

Shittu, A.R., Iwaloye, O.F., Ojewole, A.E., Rabiu, A.G., Amechi, M.O., Herve, O.F., 2023. The effects of per- and polyfluoroalkyl substances on environmental and human microorganisms and their potential for bioremediation. AIHT 74, 167–178. https://doi.org/10.2478/aiht-2023-74-3708

Shittu, A.R., Iwaloye, O.F., Ojewole, A.E., Rabiu, A.G., Amechi, M.O., Herve, O.F., n.d. The effects of per- and polyfluoroalkyl substances on environmental and human microorganisms and their potential for bioremediation. Arh Hig Rada Toksikol 74, 167–178. https://doi.org/10.2478/aiht-2023-74-3708

Siebers, R., Schultz, D., Farza, M.S., Brauer, A., Zühlke, D., Mücke, P.A., Wang, F., Bernhardt, J., Teeling, H., Becher, D., Riedel, K., Kirstein, I.V., Wiltshire, K.H., Hoff, K.J., Schweder, T., Urich, T., Bengtsson, M.M., 2024. Marine particle microbiomes during a spring diatom bloom contain active sulfate-reducing bacteria. FEMS Microbiol Ecol 100, fiae037. https://doi.org/10.1093/femsec/fiae037

Simon, M., Grossart, H.-P., Schweitzer, B., Ploug, H., 2002. Microbial ecology of organic aggregates in aquatic ecosystems. Aquatic Microbial Ecology 28, 175–211. https://doi.org/10.3354/ame028175

Skinner, J.P., Raderstorf, A., Rittmann, B.E., Delgado, A.G., 2025. Biotransforming the “Forever Chemicals”: Trends and Insights from Microbiological Studies on PFAS. Environ. Sci. Technol. 59, 5417–5430. https://doi.org/10.1021/acs.est.4c04557

Tran, Q.D., Neu, T.R., Sultana, S., Giebel, H.-A., Simon, M., Billerbeck, S., 2023. Distinct glycoconjugate cell surface structures make the pelagic diatom Thalassiosira rotula an attractive habitat for bacteria. Journal of Phycology 59, 309–322. https://doi.org/10.1111/jpy.13308

US EPA, O., 2021. Per- and Polyfluoroalkyl Substances (PFAS) [WWW Document]. URL https://www.epa.gov/sdwa/and-polyfluoroalkyl-substances-pfas (accessed 2.20.25).

Vingiani, G.M., Leone, S., De Luca, D., Borra, M., Dobson, A.D.W., Ianora, A., De Luca, P., Lauritano, C., 2022. First identification and characterization of detoxifying plastic-degrading DBP hydrolases in the marine diatom *Cylindrotheca closterium*. Science of The Total Environment 812, 152535. https://doi.org/10.1016/j.scitotenv.2021.152535

Wackett, L.P., 2022. Nothing lasts forever: understanding microbial biodegradation of polyfluorinated compounds and perfluorinated alkyl substances. Microbial Biotechnology 15, 773–792. https://doi.org/10.1111/1751-7915.13928

Wiegand, S., Jogler, M., Jogler, C., 2018. On the maverick Planctomycetes. FEMS Microbiol Rev 42, 739–760. https://doi.org/10.1093/femsre/fuy029

Wu, J., Gu, L., Hua, Z., Liang, Z., Chu, K., He, X., 2021. Per-, poly-fluoroalkyl substances (PFASs) pollution in benthic riverine ecosystem: Integrating microbial community coalescence and biogeochemistry with sediment distribution. Chemosphere 281, 130977. https://doi.org/10.1016/j.chemosphere.2021.130977

Wu, J., Hua, Z., Gu, L., 2022. Per-, poly-fluoroalkyl substances (PFASs) and planktonic microbiomes: Identification of biotic and abiotic regulations in community coalescence and food webs. Environmental Pollution 302, 119078. https://doi.org/10.1016/j.envpol.2022.119078

Xiao, Y., Li, Q., Yang, Y., Zhang, Y., Shen, Y., Liu, J., Lei, N., Zhang, W., Wang, Q., 2024. Unravelling the mechanisms of PFAS toxicity to submerged macrophytes and epiphytic biofilms at metabolic and molecular levels. Science of The Total Environment 952, 175726. https://doi.org/10.1016/j.scitotenv.2024.175726

Xin, X., Kim, J., Ashley, D.C., Huang, C.-H., 2023. Degradation and Defluorination of Per- and Polyfluoroalkyl Substances by Direct Photolysis at 222 nm. ACS EST Water 3, 2776–2785. https://doi.org/10.1021/acsestwater.3c00274

Xue, X., Gao, N., Xu, F., 2022. Toxicity of perfluooctane sulfonate (PFOS) and perfluorobutane sulfonate (PFBS) to *Scenedesmus obliquus*: Photosynthetic characteristics, oxidative damage and transcriptome analysis. Environmental Pollution 315, 120397. https://doi.org/10.1016/j.envpol.2022.120397

Yang, Z., Liu, W., Fan, X., Gao, H., Xu, X., Liu, C., Chai, Y., Zhang, M., Drosos, M., Shan, S., 2025. The molecular composition of soil organic matter is regulated by bacterial community under biochar application. Geoderma 457, 117308. https://doi.org/10.1016/j.geoderma.2025.117308

Yin, T., Tran, N.H., Huiting, C., He, Y., Gin, K.Y.-H., 2019. Biotransformation of polyfluoroalkyl substances by microbial consortia from constructed wetlands under aerobic and anoxic conditions. Chemosphere 233, 101–109. https://doi.org/10.1016/j.chemosphere.2019.05.227

Zhang, Ying, Qv, Z., Wang, Jingwen, Yang, Y., Chen, X., Wang, Jingzhen, Zhang, Yanfeng, Zhu, L., 2022a. Natural biofilm as a potential integrative sample for evaluating the contamination and impacts of PFAS on aquatic ecosystems. Water Research 215, 118233. https://doi.org/10.1016/j.watres.2022.118233

Zhang, Ying, Qv, Z., Wang, Jingwen, Yang, Y., Chen, X., Wang, Jingzhen, Zhang, Yanfeng, Zhu, L., 2022b. Natural biofilm as a potential integrative sample for evaluating the contamination and impacts of PFAS on aquatic ecosystems. Water Research 215, 118233. https://doi.org/10.1016/j.watres.2022.118233

Zhu, J., Yu, Z., He, L., Cao, X., Wang, W., Song, X., 2024. Phycosphere bacterial composition and function in colony and solitary *Phaeocystis globosa* strains providing novel insights into the algal blooms. Marine Pollution Bulletin 206, 116700. https://doi.org/10.1016/j.marpolbul.2024.116700

Zoccarato, L., Sher, D., Miki, T., Segrè, D., Grossart, H.-P., 2022. A comparative whole-genome approach identifies bacterial traits for marine microbial interactions. Commun Biol 5, 276. https://doi.org/10.1038/s42003-022-03184-4